The Formyl Peptide Receptor 2 Regulates Microglial Phenotype Through Immunometabolism: Implications for Alzheimer's Disease

Wickstead, E.

The Formyl Peptide Receptor 2 Regulates Microglial Phenotype Through Immunometabolism: Implications for Alzheimer's Disease

Edward S. Wickstead

Faculty of Science and Technology
University of Westminster

A thesis submitted to the University of Westminster for the degree of Doctor of Philosophy

July 2019

Abstract

Microglia are key players in the pathology of Alzheimer's disease (AD), driving chronic inflammation, oxidative stress, and the altered metabolism seen in the brains of patients. With clinical trials continuing to fail, new approaches towards drug development are critical. Strategies to reduce microglial activation may therefore be a viable therapeutic approach to tackling AD. Formyl peptide receptor 2 (Fpr2), which drives peripheral inflammatory resolution, is expressed in microglia. However, its functional role in neuroinflammation is unclear. This thesis provides evidence to support the peripheral findings of Fpr2 stimulation, wherein it may also hold promise for exploitation as a therapeutic for neurodegenerative disorders, including AD. We also highlight novel findings surrounding the modulation of both oxidative stress and microglial metabolism associated with Fpr2 activation.

Under inflammatory conditions, we report that selective agonists for Fpr2 modulate the microglial inflammatory response, actively shifting from a pro-inflammatory to a pro-resolving phenotype, emphasised by the reduction of pro-inflammatory cytokines and concomitant increases in both pro-resolving cytokines and phagocytosis. Metabolic shifting away from glycolysis was also observed for pro-resolving microglia. Moreover, we describe for the first time that Fpr2 completely reverses reactive oxygen species (ROS) production from the mitochondria and NADPH oxidase enzymes following an inflammatory stimulus.

We also highlight that the toxic oligomeric amyloid β 1-42 peptide (oAβ) facilitates microglial ROS production and subsequent metabolic changes without triggering an inflammatory response. oAβ facilitated NADPH oxidase activation, which in turn resulted in the activation of glucose 6-phosphate dehydrogenase (G6PD), the rate limiting step for the pentose phosphate pathway. This metabolic pathway is responsible for producing NADPH, which in turn NADPH oxidases exploit for further ROS production. These changes resulted in noticeable reductions in both microglial glycolysis and oxidative phosphorylation. We present data underlining that Fpr2/3 stimulation reverses oAβ-induced ROS production, with a resultant reduction in G6PD activity and the return of homeostatic glycolysis. These oAβ-induced microglial changes triggered the apoptosis of SH-SY5Y cells in co-culture with BV-2 microglia. However, supporting our interest in Fpr2/3 for therapeutic approaches to neurodegenerative diseases, post-treatment with a select agonist for the receptor successfully prevented apoptosis of these neuronal like SH-SY5Y cells.

This original data unveils novel functions of Fpr2/3 in the central nervous system (CNS), supplementing the well-established pro-resolving functions the receptor facilitates within the periphery. The combination of pro-resolving, anti-oxidative, immunometabolic and anti-apoptotic functions of Fpr2/3 support the exploitation of this receptor for therapeutic research into multiple different CNS disorders, including AD.

Table of contents

Table of figures

Table of tables

Acknowledgements

Whilst I understood the difficulty of undertaking a PhD from the offset, I misjudged my preparation for the physical and psychological strain the journey can inflict. However, the last four years has been an unforgettable experience of creativity, criticism, self-identification and personal progression. Despite likely being one of the most difficult challenges I will ever undertake, it will inevitability be one of the most rewarding. I realise that much of this is down to the incredible people that have supported and guided me along the way, to which I would now like to acknowledge.

First, I would like to express my deepest gratitude to my primary supervisor Dr. Simon McArthur, for selecting me to carry out this research. Your guidance and mentoring have been priceless during this journey, for which I will be eternally grateful. Your understanding and patience have been crucial for me to unlock my full potential as a scientist, facilitating my creative thinking and critical approach to research. I now feel confident about approaching familiar problems with new, previously unconsidered questions. Even during moments of frustration, this was catalysed by your genuine interest and care about my future aspirations. You have supported me through turmoil and listened to my concerns. Alongside this, your approach has really helped teach me the importance of failure in science. Inevitably, it happens. However, if you fall seven times, remember to stand up eight. I have learnt countless amounts from you over the last four years, which I am sure will stay with me for the rest of my life. You are a mentor, but also a friend. I will never be able to thank you enough for guidance over this doctoral journey.

Special thanks go out to my co-supervisors Dr. Stephen Getting and Dr. Christopher Biggs. Both specialists in different research areas, they provided exceptional insight into different areas of the PhD process. Their guidance and advice not only helped with my research and thesis, but also facilitated me to grow and move forward personally; something which will forever impact my decisions going forward.

I am incredibly thankful for the University of Westminster for funding this project, selecting me as a recipient of this scholarship. Without it, I would not been able to accumulate the funding to undertake it and my future would be appreciably different.

A special thanks also go out to Dr. Bradley Elliott, who provided me with a teaching opportunity for his undergraduate course, allowing me to gain experience before moving on to the next stage of my scientific career.

I would also like to thank all of the other PhD students I have bonded with during my journey: so thank you Nicola Fararmazi, Amy Woy, Tom Brook, Rhys Mould and Vedia Can. Friendships and discussions helped me get through some very difficult days.

I would likely to deeply thank my entire family. I sincerely believe I would not have been able to do this without your support and advice. This work is dedicated to you. To my dearest mother, without your support and guidance from a young age, I would have never really believed in my potential. I hope that this disruptive and depressed school kid with a chip on his shoulder developed into a young man that you can be proud of. To my father, thank you for your understanding and patience. You accepted how little time I have had in the past twelve months. Despite this, you happily gave me the additional space I needed to focus, and it did not go unnoticed.

Finally, to my beloved Brontë, you have picked me off the ground during my lowest moments. Without your patience, emotional support, rationality and positivity, I would certainly not have achieved all of this. The dedication I put into this thesis and the results that I have achieved during this process; they are also yours.

Publications

Wickstead, **ES.,** Getting, SJ., Biggs, C., Elliott, B., McArthur, S. Microglial Fpr2/3 activation prevents amyloid beta-induced neuronal cell death in the absence of an inflammatory response. 2019 (in preparation)

Wickstead, **ES.,** Getting, SJ., Biggs, C., McArthur, S. Activation of the pro-resolving receptors Fpr2/3 attenuates lipopolysaccharide-induced inflammatory microglial activation. 2019 (in preparation)

Wickstead, **ES.,** Getting, SJ., Biggs, C., McArthur, S. Current understanding of Alzheimer's disease pathogenesis: prominence for microglial therapeutics. 2019 review (in preparation)

Meeting attendance

Oral Communications

Society for Neuroscience Conference 2018, San Diego (05/11/18)
Presentation title: Targeting oxidative stress and metabolism in Alzheimer's: an alternative approach'

Alzheimer's Research UK 2017 Conference, Aberdeen (13/03/17)
Presentation title: 'Fpr2: a novel drug target to tackle oxidative stress and inflammation in Alzheimer's disease'

British Pharmacological Society: Pharmacology 2016, London (13/12/16)
Presentation title: 'Fpr2 – a new target for neuroinflammation'

Poster Presentations

Alzheimer's Research UK 2018 Conference, London (20/03/18)
Poster title: 'Fpr2 and neuroinflammation: a selective agonist with synergistic anti-oxidative and pro-resolving effects'

British Pharmacological Society: Pharmacology 2017, London (13/12/17)
Poster title: 'Reversal of β-amyloid induced microglial activation by an agonist of Fpr2/3'

William Harvey Day 2017, London (18/10/17)
Poster title: 'Fpr2: stimulation of this pro-resolving receptor abolishes Aβ1-42 induced oxidative stress in BV2 microglia'

13th World Congress on Inflammation, London (09/07/17)
Poster title: 'Pro-resolving agonists of Fpr2 can restrain microglial activity, controlling inflammation and oxidative stress'

University of East London Bioscience Conference, London (10/05/17)
Poster title: 'Tackling neuroinflammation: A viable approach for neurodegenerative diseases?'

British Neuroscience Association, BNA2017 – Neuroscience, Birmingham (11/04/17)
Poster title: 'Activation of the pro-resolving receptor Fpr2 attenuates inflammatory microglial activation'

Alzheimer's Research UK 2017 Conference, Aberdeen (13/03/17)
Poster title: 'Fpr2: a novel drug target to tackle oxidative stress and inflammation in Alzheimer's disease'

Author declaration of originality

I, Edward S. Wickstead, hereby declare that the work presented in this thesis is my own and to the best of my knowledge, original. Any content derived from other sources, including figures, data and other materials have been appropriately indicated, acknowledged, accepted for use and referenced within the text and the bibliography.

Signed: 

Date: 25th July 2019

Abbreviations

Abbreviation	Full Name
ABAD	Amyloid-beta alcohol dehydrogenase
ACE	Angiotensin-1-converting enzyme
ACh	Acetylcholine
Aβ	Amyloid beta
oAβ	Oligomeric amyloid beta
AD	Alzheimer's disease
ADAM	Disintegrin and metalloproteinase
ADP	Adenosine diphosphate
AGEs	Advanced glycation end-products
AICD	Amyloid precursor protein intracellular cytoplasmic domain
ALEs	Advanced lipoxidation end-products
AMPA	Alpha-amino-3-hydroxy-5-methyl-4-isoxazolepropionic acid
ANOVA	Analysis of variance
AnxA1	Annexin A1
AP	Action potential
APC	Allophycocyanin
APH-1	Anterior pharynx-defective-1
APP	Amyloid precursor protein
ApoE	Apolipoprotein E
ATP	Adenosine triphosphate
BACE1	Beta-secretase 1
BBB	Blood-brain barrier
BDNF	Brain derived neurotrophic factor
BSA	Bovine serum albumin
CAM	Cell adhesion molecule
CM-H_2DCFDA	Chloromethyl-dichlorofluores-cin-diacetate
CNS	Central nervous system
CNV	Copy number variant
CSF	Cerebral spinal fluid
CSH	Cyclosporin H
CycD	Cyclophilin D
Cys	Cysteine
Cyt C	Cytochrome C
C43	Compound-43
DAMP	Damage associated molecular pattern

ddH_2O	Double distilled water
DMEM	Dulbecco's Modified Eagle's Medium
DNA	Deoxyribonucleic acid
ECAR	Extracellular acidification rate
ECL	Enhanced chemiluminescence
EC_{50}	Half maximal effective concentration
ELISA	Enzyme-linked immunosorbent assay
EOAD	Early-onset Alzheimer's disease
ERK	Extracellular signal-regulated kinase
Ex/Em	Excitation/Emission
FCS	Fetal calf serum
FITC	Fluorescein isothiocyanate
fMet	*N*-formylmethionine
fMLP	*N*-formyl-methionyl-leucyl-phenylalanine
FPR	Formyl peptide receptor
FPR1	Human formyl peptide receptor 1
FPR2	Human formyl peptide receptor 2
Fpr2	Murine formyl peptide receptor 2
FPR3	Human formyl peptide receptor 3
Fpr3	Murine formyl peptide receptor 3
GPCR	G-protein coupled receptor
GSK-3β	Glycogen synthase kinase 3-beta
GWAS	Genome wide association study
G6P	Glucose 6-phosphate
G6PD	Glucose 6-phosphate dehydrogenase
HFIP	Hexafluoro-2-propanol
hiFCS	Heat-inactivated fetal calf serum
HPF	Hydroxyphenyl fluorescein
HO-1	Hemeoxygenase-1
HRP	Horseradish peroxidase
HSD	Honest significant difference
H_2O_2	Hydrogen peroxide
Iba1	Ionized calcium-binding adaptor molecule 1
IC_{50}	Half maximal inhibitory concentration
IDE	Insulin degrading enzyme
IgG	Immunoglobulin G
IL-1	Interleukin-1
IL-6	Interleukin-6
IL-10	Interleukin-10

iNOS	Inducible nitric oxide synthase
JNK	c-Jun N-terminal kinase
kDa	Kilodalton
KO	Knockout
LPS	Lipopolysaccharide
LOAD	Late-onset Alzheimer's disease
LTP	Long-term potentiation
LXA4	Lipoxin A4
MHCII	Major histocompatibility complex II
MAP	Microtubule-associated protein
MAPK	Mitogen activated protein kinase
MCI	Mild cognitive impairment
MDA	Malondiadehyde
MPT	Mitochondrial permeability transition
Mφ	Macrophage
NADPH	Nicotinamide adenine dinucleotide phosphate
$NaNO_2$	Sodium nitrite
NEAA	Non-essential amino acid
NFT	Neurofibrillary tangle
NF-κB	Nuclear factor kappa-light-chain-enhancer of activated B cells
NIH	National Institute of Health
NMDA	N-Methyl-D-aspartic acid
NMDAR	N-Methyl-D-aspartic acid receptor
NO	Nitric oxide
NOD	Nucleotide-binding oligomerisation-domain protein
NSAIDs	Non-steroidal anti-inflammatory drugs
OCR	Oxygen consumption rate
$OH^{\cdot}$	Hydroxyl radical
$ONOO^{\cdot-}$	Peroxynitrite
O_2^{-}	Superoxide radical
PAGE	Polyacrylamide gel electrophoresis
PAMP	Pathogen-associated molecular pattern
PBS	Phosphate buffered saline
PE	Phycoerythrin
PEN-2	Presenilin enhancer-2
PET	Positron emission tomography
PHF	Paired helical filaments
P_i	Inorganic phosphate
PMA	Phorbol 12-myristate 13-acetate

PPP	Pentose phosphate pathway
PRF-DMEM	Phenol red free
PRR	Pattern recognition receptor
PS1	Presenilin 1
PS2	Presenilin 2
PVDF	Polyvinylidene fluoride
p3	p3 peptide/amyloid beta-peptide$_{17\text{-}40/42}$
QC1	Quin-C1
rAAV	Recombinant adeno-associated virus
RAGE	Receptor for advanced-glycation end-products
REVIHAAP	Review of the evidence on health aspects of air pollution
RIPA Buffer	Radioimmunoprecipitation Assay Buffer
RLR	RIG-I-like receptor
RLU	Relative luminescence units
RNS	Reactive nitrogen species
ROS	Reactive oxygen species
RvD2	Resolvin D2
sAPPα	Soluble amyloid precursor protein alpha
sAPPβ	Soluble amyloid precursor protein beta
SDS	Sodium dodecyl sulfate
SEM	Standard error of the mean
SPMs	Specialised pro-resolving mediators
TBS	Tris-buffered saline
TBS-T	Tris-buffered saline with Triton™ X-100
TLR	Toll-like receptor
TNFα	Tumour necrosis factor alpha
tRA	*Trans*-retinoic acid
TREM2	Triggering receptor expressed on myeloid cells 2
TX-100	Triton X-100
T2DM	Type 2 diabetes mellitus
WRW$_4$	WRWWWW
WT	Wildtype
α7-nAChR	Alpha7 nicotinic acetylcholine receptor
Δψ	Mitochondrial membrane potential
3xTg	Triple transgenic
4-HNE	4-hydroxy-2-nonenal

Chapter 1: An Introduction to Innate Immunity and Alzheimer's Disease

1.1. Inflammation and the innate immune system

Inflammation is a part of a complex biological system that is essential in responding to injury or infection. It is generally a protective process, which includes the involvement of cells from the immune system and vascular endothelium, but also a vast array of molecular mediators (Sansbury and Spite, 2016). It serves to eliminate the initial cause of cell injury, but also helps to remove necrotic cells and tissues damaged as a consequence of this insult. The response also has the capacity to stimulate initiation of tissue repair. A summary of the innate inflammatory response is shown in Figure 1.1 (Bell et al., 2006).

An acute inflammatory insult therefore usually involves a biphasic innate immune response. Utilising an initial cascade involving the release of pro-inflammatory cytokines, chemokines and reactive oxygen species (ROS) amongst others, this contributes to facilitate the movement of immune cells such as neutrophils in the periphery and microglia in the central nervous system (CNS) towards the injury site, before pathogen killing commences. Following this preliminary response, cells are signalled towards a pro-resolving phenotype, resulting in degradation of cellular debris and apoptotic cells, alongside tissue reparation. When tissue damage is amended and the insult destroyed or removed, inflammation will begin to cease. If this does not occur, chronic inflammation can result (Heneka et al., 2015b). In this case, during its development and propagation, inflammation can continue for months to years. The primary reason for this can be due to the inability of the body to eliminate the causing agent of the initial acute inflammatory response, impairing inflammatory resolution. This impaired resolution response is known to occur in neurodegenerative diseases such as AD (Wang et al., 2015; Zhu et al., 2016).

1.1.1. The innate inflammatory process

The immune system is activated through the identification of two groups of biomolecules: pathogen-associated molecular patterns (PAMPs) and damage-associated molecular patterns (DAMPs). PAMPs are molecules present within diverse groups of pathogens, whilst also being absent in the host, providing exogenous signals that alert the immune system to the presence of pathogens; thereby stimulating immunity in the host (Akira and Hemmi, 2003; Tang et al., 2012). The prototypical PAMP is lipopolysaccharide (LPS), found in the outer-cell membrane of gram-negative bacteria, but others also include bacterial flagellin and peptidoglycan (Silhavy et al., 2010). DAMPs are endogenous damage/danger

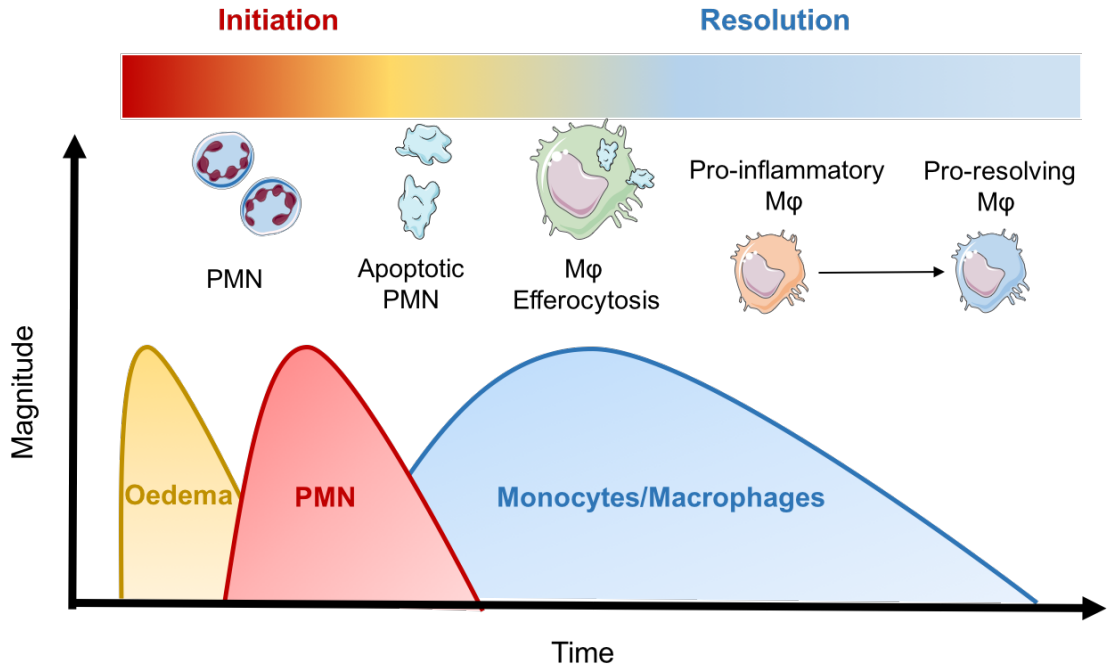

Figure 1.1 A simplified diagram of the acute innate immune inflammatory response. The ideal outcome of an acute innate inflammatory response is complete resolution and repair of the damaged area. Generally, inflammation is divided into two primary phases: initiation and resolution. The earliest stage of this process can be identified by marked tissue oedema, caused by increased blood flow and microvascular permeability. This is a direct consequence of pro-inflammatory mediators such as certain leukotrienes and prostaglandins. Polymorphonuclear neutrophils (PMN) infiltrate the tissue in response and attempt to kill the pathogens. Next, PMN undergo apoptosis. This is in parallel to switching from releasing pro-inflammatory, to pro-resolving inflammatory mediators, contributing to the resolution of inflammation. These PMN send 'eat me' signals to macrophages (Mφ) in a process referred to as efferocytosis. Pro-resolution mediators are also essential for promoting a pro-resolving macrophage phenotype, a critical process for tissue repair. Figure based around Sansbury and Spite, 2016.

signals released by host cells which alert the immune system of invading pathogens (Bours et al., 2006; Mathew et al., 2012). They also provide alerts for unscheduled/unprogrammed cell death, and can be released in response to stress (Rubartelli and Lotze, 2007). Examples of DAMPs include but are not limited to, heat-shock proteins (Panayi et al., 2004) and non-protein molecules including ATP (Bours et al., 2006) and DNA (Farkas et al., 2007). Interestingly, amyloid-beta (Aβ), which is a central pathological protein in AD, has been suggested to be an endogenously produced DAMP (Clark and Vissel, 2015; Santoni et al., 2015; Tang et al., 2012; Venegas and Heneka, 2017).

Both signals are identified by pattern recognition receptors (PRRs) on immune cell membranes, such as toll-like receptors (Beutler et al., 2006) and in the cytoplasm including nucleotide-binding oligomerisation-domain protein-like receptors (NLRs) and retinoic acid-inducible gene-I-like receptors (RLRs; Ting and Willams, 2005). Stimulation of these receptors on resident macrophages leads to the production and release of a battery of inflammatory mediators, including cytokines, chemokines and products of several proteolytic cascades. The primary and immediate effect of these mediators is the elicitation of a local inflammatory response centred in the periphery on neutrophils and macrophages, and on microglia in the CNS (Heneka et al., 2014; Rivera et al., 2016).

Macrophages are responsible for the engulfment and digestion of microbes, foreign substances, cellular debris and cancer cells. Any structure that does not contain cell surface proteins that match those of healthy bodily cells are engulfed and digested through phagocytosis. They were first identified by the Russian zoologist, Élie Metchnikoff in the 19th century (Underhill et al., 2016), and are located in essentially all tissues, whereby they constantly survey their surrounding environment for potential pathogens (Ovchinnikov, 2008). Due to their heterogeneous nature, macrophages perform tissue-specific functions. Despite their physiological distinctions, alongside their differing transcriptional profiles and functional capabilities, all macrophage cells are required for the homeostatic maintenance of the tissues they reside in. These unique cells therefore have different names and slightly alternating functions.

1.1.2. Microglia

Microglia are the resident macrophage-like innate immune cells of the CNS. Whilst often compared to macrophages, microglia (and also partially Langerhans cells) are the only myeloid cells which solely originate from erythromyeloid progenitors in the embryonic yolk sac under homeostatic conditions (Ginhoux et al., 2013; Ginhoux and Jung, 2014; Sheng et al., 2015). These progenitors then migrate into the developing neural tube before proliferating and maturing through the entire brain parenchyma. Their transcriptional

network is also unique, allowing for further distinguishability from tissue-resident macrophages (Gosselin et al., 2014; Kierdorf et al., 2013). Being the resident phagocytes of the CNS, microglia have critical roles in tissue maintenance, response to injury (Gyoneva and Ransohoff, 2015) and pathogenic defence (Ransohoff and El Khoury, 2015). Their role in neural circuit development, alongside synaptic pruning and removal of unwanted neurones is also essential for normal brain development (Figure 1.2; Paolicelli et al., 2011; Schafer et al., 2012). Additionally, microglia appear to be central regulators in activity-triggered synaptic plasticity, neurogenesis, and consequentially, learning and memory (Gemma and Bachstetter, 2013; Rogers et al., 2011).

In the healthy brain and spinal cord, microglial represent approximately 10% of the total cells in the CNS (von Bartheld et al., 2016), with cell maintenance not being dependent on circulating monocytes, but rather local self-renewal pools within the CNS (Bruttger et al., 2015). In mice, multiphoton microscopy techniques revealed that neocortical microglia are long-lived, with a median lifetime of 15 months, thus highlighting the ability of these phagocytes to survive the entire mouse lifespan (Füger et al., 2017). In humans, it has been estimated that human microglia renew slowly at a median rate of 28% per year, live for an average of 4.2 years, and some survive for more than two decades (Réu et al., 2017).

1.1.2.1. Microglial activation and immunity

Microglia have highly dynamic processes and are responsible for constant local environment surveillance (Nimmerjahn et al., 2005). Because of this, they can respond to a large variety of environmental cues, with an often highlighted hallmark of the microglial response being their ability to alter their morphology (Kirkley et al., 2017; Wadhwa et al., 2017). These changes were first described by Pío del Río Hortega over a century ago, correlating amoeboid-like morphological changes with pathology manifestation and disease (Sierra et al., 2016). However, we now know that microglial morphological changes only indicate a detectable change from homeostasis; this alone is not enough to inform us of a particular response or activity state in CNS disease (Boche et al., 2013).

In more recent years, attempts have been made to classify microglial activation as a biphasic response, utilising the terms ‘M1’ and M2’ borrowed from the now-defunct terminology used for macrophage classification (Murray et al., 2014). However as with macrophages, microglia carry out diverse functions and likely change in a variety of different ways depending on the environmental cues. Recent transcriptional analysis of murine microglia confirms this, highlighting that at least nine transcriptionally distinct microglial states exist (Hammond et al., 2019), clearly underlining the shortcomings of the M1/M2 system.

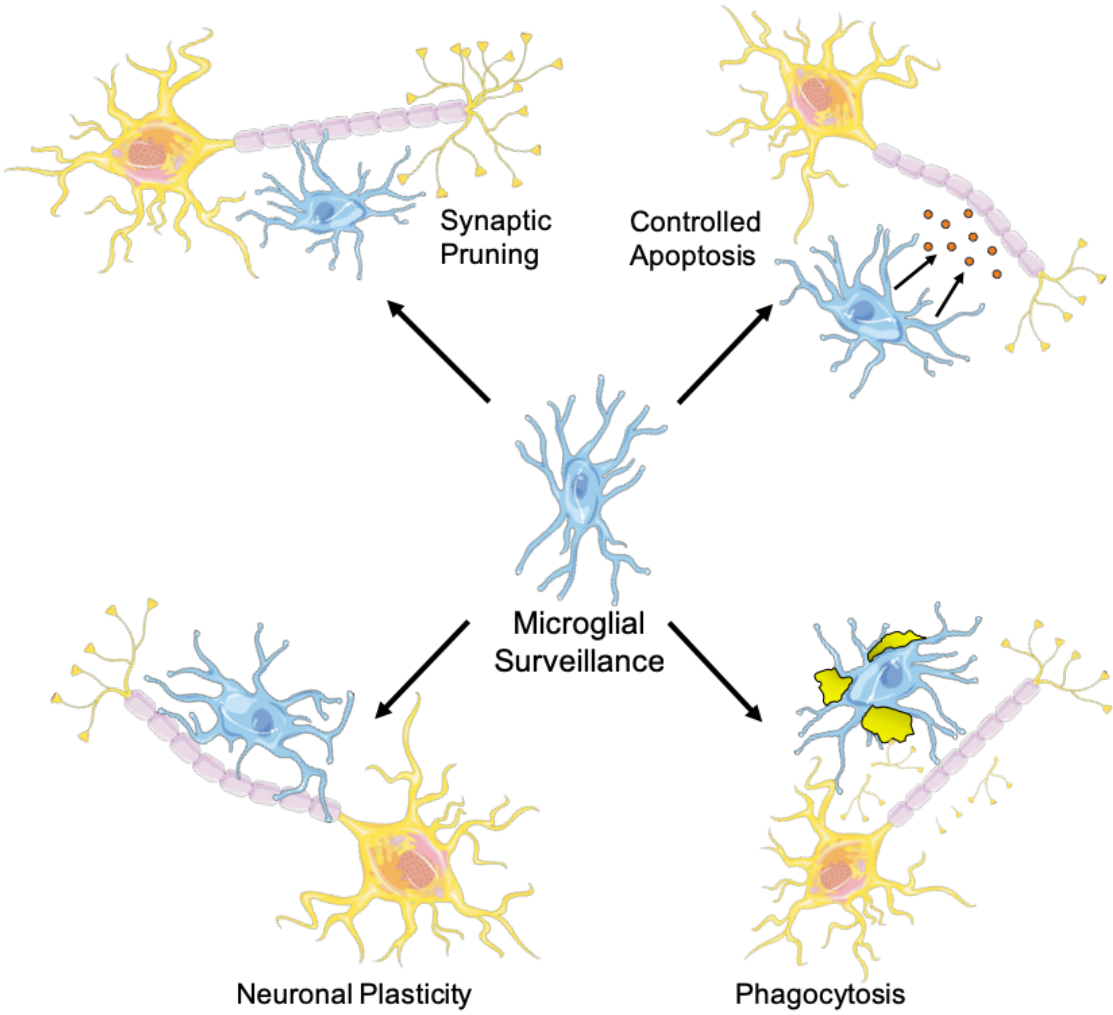

Figure 1.2 Different microglial functions involved in maintaining environmental homeostasis. Microglia have important physiological roles in synaptic pruning during development, alongside regulating neuronal plasticity. Microglia are also important for controlled apoptosis of neurones and other CNS residing cells, alongside removing cellular debris by phagocytosis. Neuroinflammation may disrupt these physiological functions, contributing to disease manifestation and progression.

Microglia express a wide variety of PRRs that detect both PAMP and DAMP signals, including TLRs and NLRs (Bordt and Polster, 2014; Yu and Ye, 2014) alongside scavenger receptors such as MARCO, CD36 and the receptor for advanced glycation end products (RAGE) which enable phagocytosis of apoptotic cells and protein aggregates (Yu and Ye, 2014). Microglial activation usually follows a similar temporal formula as that discussed for macrophage innate immunity (Figure 1.1). In this case, macrophages are often the first line of defence following infection or injury. In injured brain tissue, microglia exist in various states with differing transcriptional profiles (Hammond et al., 2019) but also retain their capacity to shift their phenotype during the course of an inflammatory response (Gobbetti et al., 2014). Following injury or infection, microglia become polarised towards inflammatory phenotypes, releasing a battery of pro-inflammatory cytokines, alongside expressing high levels of inducible nitric oxide synthase (iNOS; Orihuela et al., 2016). This action is targeted towards killing and/or removing the responsible pathogen. Whilst extensively characterised, this is primarily associated with exposure to bacteria-derived products such as LPS (Orihuela et al., 2016).

A sterile inflammatory response is more common in the CNS, often correlated to trauma, chemical exposure, ischaemic-reperfusion injury or neurodegenerative disease (Chamorro et al., 2016; Gyoneva and Ransohoff, 2015; Heneka et al., 2015; McPherson et al., 2014). This is usually associated with the release of a wide range of pro-inflammatory cytokines, chemokines and complement, alongside nitric oxide (NO) and ROS (Heneka et al., 2014b). Moreover, the overall outcome of a pro-inflammatory polarisation event depends on several factors, including the extend of ROS production or activation of NOD-like receptor family pyrin domain-containing 3 (NLRP3) inflammasome (Bordt and Polster, 2014; de Rivero Vaccari et al., 2014). A key component of the innate immune system, the inflammasome is a multiprotein complex which facilitates the activation of caspase-1 and consequential production of pro-inflammatory IL-1β and anti-inflammatory IL-18, a response which appears crucial to activate the full cytokine cascade (de Rivero Vaccari et al., 2014). This pro-inflammatory response can facilitate the death of damaged or diseased neurones, tagging them for apoptotic clearance, but it is also responsible for cognitive impairment in animal models (Chen et al., 2015).

After this initial pro-inflammatory response, microglial phenotype shifts towards inflammatory resolution. During this switch, phagocytosis is employed as the crucial mechanism to facilitate the uptake, degradation and removal of apoptotic cells, cellular debris and protein aggregates, all of which are evident in neurodegenerative disease (Felsky et al., 2019; Ossenkoppele et al., 2016). Many PRRs facilitate this switch during acute inflammation, contributing to the delayed release of pro-resolving cytokines and neurotrophic factors such as IL-10 and TGF-β, consequentially contributing to the reduction of pro-inflammatory mediator release alongside increasing tissue repair (Heneka et al.,

2014b; Lobo-Silva et al., 2016). IL-10 release also protects astrocytes from excessive inflammation alongside promoting neuronal survival, working to limit CNS damage following an inflammatory response (Balasingam and Yong, 1996; Zhou et al., 2009). Hence, some PRRs have a negative feedback system to regulate neuroinflammation. This inflammatory resolution switch helps to facilitate and re-establish homeostasis (Figure 1.3; Chang et al., 2017; McArthur et al., 2010).

1.1.3. Brain metabolism, aging and neuroinflammation

The human brain is unique in terms of its particularly high reliance on glucose utilisation, accounting for approximately 20% of the total glucose consumption of the body (Mergenthaler et al., 2013). This is in spite of the brain only comprising 2% of the typical mass of the human body (Heymsfield et al., 2009; Mink et al., 1981). This may be associated with the fact that the brain doesn't really contain any energy reserves compared to the rest of the body, despite its high-energy consuming nature (Mireille et al., 2011). Thus, the brain is dependent on the uninterrupted supply of energy substrates from the circulation. This explains why diseases which increase the risk of ischaemia, such as atherosclerosis are associated with neurological dysfunction (Moroni et al., 2016).

Interestingly, despite the high energy demand of the brain, aerobic glycolysis – which is considerably less efficient at producing ATP than oxidative phosphorylation – appears to be crucial in modulating neuronal health. Recent studies suggest that aerobic glycolysis is particularly important for synapse formation, synaptic plasticity and learning (Goyal et al., 2014; Shannon et al., 2016). The importance of aerobic glycolysis in brain activity is also supported by nuclear magnetic resonance imaging in various brain regions, identifying that increases in lactate levels correlate with brain activity (Figley and Stroman, 2011; Shulman et al., 1993).

A wide body of evidence shows that neurones can directly use lactate as an energy source (Boumezbeur et al., 2010; Schurr et al., 1997; Serres et al., 2005), even showing a preference for lactate over glucose when both energy substrates are present (Bouzier-Sore et al., 2006). In neurones, aerobic glycolysis and related metabolic pathways may also provide neuroprotection via the synthesis of intermediates which reduce oxidative damage (Mullarky and Cantley, 2015; Nciri et al., 2013). This is particularly pertinent for neurodegenerative disease, as many are associated with oxidative stress (Butterfield et al., 2013; Ma et al., 2017).

The normal aging brain experiences reductions in glucose uptake and thus consequential decreases in metabolism (Goyal et al., 2017). However, effects appear to be primarily driven

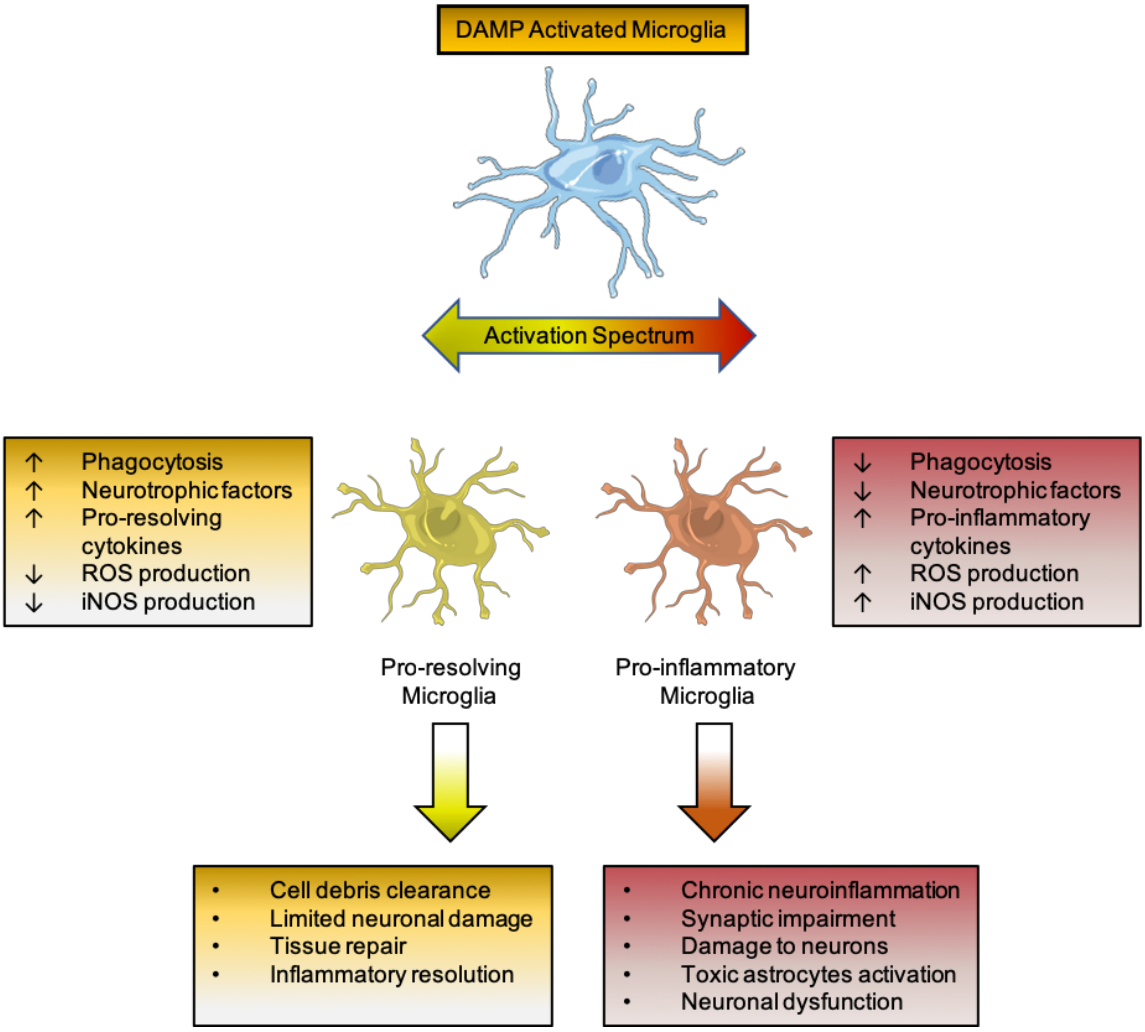

Figure 1.3 Effects of microglial activation within the brain. During sterile inflammation, microglia can be activated by various DAMP signals, including Aβ. In the healthy brain, microglia are responsible for homeostatic maintenance, wherein they removal cellular debris by phagocytosis and secrete neurotrophic factors that support the growth and survival of neurones. Cellular oxidation associated with ROS and nitric oxide production is also limited. In AD, chronic inflammation manifests, contributing to the persistent release of pro-inflammatory cytokines and considerable increase in both ROS production and iNOS synthesis. Alongside reductions in phagocytosis and neurotrophic factor release, these changes lead to synaptic impairment and neuronal damage. Chronically inflamed microglia can also activate neurotoxic astrocytes. Together, these neuroinflammatory changes all contribute to neurodegeneration. Image adapted from Heneka et al., 2014.

by the global loss of aerobic glycolysis within the brain with age (Goyal et al., 2017). As with any other organ, the functional capabilities of the brain decline progressively with aging, eventually manifesting as impairments in learning and memory, cognition and motor coordination, amongst others (Alexander et al., 2012; Dykiert et al., 2012). With a clear reduction in aerobic glycolysis during the aging process, neurones may become more vulnerable to oxidative damage. Aging neurones also accumulate dysfunctional and aggregated proteins alongside damaged mitochondria, which may be a potential consequence of metabolic modulation and oxidative damage (Castelli et al., 2019). Expanding on this, impairment of the electron transport chain alongside mitochondrial enlargement and fragmentation have all been identified in the aging brain (Morozov et al., 2017; Pollard et al., 2016; Stahon et al., 2016). Mitochondrial fragmentation can happen in microglia, whereby this process can propagate microglial inflammation and neuronal death in otherwise healthy neurones (Joshi et al., 2019), highlighting that metabolic dysfunction could be a potential catalyst to trigger neurodegeneration in disease. This process appears occur through inflamed microglial communication with astrocytes (Joshi et al., 2019; Liddelow et al., 2017), emphasising the centrality of the immune system in potentially facilitating neurodegeneration in disease.

1.2. The past, the present, and the future of Alzheimer's disease dementia

Dementia, from the Latin '*demens'*, or '*dement'*, meaning 'out of one's mind', is a chronic disorder of mental processes triggered by injury or disease. Dementia is characterised by symptoms including the impairment of memory and cognition, executive functions such as reasoning, problem solving and attentional control, and changes in personality and emotion. It was first identified in 1906 by the German psychiatrist and neuropathologist Dr. Alois Alzheimer through the behavioural study of a 55-year-old woman, Auguste Deter (Stelzmann et al., 1995), followed by examination of her brain tissue after death. However, Emil Kraepelin, a German psychiatrist who worked with Dr. Alzheimer, was the first to coin "Alzheimer's Disease" (Hippius and Neundörfer, 2003). It wasn't until 1931, following the invention of the electron microscope, that brain cells could be studied in greater resolution and detail (Knoll and Ruska, 1932; Ruska, 1986), facilitating the characterisation of AD. Two core pathological lesions exist in AD, manifesting as extracellular protein deposits in the form of neuritic plaques, now known to consist primarily of 35-45 amino acid β-amyloid (Aβ) peptides (Bergström et al., 2016; Murphy et al., 2010), and intracellular neurofibrillary tangles (NFTs), formed of hyperphosphorylated aggregates of the microtubule-associated protein, tau (Šimić et al., 2016). The importance of the neuritic plaques was revealed in seminal work published in 1968, linking the number of Aβ plaques in the brain and the risk of developing dementia (Blessed et al., 1968). This has been revised more recently, with similar findings (Cummings et al., 1996; Perry et al., 1978), with new emphasis on the role of microglia responding to these accumulating plaques (Sala Frigerio et al., 2019)

AD is the greatest cause of dementia in the aging population, affecting approximately 4% of individuals aged ≥ 65 years of age (Figure 1.4A, Hebert et al., 2013; Prince et al., 2013). As of July 2015, around 12% of the global population of 7.3 billion was over 60, leading to a global disease burden of around 37 million individuals (United Nations, 2015). AD prevalence is expected to rise due to the planet's aging population, with the numbers of AD sufferers expected to increase to around 78 million by 2050 (Prince et al., 2015). This is due to increasing age being the primary risk factor for AD (Guerreiro and Bras, 2015). Some recent evidence disputes this, because the number of people in Europe and the United States living with dementia appears to be reaching a plateau (Wu et al., 2017; Wu et al., 2015), potentially due to improved education, and declines in chronic disorders such as heart disease, stroke, and hypertension. Despite this, in comparison to most diseases, where death rates have steadily decreased in recent history, death associated with AD continues to rise (Figure 1.4B; James et al., 2014; Murphy et al., 2013; Lehman et al., 2012). This statistic helps underline dementia and AD as a public health priority.

Development of AD imposes a substantial physiological, psychological and economic burden on patients, their families, and the health care system. On average, AD patients live for 7 to 10 years following diagnosis. This can fluctuate significantly between individuals, with age at diagnosis having a large impact on life expectancy (Figure 1.4C) alongside clinical symptom manifestation rate. Regardless, in the UK the overall economic impact of AD and the other dementias is approximately £26 billion per annum (Figure 1.4D), with an approximate annual cost of £32,000 per patient (Prince et al., 2014). Emphasising this, a recent National Institutes of Health study identified that the average total health care costs for patients with dementia in the last 5 years of life were significantly greater than those who died from cancer or heart disease (Figures 1.4E and 1.4F) (Kelley et al., 2015).

Despite having been first identified over a century ago, there is still no effective therapy to slow down or halt the progressive nature of AD. There are symptomatic treatments clinically available (see Section 1.5), but these are not permanent solutions. Clinically available drugs tackle excitotoxicity (Mehta et al., 2013; Olney and Sharpe, 1969), whilst others can be utilised to inhibit the breakdown of acetylcholine (ACh), the primary neurotransmitter associated with memory (Croxson et al., 2012; Giovannini et al., 2015; Micheau and Marighetto, 2011). However, none of these slow the progression of disease. Further, as AD progresses, the exacerbation and expansion of neurodegenerative damage and a hostile extracellular environment likely lead to a lack of efficacy for these drugs in later disease stages.

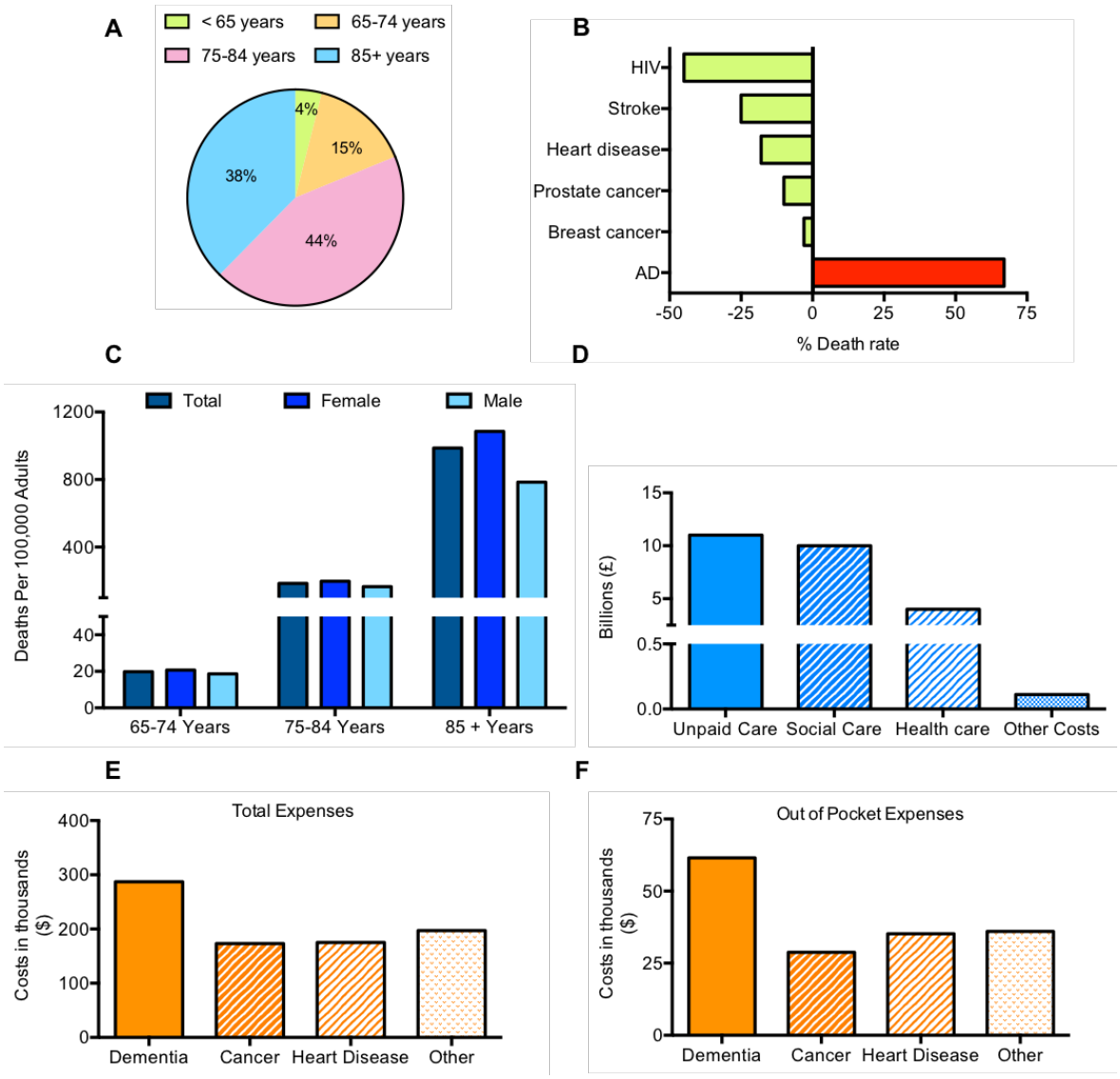

Figure 1.4 Dementia and Alzheimer's disease statistics in the UK and USA. A; Proportion of people with AD in the United States, grouped by age. Data collected from Hebert et al., 2013. **B**; Estimated percentage change in death rate of several diseases in the USA over a 10-year period (2000-10). Data collected from Murphy et al., 2013 and the National Centre for Health Statistics. **C**; Deaths in the USA in 2010 due to AD* per 100,000 adults over the age of 64. **Deaths where AD is listed as underlying cause*. Data obtained from the National Centre for Health Statistics. **D**; Estimated breakdown of dementia costs in the UK, 2013. Adapted from Prince et al., 2014. **E**; Average total expenses per decedent of dementia in the final 5 years of life. Data obtained from Kelley et al., 2015. **F**; Average out of pocket expenses per decedent of dementia in the final 5 years of life. Spending is as a proportion of household wealth. Data obtained from Kelley et al., 2015.

1.3. The pathology of Alzheimer's disease

The neurodegeneration that occurs in AD is multifactorial, with glutamatergic excitotoxicity, oxidative stress, and inflammation all contributing to neuronal death (Figure 1.5, Swaminathan and Jicha, 2014). The multifaceted and multicellular nature of the disease has been widely recognized in recent years (Bouvier and Murai, 2015; Di Scala et al., 2014; Guerrero-Muñoz et al., 2015; Talbot et al., 2012), with abnormal interactions between microglia, astrocytes and neurones highlighted as a core component in this proteinopathic neurodegenerative disorder (Goetzl and Miller, 2017).

These pathological processes and interactions are thought to sequentially contribute to the initial loss of neurones within the entorhinal cortex, before spreading to the hippocampus and frontal cortical regions. Neuronal loss leads to cognitive impairment and memory deficits seen in AD (Chen et al., 2016; Thomsen et al., 2016). As the disease progresses, there is a far greater gross loss of multiple neurones subtypes, leading to an overt reduction of brain volume. However, AD may more closely correlate with the enlargement of the ventricles, rather than the loss of brain tissue per se (Erten-Lyons et al., 2013).

Our understanding of end-stage AD pathology is relative good, but the root cause(s) of the condition remain obscure. Understanding the core pathologies of AD and their contribution to disease may be the first step in discovering ways to suppress damage, and successfully treat this condition.

1.3.1. Amyloid beta

1.3.1.1. Amyloid precursor protein processing and amyloid beta production

The amyloid precursor protein (*APP*) gene has been studied extensively since the link between Aβ production and AD was identified. The gene encodes for the integral membrane APP protein which is expressed in many cell types within the CNS, including neurones (Zhang et al., 2012; Zhang et al., 2011), where it is concentrated at the synapse (Pliássova et al., 2015). It appears to have physiological roles in synaptic plasticity and axonal outgrowth alongside others which are involved in the regulation of neuronal health (Müller et al., 2017). However, APP can be proteolytically cleaved, resulting in the production of both amyloidogenic and non-amyloidogenic peptides, depending on the nature of sequential secretase cleavage. γ-secretase can cleave APP at differing positions, resulting in the production of peptides of various length (Aβ37, Aβ38, Aβ40 and Aβ42). Whilst there are several proteases which have α- and γ-secretase activity, BACE1 is the primary β-secretase (Figure 1.6).

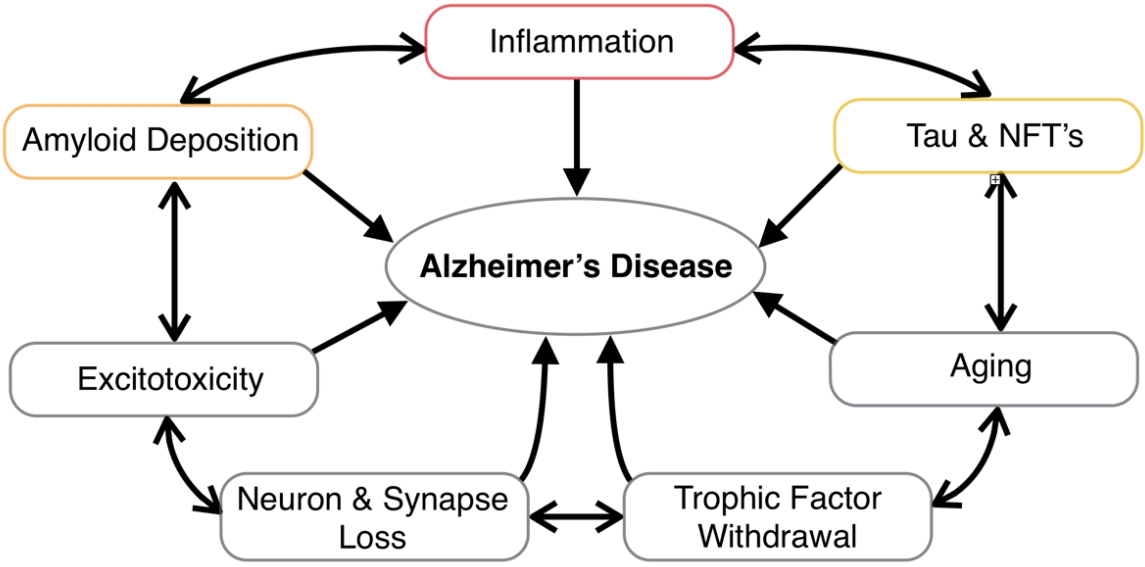

Figure 1.5 Cellular processes and pathways linked to Alzheimer's disease. These processes are likely to be additive, which is indicated by the double-headed arrows in a circular fashion. Amyloid deposition, tau hyperphosphorylation, and inflammation are three key pathologies of AD, each of which will be looked at in significant detail in Sections 1.3 and 1.4. NFT's; neurofibrillary tangles.

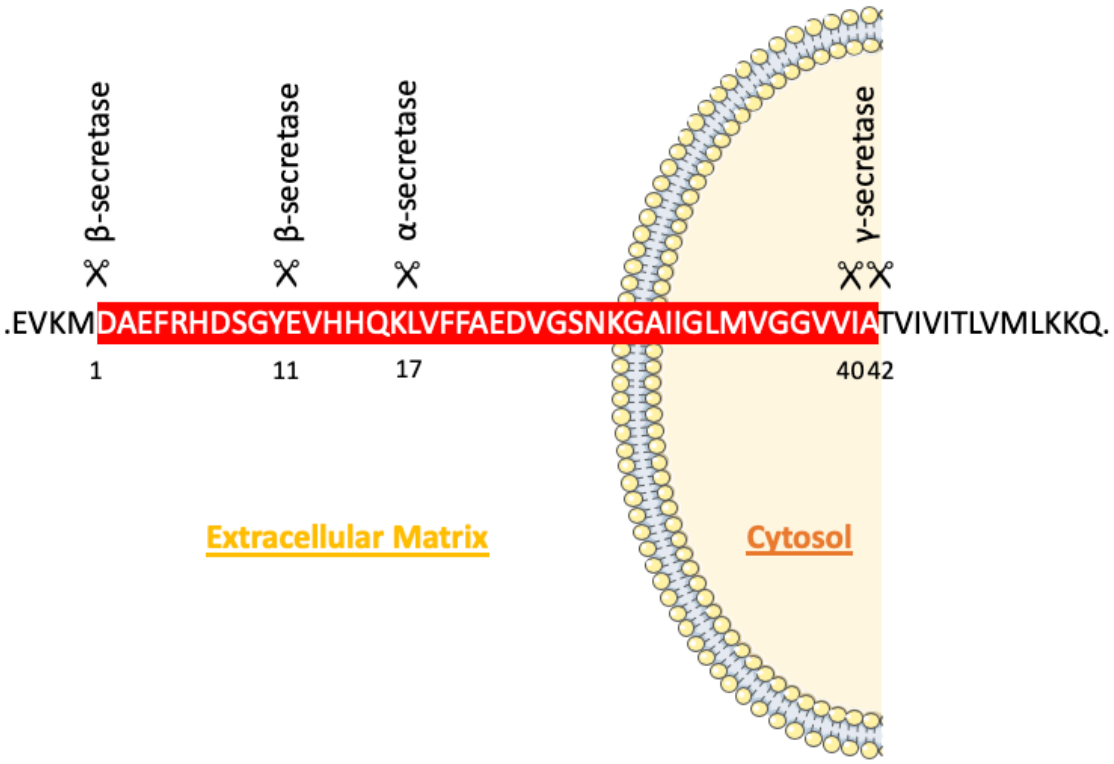

Figure 1.6 The proteolytic cleavage of APP. The APP family of proteins have a large, biologically active N-terminal ectodomain, along with a smaller C-terminus. Cleavage can occur through non-amyloidogenic means, where APP is successively cleaved by α-secretases (such as ADAM10 and ADAM17) and γ-secretase. However, cleavage can also occur through amyloidogenic means, where β-secretase (primarily BACE1) & γ-secretase cleave APP.

Several members of the disintegrin and metalloproteinase (ADAM) family exert α-secretase activity, including ADAM9, ADAM10 & ADAM17 (Colombo et al., 2013; Lericheet al., 2016; Marolda et al., 2012; Postina, 2012; Vingtdeux and Marambaud, 2012). Similarly, BACE1 is a transmembrane protease present at relatively high levels in neurones (Zhang et al., 2011), acting as the catalyst for the first step in the liberation of Aβ from APP (Vassar et al., 1999). Downregulation of BACE1 leads to the inhibition of cleavage at the two known β-cleavage sites on APP: Asp1 & Glu11 (Figure 1.6). Further, BACE1 KO mice do not produce detectable levels of Aβ (Kobayashi et al., 2008; Luo et al., 2001), and BACE1 expression alongside its activity increases in brain regions affected in AD (Johnston et al., 2005; Yang et al., 2003). The intramembrane γ-secretase protease complex is responsible for cleaving a range of transmembrane proteins including APP (Hong et al., 2017; Wang et al., 2015). It consists of four components, two of which are presenilin 1 and 2 (PSEN1/PSEN2; De Strooper et al., 2012; Zhang et al., 2014), with PSEN1/PSEN2 thought to be the primary regulator of APP processing by γ-secretase (Bai et al., 2015).

In non-amyloidogenic APP processing, APP is sequentially cleaved by α-secretase and γ-secretase. Upon α-cleavage, a large extracellular domain is released (soluble α-APP; sAPPα) through a process coined ectodomain shedding (Klevanski et al., 2015; Lichtenthaler, 2006). The α-secretase cleavage site lies within the Aβ domain, thus cleavage here prevents Aβ generation (Postina, 2008). Once ectodomain cleavage occurs, the C-fragment remains associated with the membrane, before being further cleaved by γ-secretase. In amyloidogenic processing, APP is first cleaved by BACE1 in place of α-secretase. The cleavage site for BACE1, unlike α-secretase, is not present within the Aβ domain, keeping the peptide sequence intact. Cleavage of APP by BACE1 is often noted as the rate-limiting step for the production of Aβ (Das et al., 2016). This shift in processing releases sAPPβ, which shares the same sequence as sAPPα, excluding the last few C-terminal amino acids (Chasseigneaux and Allinquant, 2012).

Aβ peptides are produced in large amounts in AD, but previous research proposed that low concentrations (picomolar) of monomeric Aβ could act as a trophic signal, alongside modulating synaptic plasticity (Puzzo et al., 2008). This therefore has implications for learning and memory (Pearson and Peers, 2006; Plant et al., 2003). However, monomeric Aβ readily and rapidly aggregates to form oligomers, protofibrils and fibrils en route to plaque deposition (Figure 1.7). The most harmful species of Aβ produced by sequential β and γ-secretase cleavage are $A\beta_{1-40}$ and $A\beta_{1-42}$ (Figure 1.8, Butterfield et al., 2013), with the latter said to be the more toxic. This is based on the observation that $A\beta_{1-42}$ peptides increase in cells expressing APP or presenilin harbouring mutations associated with early onset AD (EOAD; Benilova et al., 2012).

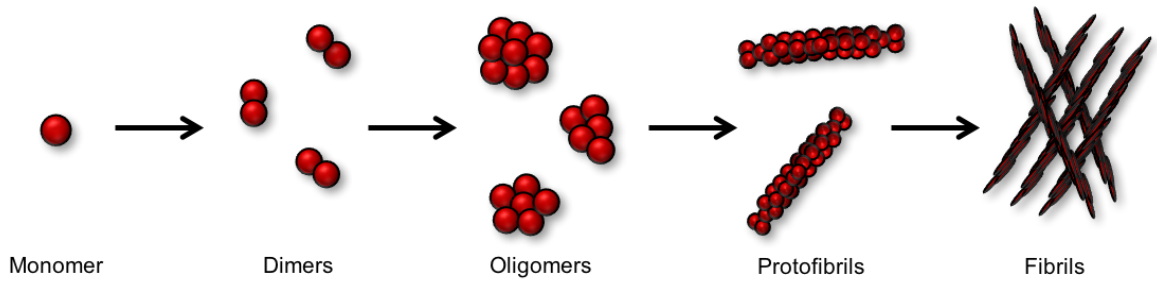

Figure 1.7 The sequential steps in aggregation of Aβ peptides. Native monomeric forms of Aβ of varying sizes initiate the process. Dimers and trimers can assemble before heavier oligomers are formed. These can range from tetramers to nonamers and beyond. Protofibrils form through the elongated cluster of Aβ oligomers. These in turn aggregate in a mesh-type pattern to form amyloid fibrils, the core component of senile plaques.

A

$A\beta_{1-40/1-42}$

H_2N-Asp[1]-Ala[2]-Glu[3]-Phe[4]-Arg[5]-His[6]-Asp[7]-Ser[8]-Gly[9]-Tyr[10]-Glu[11]-Val[12]-His[13]-His[14]-Gln[15]-Lys[16]-Leu[17]-Val[18]-Phe[19]-Phe[20]-Ala[21]-Glu[22]-Asp[23]-Val[24]-Gly[25]-Ser[26]-Asn[27]-Lys[28]-Gly[29]-Ala[30]-Ile[31]-Ile[32]-Gly[33]-Leu[34]-Met[35]-Val[36]-Gly[37]-Gly[38]-Val[39]-Val[40]-Ile[41]-Ala[42]-COOH

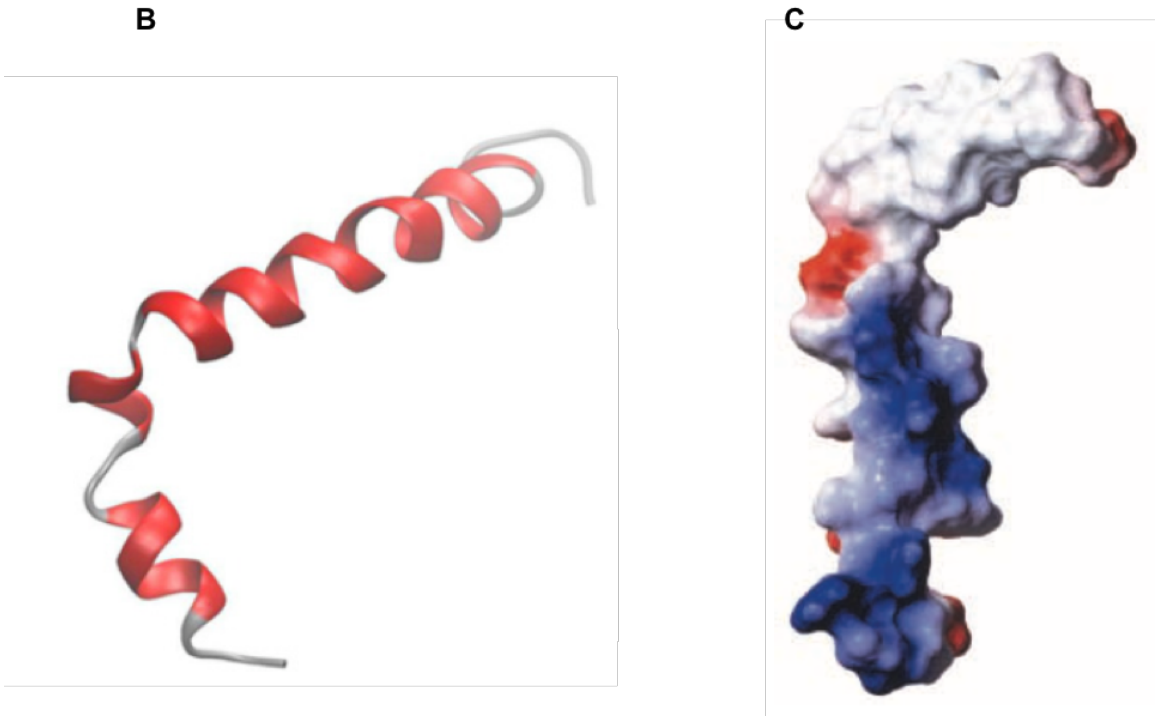

Figure 1.8 The amino acid sequence and proposed structure of $A\beta_{1-42}$. **A**; the full amino acid sequence of $A\beta_{1-42}$. If you remove the final two amino acids (isoleucine and alanine, in red), this is the amino acid sequence of $A\beta_{1-40}$. **B**; The structure of the $A\beta_{1-42}$ monomer in a non-polar microenvironment. **C**; This is the contact surface representation of the lowest energy conformation of $A\beta_{1-42}$, in terms of electrostatic potential. This representation shows a large electropositive region (blue) within the first of two alpha-helices. Interestingly, if you align this helix to face the phospholipids of the cell membrane, it results in the second alpha-helix orientated as such that it can be inserted into the membrane. Data acquired from Crescenzi et al., 2002; Zhang-Haagen et al., 2016.

Oligomers are held together non-covalently, and their formation is likely to occur due to the amphiphilic nature of Aβ peptides. Initially thought to remain static and stable (like plaques), the possibility exists that oligomers are dynamic, perhaps in a form of equilibrium with Aβ monomers and other aggregate formulations (Benilova et al., 2012). The questioning of oligomer stability is supported by the identification of a wide array of differing oligomeric Aβ (oAβ) forms, including dimers (Shankar et al., 2008), tetrameters (Bernstein et al., 2009), nonamers and dodecamers (Lesné et al., 2006). These oligomers appear to be intermediates in fibril formation, whereby their shape is modified before the transition occurs, but the nature and mechanism of the structural transition is unknown (Fu et al., 2015; Lee et al., 2011; Lomakin et al., 1997; Sabaté and Estelrich, 2005).

1.3.1.2. Amyloid beta: plaques or oligomers?

First purified in the 1980s (Palutke et al., 1987), the cardinal neuropathological feature of AD is the presence of extracellular proteinaceous Aβ plaques. Until more recently, insoluble fibrillary plaques consisting of Aβ were considered the toxic moiety, contributing to neuronal death and gross pathology seen in AD (Farrell et al., 2017; Hanna et al., 2012). As mentioned in Section 1.2, increased plaque number has been associated with an increased risk of developing AD. However, this increase in plaque number will likely correlate with the increased numbers of varying structural forms of Aβ, confounding interpretation of which species holds the highest toxicity.

oAβ also displays neuronal toxicity, and has been suggested to be a central contributor towards neuronal damage rather than accumulated insoluble extracellular aggregates which were initially suggested (Tomiyama et al., 2010; Walsh et al., 2002). Moreover, oAβ but not total plaque burden may correlate more closely with neuronal loss and the astrocytic inflammatory response in murine AD models (DaRocha-Souto et al., 2011).

Accumulation of Aβ from oligomers into plaques may act as an endogenous reservoir, sequestering oAβ and providing a defence mechanism to protect neurones against oAβ-induced damage (Treusch et al., 2009; Yang et al., 2017). Whether oligomers could dissociate from plaques, reversing this protection is unknown, but plaques are neither wholly benign or harmless, with evidence supporting their involvement in the pathological conversion of tau (Li et al., 2016), contributing towards its phosphorylation (Busciglio et al., 1995; Oliveira et al., 2015). This could be a priming step in the development of NFTs. The complexities associated with the disease are evident, and the role of Aβ in the pathophysiology of AD is not fully understood. However, the amyloid cascade hypothesis was previously proposed as the central pathogenic pathway for AD development.

1.3.1.3. The amyloid cascade

The amyloid cascade hypothesis, originally proposed in 1992 (Hardy and Higgins, 1992), states that Aβ production is the initial trigger in the manifestation of AD pathology, consequently leading to the clinical symptoms observed (Figure 1.9). The authors expanded, labelling Aβ as the causative agent for the disease process, with NFT formation, vascular damage and cell loss all being consequential of Aβ accumulation. This hypothesis has been the basis for most work surrounding the pathogenesis of AD for many years. Yet, it was developed from studies of familial AD, which are caused by mutations in either APP or the presenilin genes. In sporadic late-onset AD (LOAD), Aβ is not necessarily the causative agent, with patients still dying due to cognitive related decline following Aβ-antibody targeted immunotherapy, despite the removal of plaque pathology (Holmes et al., 2008). Thus, Aβ is unlikely to be the only important pathological target for AD. This holds true when comparing the initial localisation of amyloid pathology and neuronal death. Studies by Braak and others identified that Aβ pathology appears to begin in the cortex before spreading inwards; a progression which is opposite of that for tau (Braak and Braak, 1991). Further, neuronal death initially and more readily occurs within the entorhinal cortex and hippocampus, two brain regions with relatively few plaques when compared to regions such as the praecuneus and frontal lobes (Braak and Braak, 1991; Serrano-Pozo et al., 2011).

This does not mean that the amyloid hypothesis wrong. It can be clearly seen in EOAD that genetic mutations which result in Aβ production and accumulation lead to AD. However, with regards to LOAD, a more complicated pathway is likely to be responsible for disease development. Nevertheless, the hypothesis has come under criticism, with the key argument against it based on the poor anatomical and temporal correlation between plaque deposition, neuronal loss, and the clinical symptoms of AD. With suggestions that Aβ is simply a “bystander”, several researchers propose that tau pathology, which strongly correlates with neurone loss and clinical symptoms (Di et al., 2016; Liu et al., 2017), should be the primary target of AD research. If this were the case, it could be assumed that in EOAD, whereby Aβ accumulation is directly caused by mutations in either *APP* or *PSEN1/PSEN2*, its deposition would have a stronger anatomical correlation to neurone loss, when compared to late stage AD. However, this does not happen. Instead, Aβ pathology closely resembles that seen in sporadic AD, with plaques anatomically dissociated from brain areas with extensive neuronal loss (Bateman et al., 2012; Shepherd et al., 2009). Additionally, positron emission tomography (PET) imaging of tau using flortaucipir F 18 identified increased hyperphosphorylated tau in EOAD patients (Quiroz et al., 2018). Thus, genetic data suggests that Aβ accumulation can drive tau pathology without the two protein aggregates necessarily being anatomically co-localised.

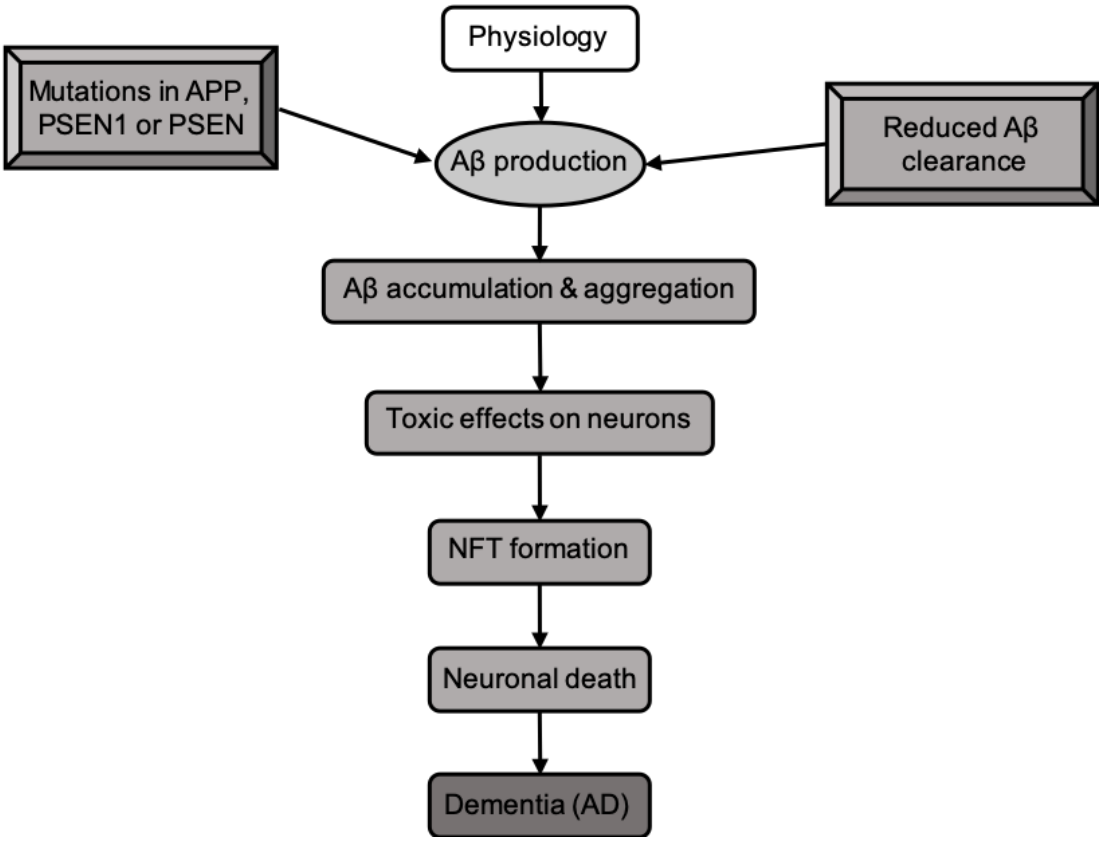

Figure 1.9 Diagrammatic representation of the amyloid cascade hypothesis. Research into EOAD identifies the importance of mutations in the *APP*, *PSEN1* and *PSEN2* genes for Aβ accumulation. Reduced clearance of Aβ due to damaged degradation and removal mechanisms likely contributes to Aβ aggregation. However, in LOAD, there is likely much more at play than Aβ alone. Aβ, amyloid beta; APP, amyloid precursor protein gene; PSEN1, presenilin 1 gene; PSEN2, presenilin 2 gene.

This anatomical disconnection linking amyloid and tau pathology to neurone loss is yet to be fully elucidated. It is likely that Aβ is necessary but not sufficient to cause AD, with evidence supporting the complex nature of neuronal damage and synapse loss in the disease process (Drachman, 2014; Herrup, 2015; Musiek and Holtzman, 2015). However, there are multiple toxic mechanisms that Aβ accumulation can utilise to facilitate neuronal damage.

1.3.1.4. Amyloid beta toxicity

Whilst the full extent of Aβ toxicity has not yet been elucidated, many pathological actions have been identified including oxidative stress (Li et al., 2017; Ojala and Sutinen, 2017), mitochondrial cytochrome C (Cyt C) & Ca^{2+} diffusion (Kim et al., 2014; SanMartín et al., 2017), loss of membrane integrity and membrane damage (Fernandez-Perez et al., 2016; Sepulveda et al., 2010) and its association with neuroinflammation (Li et al., 2017; Salminen et al., 2009; Yin et al., 2017), synaptic dysfunction (Müller-Schiffmann et al., 2016; Ripoli et al., 2014) and excitotoxicity (Pallo et al., 2016; Sáez-Orellana et al., 2016).

1.3.1.4.1. Amyloid beta and oxidative stress

The initial response of microglia to pathological forms of Aβ appears to be an oxidative stress response, well known to be a prominent and significant feature in many, if not all neurodegenerative diseases (Chiurchiù et al., 2016; Della Bianca et al., 1999; Leszek et al., 2016; Urrutia et al., 2017; Wilkinson et al., 2012). Oxidative damage to DNA, proteins and lipids occurs under basal conditions (Barone et al., 2012). However, cells have endogenous defence mechanisms which repair and replace damaged macromolecules (Andrews et al., 2014; Chondrogianni et al., 2014). Oxidative stress occurs when an imbalance arises between ROS formation and cellular antioxidant ability, due to either increased ROS generation, or a reduction in antioxidant pathways (Valko et al., 2007). The brain is vulnerable to ROS induced oxidative damage due to two reasons. Firstly, neuronal membranes are rich in polyunsaturated fatty acids, which are especially vulnerable to free radical damage (Chen et al., 2008). Secondly, despite the brain only representing approximately 2% of total body weight, it receives 15% of the cardiac output, and 20% total body oxygen (Jain et al., 2010). The resulting large O_2 consumption leads to high levels of ROS compared to other parts of the body.

Whilst not essential, the toxicity of Aβ is partly mediated through the interaction with Cu^{2+} and Fe^{3+} ions (Bush and Tanzi, 2008; Huang et al., 1999; Opazo et al., 2002). The oligomeric Aβ complex produced in the presence of Cu^{2+} and Fe^{3+} can generate hydrogen peroxide (H_2O_2) from molecular oxygen (O_2) through the reduction of Cu^{2+} to Cu^{+} and Fe^{3+} to Fe^{2+}. Yet, the presence of these ions is not essential for Aβ to produce H_2O_2. This is due

to Aβ (4 μM) increasing NADPH oxidase activation and protein in BV-2 microglia (Yao et al., 2015). This enzyme produces superoxide ($O^{\cdot -}_2$) radicals which can undergo reactions to generate additional ROS species, including H_2O_2. Further, ROS species such as H_2O_2 are known to trigger the nuclear translocation of the transcription factor NF-κB (Hara-Chikuma et al., 2015; Henríquez-Olguín et al., 2015), a central component for the microglial inflammatory response (Bordt and Polster, 2014; Kirkley et al., 2017; Taetzsch et al., 2015). NADPH oxidase enzymes, including microglial NOX2 are activated by Aβ (Della Bianca et al., 1999; Wilkinson et al., 2012), which in turn upregulates NF-κB activity (Fan et al., 2017; Vara et al., 2018). Activation of NADPH oxidase enzymes also appear to be crucial for astrogliosis and cortical neurone apoptosis (Qin et al., 2002; Wyssenbach et al., 2016), with microglia being prime cellular candidates responsible (Choi et al., 2012; Fischer et al., 2012; Floden et al., 2005). Microglial activation associated with Aβ-induced ROS production may therefore be a central component in developing the chronic neuroinflammatory environment observed in AD (Heneka et al., 2015).

In the absence of sufficient antioxidative defence mechanisms, H_2O_2 can further react with the reduced Cu^{+} and Fe^{2+} ions to produce the highly reactive and toxic hydroxyl radicals ($OH^{\cdot}$) through the Fenton reaction or via reaction with nitric oxide (NO), the latter forming peroxynitrite ($ONOO^{\cdot -}$). As with most ROS species, $OH^{\cdot}$ is highly-mobile and water soluble, reacting with a vast array of cellular components, including DNA, proteins and membranous lipids, resulting in DNA fragmentation, inhibition of DNA and protein synthesis but also blockage of mitochondrial respiration (Figure 1.10; Halliwell and Gutteridge, 1992), with $OH^{\cdot}$ accumulation leading to cell death (Shoeb et al., 2014). Microglial activation of NADPH oxidase may therefore have considerable consequences not only for microglial inflammation, but also neuronal damage and death associated with multiple different oxidative species (Haslund-Vinding et al., 2017).

Lipid peroxidation results in the production highly reactive 4-hydroxy-2-nonenal (4-HNE) and malondialdehyde (MDA), the latter of which can activate the immune response and RAGE (Aldini et al., 2013; Vistoli et al., 2013), with RAGE itself being an inflammatory intermediary (Sanders et al., 2017) and inducer of oxidative stress (Hong et al., 2016). Aβ can also activate microglial expressed RAGE, increasing oxidative stress, pro-inflammatory cytokine production and further Aβ accumulation (Bierhaus et al., 2001; Kierdorf and Fritz, 2013; Tóbon-Velasco et al., 2014), with RAGE overexpression exaggerating the neuroinflammatory response in mice (Fang et al., 2010). This underlines that neuronal Aβ production can stimulate microglial activation and ROS production via a variety of different sources, including NADPH oxidase and RAGE, which could consequentially drive a positive feedback system to increase Aβ accumulation. RAGE is also an important transporter in regulating Aβ influx from the circulation into the brain (Cai et al., 2016). It is no surprise then, that advanced lipid peroxidation end products (ALEs) such as MDA are associated

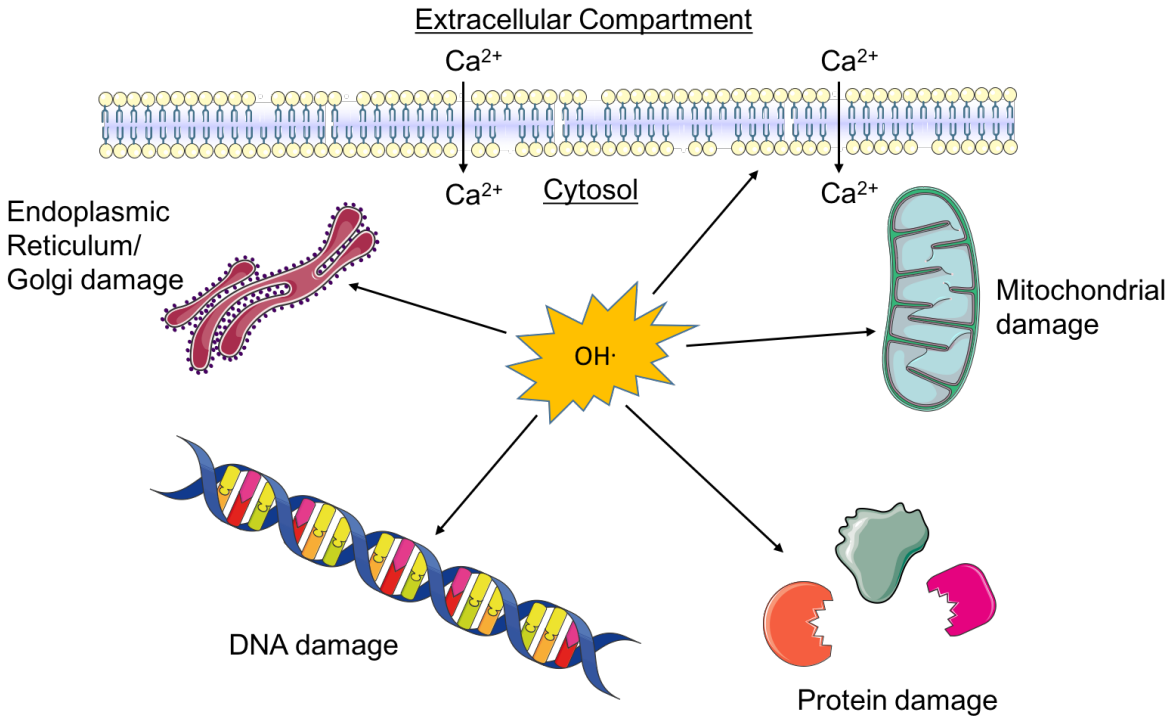

Figure 1.10 Hydroxyl radicals induce macromolecular damage. These radicals can damage all manner of cellular components, from DNA, to mitochondria, and to proteins. Further, free radical-induced lipid peroxidation leads to the damage and increased permeability of cellular membranes, allowing amplified Ca^{2+} influx. This results in the disruption of cellular Ca^{2+} homeostasis, which has particular significance for neurones, because it can contribute towards excitotoxicity in those of a glutamatergic subtype.

with AD (López et al., 2013).

1.3.1.4.2. Amyloid beta and mitochondrial dysfunction

Aβ-induced disruption of cytosolic Ca^{2+} signalling can lead to mitochondrial permeability transition (MPT) pore formation (Figure 1.11, Elkamhawy et al., 2017; Sun et al., 2014; Ye et al., 2015) This can result in severe mitochondrial dysfunction, leading to ROS overproduction, mitochondrial respiratory cessation and the release of pro-apoptotic factors, all contributing to cell death (Du and Yan, 2010). ROS induced-lipid peroxidation might also contribute, with 4-HNE triggering MPT pore opening in cortical neurones (Figure 1.11; Choi et al., 2013).

Aβ can accumulate within the mitochondrial matrix (Hansson Petersen et al., 2008; Muirhead et al., 2010; Pinho et al., 2014; Rosales-Corral et al., 2012), where it binds to amyloid-β alcohol dehydrogenase, (ABAD; Borger et al., 2013; Takuma et al., 2005; Yan and Stern, 2005; Yao et al., 2011), an enzyme which exhibits important metabolic functions. This includes sequestering cyclophilin D (CycD) in the mitochondrial matrix (Figure 1.11), preventing CycD to regulate opening of the MPT pore (Gutiérrez-Aguilar and Baines, 2015; Naga et al., 2007; Yan and Stern, 2005). Interaction of ABAD-Aβ appears to displace CycD, leading to its translocation to the inner mitochondrial membrane, triggering its involvement in opening of the MPT pore. This is of particular importance, because microglial oxidative phosphorylation is reduced during an inflammatory response (Orihuela et al., 2016), holding promise that ABAD-Aβ interactions in microglia may, in part, correlate with neuroinflammation.

Increased intracellular Ca^{2+}, $^{\cdot}OH$, and Aβ levels in AD can all converge to trigger mitochondrial dysfunction and damage, with increased mitochondrial permeability and consequential abolishment of the mitochondrial membrane potential (Δψ) linked to both apoptotic and necrotic cell death pathways (Barnwal et al., 2016; Ni et al., 2014; Vessoni et al., 2016). Reduced Δψ in macrophages also appears to be associated with increased mitochondrial ROS production and inflammatory activation (Yaron et al., 2015), suggesting a similar response is likely in microglia, further implicating Aβ in their activation and consequent inflammatory response.

1.3.1.4.3. Amyloid beta and excitotoxicity

Aβ appears to propagate several mechanisms which can lead to neuronal dysfunction and apoptosis. One of which is binding to and inhibiting neuronal α7 nicotinic acetylcholine receptors (α7-nAChRs), which are critical for cognition and long-term memory

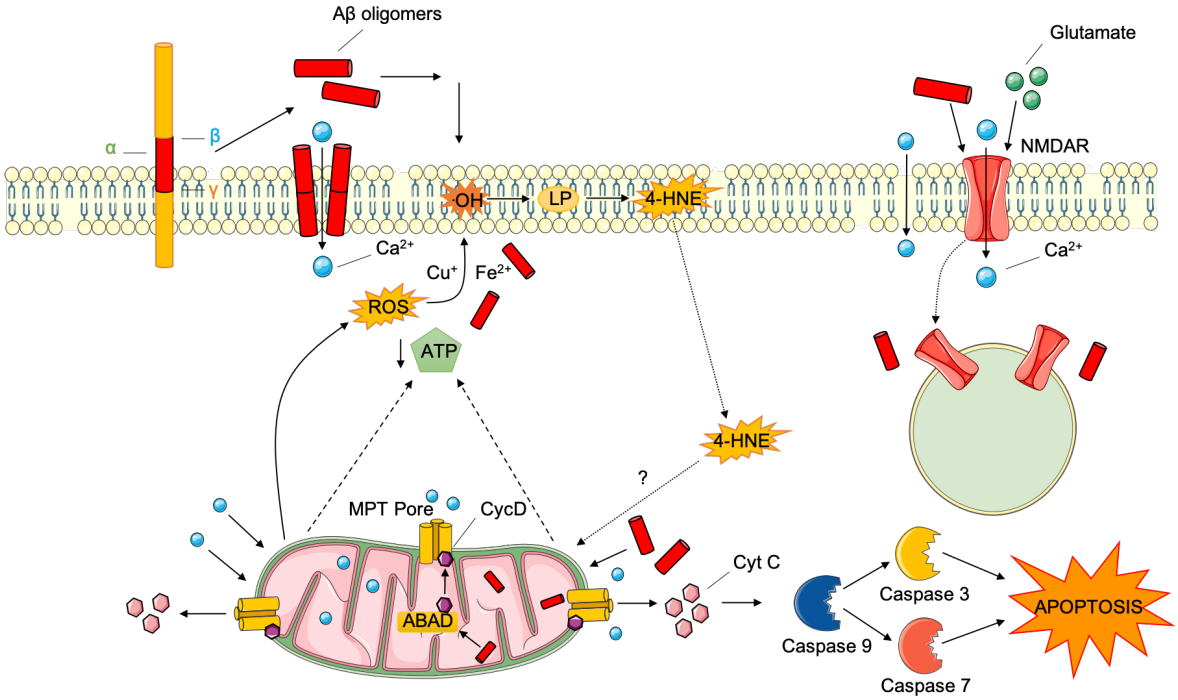

Figure 1.11 Summary diagram depicting several cellular processes contributing to neuronal apoptosis in response to Aβ oligomer formation and accumulation. 4-HNE has been identified to open the MPT pore in cortical neurones *in vitro*, in the presence of NMDA. However, whether this occurs *in vivo* needs to be determined. Excess glutamate release which is seen in AD could substitute for the NMDA. Mitochondrial ROS production can contribute towards lipid peroxidation and further mitochondrial damage. Microglial ROS production can also lead to neuronal plasma membrane peroxidation, leading to increased Ca^{2+} influx, which could result in opening of the MPT pore and mitochondrial release of cytochrome C, leading to caspase activation and neuronal apoptosis. ABAD, amyloid-β alcohol dehydrogenase; ATP, adenosine triphosphate; Cyt C, cytochrome C; CycD, cyclophilin D; 4-HNE, 4-hydroxy-2-nonenal; LP, lipid peroxidation; MPT, mitochondrial permeability transition; NMDAR, N-methyl-D-aspartate receptor.

(Albuquerque et al., 2009; Liu et al., 2001; Ni et al., 2013; Oz et al., 2013). Also vital for cognition are NMDARs, with roles in synaptic plasticity and long-term potentiation (LTP; Niciu et al., 2012), the persistent and long-lasting strengthening of synapses as a result of high frequency stimulation (Bliss and Lomo, 1973). They are receptors for glutamate, a neurotransmitter responsible for around 70% of the excitatory neurotransmission that occurs in the CNS. As previously discussed, Aβ can reduce the surface expression of NMDARs through direct interaction and consequential endocytosis (Tang, 2009). Aβ oligomers have also been shown to directly activate these receptors (Texidó et al., 2011). As Aβ continues to accumulate, Aβ-induced NMDA activation may contribute to excitotoxicity (Figure 1.12; Vandresen-Filho et al., 2013; Wang et al., 2013).

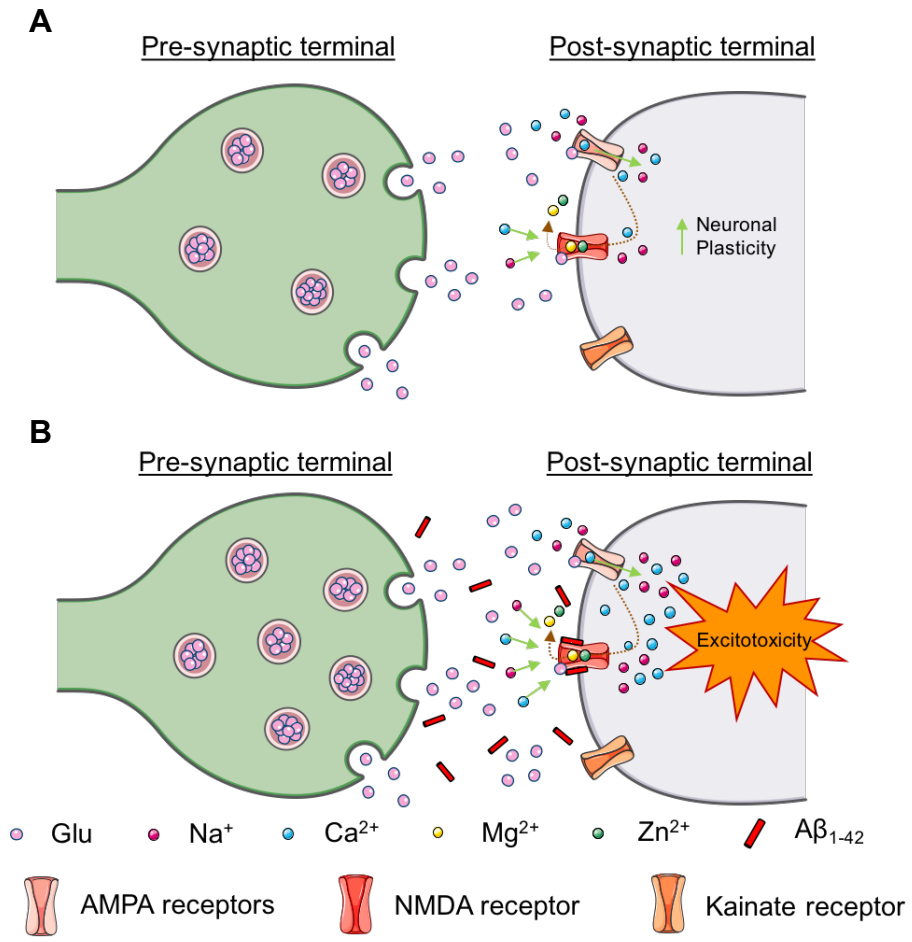

Figure 1.12 A simplified representation of neurotransmitter signalling at the glutamatergic synapse. A; Under physiological conditions, excitation of the presynaptic neurone results in the release of glutamate. Glutamate binds to AMPA and NMDA receptors, initiating Na^+ and Ca^{2+} influx, leading to the synthesis of brain derived neurotrophic factor (BDNF; not shown), and the upregulation of neuronal plasticity. **B**; In late stage AD, Aβ oligomer accumulation and excessive extracellular glutamate (mainly resulting from neuronal death) have been linked to overactivation of AMPA and NMDA receptors, leading to Ca^{2+}-induced excitotoxicity. $Aβ_{1-42}$, amyloid-beta 42 peptide; AMPA, α-amino-3-hydroxy-5-methyl-4-isoxazolepropionic acid; Glu, glutamate; NMDA, N-methyl-D-aspartate.

1.3.2. Tau hyperphosphorylation

Alongside extracellular Aβ plaques, the second major neuropathological feature of AD is the presence of intraneuronal inclusions, so-called NFTs. These are formed by paired helical filaments of hyperphosphorylated tau proteins. Tau is abundant in CNS neurones, primarily localised in axons (Morris et al., 2011) and has a physiological role in stabilising microtubules, a component of the eukaryotic cytoskeleton. However, phosphorylation of tau results in its detachment from the cytoskeletal filament. In certain conditions such as AD, tau can become hyperphosphorylated (Quiroz et al., 2018), and this could therefore lead to mass detachment of the protein from microtubules, leading to decreased cytoskeletal stability and neuronal damage (Di et al., 2016; Spires-Jones and Hyman, 2014). During the aggregation process, tau undergoes oligomerisation and fibrillarisation. Fibrillary tau clumps together into insoluble NFTs that gradually overburden neurones, inhibiting the machinery involved in fundamental cell functions (Cheng and Bai, 2018; Chiasseu et al., 2017), ultimately, leading to neuronal death (Ward et al., 2012). This is emphasised by the presence of extracellular ghost tangles present in the brain long after the neurones they resided in have been removed (Serrano-Pozo et al., 2011). Further, tangle number and localisation are often correlated to dementia status, something which has not been not been associated with Aβ senile plaques (Arriagada et al., 1992).

As with Aβ, the soluble forms of tau may be the toxic moiety, whilst NFTs act as a sink for these species. This would push the idea that NFTs are neuroprotective, even at the expense of synaptic plasticity. On the other hand, it has been suggested that both NFTs and soluble tau are toxic in differing ways, and on different time scales (Kopeikina et al., 2012). It has been demonstrated in several animal studies, where non-aggregated tau is linked to synaptic dysfunction, microgliosis alongside memory, LTP and other functional deficits (Berger et al., 2007; Fá et al., 2016; Hoover et al., 2010; Sydow et al., 2011; Yoshiyama et al., 2007). However, targeting tau pathology alone may not be sufficient to effectively dampen neuronal damage seen in AD. This is further emphasised by clinical trial failure of tau therapeutics (Gauthier et al., 2016).

1.3.2.1. Synergy between tau and amyloid beta pathology

The synergistic actions of oAβ and tau in promoting synaptic dysfunction in AD is well supported (Guerrero-Muñoz et al., 2015; Spires-Jones and Hyman, 2014). Interactions between oAβ and phosphorylated tau have been observed in neurones, and this increases in correlation with disease progression (Manczak and Reddy, 2013). Further, it appears that Aβ accumulation may contribute to tau-induced neuronal disruption and disturbance of axonal projections (Pooler et al., 2013). Thus, inhibiting this interaction may be an avenue to help reduce neuronal damage and synapse loss, rather than targeting one or the other

independently. Nevertheless, the prevailing theory is that Aβ pathology occurs upstream of tau, whereby it initiates tau's pathological spread, thus acting as an initiator for the disease process. However, the spread of Aβ throughout the brain is distinct from that of tau (Jucker and Walker, 2013), with deposition appearing to begin in the frontal and temporal lobes, before spreading to the hippocampus and limbic system; gross cortical pathology then follows (Masters et al., 2015). Tau tangles start in the entorhinal cortex, before spreading into the hippocampus, limbic structures, and finally the primary visual, sensory and motor systems (Figure 1.13; Braak and Braak, 1991). Despite this temporal discrepancy, cortical tangle burden only increases in people with amyloid pathology, a feature which coincides with clinical symptoms (Pontecorvo et al., 2019); highlighting a clear link between the two pathologies. Thus, which is the more toxic species is still heavily debated. Although, as tau pathology is primarily observed in brain regions relating to clinical symptoms, and its deposition correlates with dementia status and reduced cognitive performance with better reliability than Aβ (Brier et al., 2016), tau PET imaging may serve as a biomarker for neuronal injury in disease. (Dronse et al., 2016).

1.3.3. The links and risks of Alzheimer's disease

Approximately 90% of all AD cases are sporadic, with the remainder showing some degree of heritability (Tanzi, 2012). Most inherited forms manifest as EOAD, which is primarily triggered by familial autosomal dominant mutations linked to genes responsible for the processing of APP, amongst which *PSEN1*, *PSEN2* and *APP* dominate (Goate et al., 1991; Raux, 2005; Rogaev et al., 1995; Sherrington et al., 1995). Mutations in these three genes are responsible for approximately 70% of familial AD cases (Rovelet-Lecrux et al., 2012). As discussed in Section 1.3.1, *PSEN* genes encode for presenilin-1 and -2, transmembrane proteins which are components of the γ-secretase complex. Mutations in these genes therefore appear to increase the efficiency of γ-secretase cleavage of APP. However, *APP* mutations can modify the cleavage of its product by all secretase enzymes. For example, the *E682K* mutation in *APP* favours BACE1 cleavage of APP at an alternative β-cleavage site (β'), resulting in increased Aβ production, as identified in an early onset AD case (Zhou et al., 2011).

Sporadic cases are non-heritable and have a late-onset (LOAD). Numerous factors seem to be associated with increased LOAD risk, with age being the most common. Risk of AD increases exponentially as an individual gets older (Imtiaz et al., 2014). Sex differences also exist, with women having a higher risk of developing AD post-menopause (Cahill, 2006; Pike et al., 2009). These risk factors are highlighted in Figure 1.14 (Seshadri et al., 2006).

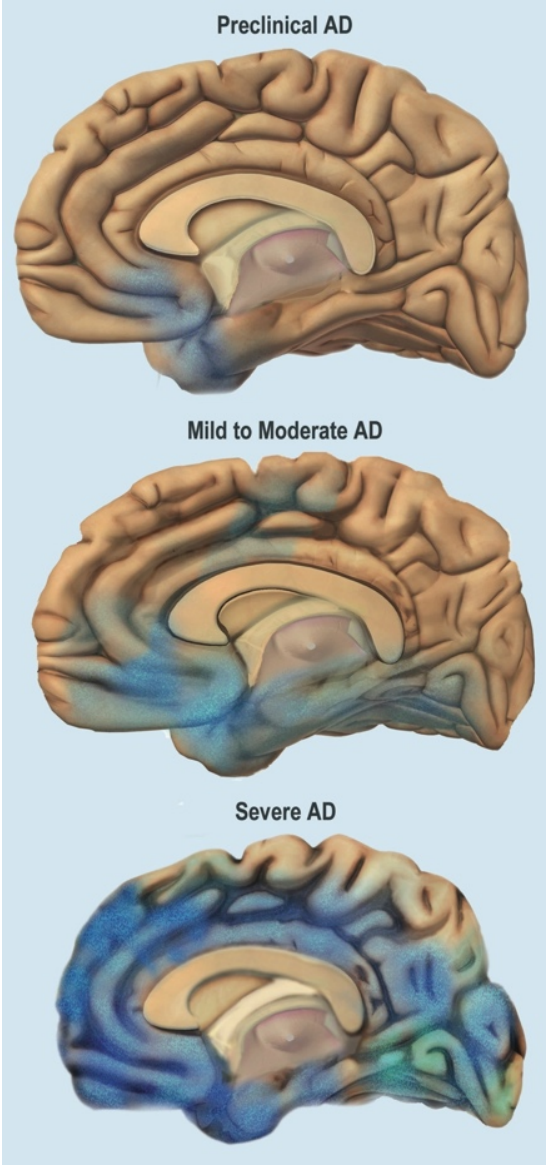

Figure 1.13 Tau pathology progression in AD. The diagram presented represents Braak staging. Braak staging is utilised to refer to NFT pathology, whereby the stage aligns with AD symptoms. Stage I-II tangles are primarily confined to the transentorhinal cortex, III-IV enter the limbic regions of the brain including the hippocampus and amygdala whilst V & VI includes extensive neocortical distribution (Braak and Braak, 1991). The brain of someone with preclinical AD will likely have I-II staging, whilst mild to moderate AD and severe AD would likely have stages III-IV and V-VI, respectively. Diagram was acquired from the National Institute of Health (NIH) and is open access.

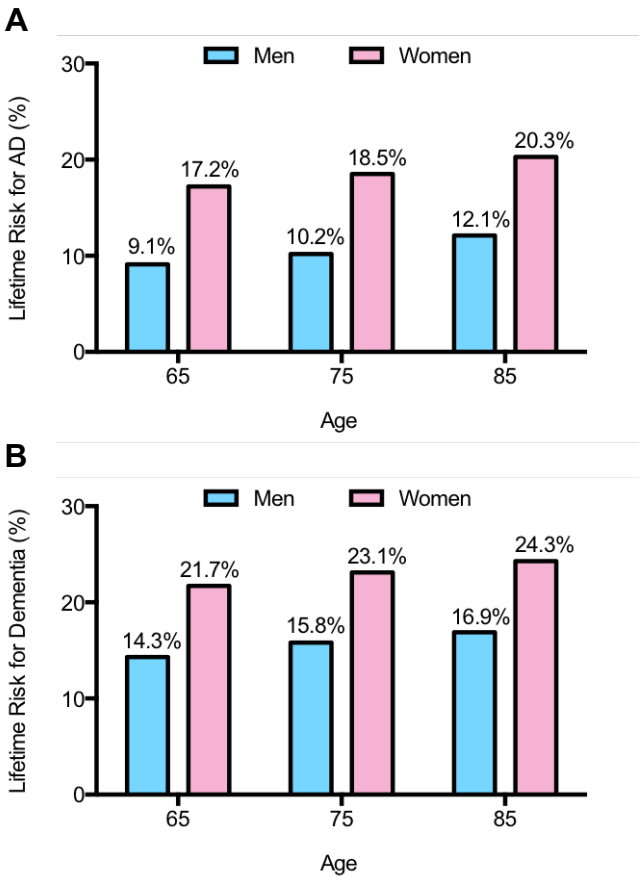

Figure 1.14 Estimated lifetime risk for developing dementia and AD at differing ages for both men and women. A; AD risk with increasing age. **B**; total dementia risk with increasing age. Women having a heightened AD and total dementia risk when compared to men of the same age group. Lifetime risk is defined here as the percentage likelihood of developing either AD or another manifestation of dementia at the ages examined. Data was acquired from participants of the Framingham Study, which was initiated in 1948. 4897 individuals who were stroke and dementia-free at the age of 55 were followed biennially for up to 51 years. Adapted from Seshadri et al., 2006.

The strongest genetic risk factor for LOAD is an allelic variation in the apolipoprotein E (*APOE*) gene, encoding for ApoE, a major cholesterol carrier protein with a supporting role in lipid transport and tissue repair (Liu et al., 2013). Individuals bearing this allele accounting for approximately 60% of all AD cases (Huang, 2011). In the CNS, ApoE is mainly produced by astrocytes, transporting cholesterol to neurones through ApoE receptors (Liu et al., 2015). It also helps promote the clearance and degradation of soluble forms of Aβ (Bachmeier et al., 2013; Castellano et al., 2011). There are three polymorphic alleles of ApoE: ε2, ε3 and ε4 (Farrer et al., 1997). Aβ levels and plaque load are ApoE isoform dependent (Bales et al., 2009; Castellano et al., 2011; Reiman et al., 2009), with AD patients positive for the ε4 allele having the highest plaque load, and those with ε2 having the lowest.

GWAS analyses have identified over 20 other genes associated with LOAD, many of which encode proteins related to microglial function and inflammation, including *CD33*, *CR1*, and *TREM2* (Beecham et al., 2014; Hollingworth et al., 2011; Hu et al., 2017; Kauwe et al., 2014; Lambert et al., 2009; Malik et al., 2015; Naj et al., 2011; Villegas-Llerena et al., 2016). Other risk factors of interest include air pollution (Calderón-Garcidueñas et al., 2016; Jung et al., 2015), smoking (Durazzo et al., 2014), traumatic brain injury (TBI; Gupta and Sen, 2015; Mendez et al., 2015), periodontitis (Cerajewska et al., 2015), high blood pressure (Meng et al., 2014), high cholesterol intake/hypercholesterolemia (Brooks et al., 2017), heart failure (Cermakova et al., 2015) and type 2 diabetes (T2DM; De Felice and Ferreira, 2014; Li and Huang, 2016; Moran et al., 2015; Steen et al., 2005).

Patients diagnosed with T2DM have a significantly greater risk of developing AD (De Felice and Ferreira, 2014), with diabetes contributing to structural deficits in the brain, potentially linking it to the modulation of neurodegeneration (Sato and Morishita, 2014). Metabolic disorders such as T2DM and the associated inflammatory signalling which accompanies them can reduce insulin signalling and inhibit cellular responsiveness to insulin (Gregor and Hotamisligil, 2011). In the brains of AD patients, similar abnormalities can manifest, primarily metabolic stress and neuroinflammation (Talbot et al., 2012; Verdile et al., 2015; Yoon et al., 2012). Insulin is broken down by insulin degrading enzyme (IDE; Farris et al., 2003). In the brain, IDE is also the main enzyme responsible for the degradation of extracellular Aβ (Pivovarova et al., 2016; Vekrellis et al., 2000). As a consequence, IDE appears to represent the pathological link between T2DM and AD.

1.4. Neuroinflammation in Alzheimer's disease

For decades, Aβ and tau have been considered the primary neuropathological hallmarks associated with AD and its clinical manifestations. Despite this, some discrepancies have been proposed in recent years. Whether Aβ and tau alone are enough to cause the extensive neuronal death that is seen in late stage disease is debated. Today, considerable

support exists underpinning the critical involvement of neuroinflammation in the progression of AD (Bagyinszky et al., 2017; Guerreiro et al., 2013; Heneka et al., 2014; Heneka et al., 2015; Jiang and Bhaskar, 2017; Latta et al., 2015; Yin et al., 2017; Yu and Ye, 2014). However, inflammation is unlikely to just result as a consequence of plaque and tangle accumulation, rather it appears to have a causal role in disease, contributing to pathogenesis as much so, if not more than Aβ and tau (Bate et al., 2006; Heneka et al., 2015; Morales et al., 2014). This has been corroborated through an array of methods including genetic screening (Heneka et al., 2014; Malik et al., 2015; Villegas-Llerena et al., 2016), the use of animal models (Hong et al., 2016; Orre et al., 2014; Spangenberg et al., 2016; Zenaro et al., 2015), and the histological analysis of AD patients' brain immune cells post-mortem (Gomez-Nicola and Boche, 2015; Gomez-Nicola and Perry, 2016; Hopperton et al., 2018; Taipa et al., 2018).

1.4.1. Evidence to support neuroinflammatory damage in Alzheimer's disease

1.4.1.1. Animal models

Animal studies underline that inflammatory challenge alone may be sufficient to induce the development of sporadic AD, wherein systemic immune stimulation with a viral mimetic contributed towards both Aβ and tau deposition, memory impairments and microglial activation (Krstic et al., 2012). This may explain why many risk factors for AD development involve inflammation (Brooks et al., 2017; Calderón-Garcidueñas et al., 2016; Cerajewska et al., 2015; De Felice and Ferreira, 2014; Durazzo et al., 2014; Gupta and Sen, 2015; Meng et al., 2014). Further, animal model data has identified that the development of neuroinflammation can occur downstream of Aβ deposition (Akiyama et al., 2000). In addition, markers for complement, a part of the immune response which normally occurs as an attempt to remove cellular debris, have been identified in transgenic mouse models of AD (Fan et al., 2007; Matsuoka et al., 2001; Zhou et al., 2008); most of which co-localise with fibrillary Aβ. Being a strong activator of complement, Aβ can stimulate both the classical, and alternative complement pathways. A recent study identified that oAβ-induced microglial and complement activation can mediate synapse loss and the depression of LTP (Hong et al., 2016). The classical complement cascade appears to be crucial for this, as an anti-C1q antibody prevented synapse loss. C1q is the first subcomponent of the C1 complex within the classical cascade of complement (Kishore and Reid, 2000). Complement activation also attracts microglia, resulting in their production and release proinflammatory cytokines (Orsini et al., 2014; Silverman et al., 2016). Finally, microglial activation and inflammation has been reported in at least seven independent animal models of AD, including both Aβ and tau transgenics (Apelt and Schliebs, 2001; Crawford et al., 2007; Fan

et al., 2007; Frautschy et al., 1998; Hock and Lamb, 2001; Sturchler-Pierrat et al., 1997; Yoshiyama et al., 2007).

1.4.1.2. Genetic/genomic studies

In mice, Aβ plaque-associated microglia express higher levels of proinflammatory genes, including several encoding chemokines (Yin et al., 2017), with these microglia taking on an "activated" morphology. This shift broadly encompasses microglial transformation from a ramified to an amoeboid morphology, which includes the retraction of cellular processes, and can be followed by cellular locomotion (Davis et al., 2017). Further, a loss-of-function variant of the microglial regulator TREM2, which controls inflammation and phagocytosis in microglia (Mecca et al., 2018; Ulrich et al., 2017), has a highly significant association with AD, increasing the risk of developing AD approximately threefold (Guerreiro et al., 2013).

1.4.1.3. Post-mortem analysis

In AD patients, complement is activated in both early and late stage disease, with differencing complement species co-localising with diffuse and neuritic plaques, alongside neurofibrillary tangles (Loeffler et al., 2008; Yasojima et al., 1999; Zanjani et al., 2005). In addition, microglial inflammation appears to be positively correlated with total Aβ load, wherein it may indirectly contribute towards cognitive decline by facilitating NFT formation (Felsky et al., 2019). Increases in microglial activation markers have been identified in multiple post-mortem analyses of AD patients. A systematic review published in 2018 identified thirty-six papers reporting higher levels of major histocompatibility complex II (MHCII) in AD patients relative to control patients in at least one of the brain regions measured (Hopperton et al., 2018).

A further twenty-one studies compared CD68 between control and AD patients. Although there is some CD68 expression in surveillant microglia (Lee et al., 2002), CD68 is primarily considered a marker of microglial activation, wherein in labels the lysosome (Walker and Lue, 2015). Seventeen of these studies discovered an increase in CD68 expression, staining, or CD68 positive cell counts in AD brains compared to control. Twenty papers were also identified to quantitatively compare the levels of ionized calcium-binding adaptor molecule 1 (Iba1), a protein considered to be a general marker of microglia (Walker and Lue, 2015). Data for Iba1 was conflicting, suggesting microglia are primarily activated in AD, rather than upregulated (Hopperton et al., 2018). In addition, both familial and sporadic AD patients had higher neuroinflammatory pathological markers in brain areas damaged in disease including the entorhinal and temporal cortices, hippocampus and dentate gyrus (Taipa et al., 2018).

Wang et al. analysed the levels of specialised pro-resolving mediators (SPMs), which are fatty acid derivatives actively involved in the resolution of inflammation, in hippocampal tissue and the cerebrospinal fluid (CSF) from AD and non-AD subjects. Levels of the SPM lipoxin A4 (LXA4), which is an endogenous ligand for formyl peptide receptor 2 (FPR2), were significantly reduced in both the CSF and hippocampus (Wang et al., 2015).

The link between proteineous pathology and neuroinflammation is therefore becoming clearer. However, the association is unlikely to be a passive process. Meaning inflammation does not just result as a consequence of plaque and tangle accumulation. Rather, it has a causal role in the disease, contributing to pathogenesis of AD.

1.4.2. Microglia in Alzheimer's disease

Several cell types are involved in the neuroinflammatory response, including astrocytes (Colombo and Farina, 2016; Wang et al., 2013) and blood-derived mononuclear cells, such as perivascular macrophages (Agrawal et al., 2013; Zhang et al., 2012). The primary cells responsible for neuroinflammation however, are microglia (Heneka et al., 2015; Ransohoff et al., 2015). These CNS resident macrophage-like immune cells are phagocytic in nature (Lucin et al., 2013; Savage et al., 2015), able to degrade various molecules through enzymatic cleavage (Paolicelli et al., 2017). In healthy individuals, microglial phenotype is relatively homeostatic, whereby cells are able to remove dead cells and debris, preventing accumulation in the brain (Ransohoff and El Khoury, 2015). However, as phagocytic cells such as microglia age, their degradative capacity becomes less efficient (Koellhoffer et al., 2017; Li, 2013; Ritzel et al., 2015), leading to the slow and progressive build-up of unwanted cellular debris (Thériault and Rivest, 2016). In terms of microglia and the CNS, this includes the aggregation of damaging peptides such as $A\beta_{1\text{-}42}$ (Floden and Combs, 2011).

1.4.2.1. Amyloid beta, microglia and neuroinflammation

In patients developing AD, large quantities of fibrillar Aβ begin to accumulate. Unlike soluble Aβ however, fibrillar forms of the peptide are mostly resistant to enzymatic degradation, and thus microglial phagocytosis does not successfully remove accumulating plaques (Saido and Leissring, 2012; Shen et al., 2006). This aligns to the observation of microglia in close proximity to Aβ plaques in histology stains, with reduced clearance identified as a major pathogenic pathway in AD (Mawuenyega et al., 2010), whereby an inefficient microglial phagocytic response leads to further accumulation of soluble Aβ. In addition, Beclin 1, a key regulator of microglial phagocytosis, appears to be impaired in AD (Lucin et al., 2013), whilst accumulation of oAβ can attenuate phagocytosis of fibrillar amyloid species (Pan et al., 2011); multiple observations therefore appear to contribute to the reduced phagocytic

capacity of microglia in AD.

This extensive Aβ accumulation appears to be directly responsible for the manifestation of chronic neuroinflammation in AD, with deposition following a positive correlation with inflammation in the brains of transgenic mice (López-Picón et al., 2018). PRRs such as TLRs and RAGE both recognise Aβ, resulting in the stimulation of an immune response and the release of pro-inflammatory mediators (Zhou et al., 2014). This appears to be in part mediated by NF-κB activation (Zhao et al., 2018; Zhou et al., 2014). This RAGE and TLR mediated neuroinflammatory response appears to impair learning and memory in APP transgenic and C57 naïve oAβ-injected mice (Balducci et al., 2017; Fang et al., 2010). Further, age-related cognitive impairment in mice was directly associated with long-term neuroinflammation (d'Avila et al., 2018). Thus, animal studies suggest that Aβ-induced inflammatory responses are accountable for neuronal dysfunction.

Although the inflammatory reaction is key in homeostatic regulation, whereby it helps to remove dying neurones and cell debris, as well as assisting in repair and regeneration (Merino et al., 2015; Zilkha-Falb et al., 2016), chronically activated microglia may also damage and remove healthy neurones, thereby further contributing to the pathogenic process (Bouvier and Murai, 2015). Microglial interaction with Aβ appears to result in a shift of function, causing the release of a battery of pro-inflammatory mediators, including cytokines such as IL-1, IL-6 and TNFα (Floden et al., 2005; Heneka et al., 2001), chemokines including CXCL1 and CCL-2 (Liu et al., 2015) ROS (Pan et al., 2011; Wilkinson et al., 2012), and reactive nitrogen species (RNS; Song et al., 2012). This can result in the development of a positive feedback loop between inflammation and Aβ production, wherein Aβ-activated microglia have hindered phagocytic ability (Heneka et al., 2015), and thus Aβ accumulates, further stimulating microglia, resulting in the manifestation of a self-propagating chronic inflammatory cycle (Herbst-Robinson et al., 2016; Sastre et al., 2008).

Microglial activation alongside the expression of neuroinflammatory markers such as TSPO positively correlate with AD severity in patients and cognitive decline (Cagnin et al., 2001; Kreisl et al., 2013). This may explain why eliminating microglia from AD mice can prevent neuronal loss without modulating Aβ pathology (Spangenberg et al., 2016). Interestingly, microglial activation in post-mortem cortical tissue has a strong association with both Aβ and tau pathology, with models supporting that microglial activation is upstream of tau accumulation (Felsky et al., 2019). This is supplemented by animal work, wherein microglial activation correlated with both memory deficits and tau pathological spread (Maphis et al., 2015), whilst in contrast microglial depletion prevented tau accumulation (Asai et al., 2015). This is further supported by the observation that chronic neuroinflammation occurs relatively early in the disease process (Misiak et al., 2012; Monson et al., 2014; Wilcock and Griffin, 2013; Zhang et al., 2013), identified through neuropathological studies detecting

inflammatory mediators and activated microglia in the cerebral cortex of patients post-mortem, despite a low Braak staging (Eikelenboom et al., 2010). PET imaging studies in patients have also shown microglial activation to occur well before clinical symptoms manifest (Hamelin et al., 2016; Yasuno et al., 2012), and brain inflammation also accompanies Aβ deposition in the majority of MCI patients that progress to AD (Parbo et al., 2017). Further, many risk gene variants identified via GWAS are involved in innate immunity and are highly expressed in microglia (Beecham et al., 2014; Hansen et al., 2018; Villegas-Llerena et al., 2016). These expression profiles have been identified both in the brains of mice and humans (Figure 1.15).

1.4.2.2. Tau hyperphosphorylation, microglia and neuroinflammation

In humans, microglial activation appears to be primarily associated with Aβ load, indirectly contributing to cognitive decline via induction of hyperphosphorylated tau (Felsky et al., 2019). However, progression of Aβ does not corelate closely to clinical symptom progression (Serrano-Pozo et al., 2011). In contrast, both neuroinflammation and tau pathology correlate with AD severity in humans (Bejanin et al., 2017; Kreisl et al., 2013; Ossenkoppele et al., 2016), with the former potentially being critical for the latter. For example, immunohistochemical analysis of AD patient brains highlighted the importance of local grey matter inflammation for tau pathology (Zotova et al., 2013). It may not be surprising then that microglial have been proposed to contribute towards the pathological seeding of tau (Hopp et al., 2018). In transgenic mice, inflammatory microglia correlate with spatial memory deficits and the spread of tau pathology, with an IL-1 receptor antagonist significantly reducing this microglial-induced tau pathology (Maphis et al., 2015). Additionally, purified microglia transferred from these transgenic mice induced tau hyperphosphorylation within the brains of non-transfected mice (Maphis et al., 2015). Thus, considerable evidence supports a central pathological role for microglia in AD, wherein it may act as a ‘gatekeeper’ between Aβ and tau pathological spread and neurodegeneration.

The widespread and diverse evidence available therefore warrants a focus on research to combat neuroinflammation in AD. Additionally, because neuroinflammation is associated with a plethora of both neurodegenerative and neuropsychiatric disorders (Furtado and Katzman, 2015; Müller et al., 2015; Najjar and Pearlman, 2015; Russo et al., 2014; Zhang, 2015), the identification of a mechanism to microglial-induced neuroinflammatory damage could be beneficial and translatable to differing diseases. We believe that microglial activation can be modulated by an appropriate therapeutic agent(s), allowing promotion of anti-inflammatory and immunomodulatory pathways to fight back against chronic inflammatory and oxidative damage.

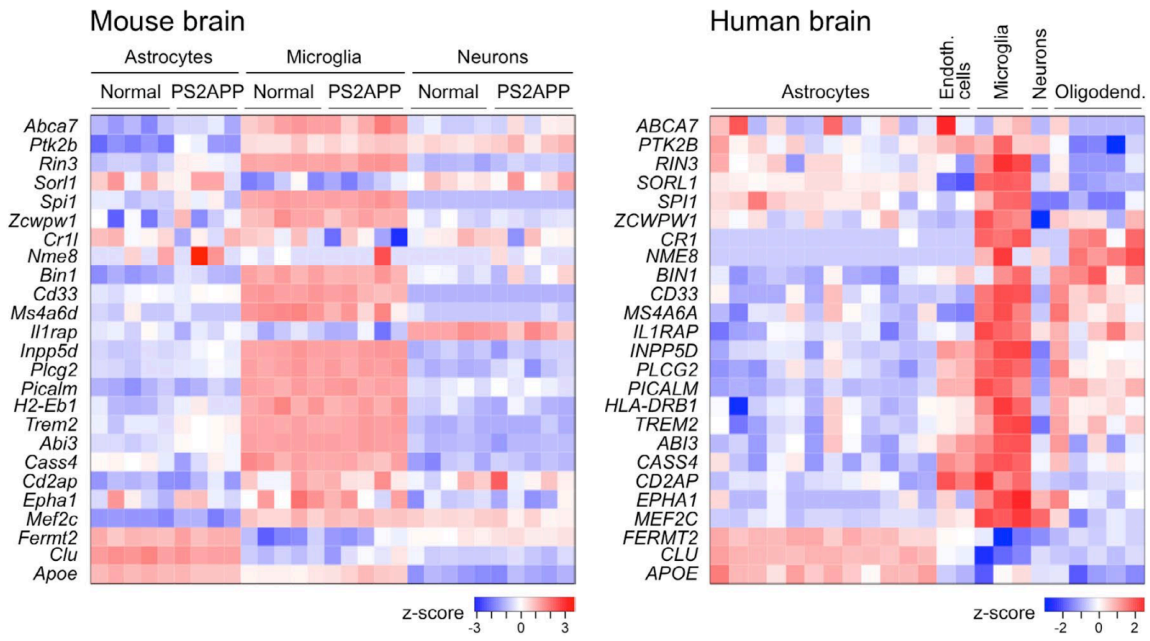

Figure 1.15 Expression profile of AD risk genes in microglia. These heat maps depict the relative expression profile of AD risk genes purified from mouse (**A**) or human (**B**) brain tissue (Srinivasan et al., 2016; Zhang et al., 2016). RNA sequencing was used for tissue analysis. Each column within a cell type represents one sample of those purified cells from a different brain. For the mouse dataset, cortical samples from 13-mo old PS2APP Aβ model or age-matched non-transgenic littermates were plotted. For the human dataset, "normal" cortical samples were plotted, with samples ranging in age from 8 to 63 years. The Z-score represents the number of standard deviations by which a sample's expression level for a gene varies in comparison to mean expression level for that gene across all samples analysed. For human genes which do not appear to have mouse orthologues, suitably selected mouse homologues were utilised. The use of this figure was signed off by the original authors (Hansen et al., 2018), and the Journal of Cellular Biology.

1.5. Current therapies and recent clinical research

Several medicines are available which can slow down the progression of clinical symptoms. Donepezil, rivastigmine and galantamine are acetyl-cholinesterase inhibitors central to symptomatic treatment of AD, showing to be mostly effective in mild to moderate stages of disease (Grutzendler and Morris, 2001). However, there is no evidence to suggest that one drug in this class is more efficacious than the others (Grutzendler and Morris, 2001). Nevertheless, withdrawal of donepezil treatment has been associated with potential risks, even when the benefits of continuing treatment are not apparent (Howard et al., 2015). An alternative symptomatic treatment is memantine, a low affinity NMDA receptor antagonist. The aim of its use is to reduce glutamate-induced excitotoxicity without interfering with the physiological functions of this neurotransmitter (Wang and Reddy, 2017). Evidence also suggests that combination therapy with these two treatments may improve clinical symptoms in comparison to singular regimens (Parsons et al., 2013).

Approaches targeted towards disease pathology are essential, with a significant focus being on reducing Aβ load to improve clinical outcome (Bales et al., 2016; Gilman et al., 2005; Salloway et al., 2014). However, fighting Aβ alone may not be enough to prevent the extensive synapse and neuronal loss that occurs in AD. Aβ immunisation has become a central research focus in more recent years (Salloway et al., 2014; Wisniewski and Goñi, 2015). Pre-clinical studies contained promise, providing evidence that different antibodies could alleviate both Aβ-associated synaptic and cerebral amyloid angiopathy pathology in transgenic AD mouse models (Bales et al., 2016; Dorostkar et al., 2014). However, another study highlighted that immunotherapy may not be effective at repairing neuronal dysfunction (Busche et al., 2015), perhaps foreshadowing the extensively documented failures of Aβ immunotherapy clinical trials (Holmes et al., 2008; Honig et al., 2018; Panza et al., 2019). Whether Aβ alone is enough to facilitate neurodegeneration is unclear, with PET imaging identifying a reduction in plaque load in APOE ε4 carriers, despite a lack of clinical outcome improvements (Salloway et al., 2014). Pittsburgh Compound-B (PiB) is the primary radioactive tracer used for PET imaging of plaques, also binding to protofibrils (Yamin and Teplow, 2017).

The importance of oligomeric Aβ to disease progression is clearly evident (Benilova et al., 2012; Bernstein et al., 2009; Ferreira et al., 2015). Though whilst a new approach is available to radiolabel oligomers in mice (Sehlin et al., 2016), lowering radioactivity will be essential to make this technique safe in humans, allowing us to determine the effects of immunotherapies on soluble Aβ accumulation. The clear conclusion that arises from continual clinical trial failure is that new research approaches are warranted.

As discussed previously, initial exposure of microglia to Aβ likely facilitates ROS production, which can further fuel Aβ production but also instigate an inflammatory response. Whether Aβ sets in motion a self-propagating disease involving extensive microglial involvement needs further elucidation. However, neuronal loss in AD appears to be facilitated by multiple causes which develop as the disease progresses (Hoover et al., 2010; Kreisl et al., 2013; Nation et al., 2019), underlining the importance of a multifaceted approach for AD therapeutics.

As a consequence, therapies targeting Aβ in patients with late stage disease are unlikely to have a significant impact on clinical outcome. This is due to the recruitment of a plethora of other factors from both neurones and glia, which can further contribute to, and propagate, neurodegenerative damage (Liddelow et al., 2017; Salter and Stevens, 2017); likely resulting in a vicious cycle of neurodegeneration. Targeting Aβ earlier in disease progression is a more sought-after approach to slow down the rate of clinical onset, but whether this is enough to combat sporadic disease, which is not directly related to mutations in amyloid processing genes, can be debated. It is nevertheless important to go into detail about how Aβ is toxic to neurones, and later on, how it could link to the other characteristic pathological hallmarks of AD.

Simply put, focusing solely on the amyloid cascade hypothesis or tau-related neuronal disruption has not developed effective therapies for AD. This suggests that the pathological processes responsible for disease progression are far more expansive than just the dysfunctional processing of APP or microtubule associated proteins. However, it could also suggest that the therapies targeting towards amyloid and tau are just poor in quality. Regardless, there are molecular pathways and cells which are clearly responsible for bridging the gap between proteineous pathology and cell death. As covered in Section 1.4, chronic inflammation could play a central role, either in response to protein accumulation, or as a causative driver of disease (McGeer and McGeer, 2013).

1.6. Formyl peptide receptor 2

The formyl peptide receptors, abbreviated as FPRs in humans, are G-protein coupled receptors (GPCR) with known roles in chemotaxis, host defence and inflammation (Dalli et al., 2012; McArthur et al., 2015; Migeotte et al., 2006; Ye et al., 2009). Mainly expressed by mammalian leukocytes, their roles in inflammation vary, from cellular adhesion and directed migration through chemotaxis, to granule release and superoxide formation (He and Ye, 2017). However, FPRs may function to suppress the immune system in certain conditions, including exposure to human immune-deficiency virus derived peptides (Braun et al., 2001). There are three human FPRs: FPR1, FPR2/ALX, and FPR3. All three share similar sequence homology, encoded by genes in a gene cluster (Gao et al., 1998; Yi et al., 2007).

FPR1 and FPR2 in particular share an overall high sequence homology, with some overlapping functionality. However, in mice, two receptors exist which work together to carry out similar functions to that of human FPR2: Fpr2/3 (Dufton et al., 2010; Stempel et al., 2016). These receptors are functional equivalents of human FPR2, with both having more or less identical pharmacology and signalling behaviour (Ye et al., 2009). However, the presence of the Fpr3 protein complicates several experimental approaches, such as knock-down and knock-out experiments. Nevertheless, Fpr3 has 74% identity (Fpr2 has 75%) and 81% homology to human FPR2, whilst murine Fpr2 and Fpr3 have 82% identity and 88% homology to each other (Ye et al., 2009), highlighting their similarities.

The receptors themselves were initially identified and named through their ability to bind N-formyl peptides such as N-formylmethionine (fMet), a peptide that is produced through the degradation of bacterial or host cells (Le et al., 2002; Panaro et al., 2006). The ability to recognise peptides containing N-formylated methionine, including the potent *N*-formyl-methionyl-leucyl-phenylalanine (fMLP or fMet-Leu-Phe) thereby leads to the conclusion that FPRs can act as PRRs. Collectively, these receptors bind to a substantial repertoire of ligands, something that has only increased in recent years with the development of new synthetic substrates. Agonists are not limited to *N*-formyl peptides though, with non-formyl peptides from both microbial and host origins, alongside synthetic small molecules and an eicosanoid, all binding to one, or several of these receptors (He and Ye, 2017). How these receptors recognise such a diverse array of ligands remains largely unclear. In the absence of crystalline structures of these receptors, computer-aided ligand docking (He et al., 2014; Stepniewski and Filipek, 2015) and structural simulation (Schepetkin et al., 2014), alongside site-directed mutagenesis (Ferrari et al., 2006) have led to the identification of amino acids within both FPR1 and FPR2 responsible for receptor interactions with several different molecules (He and Ye, 2017). Interestingly, ligands identified for FPR3 are currently minimal. The amino acid sequences for FPR1 and FPR2 are shown in Figure 1.16.

Both FPR1 and FPR2 receptors are expressed in several cell types, including monocytes, neutrophils, and microglia (He and Ye, 2017; Yu and Ye, 2014). Whereas FPR3 is expressed in monocytes, but not neutrophils (He and Ye, 2017). The distribution pattern of the former two receptors does expand though, with both also found in microvascular endothelial cells, alongside others (Table 1.1; He and Ye, 2017). However, neither have been identified as being present in neurones. Conventionally, FPR1 ligands tend to be pro-inflammatory, with activation of FPR1 contributing to inflammatory responses (Dorward et al., 2015; Liu et al., 2012; Prevete et al., 2015; Wang et al., 2015). Conversely, FPR2 ligands are mostly, but not all, anti-inflammatory and immunomodulatory (Al-Madol et al., 2017; de Oliveira et al., 2017; Mottola et al., 2017; Tan et al., 2017). Some FPR2 agonists are pro-inflammatory, including serum amyloid A and Aβ (Yu and Ye, 2014). Nevertheless, FPR2 may be able to regulate microglial phenotype following challenge by toxic Aβ, highlighted

FPR1 (1-90)

METNSSLPT--------NISGGTPAVSAGYLFLDIITYLVFAVTFVLGVLGN

GLVIWVAGFRMTHTVTTISYLNLAVADFCFTSLPFFMVRKAMGGH

FPR2 (1-90)

METNFSTPL--------NEYEEVSYESAGYTVLRILPLVVLGVTFVLGVLG

NGLVIWVAGFRMTRVTTICYLNLALADFSFTATLPFVLIVSMAMGEK

FPR1 (91-185)

WPFGWFLCKFLFTIVDINLFGSVFLIALIALDRCVCVLHPVWTQNHRT

VSLAKKVIIGPWVMALLLTLPVIIRVTTVPGKT---GTVACTFNFSPWTN

FPR2 (91-185)

WPFGWFLCKLIHIVVDINLFGSVFLIGFIALDRCICVLHPVWAQNHRTV

SLAMKVIVGPWILALVLTLPVFLFLTTVTIPN---GDTYCTFNFASWGG

FPR1 (186-281)

DPKERINVAVAMLTVRGIIRFIIGFSAPMSIVAVSYGLIATKIHKQGLIKS

SRPLRVLSFVAAAFFLCWSPYQVVALIATVRIRE-L-LQGMYKEIGI

FPR2 (186-282)

TPEERLKVAITMLTARGIIRFVIGFSLPMSIVAICYGLIAAKIHKKGMIKS

SRPLRVLTAVVASFFICWFPFQLVALLGTVWLKE-MLFYGKYKIIDI

FPR1 (282-350)

AVDVTSALAFFNSCLNPMLYVFMGQDFRERLIHALPASLERALTEDS

TQTSDTATNSTLPSAEVALQAK

FPR2 (283-351)

LVNPTSSLAFFNSCLNPMLYVFVGQDFRERLIHSLPTSLERALSEDS

APTNDTAANCASPPAETELQAM

Figure 1.16 Sequence alignment of human FPR1 and FPR2. The amino acid sites highlighted in red give rise to the differences seen in these receptor subtypes. The sequence differences encode for varying amino acids on the II and IV transmembrane domains of these FPRs, alongside changes on the third extracellular chain, connecting intracellular domains VI and VII. Adapted from He and Ye, 2017.

by the pro-resolving nature of many of the receptor's ligands (Hughes et al., 2017; Perretti et al., 2017b; Petri et al., 2017). This receptor could therefore, if modulated correctly, blunt inflammation in AD and contribute towards a restriction of disease progression.

Table 1.1 Summary of human FPR receptor subtype location.

Receptor Subtype	Cellular Location
FPR1	Monocytes, neutrophils, astrocytes, microglia, hepatocytes, dendritic cells
FPR2	Monocytes, neutrophils, microglia, epithelia, hepatocytes, microvascular endothelial cells

Studies in recent years have provided evidence supporting that FPR2 modulation can lead to a reduction in inflammation in different pathological conditions. For example, murine Fpr2 appears to be crucial to facilitate effective protection against bacterial infection (Sharba et al., 2019). When the receptor was inhibited by the FPR2 antagonist WRW_4, it resulted in the impairment of inflammatory resolution in murine acute heart failure (Kain et al., 2019). Many studies have focused on annexin A1 (AnxA1), an endogenous signalling molecule well characterized to be a highly potent FPR2 agonist (Gobbetti et al., 2014; McArthur et al., 2015, 2010). Published research highlights how AnxA1 promotes the resolution of inflammation via FPR2 (Corminboeuf and Leroy, 2015; Perretti and D'Acquisto, 2009), including a recent study underlining that AnxA1 attenuates neuroinflammation after intracerebral haemorrhage in mice (Ding et al., 2019).

The effects of other FPR2 ligands have also been investigated. In a mouse model of silicosis, wherein lung fibrosis is triggered by the inhalation of particulates containing silica, Ac2-26, an N-terminal peptide of AnxA1, abolished leukocyte infiltration and inhibited the generation of pro-inflammatory cytokines (Trentin et al., 2015). Ac2-26 also has a protective role in atherosclerosis, whereby administration was shown to reduce sclerotic lesion sizes and macrophage accumulation in these lesions (Drechsler et al., 2015). Given that microglia are the resident macrophage-like myeloid cells of the CNS (Perry and Teeling, 2013), FPR2 activation may have similar protective roles here. This appears to hold promise, as a second AnxA1 peptide, AnxA1sp, can promote neuroinflammation resolution in a model of exsanguinating cardiac arrest (Ma et al., 2019).

Lipoxin A4 (LXA4), a bioactive metabolite of arachidonic acid, is classified as a type of specialized pro-resolving mediator (SPM; Serhan et al., 2015). It also appears to be an FPR2 agonist, wherein stimulation of this receptor blocks atherosclerotic lesion progression in both the aortic root and thoracic aorta in mice through binding with FPR2 (Petri et al., 2017). Alongside this, LXA4 reduced macrophage infiltration, the number of apoptotic cells associated with atherosclerotic lesions, and both chemokine and pro-inflammatory cytokine

levels including TNFα and IL-6 (Petri et al., 2017). It can also reduce inflammation following subarachnoid haemorrhage in rats (Guo et al., 2016). Resolvin D2 (RvD2), another SPM and FPR2 agonist, was identified to reduce inflammation in an *in vitro* model of human bronchi (Khaddaj-Mallat et al., 2016), which was inhibited upon the addition of the FPR2 antagonist, WRW_4.

Several small molecular compounds have been shown to act through FPR2, each displaying a variety of pro-resolving actions, including WKYMVm. Administration of this small compound into a murine model of acute myocardial infarction provided myocardial protection from apoptosis, alongside preservation of cardiac function (Heo et al., 2017). Compound-17b has been shown to be cardioprotective both *in vitro*, and *in vivo*, protecting mice against myocardinal ischaemia-reperfusion injury (Qin et al., 2017). In a mouse model of rheumatoid arthritis, which is a chronic systemic inflammatory disorder, another small molecule FPR2 agonist, Compound-43 (C43), reduced clinical disease severity and attenuated synovial TNFα (Kao et al., 2014); deleting the AnxA1 gene severely exacerbated observable symptoms. The small molecular agonist Quin-C1 (QC1) also significantly reduced inflammation in a mouse model of bleomycin-induced lung injury (He et al., 2011).

1.6.1. A new approach: targeting FPR2 for Alzheimer's disease

In AD, chronic neuroinflammation manifests (Heneka et al., 2015; Kreisl et al., 2013; Togo et al., 2000), underlining that the homeostatic control of inflammatory resolution appears to be impaired in AD (Wang et al., 2015; Zhu et al., 2016). Interestingly, surveillant murine microglia only express low levels of Fpr2, but this is upregulated following inflammatory insult (Cui et al., 2002b, 2002a). Exploitation of this receptor under neuroinflammatory conditions therefore makes it a prime candidate for modulating the microglial inflammatory response for AD research.

The therapeutic potential of FPR2 is evident when AnxA1, LXA4 and resolvin D1 are expressed in both human and mouse brain tissue (Bisicchia et al., 2018; McArthur et al., 2010; Wang et al., 2015). In AD models, both Aβ induced and pro-inflammatory microglia upregulate Fpr2 gene expression (Pan et al., 2011). AnxA1 induced stimulation of FPR2 can also inhibit Aβ-induced microglial inflammatory mediator release, alongside upregulating their ability to phagocytosis Aβ (Ries et al., 2016). Because microglial phagocytosis is reduced in AD (Hellwig et al., 2015; Wolf et al., 2017), FPR2 modulation may therefore be able to ablate further cellular damage by clearance of pathological Aβ and cellular debris. Data with LXA4 supports this, wherein it reduced both Aβ and tau pathology alongside improving cognitive performance in AD-transgenic mice (Dunn et al., 2015).

In humans, there is reduced expression of several pro-resolving mediators in the hippocampus, entorhinal cortex and CSF of AD patients, including resolvin D5 and LXA4 (Wang et al., 2015; Zhu et al., 2016). With both brain regions highly affected by AD pathology, we theorise that neuroinflammatory resolution pathways are critical to prevent extensive neuronal damage associated with microglial activation and neuroinflammation in AD.

Evidence therefore supports the notion that endogenous resolution pathways are disturbed in AD, and that an immuno-modulatory FPR2 agonist could help reverse the disruption of this system. Thus, FPR2 might be a viable drug target for tackling neuroinflammation in AD, at a time where AD and neurodegenerative diseases as a whole are in desperate need for new therapeutics.

1.7. Hypothesis

I hypothesise that microglial Fpr2/3 activation will successfully reverse the onset of neuroinflammation, priming the receptor as a central target for immunomodulation in AD. This hypothesis was based on peripheral research by both our group and others, identifying the immunomodulatory capability of both the human FPR2 and murine Fpr2/3 receptors (Sadani N. Cooray et al., 2013; McArthur et al., 2018, 2015; Trentin et al., 2015).

1.8. Aims

I will use *in vitro* microglial cultures to investigate this hypothesis by establishing whether Fpr2/3 stimulation can reverse (a) LPS and (b) oligomeric $A\beta_{1\text{-}42}$ (oAβ) induced inflammation, identifying any mechanisms involved. I will determine whether Fpr2/3 activation can modulate the expression of inflammatory phenotypic markers following toxin exposure, and whether metabolic changes link to any of the inflammatory responses observed. Next, I will ascertain whether LPS or $oA\beta_{1\text{-}42}$-induced ROS production is affected by Fpr2/3, underlining any mechanism involved in this change. Finally, I will investigate whether Fpr2/3 stimulation post-$oA\beta_{1\text{-}42}$ exposure can protect differentiated SH-SY5Y cells from apoptosis by $oA\beta_{1\text{-}42}$-induced microglial activation.

1.9. Selecting FPR2 ligands

One of the main issues with neurodegenerative disease drug treatments is the ability for therapeutics to cross the BBB and enter the brain (Patel and Patel, 2017). Despite the clear benefits of utilising previously named SPMs, issues arise regarding their ability to be druggable. For example, LXA4 and resolvin D1 appear to be chemically unstable and have a short half-life (Maderna and Godson, 2009; Mozurkewich et al., 2016; Skarke et al., 2015),

whereas AnxA1 is a large molecule (37 kDa), likely preventing its ability to cross the BBB. Whilst direct intracerebroventricular injections are often incorporated to animal studies (Guo et al., 2016), this is not possible for humans. Instead, small molecules likely to cross the BBB are essential to support any translational applications for preliminary *in vitro* research. For our study, small peptide mimetics such as Ac2-26 from AnxA1 were originally considered, but limitations were apparent. For example, it also binds to FPR1 (Dalli et al., 2012), confusing any potential immunomodulatory mechanisms. Further, recent research has returned to focus on AnxA1 (Lima et al., 2017; Ries et al., 2016), suggesting a lack of potency or full efficacy compared to the parent molecule.

Instead, we have selected two small molecule FPR2 ligands, the pyrazolone derivative C43 and quinazolinone compound QC1 (He and Ye, 2017). Pyrazolones are 5-membered heterocyclic compounds that have been known to reduce markers of inflammation for over thirty years (Brogden, 1986). Quinazolinones are also heterocyclic compounds, possessing a diverse array of biological activity including antibacterial and anti-inflammatory (Jafari et al., 2016). The anti-inflammatory effects showcased by both of these FPR2 agonists in peripheral inflammatory models is therefore unsurprising (He et al., 2011; Kao et al., 2014), but their effects on neuroinflammation is yet to be documented. Both compounds are also cheap and readily available commercially. The structures of these compounds are displayed in Figure 1.17.

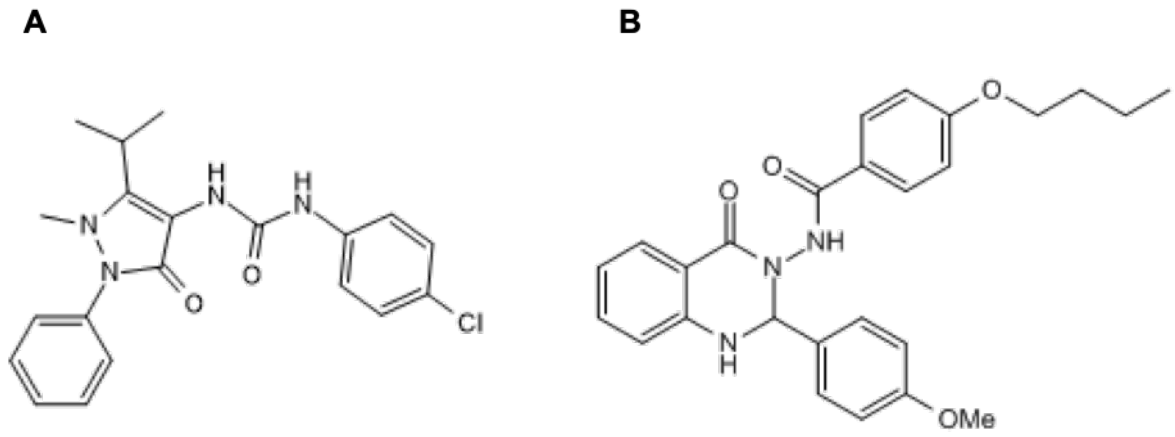

Figure 1.17 The chemical structures of Compound-43 (C43) and Quin-C1 (QC1). C43 (**A**) is a pyrazolone derivative, whilst QC1 (**B**) is a quinazolinone based compound. Structural images were available on the Tocris Bioscience website, and via He and Ye, 2017.

Chapter 2: Methods

2.1. Drugs and reagents

N-(4-Chlorophenyl)-*N*-[2,3-dihydro-1-methyl-5-(1-methylethyl)-3-oxo-2-phenyl-1*H*-pyrazol-4-yl]-urea (Compound 43), 4-Butoxy-*N*-[1,4-dihydro-2-(4-methoxyphenyl)-4-oxo-3(2*H*)-quinazolinyl]benzamide (Quin-C1), LESIFRSLLFRVM (MMK 1), WRWWWW (WRW_4), 4-[5-(4-Fluorophenyl)-2-[4-(methylsulfonyl)phenyl]-1*H*-imidazol-4-yl]pyridine (SB 203580), 5-(2-Phenyl-pyrazolo[1,5-*a*]pyridin-3-yl)-1*H*-pyrazolo[3,4-*c*]pyridazin-3-ylamine (FR 180204), diphenyleneiodonium chloride, N^6-[2-[[4-(Diethylamino)-1-methylbutyl]amino]-6-methyl-4-pyrimidinyl]-2-methyl-4,6-quinolinediamine trihydrochloride (NSC 23766), 4-[4,5-Dihydro-5 (4-methoxyphenyl)-3-phenyl-1*H*-pyrazol-1-yl]benzenesulfonamide (ML 141), rhosin hydrochloride and dorsomorphin dihydrochloride were bought from Tocris Bioscience (Bio-Techne Limited, Bristol, UK). 6E-(bromomethylene)tetrahydro-3-(1-naphthalenyl)-2H-pyran-2-one (Bromoenol lactone) and 3-(2-methyl-1-oxopropyl)-1-[2-oxo-3-(4-phenoxyphenoxy)propyl]-1H-indole-5-carboxylic acid (CAY10650) were bought from Cayman Chemical Company (Ann Arbor, Michigan, USA). Coomassie Brilliant Blue R-250 was purchased from Alfa Aesar (Lancashire, UK). Hexafluoro-2-propanol (HFIP), a solvent which can monomerise β-sheet protein aggregates (Broersen et al., 2011), treated $A\beta_{1-42}$ was purchased from JPT Peptide Technologies (Berlin, Germany). Isolated and purified lipopolysaccharides from *Escherichia coli*, Serotype O111:B4 and trans-retinoic acid alongside all other chemicals and reagents unless otherwise indicated were purchased from Merck Millipore Limited (Poole, UK)

2.2. Native tricine-PAGE electrophoresis and Coomassie staining

Coomassie Brilliant Blue was used as a dye-based protein stain for the visualisation of $A\beta_{1-42}$ protein bands by gel-electrophoresis. To determine whether the oligomerisation protocol previously described (Stine et al., 2011) worked successfully, a native tricine-PAGE was used to separate the $A\beta_{1-42}$ peptides, according to their molecular weight. In sample buffer (62.5 mM Tris-base, 25% glycerol, 1% (w/v) Coomassie Blue R-250), 2 µg $A\beta_{1-42}$ was added to each well, in triplicate. Running buffer used consisted of 25 mM Tris and 192 mM glycine (pH = 8.3). Following electrophoresis, gels were stained (60 mg/L Coomassie Blue R-250, 10% (w/v) acetic acid in distilled water) for 2 h. Gels were then washed (10% (v/v) acetic acid, 50% (v/v) HPLC-grade methanol, in distilled water) over 24 h. The representative photograph in Figure 2.1 highlights Coomassie stained oligomeric $A\beta_{1-42}$ bands, with molecular weight compared against a ladder of know molecular weight proteins.

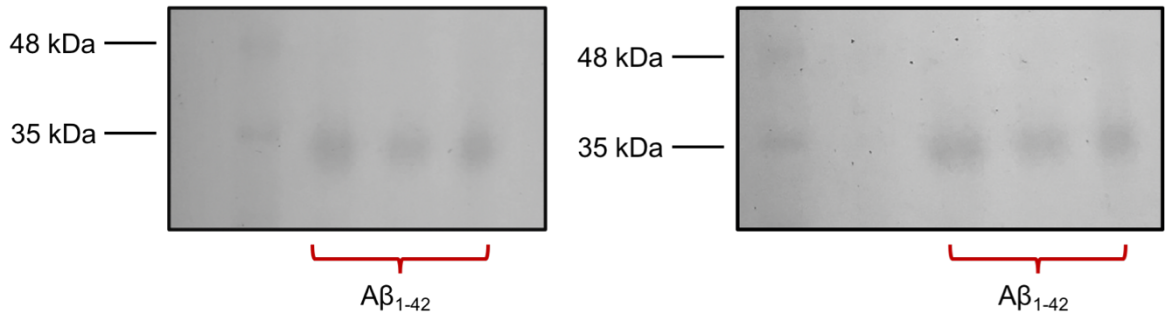

Figure 2.1 $A\beta_{1-42}$ bands following native tricine-PAGE and Coomassie Brilliant Blue staining. Monomeric $A\beta_{1-42}$ has a molecular weight of 4.51 kDa. Thus, following the oligomerisation protocol, acquired $A\beta_{1-42}$ were hexa/heptamers.

2.3. Cell culture

2.3.1. BV-2 microglia

The murine BV-2 immortalised microglial line (from C57BL/6 mice) which is known to express Fpr2/3 (McArthur et al., 2010; Ries et al., 2016), was used as a model system. It was a generous gift from Dr E. Blasi (Department of Hygienic, Microbiological and Biostatistical Sciences, Modena, Italy). BV-2 cells were cultured in Dulbecco's Modified Eagle's Medium (DMEM) with 15 mg/L phenol red, 4 mM L-glutamine and 4.5 g/L glucose, supplemented with heat-inactivated fetal calf serum (hiFCS, 5% final), 100 µM non-essential amino acids (NEAAs), and 50 mg/ml penicillin-streptomycin. Cells were grown in T-75 culture flasks (Sarstedt Limited, Leicester, UK), at 37°C in a humidified incubator (5% CO_2 and 95% air). Medium was changed and cells were sub-cultured three times a week. The passage range used was p33-p53, unless otherwise indicated.

2.3.1.1. Routine sub-culturing

Cells were observed under the microscope and confluency estimated. Upon reaching 70% confluency, cells were prepared for sub-culturing. Spent medium was aspirated and cells were washed with room temperature phosphate buffered saline (PBS-/-; 0.01 M, no Ca^{2+} or Mg^{2+}). Cells were removed by the gentle use of a Corning cell scraper (Sigma-Aldrich Corporation, Dorset, UK) in fresh medium, before cell numbers were calculated using a Neubauer haemocytometer (Agar Scientific, Stansted, UK). Cells were then centrifuged at 800 g for 5 min at 22°C and resuspended in warm medium prior to re-plating in fresh flasks, at 30,000 cells/cm^2.

2.3.1.2. Experimental sub-culturing

Cells were washed, collected, counted and centrifuged as described for routine sub-culturing. However, instead of being re-plated in cell culture flasks, BV-2 microglia were seeded onto experimental assay tissue culture plates. The relative densities for different culture plates are shown in Table 2.1. Relative densities for each experiment will be detailed in appropriate methodological sections. Any differences were recommended and applied according to manufacturer's instructions. For experimentation, cells were plated and allowed to adhere for 2 h prior to serum-starvation for 24 h in DMEM supplemented with 4 mM L-glutamine, 100 µM NEAAs, and 50 mg/ml penicillin-streptomycin at 37°C in 5% CO_2 and 95% air overnight. Any cell density changes applied were due to manufacturer assay protocols.

Table 2.1 Relative seeding densities for BV-2 microglia on different cell culture plates.

Culture Plate	Cell Density (cells/cm^2)
6 Well Plate	100,000
12 Well Plate	100,000
24 Well Plate	150,000
Agilent Seahorse 24 Well Plate	1,800,000
96 Well Plate	200,000
Tissue Culture Chamber Slides	21,500

2.3.2. SH-SY5Y neuroblastoma

The human neuroblastoma SH-SY5Y cell line was purchased from the European Collection of Authenticated Cell Cultures (ECACC, Salisbury, UK). SH-SY5Y cells were cultured in DMEM supplemented with 15 mg/L phenol red, 4 mM L-glutamine, 4.5 g/L glucose, 5% hiFCS, 100 µM NEAAs and 50 mg/ml penicillin-streptomycin, with medium changed three times a week. Cells were sub-cultured once a week and incubated at 37°C in 5% CO_2 and 95% air. Maximum passage used was p20, since ECACC have reported that SH-SY5Y cells begin to lose their neuronal characteristics beyond this passage number.

2.3.2.1. Routine sub-culturing

When a visually estimated confluency of 80% was reached, spent medium was aspirated, and cells were washed in room temperature PBS-/-. SH-SY5Y cells were then exposed to trypsin-EDTA (2,500 and 380 mg/L respectively), solution for 5 min to initiate cellular dissociation from the plastic; trypsin-EDTA was then quenched by the addition of new warmed medium (6x the volume of that for trypsin-EDTA administered). Cells were counted using a Neubauer haemocytometer, before being centrifuged at 800 g for 5 min (22°C). Medium/trypsin/EDTA mixture was aspirated and cells were resuspended in fresh medium and plated at 30,000 cells/cm^2 for sub-culturing.

2.3.2.2. Experimental sub-culturing and neuronal differentiation

Cells were treated as for routine sub-culturing in Section 2.3.2.1 but were seeded on cell culture plates at densities shown in Table 2.2. Cells were plated in DMEM containing 15 mg/L phenol red, 5% hiFCS, 4 mM L-glutamine, 4.5 g/L glucose, 100 µM NEAAs and 50 mg/ml penicillin-streptomycin for 24 h. This was then aspirated and replaced with differentiation medium (DMEM; 1% hiFCS, 10 µM trans-retinoic acid (tRA), 4 mM L-glutamine, 4.5 g/L glucose, 100 µM NEAAs and 50 mg/ml penicillin-streptomycin), previously reported to trigger neuronal differentiation in SH-SY5Y cells (Shipley et al.,

2016). Cells were differentiated for 5 days at 37°C and 5% CO_2, with differentiation media replaced on day 3. On day 5, differentiation media was replaced with standard culture medium (DMEM; 1% hiFCS, 4 mM L-glutamine, 4.5 g/L glucose, 100 µM NEAAs and 50 mg/ml penicillin-streptomycin) for 24 h. Cells were used for experimentation from day 6 onwards. As shown in Figure 2.2, tRA treatment begins to alter the morphology of SH-SY5Y cells on day 3, but neurites do not appear until day 4, before becoming extensive on day 5.

Table 2.2 Plating densities for SH-SY5Y neuroblastoma cells in different culture dishes.

Cell Plate	Cell Density (cells/cm^2)
6 Well Plate	30,000
24 Well Plate	35,000
Tissue Culture Slides	21,500

2.3.3. Cryopreservation and thawing of cell lines

Frozen stocks of both cell lines were produced regularly. Following detachment as described in Sections 2.3.1.1 and 2.3.2.1, cells were centrifuged at 800 g at room temperature for 5 min and resuspended at 1 x 10^6/ml in freezing medium (hiFCS with 1/11th DMSO). 1 ml of cells were added to each 2 ml cryotube before being stored at -80°C in an isopropanol filled Mr. Frosty freezing container (ThermoFisher. Scientific, Dartford, UK). After 24 h, samples were transferred to liquid nitrogen (-196°C) for long term storage.

To thaw these stock samples, frozen vials were slowly defrosted at room temperature by immediate dilution with pre-warmed culture medium. Once completely thawed, cells were centrifuged at 800 g for 5 min at room temperature to remove DMSO before being resuspended in culture medium as described previously. Cells were cultured at 37°C in 5% CO_2 and 95% air overnight, and medium was replaced the following day, removing any dead cells which did not survive the freeze-thaw process.

2.3.4. SH-SY5Y BV-2 co-culture

In SH-SY5Y/BV-2 co-culture experiments, SH-SY5Y cells were differentiated and cultured at a density of 30,000 cells/cm^2 as described in Section 2.3.2.2. On day 5, differentiation medium was replaced with fresh standard culture medium. At the same time, BV-2 cells were collected and seeded onto the plates at a density of 25,000 cells/cm^2. On day 6, medium was replaced before drug treatment. The identification of both cell types is shown in Figure 2.3.

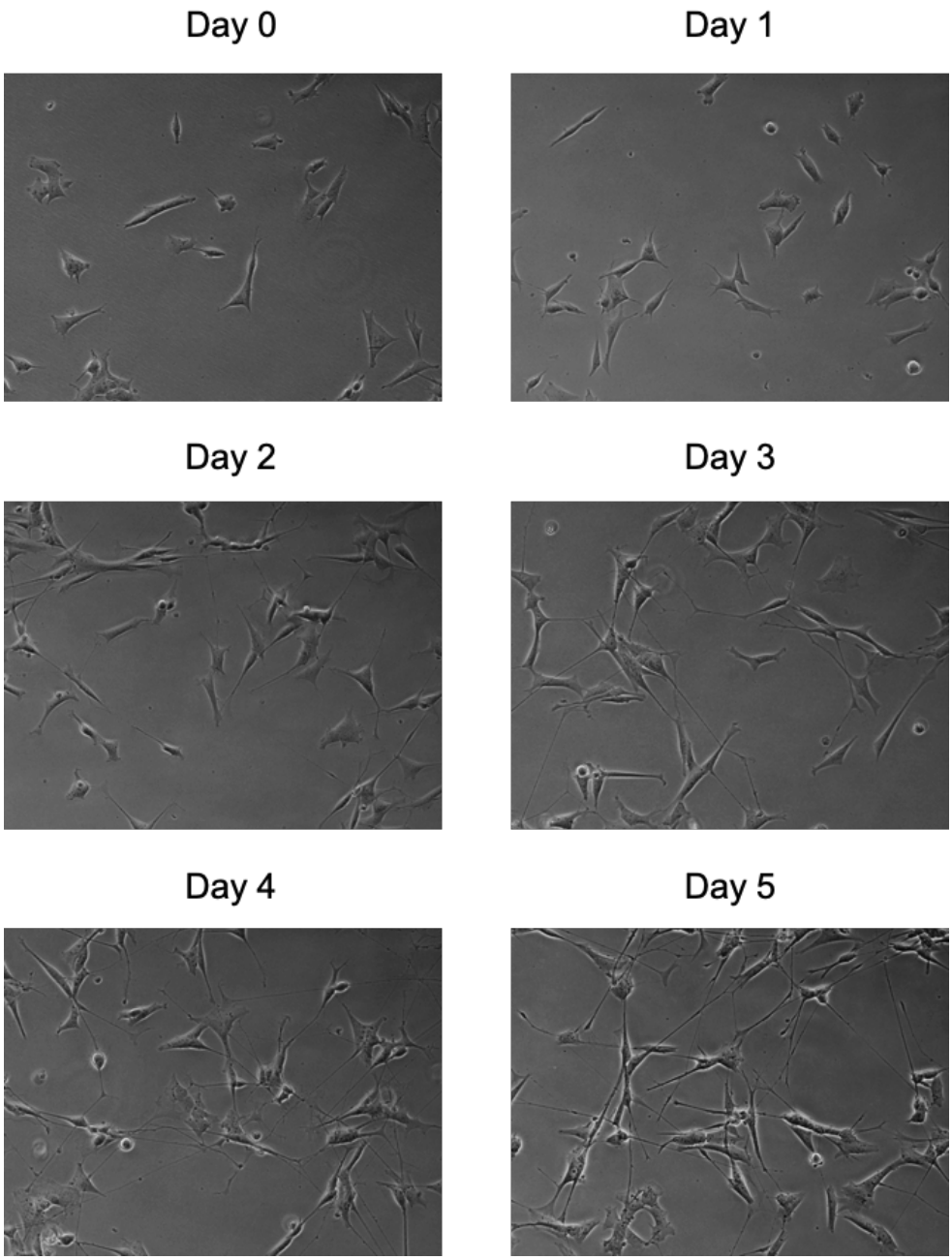

Figure 2.2 Phase-contrast photomicrographs of tRA-induced SH-SY5Y differentiation over 5 days. After day 3, cells morphology changes can be detected, with neurites clearly evident at days 4 and 5. 20x magnification

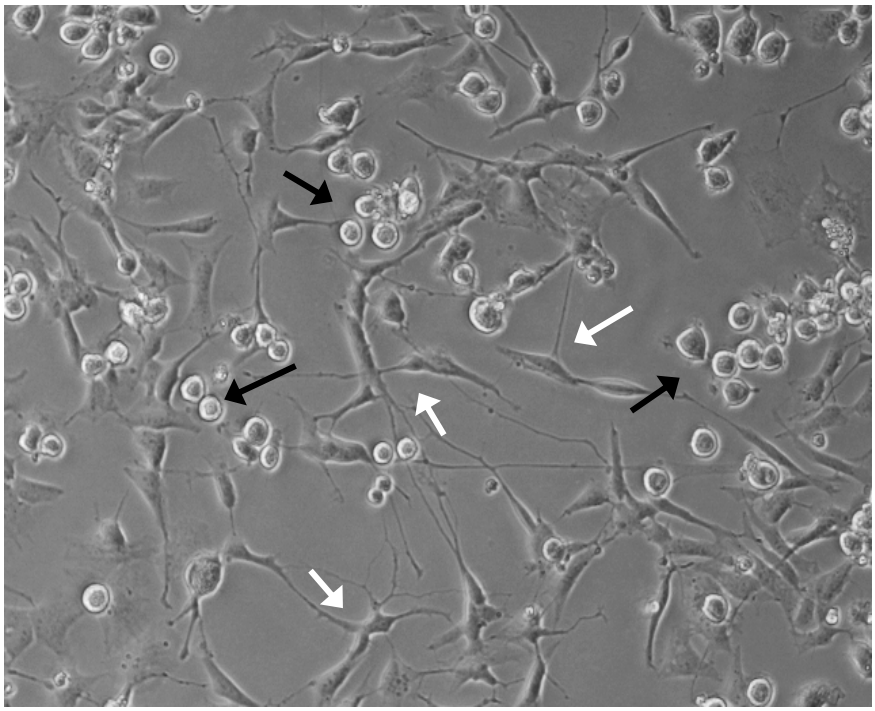

Figure 2.3 20x phase-contrast micrographs of BV-2-SH-SY5Y co-culture. BV-2 microglia (black arrows) are primarily spherical cells, with some exhibiting a few small processes. SH-SY5Y cells (white arrows) express extended neurite processes following a 5-day differentiation protocol in tRA. Images were taken on day 6, a day after BV-2 administration. 20x magnification.

2.3.5. Primary murine microglia isolation and culturing

Male wild-type or Fpr2/3$^{-/-}$ C57Bl/6 (Fontaine and Davis, 2016; Vital et al., 2016) mice aged 8-9 weeks were anaesthetised by intraperitoneal (i.p.) injection of sodium pentobarbitone (100 µl/mouse). Animals were then transcardially perfused with ice-cold sterile 0.9% saline, before brains were collected into collection buffer (ice-cold sterile PBS-/- with 15 mM HEPES, 0.5% D-Glucose and 50 mg/ml penicillin/streptomycin) on ice. 5 ml ice-cold PBS-/- was then added to a sterile Petri dish, before brains were transferred from the collection buffer. Brain tissue was chopped into fine pieces (approximately 1 mm^3) with a sterile scalpel blade. Tissue fragments were collected, centrifuged at 300 g for 2 min at 4°C and supernatant aspirated. 5 ml pre-warmed (37°C) enzyme buffer (PBS-/- with 20 mM HEPES, 40 µM BSA solution, 200 U/ml deoxyribonuclease I (Sigma-Aldrich Corporation, Dorset, UK), 5 mM L-Cysteine, 5 mg/ml D-Glucose, 1.5 U/ml Papain (Sigma-Aldrich Corporation, Dorset, UK) and 50 mg/ml penicillin/streptomycin) was added and fragments were incubated at 37°C for 30 min with occasional agitation and trituration with a 1 ml Gilson pipette. Resulting cell suspensions were passed through a 40 µm cell strainer and centrifuged at 300 g for 10 min at room temperature. The cell pellet was re-suspended in ice-cold 0.9 M sucrose in PBS-/- and centrifuged at 800 g for 10 min at 4°C to remove myelin debris. Cells were washed and resuspended in cold PBS-/- at 300 g for 10 min (4°C).

Microglia were isolated from crude cell digests by Percoll density gradient separation (De Haas et al., 2007). Each cell pellet was resuspended (3.5 ml/brain) in ice-cold 75% Percoll in PBS-/- and slowly overlayed with 5 ml ice-cold 25% Percoll in PBS-/-, then with 3.5 ml ice-cold PBS-/-. Gradients were centrifuged at 800 g for 30 min at 4°C without braking, and the cells at the 25/75% interphase were collected. Cells were washed in 3x volumes of ice-cold PBS-/-, centrifuged at 1000 g for 10 min at 4°C and resuspended in warmed culture medium (DMEM with L-glutamax, 20% hiFCS and 50 mg/ml penicillin/streptomycin) and plated at 150,000 cells/cm^2. Cells were given 3 h to adhere, before medium was replaced with fresh culture media. Medium was changed every 4 days. Microglia were ready for experimentation 2 weeks after initial plating.

2.4. SDS-PAGE and western blot

Expression of phosphorylated and total ERK$_{1/2}$, p38 mitogen activated protein kinase (p38), alongside total expression of haem oxygenase-1 (HO-1), iNOS, IκBα, AnxA1 and superoxide dismustase 2 (SOD2) were examined by SDS-PAGE and western blot. Cells were serum-starved overnight and treated according to the experimental design. Supernatant was aspirated and cells were lysed in 150 µl pre-cooled RIPA lysis buffer (pH 8, 150 mM NaCl, 50 mM Tris, 1% Triton X-100, 0.5% deoxycholic acid, 0.1% sodium dodecyl sulfate (SDS), and phosphatase/protease tablets (Roche Holding, Basel,

Switzerland; 1 of each per 10 ml of RIPA buffer) were added. Cell lysates were then subjected to 5 rounds of freeze-thawing on dry ice.

Protein content was determined using Bradford's reagent (Walker and Kruger, 2003), and a standard curve of BSA (0.2 - 1 mg/ml; Figure 2.4). Equal amounts of protein samples (40 µg) were added to 6x Laemmli SDS sample buffer (375 mM Tris-HCl, 9% SDS, 50% glycerol, 9% beta-mercaptoethanol, 0.03% bromophenol blue, pH 6.8; Alfa Aesar, Lancashire, UK), and heated at 97°C for 5 min, prior to centrifugation at 800 g for 2 min at 4°C. Samples were then loaded into an appropriate gel, depending on the molecular weight ladder of the protein of interest (Table 2.3) within an OmniPAGE mini vertical system (Cleaver Scientific, Rugby, UK) alongside 2 µl of pre-stained Prism Ultra broad molecular weight (10-245 kDa; Abcam, Cambridge, UK). Electrophoresis was performed at room temperature for approximately 1 h using a constant voltage (180 V) and current (60 mA), utilising a nanoPAC-300 (Cleaver Scientific, Rugby, UK) in NuPAGE MOPS SDS running buffer (50 mM MOPS, 50 mM Tris base, 1 mM EDTA, 0.1% SDS, pH 7.7; ThermoFisher Scientific, Dartford, UK).

Following electrophoresis, proteins were transferred to polyvinylidene fluoride (PVDF) membranes (pre-activated by incubation in methanol for 1 min, 0.2 µm pore; Bio-Rad Laboratories, Watford, UK) in 25 mM Tris-base, 0.2 M glycine, pH 7.4 at 400 mA for 90 min using an OmniPAGE mini vertical system on ice. Protein transfer was confirmed by visualisation with Ponceau S red (Alfa Aesar, Lancashire, UK) and membranes were blocked in either 5% BSA (ThermoFisher Scientific, Dartford, UK) or non-fat milk for 1 h, depending on the primary antibody. Membranes were then washed in TBS, before probing with primary antibodies (dilutions as in Table 2.8) overnight at 4°C, Membranes were washed with TBS-T and incubated with horseradish peroxidase (HRP)-conjugated goat anti-mouse rabbit secondary antibodies for 1 h (1:5000 dilution). Membranes were washed extensively in TBS-T and protein was visualised by enhanced chemiluminescence (2.5 mM luminol, 0.4 mM p-coumaric acid, 7.56 mM H_2O_2 in 1 M Tris, pH 8.5) using X-ray film (Scientific Laboratory Supplies Limited, Nottingham, UK). For phosphorylated blots, the total protein per-well was used as protein loading controls. For all other experiments, red Ponceau S stain was employed.

For phosphorylated/total protein blots, following initial ECL exposure to detect phosphorylated proteins, membranes were washed in TBS-T, before the HRP enzyme was inactivated by administration of 10 M H_2O_2 for 15 min at 37°C. Membranes were then washed with TBS-T three times for 5 min prior to re-blocking with 5% BSA or non-fat milk for 1h. PVDF membranes were then re-probed and bands visualised as previously described. Quantification of band density was determined through densitometric analysis using NIH ImageJ 1.50 software (National Institute of Health, Maryland, USA).

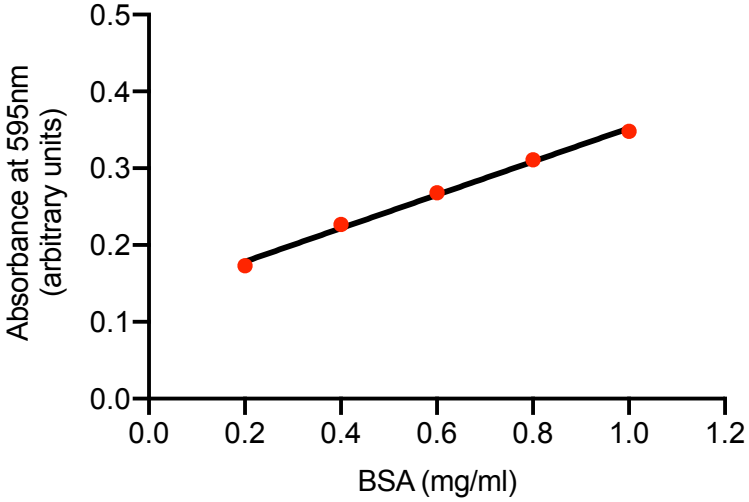

Figure 2.4 Standard curve of BSA for the Bradford reagent. Relative concentrations of samples were determined through the linear regression line from the data.

Table 2.3 The weight (kDa) of proteins of interest targeted for western blotting. The respective acrylamide gel percentages which used for each protein is also shown.

Protein	Protein size (kDa)	Gel (%)
SOD2	22	15%
HSP27	27	15%
HO-1	28	15%
p38 MAPK	38	10%
IκBα	39	10%
Annexin A1	40	10%
ERK1/2	44/42	10%
AMPK	62	10%
iNOS	130	8%

2.5. Flow cytometry

2.5.1. Fluorochromes, lasers and filters

For all flow cytometry experiments, a BD FACSCanto II (BD Biosciences, Berkshire UK) flow cytometer equipped with three lasers (405 nm violet, 488 nm blue, and 633 nm red) was used, see Table 2.4. A number of different fluorochromes were used in this project, as listed in Table 2.5, alongside the type of experiment that they were used in.

Table 2.4 Fluorescent signals (fluorochromes) which can be detected by the BD FACS Canto II flow cytometry system.

Fluorochrome	Fluorescence	Maximal Excitation/Emission Filter wavelengths (nm)
405 nm Violet		
Pacific Blue	Blue	401/452
AmCyan	Green	475/491
488 nm Blue		
FITC	Green	494/520
PE	Yellow	496/578
PerCP-Cy5.5	Far Red	482/676
Pe-Cy7	Far Red	496/785
633 nm Red		
APC	Red	650/660
APC-Cy7	Far Red	650/785

Table 2.5 A list of antibodies, molecules and conjugated fluorochromes alongside the respective lasers and filters used for flow cytometry analysis. APC, allophycocyanin; DAPI, 4', 6-diamidino-2-phenylindole; FITC, fluorescein isothiocyanate; FPR2, formyl peptide receptor 2; HPF, hydroxyphenyl fluorescein; IgG, immunoglobulin G; PE, phycoerythrin.

Antibody/Molecules	2nd Antibody/ Conjugates/ Fluorochrome	Laser	Filter	Experiment	Section
Annexin A1	Alexa Fluor-goat anti-mouse IgG	Blue	FITC	Annexin A1 Expression	2.11
Annexin V	FITC	Blue	FITC	Annexin V/PI	2.7.3
CD11b	APC	Red	APC	BV-2 Phenotyping	2.5
CD38	APC	Red	APC	BV-2 Phenotyping	2.5
CD40	APC	Red	APC	BV-2 Phenotyping	2.5
CD68				BV-2 Phenotyping	2.5
CD86	FITC	Blue	FITC	BV-2 Phenotyping	2.5
CD200	PerCP-Cy5.5	Blue	PerCP-Cy5.5	Co-Culture Apoptosis	2.7.3
CD206	PE	Blue	PE	BV-2 Phenotyping	2.5
CM-H_2DCFDA	FITC	Blue	FITC	ROS Production	2.12.1
DAPI	DAPI	Violet	Pacific Blue	Cell Cycle	2.7.2
E.Coli BioParticles	BODIPY FL	Blue	FITC	BV-2 Phagocytic Capacity	2.13
FPR2	Alexa Fluor 488-goat anti-mouse IgG	Blue	FITC	SH-SY5Y FPR2 Expression	2.6
HPF	FITC	Blue	FITC	Hydroxyl/Peroxynitrite Detection	2.12.4
2-NBDG	7-nitrobenzofurazan	Blue	FITC	Glucose Uptake	2.15.2

2.5.2. Cell Gating and controls

Live cells were initially gated according to forward scatter (FSC) and side scatter (SSC) as indicators of size and granularity, respectively, as shown in Figure 2.5A. Debris and dead cells often express a lower level of FSC and are often found in the bottom left corner of the histogram plot with appropriate voltage and gain settings (Figure 2.5A). Dead cells can also have increased an autofluorescent signal hence why a cell gate was selected around the population of interest. Aggregated cells were excluded by further comparison of FSC signal peak height with peak area, with events showing a non-linear relationship between the two

being excluded (Figure 2.5B). This second step was not included in the analysis of co-culture experiments given the ability of microglia to phagocytose (Solito and Sastre, 2012) and hence aggregate with other cells. A total of 10,000 singlet events were analysed in each experiment per sample, except for co-culture assays, where 50,000 events per sample were used. Data was analysed using Flow Jo 8.8.7 software (Tree Star Incorporated. OR, USA).

Several controls were used for all flow cytometry experiments. This included an unstained population of cells to determine any autofluorescence, alongside single stained controls which reveal spectral overlap between two or more different fluorophores, allowing for removal by compensation when analysing. Finally, a Fc receptor blocking control antibody (1 µg/ml CD16/32; ThermoFisher, Dartford, UK) was utilised for IgG experimental antibodies, to ensure only antigen specific binding was observed.

2.6. Cell surface marker expression

Expression of pro-inflammatory (CD11b, CD38, CD40, CD86) and anti-inflammatory (CD206) cell surface markers was detected by flow cytometry. Cells were collected and fixed with 2% formaldehyde in PBS-/- 0.01 M for 10 min at 4°C, washed twice in PBS-/- prior to incubation in blocking buffer (0.01 M PBS-/-, 1 µg/ml CD16/32 Fc-receptor block, 1% FCS, 1 mM $CaCl_2$) on ice for 15 min. Following centrifugation at 1000 g for 1 min, cell pellets were resuspended in appropriate antibody mix (Table 2.6) in PBS-/- on ice in the dark for 30 min. Cells were centrifuged at 1000 g and washed in 4°C PBS-/- and kept on ice until analysed using a BD FACSCanto™ II system as described in Section 2.5. Representative histograms for CD11b and CD38 expression in BV-2 microglia are shown in Figure 2.5.

Table 2.6 List of conjugated antibodies used for BV-2 phenotypic analysis by flow cytometry. The maximal experimental concentrations used alongside the appropriate dilution factors have also been listed. Experimental concentration of antibody mix was per million cells in 100 µl volume.

Antibody	Clone	Company	Maximal Experimental Concentration	Dilution
CD11b-APC	M1/70	BioLegend®	2.5 µg/ml	1:80
CD38-APC	90	BioLegend®	2.5 µg/ml	1:80
CD40-APC	1C10	BioLegend®	10 µg/ml	1:20
CD45-PE	30-F11	BioLegend®	2.5 µg/ml	1:80
CD86-FITC	GL1	BioLegend®	2.5 µg/ml	1:80
CD206-PE	C068C2	BioLegend®	5 µg/ml	1:40

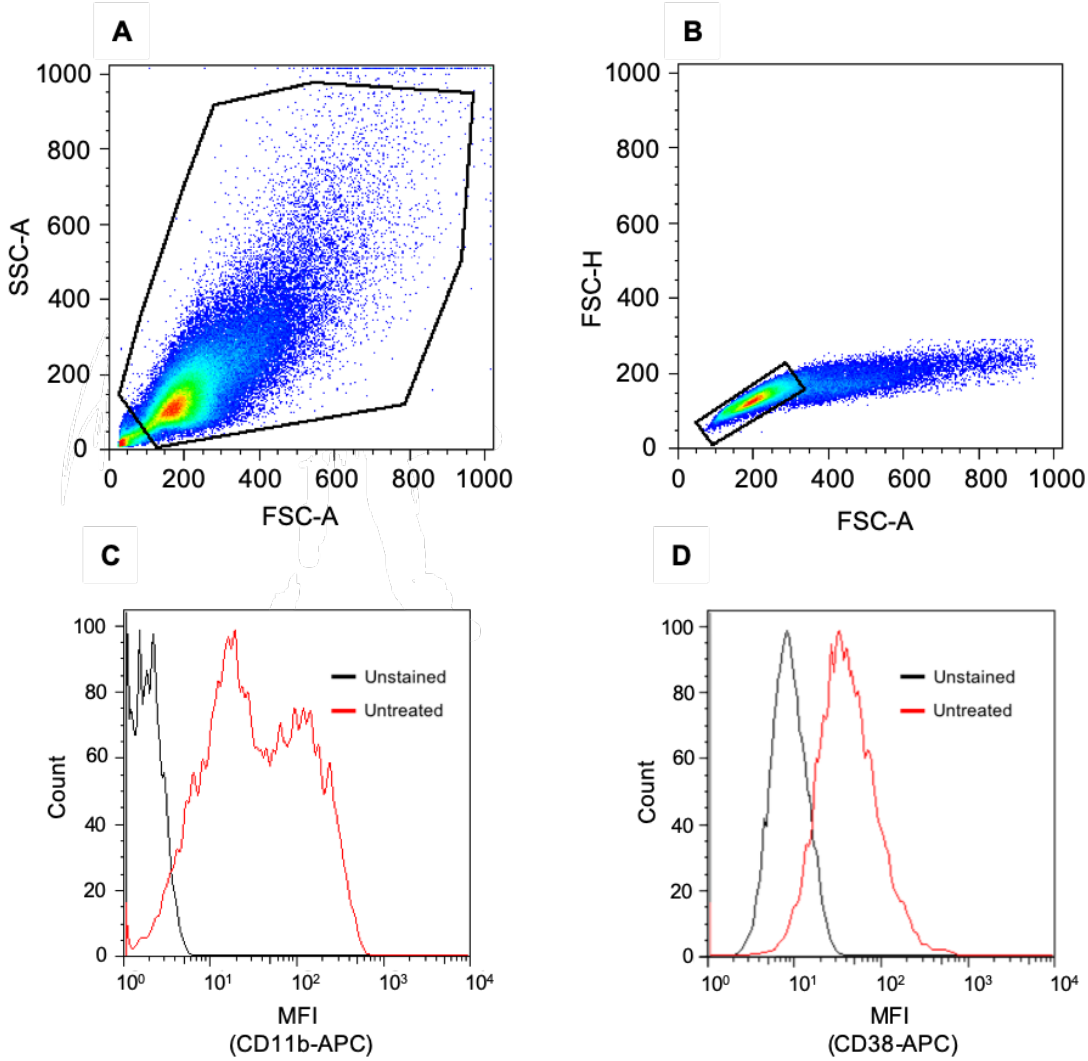

Figure 2.5 Flow cytometry gating strategy and histogram traces for cell surface marker fluorescence. A; cell gating around living population. Debris (bottom left corner) were excluded. **B**; gating strategy to identify singlet events. **C** and **D**; representative histograms for CD11b and CD38 staining in BV-2 microglia respectively. Samples are unstained (black) and untreated (red). Marker expression was recorded via flow cytometry 48 h after plate seeding. MFI, median fluorescence intensity.

2.7. Immunofluorescence

For immunofluorescent staining and visualisation, cells were fixed in 2% formaldehyde in PBS-/- for 10 min at 4°C and washed in PBS-/-, before being blocked for 30 min with PBS-/- containing 10% hiFCS ± 0.05% Triton-X 100. Cells were then incubated with appropriate primary antibody in PBS-/- with 1% FCS ± 0.05% Triton-X 100 overnight at 4°C. Cells were washed twice in PBS-/- with 1% hiFCS ± 0.05% Triton-X 100, before being incubated with secondary antibody in PBS-/- with 1% hiFCS ± 0.05% Triton-X 100 at room temperature for 1 h. For FPR2 staining only, cells were then washed in PBS-/- and incubated with the plasma membrane marker CF640R conjugated wheatgerm agglutinin (5 ug/ml) for 20 min at room temperature. For all other immunofluorescent stains, cells were then washed in PBS-/- and incubated with AF488-conjugated phalloidin (1:1000 dilution), which also stains the plasma membrane, for 20 min at room temperature. These plasma membrane stains were added to the secondaries for the last 20 min of secondary antibody exposure. Cells were then washed in PBS-/- three times. Nuclei were defined by incubation with 4', 6-diamidino-2-phenylindole (DAPI), 180.3 nM) in ddH_2O for 5 min, prior to rinsing with ddH_2O. Cells were then mounted under Mowiol mounting solution (10% w/v Mowiol with 25% v/v glycerol, 25% v/v ddH_2O, 0.02% w/v sodium azide, 50% v/v tris.HCl, pH 8.5; Harlow and Lane, 2006). Slides were kept in the dark before images were taken using the LSM 710 Meta Confocal microscope and ZEN Black software (Zeiss, Cambridge, UK) or the Leica DM5000 B, as appropriate (see Table 2.7).

2.7.1. NADPH oxidase co-localisation

BV-2 microglia were plated on tissue culture slides (ThermoFisher Scientific, Dartford, UK) at a density of 21,500 cells/cm^2 before being serum starved for 24 h. Cells were then treated according to experimental design, washed once with pre-warmed PBS-/- and fixed in 2% formaldehyde in PBS-/- for 10 min at 4°C and blocked as described in Section 2.6. Cells were then incubated at 4°C overnight with primary anti-mouse monoclonal and rabbit polyclonal antibodies for gp91phox (NOX2) and p67phox, respectively. Cells were washed twice with PBS-/- containing 1% hiFCS and 0.05% Triton X-100 and incubated with AF647-goat anti-rabbit and AF488-goat anti-mouse secondary antibodies for 1 h at room temp in the dark. Cells were washed with PBS-/- and nuclei were identified by incubation with DAPI (80.3 nM) for 5 min in ddH_2O. Cells were then mounted with Mowiol and imaged using a LSM 710 Meta Confocal microscope and ZEN Black software (Zeiss, Cambridge, UK). The 405 nm and 488 nm lasers were used for visualisation of DAPI and gp91phox, respectively. The 633 nm laser was selected for identification of p67phox.

Table 2.7 Primary and secondary antibodies used for immunofluorescence observation, alongside appropriate filters and lasers used for each. The 405 nm laser with BP 365 FSET01 filter was used to detect DAPI fluorescence on the LSM 710.

Primary Antibody	Source	Secondary Antibody	Source	Microscope	Laser	Filter
gp91phox (NOX2)	Mouse	Alexa Fluor ® 488	Goat	LSM 710	488 nm	FSet10 FITC
p67phox	Rabbit	Alexa Fluor ® 647	Goat	LSM 710	633 nm	647
NF-kB p65	Rabbit	Alexa Fluor ® 647	Goat	LSM 710	633 nm	647

2.7.2. NF-κB nuclear translocation

Cells were plated on tissue culture slides and treated according to experimental design before being fixed and blocked as described in Section 2.7. Cells were then incubated with a primary rabbit anti-mouse antibody for NF-κB p65 (1:400 dilution) overnight at 4°C. Cells were then washed as described previously and incubated with AF647-goat anti-rabbit secondary antibody for 1 h at room temperature in the dark. Cells were washed, nuclei identified and mounted as described in Section 2.7. Cells were imaged using an LSM 710 Meta Confocal microscope and ZEN Black software (Zeiss, Cambridge, UK). Filter set 10 was used for visualisation of DAPI with the 405 nm laser, whilst NF-κB was detected using the 633 nm laser with the 647 filter.

2.8. Cell viability, cell cycle and apoptosis assays

2.8.1. PrestoBlue cell viability assay

Cell viability was determined using the PrestoBlue cell viability reagent, 24 h and 48 h after drug administration. This non-toxic resazurin-based assay measures the mitochondrial activity of viable cells and reflects their intracellular redox state (Boncler et al., 2014). PrestoBlue solution diluted 1:10 in PBS-/- was added to cells and incubated at 37°C in the dark for 15 min. Fluorescence was measured using a CLARIOstar microplate reader (BMG Labtech, Aylesbury, UK), with excitation and emission filters set at 560 and 590 nm, respectively. All drugs had their fluorescence measured in PBS-/- without cells to determine quenching and to confirm they did not contribute to alterations in the fluorescent signal. Background correction was performed using unlabelled cells in PBS-/-. Data were expressed as percentage of untreated cells.

2.8.2. Analysis of cell cycle

BV-2 cells were seeded at 100,000 cells/cm^2 and treated according to experimental design. Cell medium was aspirated, cells were washed twice in warm PBS-/- and collected in ice cold PBS-/-. Following centrifugated at 800 g for 5 min, cells were resuspended in 0.1% Triton-X 100 and 3.6 µM DAPI in 200 µl PBS-/- for 10 min at room temperature in the dark. Samples were then immediately analysed by flow cytometry, with the violet laser and pacific blue filter used to determine DAPI fluorescence. A typical cell histogram profile is shown in Figure 2.6.

2.8.3. Annexin V apoptosis assay

SH-SY5Y cells were differentiated as described in the Section 2.3.2.2 and treated according to experimental design, either alone or in co-culture with BV-2 microglia. Cells were washed with PBS-/- and centrifuged at 1000 g for 5 min at room temperature. Cells were then resuspended in binding buffer (0.01 M PBS-/- with 0.1% BSA and 1 mM $CaCl_2$) containing annexin A5-FITC (0.45 µg) before being incubated at room temperature in the dark for 15 min. After incubation, 400 µl of additional binding buffer was added to the cell suspension, and gently mixed. Samples were kept on ice in the dark, until analysed by flow cytometry, using the 488 nm blue laser and the FITC filter. Single stains were used for compensation of these fluorochromes. A typical annexin V-FITC profile for SH-SY5Y cells is shown in Figure 2.7. For co-culture with BV-2 microglia, SH-SY5Y cells were separated using the neuronal marker CD200-PerCP/Cy5.5 and microglial marker CD11b-APC.

2.9. Nitrite determination by Griess assay

As nitric oxide is too short-lived in solution to easily measure directly, its stable oxidative metabolite, nitrite (NO_2-) was used as a proxy marker, detected using the Griess reaction (Bryan and Grisham, 2007). Following serum starvation for 24 h, BV-2 cells were treated according to experimental design, with cell supernatant collected and incubated 1:2 with Griess reagent (3.85 µM napthylethylenediamine dihydrochloride, 58.1 µM sulphanilamide, 5% ortho-phosphoric acid), at room temperature in the dark for 15 min. Absorbance was detected at 540 nm with a CLARIOstar microplate reader (BMG Labtech, Aylesbury, UK), with background correction performed using absorbance values of media alone. Absorbance was calculated against a standard curve of sodium nitrite ($NaNO_2$, 1.56 - 100 µM**;** Figure 2.8). The Griess assay has a sensitivity limit of 3 µM (Misko et al., 1993); any values below this were considered ‘non-detectable’.

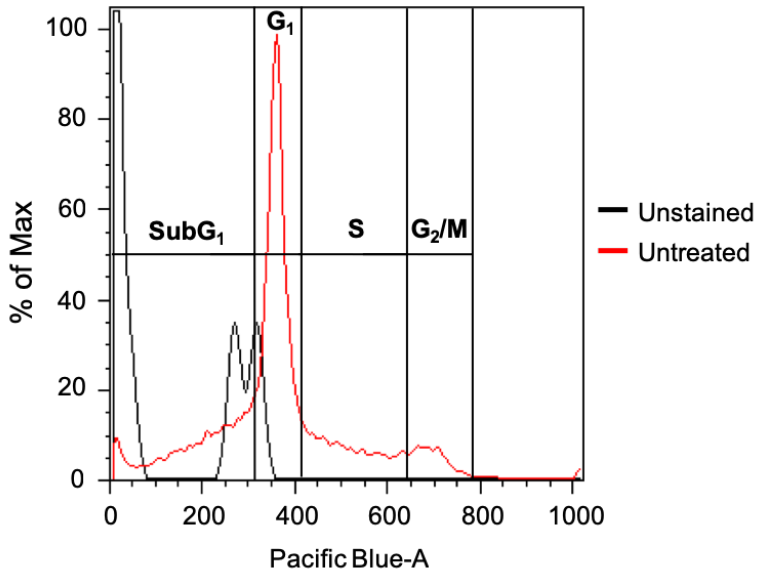

Figure 2.6 DAPI cell cycle histogram of BV-2 microglia. Appropriate gates have been included to highlighting the different areas which correlate to respective components of the cell cycle.

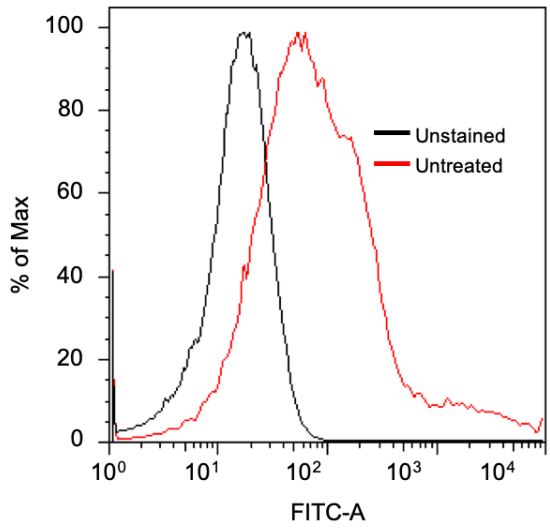

Figure 2.7 Annexin A5-FITC stained and unstained cells, identified with flow cytometry. Stained cells are red, with unstained represented by the black curve, respectively. The cell population consists of both SH-SY5Y and BV-2 cells.

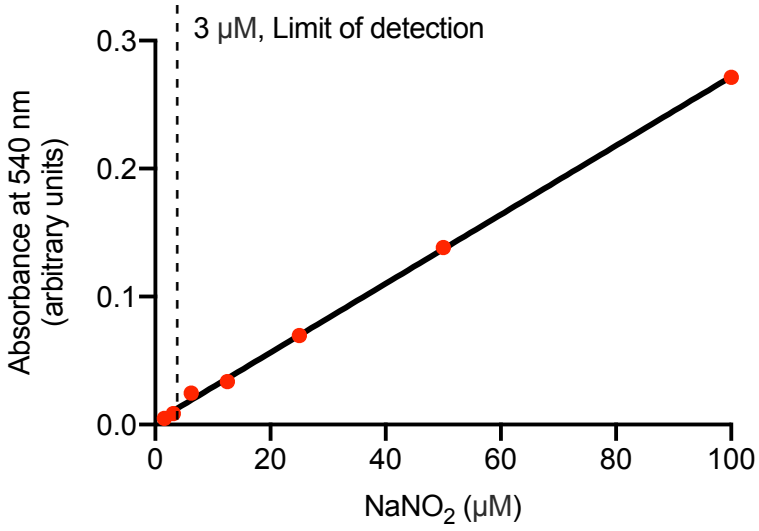

Figure 2.8 A standard curve of sodium nitrite, $NaNO_2$. Absorbance was detected at 540 nm using the CLARIOstar microplate reader. Detection limit of the assay is labelled. Absorbance is expressed as optical density, OD.

2.10. Measurement of cytokine levels

TNFα, IL-1β and IL-10 production were determined using commercially available ELISA kits (ThermoFisher Scientific, Dartford, UK), according to the manufacturer's protocol. Following overnight serum starvation, cells were seeded at 100,000 cells/cm^2 and treated according to experimental design. Cellular supernatant was then extracted and centrifuged at 1000 g for 5 min to remove cellular debris, before being frozen at -80^{o}C prior to assay. Following the assay, optical absorbance at 450 nm and 570 nm was assessed using a CLARIOstar microplate reader. Background correction was performed by subtraction of absorbance values at 570 nm. TNFα, IL-1β and IL-10 concentrations were calculated by comparison with a standard curve for each cytokine (TNFα: 15.875-1000 pg/ml; IL-1β: 15.875-1000 pg/ml; IL-10: 62.5-4000 pg/ml). Representative standard curves for each cytokine are shown in Log_{10} scale in Figure 2.9. The sensitivity limits of TNFα and IL-1β were 8 pg/ml, whilst that for IL-10 was 5 pg/ml. A power regression equation best fitted the standard curves and was used for determining the concentration of each cytokine released by BV-2 microglia.

2.11. p38 MAPK signalling ELISA

BV-2 microglia were plated at 100,000 cm^2 and treated according to experimental design. Samples were prepared and normalized for use in an InstantOne^{TM} total/phospho multispecies p38 ELISA kit (ThermoFisher, Dartford, UK) according to the manufacturer's instructions.

2.12. Annexin A1 expression

BV-2 microglia were seeded at 100,000 cells/cm^2, serum starved for 24 h and treated according to experimental design. Cells were washed with pre-warmed PBS-/- collected and incubated in PBS-/- with 1% hiFCS, 1 mM $CaCl_2$ for 30 min at room temperature to block non-specific antibody binding. Cells were then incubated with primary rabbit anti-mouse AnxA1 (ThermoFisher, Dartford, UK) diluted 1:1000 in PBS-/- with 1% hiFCS, 1 mM $CaCl_2$ for 1 h at room temperature. For total cellular expression only, 0.05% TX-100 was included for both blocking and antibody treatment steps. Cells were washed and incubated with AF488-conjugated goat anti-rabbit secondary antibody (1:500, ThermoFisher, Dartford, UK) for 30 min at room temperature. Cells were centrifuged at 800 g for 5 min at room temperature, washed, and analysed via flow cytometry.

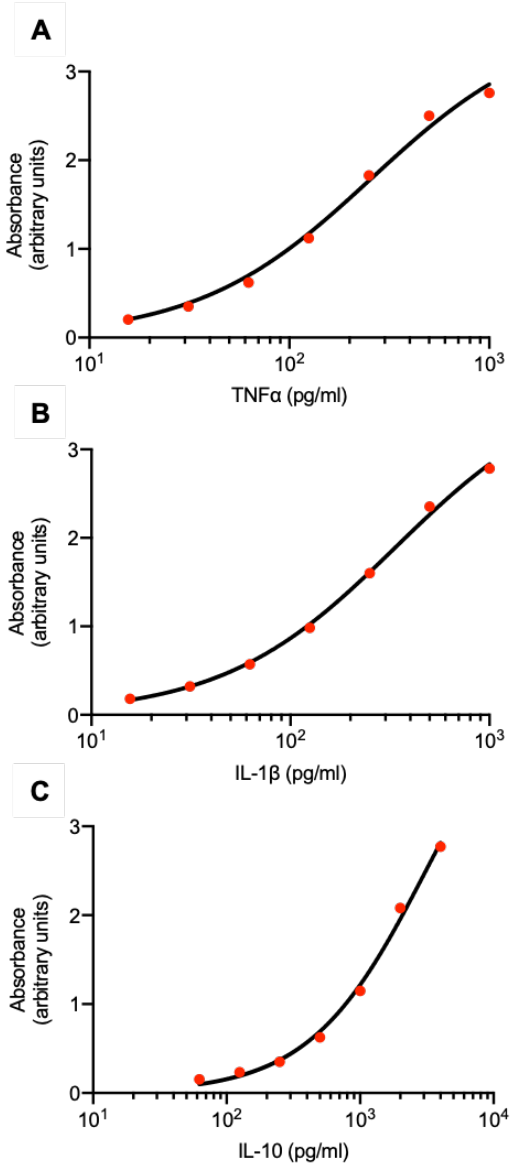

Figure 2.9 Standard curves for Log_{10} TNFα (A), IL-1β (B), and IL-10 (C). Absorbance values expressed as optical density were calculated through the subtraction of values at 570 nm from 450 nm. The curve begins to plateau at higher concentration ranges as the samples reach saturation. Samples were diluted to prevent values towards the upper end of the curve. R^2 = 0.9947, 0.9832 and 0.9993 for TNFα, IL-1β and IL-10, respectively.

2.13. Reactive oxygen species and antioxidant detection

2.13.1. Total intracellular reactive oxygen species detection

Total intracellular ROS production was quantified using the fluorescent tracer, chloromethyl-dichlorofluores-cin-diacetate (CM-H_2DCFDA; Wu and Yotnda, 2011). Cells were plated at 200,000 cells/cm^2 in phenol-red free (PRF) DMEM (phenol red is known to quench fluorescein fluorescence signal (Ettinger and Wittmann, 2014)), and serum starved overnight before being pre-incubated with CM-H_2DCFDA (10 μM) in PRF-DMEM for 20 min at 37°C. The tracer was then removed and replaced with fresh PRF-DMEM for 5 min at 37°C before experimental protocols were undertaken. Fluorescence of the carboxy-DCF product was determined every 5 min for up to 1 h at 37°C using a CLARIOstar plate reader (BMG Labtech, Aylesbury, UK) with excitation and emission wavelengths of 492 nm and 517 nm, respectively. Hydrogen peroxide (100 μM) was used as a positive control for the assay. Cells with no dye and wells with CM-H_2DCFDA alone or in combination with drug treatments but no cells were used as negative controls.

2.13.2. Mitochondrial reactive oxygen species detection

MitoSOX Red (MitoSOX), was used to define mitochondrial superoxide production. Cells were serum starved overnight in PRF-DMEM and pre-treated with 2 μM MitoSOX in PRF-DMEM at 37°C in the dark for 15 min. Following incubation, medium was replaced and fresh PRF-DMEM added. Cells were then treated as per experimental protocol. The mitochondrial respiratory chain complex I inhibitor rotenone (2.5 μM) was administered as a positive control. Detection of ROS was carried out every 5 min for up to 1 h at 37°C using a CLARIOstar (BMG Labtech, Aylesbury, UK) plate reader, set at 37°C with excitation and emission wavelengths of 510 nm and 580 nm, respectively.

2.13.3. Hydrogen peroxide detection

H_2O_2 was detected using a commercial assay (ROS-Glo H_2O_2, Promega, Southampton, UK). BV-2 cells were seeded at 156,250 cells/cm^2 and serum starved overnight in PRF-DMEM. Media was then aspirated and replaced with pre-warmed PBS-/- before H_2O_2 substrate (25 μM) was added alongside experimental treatments, as per manufacturer's instructions. Cells were then incubated at 37°C for 2 h before ROS-Glo detection solution was added to each well. Cells were then incubated for 20 min at room temperature before cell lysates were transferred to a white opaque-based 96-well plate. Detection of relative luminescence units (RLU) was determined using a CLARIOstar microplate reader. Sample

RLU readings were compared to that of a H_2O_2 standard curve (0.013 µM – 10 mM, Figure 2.10A).

2.13.4. Hydroxyl/peroxynitrite detection

Hydroxyl (•OH) radicals and peroxynitrite ($ONOO^-$) ion production were determined using the Fluoro Hydroxyl/Peroxynitrite Assay (Cell Technology Incorporated, California, USA). BV-2 cells were seeded at 100,000 cells/cm^2 and serum starved in PRF-DMEM overnight. Cells were pre-treated with hydroxyphenylfluorescein (HPF; 5 µM, 45 min at 37ºC) then treated immediately according to experimental design; 2 ng/ml of phorbol 12-myristate 13-acetate (PMA) was used as a positive control. HPF-DMEM was then aspirated and cells were washed twice and collected in pre-cold PBS-/- using a Corning cell scraper. Cells were kept on ice in the dark until analysed on a BD FACSCanto II flow cytometer (BD Biosciences, Berkshire UK). Fluorescence was determined using the 488 nm blue laser with the FITC filter. Cellular fluorescence was compared against unstained and PMA treated stained cells.

2.13.5. GSH:GSSG ratio detection

The relative ratios of reduced (GSH) and oxidised (GSSG) glutathione was determined using a commercial assay (GSH:GSSG-Glo, Promega Co, Southampton, UK) according to manufacturer's instructions. Cells were plated at 200,000 cells/cm^2 and serum starved in PRF-DMEM overnight prior to experimental treatment. RLU for cells treated with total vs. oxidised glutathione lysis reagent was determined through comparison to a total glutathione standard curve (0.25 – 16 µM) to calculate the relative GSH:GSSG ratio. The standard curve (Figure 2.10B) was halved to work out the relative GSSG values, as described in the manufacturer's protocol.

2.14. Phagocytic capacity

Phagocytic ability was determined by incubation with BODIPY FL conjugated *Escherichia coli* (K-12 strain) BioParticles (ThermoFisher, Dartford, UK; Ragsdale and Grasso, 1989; Wan et al., 1993). Cells were plated at 100,000 cells/cm^2, serum starved overnight and treated according to experimental design. Cell medium was aspirated and replaced with pre-warmed PBS-/- containing BioParticle conjugates at 50 particles per cell, before being incubated in the dark for 30 min at 37ºC. The PBS-BioParticle supernatant was then removed, and fluorescence of non-engulfed particles was quenched by incubation with 0.2% Trypan blue for 1 min. Cells were washed in PBS-/-, collected, and kept on ice. Fluorescence was determined using a BD FACSCanto II system (BD Biosciences,

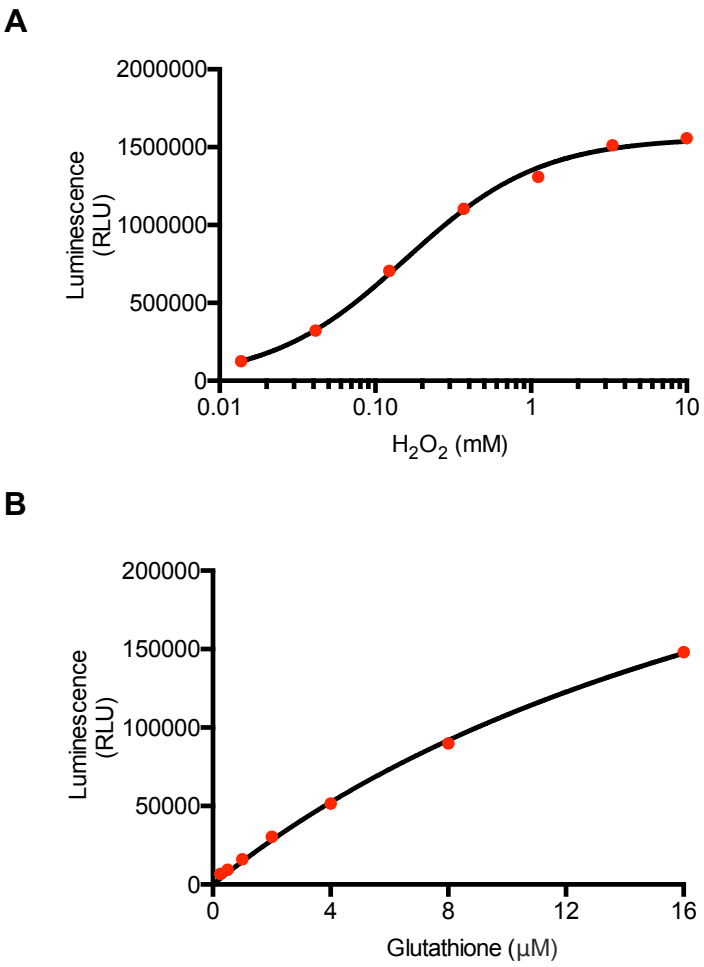

Figure 2.10 Luminescence standard curves for log_{10} H_2O_2 and glutathione. A; Luminescence standard curve for H_2O_2, with RLU identified to plateau around 3 mM. **B**; standard luminescence curve for glutathione. The standard range used was 0.25 to 16 µM. RLU, relative luminescence units.

Berkshire UK), with blue 488 nm laser and FITC filter selected. Samples were compared to cells treated with PBS-/- only. Data were analysed using Flow Jo 8.8.7 software (Tree Star Incorporated. Ashland, USA). Representative histograms of cellular phagocytosis are shown in Figure 2.11.

2.15. Lactate and glucose determination

L-Lactate production and glucose usage were simultaneously determined using a YSI 2300 Stat Plus machine (YSI Life Sciences Inc. Tunbridge Wells, UK). Cells were initially seeded at 70,000, 100,000 and 140,000 cells/cm^2 and serum starved overnight. Cells were then exposed to LPS (50 ng/ml) to determine whether L-lactate production and glucose usage depended on cell plating densities. However, proportional increases in L-lactate production and glucose utilisation were observed at each of the three densities (Figure 2.12A and 2.12B). For the following experiments, cells were plated at 100,000 cells/cm^2 and serum starved overnight prior to experimental treatment. Supernatant was collected and stored at -80^{o}C until required. Linear range of concentration readings for glucose and L-lactate are 50.0 mM/L and 30.0 mM/L respectively, which are suitably spaced from the detection limits of the machine, providing accurate results if values remain below these concentrations.

2.16. Metabolic assays

2.16.1. Glucose 6-phosphate dehydrogenase (G6PD) activity assay

Glucose 6-phosphate dehydrogenase (G6PD) activity was assessed using a commercial assay (Cell Signalling Technology, Massachusettes, USA). BV-2 microglia were seeded at 100,000 cells/cm^2, serum starved overnight in PRF-DMEM and treated according to experimental design. Cells were lysed into ice-cold 1x cell lysis buffer (22 mM Tris-HCl (pH 7.5), 150 mM NaCl, 1 mM disodium EDTA, 1 mM EGTA, 1% Triton-X 100, 20 mM sodium pyrophosphate, 25 mM sodium fluoride, 1 mM β-glycerophosphate, 1 mM sodium orthovanadate, 1 µg/ml leupeptin, 1 mM phenylmethane sulfonyl fluoride, pH 7.5; Cell Signalling Technology, Massachusettes, USA). Samples were then ultrasonicated (two 20 second bursts at 20 kHz per sample) with a Soniprep 150 (BMG Labtech, Aylesbury, UK) on ice, centrifuged at 14000 g for 10 min at 4^{o}C and lysates were collected. Following protein estimation by Bradford's method (Walker and Kruger, 2003), samples were diluted to 0.2 mg/ml in assay buffer and added to an opaque black 96-well plate. Samples were incubated at 37^{o}C for 15 min before relative fluorescence was measured using a CLARIOstar microplate reader (BMG Labtech, Aylesbury, UK), with excitation and emission filters at 540 and 590 nm, respectively.

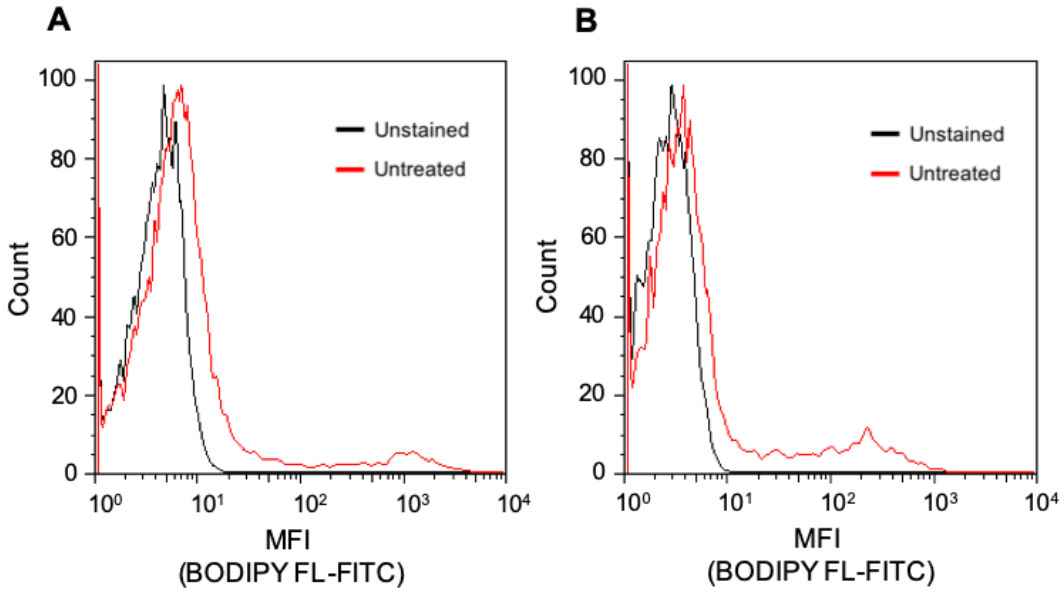

Figure 2.11 FACS histogram showing BODIPY^{TM} FL conjugated *E. coli* fluorescence in BV-2 microglia. A and **B**; fluorescence observed at 24 h and 48 h post-plate seeding, respectively. Samples are unstained (black) and untreated (red).

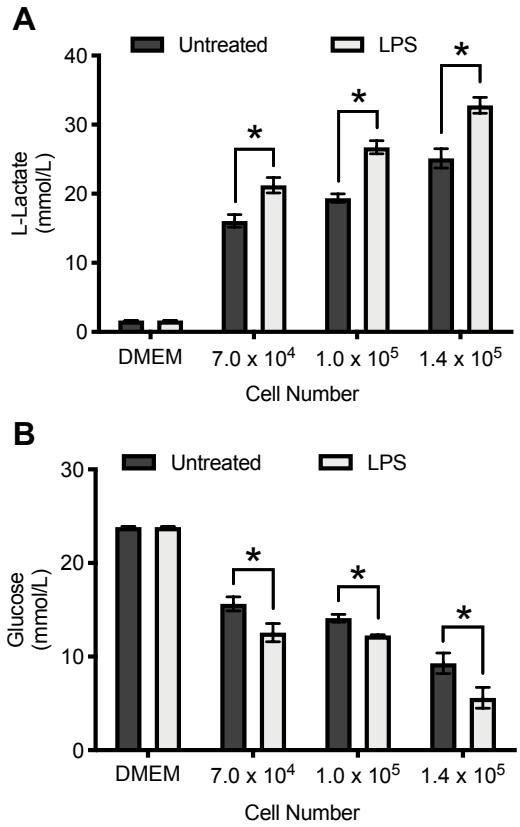

Figure 2.12 LPS (50 ng/ml) induced effects on L-lactate production and glucose usage in BV-2 microglia at different seeding densities. Cells were exposed to LPS for 24 h before supernatant was collected for analysis. **A**; L-lactate production of LPS treated cells compared to untreated. The concentration of L-lactate in DMEM without cells is also shown. **B**; the effect of LPS on glucose concentration in the cellular supernatant at 24 h compared to untreated. Reduced glucose in the medium corresponded to increased glucose usage. Glucose in DMEM alone is also shown. Data are means ± SEM of 3 independent cultures in triplicate. *$P < 0.05$.

2.16.2. Mitochondrial function

Mitochondrial function was assessed using a Seahorse XF24 cell MitoStress Test (Agilent Technologies, California, USA). This test incorporates serial injections of several inhibitors of mitochondrial complex elements and ATP synthase to determine different mitochondrial respiratory functions, including maximal respiration and ATP production. Initially, cells were plated at different seeding densities (1.0, 1.25, 1.5 and 2.0 x 10^6 cells/cm^2) to determine which one was most appropriate for distinguishable data points between the different injection timepoints. 1.5 and 2.0 x 10^6 cells/cm^2 produced the most distinct responses for both oxygen consumption rate (OCR) and extracellular acidification rate (ECAR), with the last assay measurement recorded at 97 min (Figure 2.13A and 2.13B). Due to its lower group variation, 2.0 x 10^6 cells/cm^2 was selected as the plating density for subsequent experiments. Following initial assay set up, BV-2 microglia were cultured at 2 x 10^6 cells/cm^2, serum starved overnight in PRF-DMEM and treated according to experimental design. Medium was replaced with Seahorse XF DMEM supplemented with 1 g/L glucose and 1 mM sodium pyruvate, to both match physiological glucose levels but also to facilitate mitochondrial respiration, respectively, due to XF DMEM not containing any pyruvate. The pH of the medium was then equilibrated to pH 7.4. Cells were incubated at 37°C without CO_2 for 45 min before analysis of oxygen consumption rate (OCR) and extracellular acidification rate (ECAR), allowing for de-gassing of the plate and diffusion of CO_2 from the cells and XF DMEM medium.

Basal respiration was initially determined prior to subsequent serial cellular treatments with 4 µM oligomycin, 0.6 µM FCCP and 1 µM rotenone/antimycin A to measure ATP production, maximal respiratory capacity and non-mitochondrial respiration, respectively. A summary of how each aspect of cellular respiration was calculated and what it means is highlighted in both Figure 2.13 and Table 2.8.

For each treatment, OCR readings were carried out in triplicate, with a reading every 5 min. Cells were then lysed in RIPA buffer and protein content assessed by Bradford's method (Walker and Kruger, 2003) for sample normalisation. Intracellular rates of glycolytic and oxidative ATP production were then quantified utilising a bioenergetics spreadsheet formulated by Ma et al. at the Van Andel Research Institute (Michigan, USA). Data was analysed as guided by the institute website, alongside previous descriptions (Mookerjee et al., 2017).

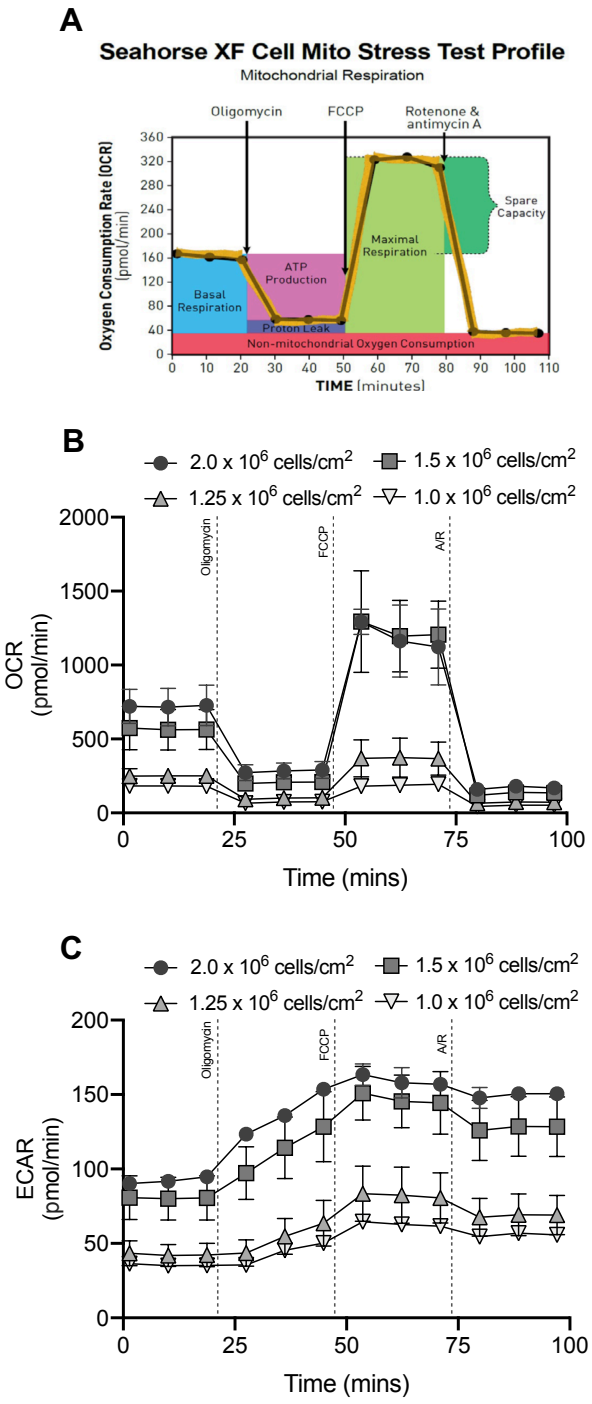

Figure 2.13 The effects of different BV-2 microglial seeding densities on oxygen consumption rate (OCR) and extracellular acidification rate (ECAR) at 24 h. All cells were untreated and cultured in medium containing 1 g/L glucose. OCR and ECAR rates were measured in triplicate per sample at baseline and following serial injection of oligomycin (4 μM), FCCP (0.6 μM) and antimycin A/rotenone (1 μM; A/R). **A**; representative plot of the Seahorse XF Cell Mito Stress Test metabolic profile for OCR. **B**; OCR acquired in this study with different BV-2 microglial cellular densities. **C**; ECAR acquired in this study for multiple BV-2 cellular densities. Data are means ± SEM of 3-4 independent cultures in triplicate.

Table 2.8 List of metabolic parameters and calculations used for Agilent Seahorse data analysis

Parameter	Equation
Basal Respiration	(Last rate measurement before final injection) – (Non-mitochondrial respiration rate)
ATP Production	(Last rate measurement prior to oligomycin injection) – (Minimum rate measurement after oligomycin injection)
Maximal Respiration	(Maximum rate measurement after FCCP) – (Non-mitochondrial respiration)
Spare Respiratory Capacity	(Maximal respiration) – (Basal respiration)
Proton Leak	(Minimum rate measurement after oligomycin injection) – (Non-mitochondrial respiration)
Non-mitochondrial Oxygen Consumption	Minimum rate measurement after rotenone/antimycin A injection

2.17. Antibodies

Antibodies used throughout the project are listed here, alongside their host species, commercial source, catalog number, dilution factor and their application(s).

2.17.1. Primary antibodies

Table 2.9 List of primary antibodies used through the study.

Antibody	Species	Company	Clone	Dilution	Applications
Monoclonal Anti-ANXA1	Rabbit	ThermoFisher Scientific	7H46L26	1:1000	Flow cytometry
Monoclonal Anti-CD16/CD32	Rat	ThermoFisher Scientific	93	1:250	Flow cytometry
Monoclonal Anti-SOD2	Rabbit	Cell Signaling Technologies Ltd.	D3X8F	1:1000	Western blot
Monoclonal Anti-NF-κB p65	Rabbit	Cell Signaling Technologies Ltd.	D14E12	1:400	Immunofluroescence
Monoclonal Anti-IkBα	Mouse	Cell Signaling Technologies Ltd.	L35A5	1:1000	Western blot
Monoclonal Anti-FPR2	Mouse	Santa Cruz Technology Inc.	GM1D6	1:10	Immunofluroescence
Monoclonal Anti-iNOS	Rabbit	Cell Signaling Technologies Ltd.	D6B6S	1:1000	Western blot
Polyclonal Anti-HO-1	Rabbit	Cell Signaling Technologies Ltd.	70081S	1:1000	Western blot
Monoclonal Anti-Phospho-p44/42 MAPK (Erk1/2) (Thr202/Tyr204)	Mouse	Cell Signaling Technologies Ltd.	E10	1:2000	Western blot
Monoclonal Anti-p44/42 MAPK (Erk1/2)	Rabbit	Cell Signaling Technologies Ltd.	137F5	1:1000	Western blot
Monoclonal Anti-Phospho-p38 MAPK (Thr180/Tyr182)	Mouse	Cell Signaling Technologies Ltd.	28B10	1:2000	Western blot
Polyclonal Anti-p38 MAPK	Rabbit	Cell Signaling Technologies Ltd.	9212S	1:1000	Western blot
Monoclonal Anti-TNFα	Armenian Hamster	eBioscience	TN3-19.12	1:250	ELISA
Monoclonal Anti-IL-1 beta	Armenian Hamster	eBioscience	B122	1:250	ELISA
Monoclonal-Anti-IL-10	Rat	eBioscience	JES5-16E3	1:250	ELISA

2.17.2. Secondary antibodies and conjugates

Table 2.10 List of secondary antibodies and fluorescent conjugates used in the study.

Antibody/Fluorescent Conjugates	Species	Company	Clone	Dilution	Applications
Polyclonal Anti-Mouse Alexa Fluor 405	Goat	ThermoFisher Scientific		1:300	Immunofluorescence
Polyclonal Anti-Rabbit Alexa Fluor 405	Goat	ThermoFisher Scientific		1:300	Immunofluorescence
Polyclonal Anti-Mouse Alexa Fluor 488	Goat	ThermoFisher Scientific		1:300	Immunofluorescence
Polyclonal Anti-Rabbit Alexa Fluor 488	Goat	ThermoFisher Scientific		1:300	Immunofluorescence
Polyclonal Anti-Mouse Alexa Fluor 647	Goat	ThermoFisher Scientific		1:300	Immunofluorescence
Polyclonal Anti-Rabbit Alexa Fluor 647	Goat	ThermoFisher Scientific		1:300	Immunofluorescence
Monoclonal CD11b-APC	Rat	BioLegend	M1/70	1:80	Flow cytometry
Monoclonal CD38-APC	Rat	BioLegend	90	1:80	Flow cytometry
Monoclonal CD40-APC	Rat	BioLegend	1C10	1:20	Flow cytometry
Monoclonal CD45-PE	Rat	BioLegend	30-F11	1:80	Flow cytometry
Monoclonal CD86-FITC	Rat	BioLegend	GL1	1:80	Flow cytometry
Monoclonal CD206-PE	Rat	BioLegend	C068C2	1:40	Flow cytometry
Monoclonal CD200-PerCP/Cy5.5	Mouse	BioLegend	OX-104	1:20	Flow cytometry
Annexin A5-FITC		BioLegend		1:20	Flow cytometry
Propidium Iodide		BioLegend		1:10	Flow cytometry
Polyclonal Anti-TNFα-Biotin	Rabbit	ThermoFisher Scientific		1:250	ELISA
Polyclonal Anti-IL-1 beta-Biotin	E.coli	ThermoFisher Scientific		1:250	ELISA
Monoclonal Anti-IL-10-Biotin	Rat	ThermoFisher Scientific	JES5-2A5	1:250	ELISA

2.18. Statistical analysis

All data are presented as mean ± SEM and were analysed with Graph Pad Prism 8 (GraphPad Software, CA, USA). All experiments were repeated using a minimum of 3 independent culture flasks. Statistical significance was detected using two-tailed Student's t-tests or one-, two- or three-way ANOVA with Tukey's HSD *post hoc* test, as appropriate. Levene's test was used to determine whether samples had equal variances. $P < 0.05$ was considered as statistically significant.

Chapter 3: Stimulation of Fpr2/3 Reverses Microglial Pro-inflammatory and Pro-oxidative Behaviour

3.1. Overview of the Chapter

Neurodegenerative disorders such as Alzheimer's disease (AD) have for many decades primarily been thought of as proteinopathies, diseases which manifest as a consequence of misfolded protein aggregation. In AD however, a central role for neuroinflammation in disease progression is increasingly clear (Heneka et al., 2015). Chronic neuroinflammation does not appear to be a consequence of amyloid plaques and neurofibrillary tangle development, but may actively contribute to disease pathogenesis just as much or perhaps even more than protein aggregates (Zhang et al., 2013). This is highlighted by PET imaging studies showing that expression of the microglial inflammatory marker TSPO correlates with AD severity in humans (Kreisl et al., 2013). A similar finding has been observed in the human AD brain for tau (Bejanin et al., 2017; Ossenkoppele et al., 2016), but this cannot be said for Aβ (Serrano-Pozo et al., 2011). As such, modulating neuroinflammation may provide a new avenue for therapeutic approaches.

Research interest associated with potential AD neuroinflammatory therapeutics is becoming more evident (Mudò et al., 2019; Raikwar et al., 2019; Zhang et al., 2019). The most extensively studied approach is the use of non-steroidal anti-inflammatory drugs (NSAIDs), which inhibit the cyclooxygenase enzymes COX-1 and COX-2; but despite promising findings in animal models (Wilkinson et al., 2012; Woodling et al., 2016) and epidemiological studies (Zhang et al., 2018), randomized placebo-controlled trials looking at the therapeutic benefit of NSAIDs such as rofecoxib (Reines et al., 2004) aspirin (AD Collaborative Group, 2008) and most recently naproxen (Meyer et al., 2019) failed to show significant changes in cognitive outcomes in AD patients. Inhibiting one aspect of a broad inflammatory response, such as the COX enzymes is unlikely to sufficiently resolve the chronically activated inflammatory phenotype that microglia adopt in AD (Meyer et al., 2019). Actively stimulating inflammatory resolution rather than simply inhibiting pro-inflammatory mediators looks to be a promising research approach for neurodegenerative diseases with a considerable inflammatory component (Frigerio et al., 2018; Hopperton et al., 2018).

Our methodology concentrates on modulating the endogenous pro-resolving phenotype that microglia/macrophages naturally adopt during acute episodes of inflammation. Successfully modulating this process pharmacologically via Fpr2/3 may be a novel way to

actively prevent tissue damage in neurodegenerative disease, and concomitantly upregulate repair mechanisms. Extensive research emphasises the essential role that both murine and human versions of the Fpr2/Fpr3 proteins have in modulating peripheral inflammatory resolution (Sadani N Cooray et al., 2013; Dalli et al., 2012; Gobbetti et al., 2014; McArthur et al., 2015; Vital et al., 2016). In addition, selective agonists have been identified to reduce chronic inflammation in a range of animal models including mouse models of rheumatoid arthritis and bleomycin-induced lung injury (He et al., 2011; Kao et al., 2014). Targeting Fpr2/3 stimulation may therefore hold therapeutic potential for neuroinflammatory disease.

3.2. Aim and hypothesis

We hypothesised that Fpr2/3 stimulation would reverse inflammation in BV-2 microglia and promote pro-resolving microglial characteristics. The primary aim of the experiments in this Chapter was to determine whether Fpr2/3 agonists could reverse inflammatory microglial activation following stimulation with the potent model inflammogen, LPS.

Stimulation of Fpr2/3 has been shown to signal through both ERK1/2 and p38 MAPK (Sadani N Cooray et al., 2013; Dalli et al., 2012; Guo et al., 2016; He and Ye, 2017; McArthur et al., 2015). Previous work identified that the Fpr2/3 agonist LXA4 lessens inflammation in rats by decreasing the activation of phosphorylated ERK1/2 but not p38 (Miao et al., 2015), with another group emphasising that LXA4 elicited reductions in stroke-associated inflammation via a p38 dependent mechanism (Guo et al., 2016). With previous work highlighting that pro-inflammatory activation of Fpr2/3 is associated with ERK1/2 signalling (Sadani N Cooray et al., 2013), we further hypothesised that the pro-resolving effects of Fpr2/3 stimulation would instead be p38 MAPK mediated.

3.3. Drug dose determination and experimental design

The potent pro-inflammatory stimulus LPS was selected as a model inflammogen, used at a concentration of 50 ng/ml. This concentration was selected on the basis of previous work within the laboratory showing it to be sufficient to induce the release of pro-inflammatory cytokines and upregulate the expression of pro-inflammatory surface markers in BV-2 microglia (McArthur et al., 2010). LPS elicits its pro-inflammatory effects through binding the CD14/TLR4 receptor complex in a range of immune cells including macrophages and microglia (Parajuli et al., 2012; Rajaiah et al., 2015), resulting in the phosphorylation of a range of signalling kinases such as ERK1/2, Akt and p38 (Khan et al., 2017; Lu et al., 2008). The resulting response triggers the nuclear translocation of NF-kB and the transcription of a range of pro-inflammatory molecules (Parajuli et al., 2012; Youssef et al., 2019).

To determine the most appropriate concentration of the Fpr2/3 agonists C43 and QC1, concentration-response curves were initially set up for both, centred around their EC_{50} values at FPR2, reported as 44 nM for C43 (Bürli et al., 2006) and 40 nM for QC1 (Zhou et al., 2007), respectively. BV-2 microglia were serum starved for 24 h before treatment. For cell viability and cell cycle assays, measures of inflammatory mediator production, phagocytic capacity, antioxidant enzyme and AnxA1 expression, alongside L-lactate and glucose detection, BV-2 microglia were exposed to LPS for 1 h unless otherwise stated. Cells were then treated with C43 or QC1 and analysed 24 or 48 h post-LPS addition. For phenotypic marker analysis, BV-2 microglia were treated with LPS for 24 h prior to the addition of Fpr2/3 agonists, with analysis 48 h post-LPS. For ROS experiments and confocal imaging, LPS was administered 10 min prior to FPR2 agonists, with ROS production analysed for up to 1 h. Samples acquired for respective imaging analysis and western blot of NF-κB, NADPH oxidase and IκBα expression were fixed at 30 min post-LPS. Fpr2/3 ligands were administered 10 min-post LPS. A summary of the different experimental procedures are detailed in Figure 3.1. Different treatment timings were utilised based on the time frame for successful response detection. For example, ROS production in immune cells happens almost immediately following a noxious response (Rawson et al., 2015), which can facilitate the transcription of pro-inflammatory markers through NF-kB (Mittal et al., 2014), although the detection for the latter is often described at 24-48 h post-noxious insult *in vitro* (Cai et al., 2017; Siddiqui et al., 2016). For phenotypic marker expression analysis, Fpr2/3 agonists were administered 24 h post-LPS to determine whether a microglial pro-inflammatory phenotype could be reversed following prolonged noxious stimulation.

3.4. Results

3.4.1. Fpr2/3 agonists do not affect BV-2 cell viability

Initial studies investigated any potential toxicity of either Fpr2/3 agonist alone or in combination with LPS pre-treatment. Neither C43, QC1 or LPS affected cell viability as assessed by the PrestoBlue assay (Figure 3.2A-3.2F), when compared to untreated cells at 24 h. Both H_2O_2 (200 μM) and actinomycin D (1 μg/ml) were administered as positive controls (Figure 3.2A and 3.2B).

As the PrestoBlue assay assesses cell number and cannot readily distinguish between cell survival and proliferation, the effects of LPS and Fpr2/3 agonists on BV-2 cell cycle was examined. Exposure to LPS for 24 h resulted in a significant decrease in the proportion of cells in G_2/M phase accompanied by an increase in the $SubG_1$ population (Figure 3.2G and 3.2H). Addition of C43 following LPS stimulation successfully reversed the reduction in G_2/M but had no effect on the $SubG_1$ population. Cells treated with both LPS and C43 had significantly increased $G_0/_1$ populations, but also concomitant reductions in the S-phase

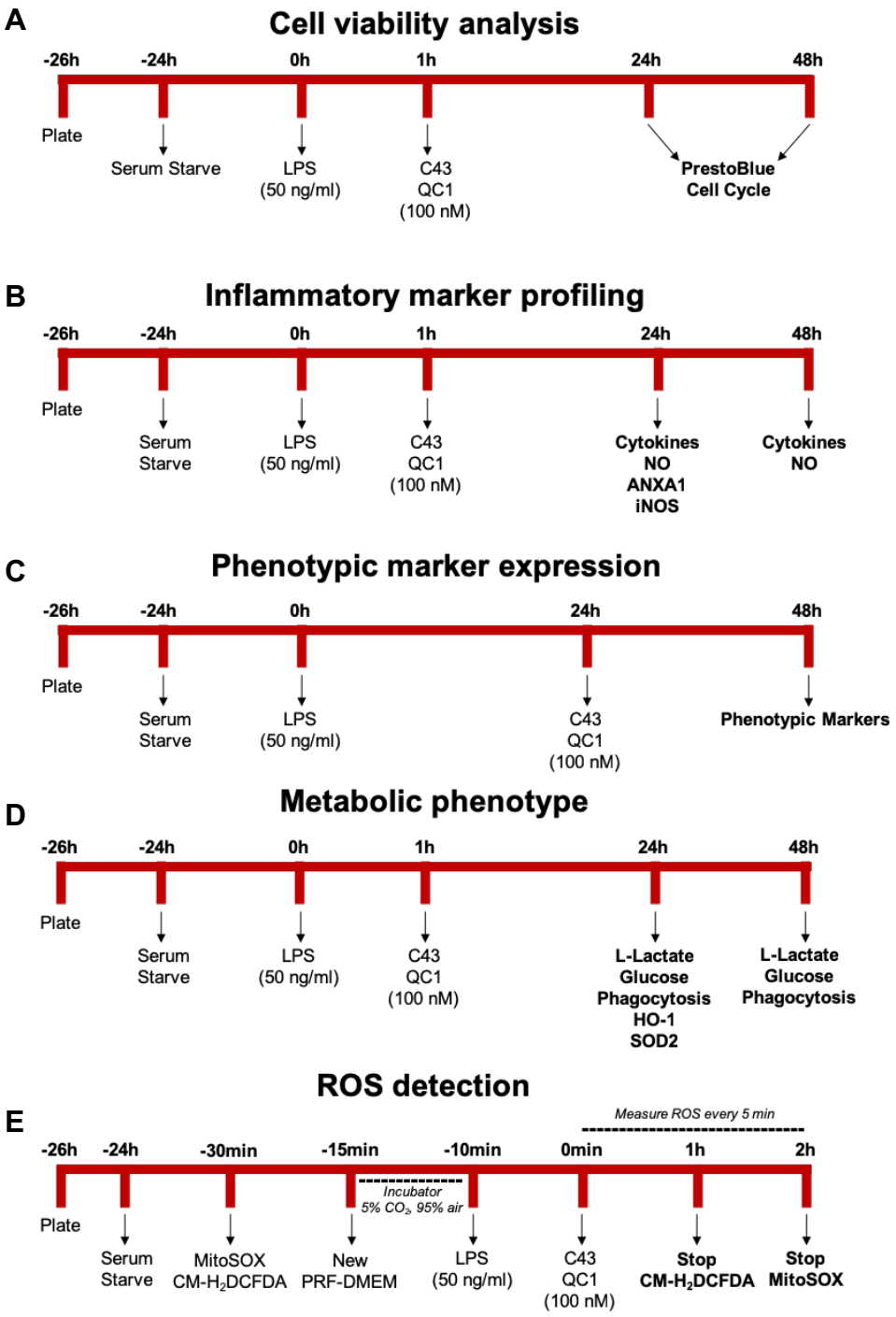

Figure 3.1 Summary of different experimental protocols. A; cell viability analysis, which included 1 h pre-treatment of LPS. PrestoBlue was used for cell viability analysis at both 24 h and 48 h. DAPI was used for cell cycle analysis at 24 h. **B**; for inflammatory marker profiling, LPS was administered 1 h prior to Fpr2/3 agonists, unless otherwise specified elsewhere in the chapter. Cytokines and nitric oxide release were detected at both 24 h and 48 h. Protein expression was analysed at 24 h unless otherwise specified. **C**; analysis of phenotypic marker expression was carried out at 48 h post-LPS administration. Fpr2/3 agonists were added 24 h after initial LPS exposure. **D**; for metabolic phenotype profiling, such as analysing phagocytic ability and L-lactate production, cells were treated as for inflammatory marker profiling, with protein expression measured at 24 h only, whilst other components were analysed at both 24 h and 48 h. **E**; ROS detection occurred every 5 min for 1 h (CM-H_2DCFDA) and 1 h (MitoSOX Red). Measurements for specific ROS species are highlighted in select sections within the Chapter.

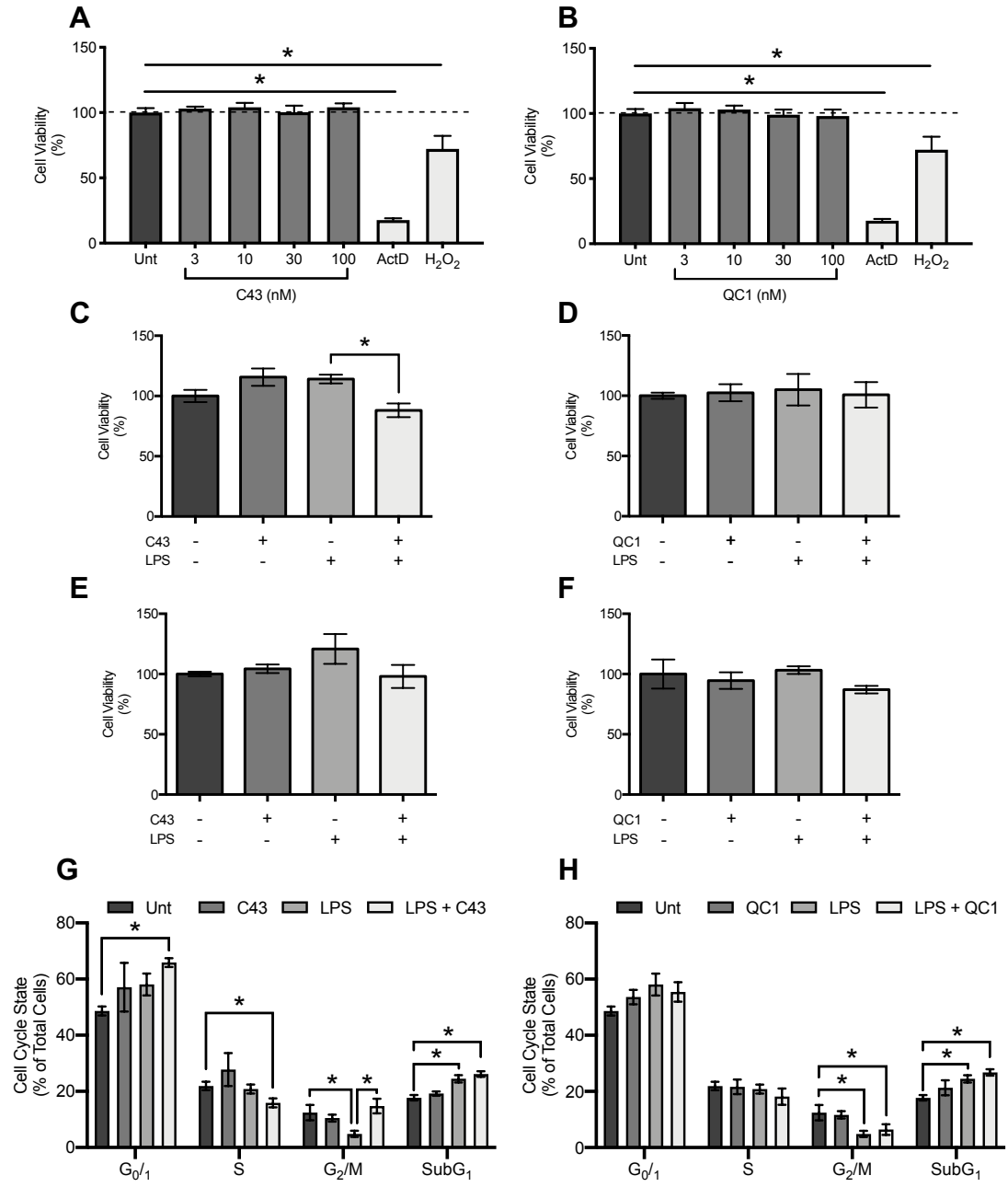

Figure 3.2 The effects of Fpr2/3 agonists and LPS on cell viability and relative cell cycle populations of BV-2 microglia. A; C43 (3, 10, 30, 100 nM) does not affect cell viability at 24 h. **B**; no tested concentration of QC1 (3, 10 30 and 100 nM) affects cell viability at 24 h. Actinomycin and H_2O_2 were used as positive controls. **C** and **D**; neither LPS or C43/QC1 (100 nM) affect cell viability at 24 h compared to untreated cells. **E** and **F**; neither Fpr2/3 agonist (100 nM) or LPS affect cell viability at 48 h when compared to untreated cells. **G**; cell phase populations following C43 and LPS treatments at 24 h. LPS ± C43 significantly increases cells in the G_1 and $SubG_1$ phase, alongside reducing cells in the S phase and rescuing the reduction in G_2/M cells triggered by LPS administration alone. **H**; cell phase populations following LPS and QC1 treatment at 24 h. Data are means ± SEM for 3-6 independent cultures in triplicate. *P < 0.05.

population (Figure 3.2G). Stimulation with QC1 did not elicit any effects on BV-2 cell cycle (Figure 3.2H). In summary, Fpr2/3 activation did not elicit toxicity or changes in cell cycle in BV-2 microglia.

3.4.2. Fpr2/3 agonists reverse LPS-induced pro-inflammatory mediator release

Nitric oxide (NO), TNFα and IL-1β are all pro-inflammatory mediators linked to the neuroinflammatory environment in AD (Brosseron et al., 2014; Heneka et al., 2015; Malinski, 2007). As microglia are thought to be the primary source of these mediators in the CNS (Ransohoff and El Khoury, 2015), the levels of each were determined at 24 h and 48 h post-initial drug treatment. Addition of LPS significantly upregulated NO release at both time points (Figure 3.3A-I) as indirectly measured by the Griess assay (Bryan and Grisham, 2007), supporting previous results (Xiang et al., 2018). This was reduced at 24 h post-LPS by C43 and QC1 when added 1 h prior to or after LPS stimulation. (Figure 3.3A, 3.3B, 3.3D). Post-treatments with C43 or QC1 at 48 h post-LPS similarly resulted in reduced NO release compared to cells treated with LPS alone (Figure 3.3C and 3.3D). In these experiments (Figure 3.3A-3.3D), neither untreated cells nor Fpr2/3 agonists alone effected nitrite levels (data not shown).

To confirm that the effects of C43 and QC1 were due the selective activation of Fpr2/3 and not the closely related receptor Fpr1, cells were treated with LPS for 50 min prior to the addition of the Fpr2/3 antagonist WRW_4 (10 μM; (McArthur et al., 2015)) or the selective Fpr1 antagonist cyclosporin H (CSH, 0.7 μM; (Wenzel-Seifert and Seifert, 1993)). C43 or QC1 were next added as prior. Pre-treatment with WRW_4 ablated the effects of C43 and QC1 on NO release at 48 h post-LPS administration (Figure 3.3E and 3.3F), whereas CSH was without effect (Figure 3.3G and 3.3H). Complex pharmacology surrounds Fpr2/3, with both pro- and anti-inflammatory agonists existing (Sadani N Cooray et al., 2013; He and Ye, 2017). We therefore tested the specificity of these anti-inflammatory effects through use of the pro-inflammatory agonist MMK-1 (2 nM, EC_{50}; (Hu et al., 2001)). Whilst having no effect on NO alone, addition 1 h post-LPS significantly increased NO production at 48 h (Figure 3.3I).

The principal source of NO in microglia is iNOS (Du et al., 2017). Hence, we studied the effects of Fpr2/3 agonists upon iNOS expression. Whilst 24 h LPS exposure upregulated iNOS expression after compared to untreated cells (Figure 3.4A), confirming previous reports (Lecca et al., 2018), this was not affected by C43 or QC1 post-treatment, nor did these Fpr2/3 agonists alter iNOS expression when administered alone. Ponceau S stain was used as a loading control, due to the altered banding pattern of β-actin following LPS treatment (Figure 3.4A). The relative ratios of iNOS expression compared to LPS alone is

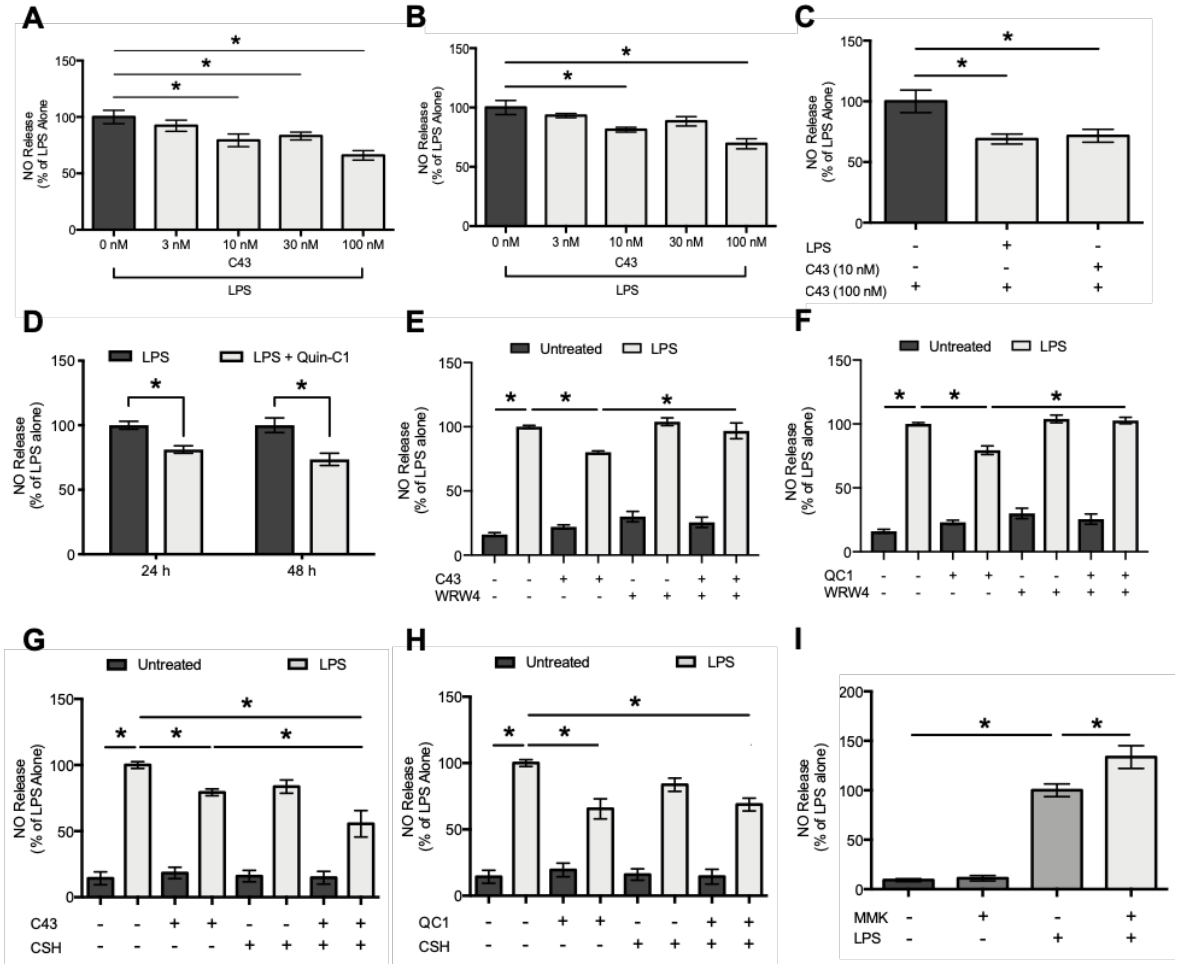

Figure 3.3 The effects of Fpr2/3 agonists and LPS on nitric oxide release. A; C43 (3, 10, 30 or 100 nM) was administered to BV-2 cells 1 h prior to LPS with nitrite levels – an indirect measure of NO production – detected at 24 h post-C43 addition. All groups were treated with LPS. Neither C43 or untreated cells produced detectable nitrite levels and were excluded. **B**; nitrite levels were detected following 24 h LPS stimulation with or without 1 h post-treatment with C43 (3, 10, 30 or 100 nM). All groups were treated with LPS, with untreated and C43 treated cells excluded as for A. **C**; C43 1 h post-treatment (10 and 100 nM) reduced LPS-induced nitrite release measured at 48 h post-LPS. **D**; QC1 (100 nM) 1 h post-treatment reduced LPS-induced nitrite release measured at both 24 h and 48 h post-LPS. **E** and **F**; the selective Fpr2/3 antagonist WRW_4 (10 μM) inhibits the nitrite reducing abilities of both C43 and QC1 at 48 h, respectively. WRW_4 was administered 10 min prior to these Fpr2/3 agonists, 50 min post-LPS. Nitrite was measured 48 h post-LPS. **G** and **H**; at 48 h post-LPS, the Fpr1 inhibitor CSH had no effect on C43 or QC1, respectively. CSH was administered 10 min prior to the Fpr2/3 agonists, and thus 50 min post-LPS. **I**; MMK-1 (2 nM) 1 h post-treatment significantly increased nitrite release when compared to untreated and LPS alone at 48 h-post LPS. Data are presented as means ± SEM for 3-7 independent cultures in triplicate. **P* < 0.05.

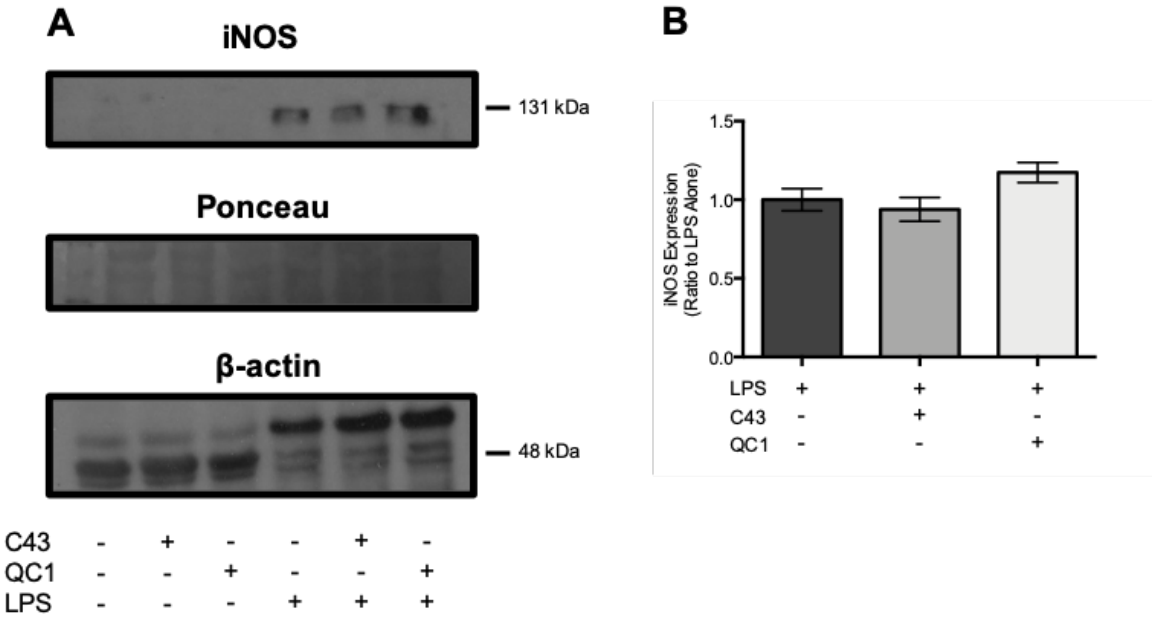

Figure 3.4 The effects of Fpr2/3 ligands and LPS on iNOS expression. A; BV-2 microglia exposed to LPS for 24 h significantly increased iNOS expression. Ponceau stain was used as a protein loading control. LPS altered the banding pattern of β-actin and thus was not used as a loading control. **B**; 1 h post-treatment with Fpr2/3 agonists did not affect iNOS expression following 24 h LPS stimulation. Data are presented as means ± SEM for 3 independent cultures in triplicate.

shown in Figure 3.4B.

Whilst NO can be a potent inflammatory mediator, it can also have other physiological functions (Chachlaki et al., 2017; Kakizawa et al., 2012). Hence, we next examined production of the major pro-inflammatory cytokines TNFα and IL-1β. As with NO, neither C43 nor QC1 addition upregulated TNFα production (Figure 3.5A, 3.5D-3.5F). However, LPS increased TNFα production approximately 10-fold in comparison to untreated cells (Figure 3.5B and 3.5C), an effect prevented by 1 h C43 pre-treatment (Figure 3.5B) and ameliorated by C43 and QC1 1 h post-LPS administration at 24 h (Figure 3.5C and 3.5E) and 48 h (Figure 3.5D and 3.5F). The effects of both C43 and QC1 at 48 h were inhibited by pre-treatment with 10 μM WRW_4 10 min prior to Fpr2/3 agonist administration (Figure 3.5G and 3.5H) but not by 0.7 μM CSH pre-treatment (Figure 3.5I and 3.5J). These anti-inflammatory Fpr2/3 responses were agonist specific, with MMK-1 having no effect at 48 h when administered alone or 1 h post-LPS (Figure 3.5K). In contrast to TNFα, IL-1β was not detectable in any groups using a well-characterised commercial IL-1β ELISA shown to be functional in murine systems (data not shown).

3.4.3. Administration of Fpr2/3 agonists post-LPS stimulation increases release of the pro-resolving cytokine IL-10

The reductions in LPS-induced TNFα and NO release caused by both Fpr2/3 agonists supports an anti-inflammatory role for this receptor. To determine whether activation in microglia is actively pro-resolving, as has been shown for peripheral monocytes (Sadani N Cooray et al., 2013), we investigated the effects of Fpr2/3 stimulation upon IL-10 production; a key anti-inflammatory cytokine (Cherry et al., 2014; Yang et al., 2009). Stimulation with LPS significantly suppressed baseline IL-10 release after 24 h (Figure 3.6A), whilst C43 treatment alone had no effect. Treatment with C43 (100 nM) 1 h prior to LPS did however increase IL-10 release at 24 h post-LPS when compared with LPS alone (Figure 3.6B). Post-treatment of C43 or QC1 significantly increased IL-10 release at 48 h but not 24 h post-LPS (Figure 3.6C-3.6F). Further, just like C43, QC1 had no direct effects on IL-10 release alone. Confirming that these observations at 48 h were Fpr2/3 mediated, the effects of C43 were inhibited by 10 min pre-treatment with WRW_4 (Figure 3.6G). The IL-10 modulating effects of Fpr2/3 stimulation were agonist specific, as 1 h post-treatment with MMK-1 had no effect on IL-10 release at 48 h (Figure 3.6H). In summary, Fpr2/3 activation successfully promotes the release of pro-resolving IL-10 whilst concomitantly reducing pro-inflammatory mediator production.

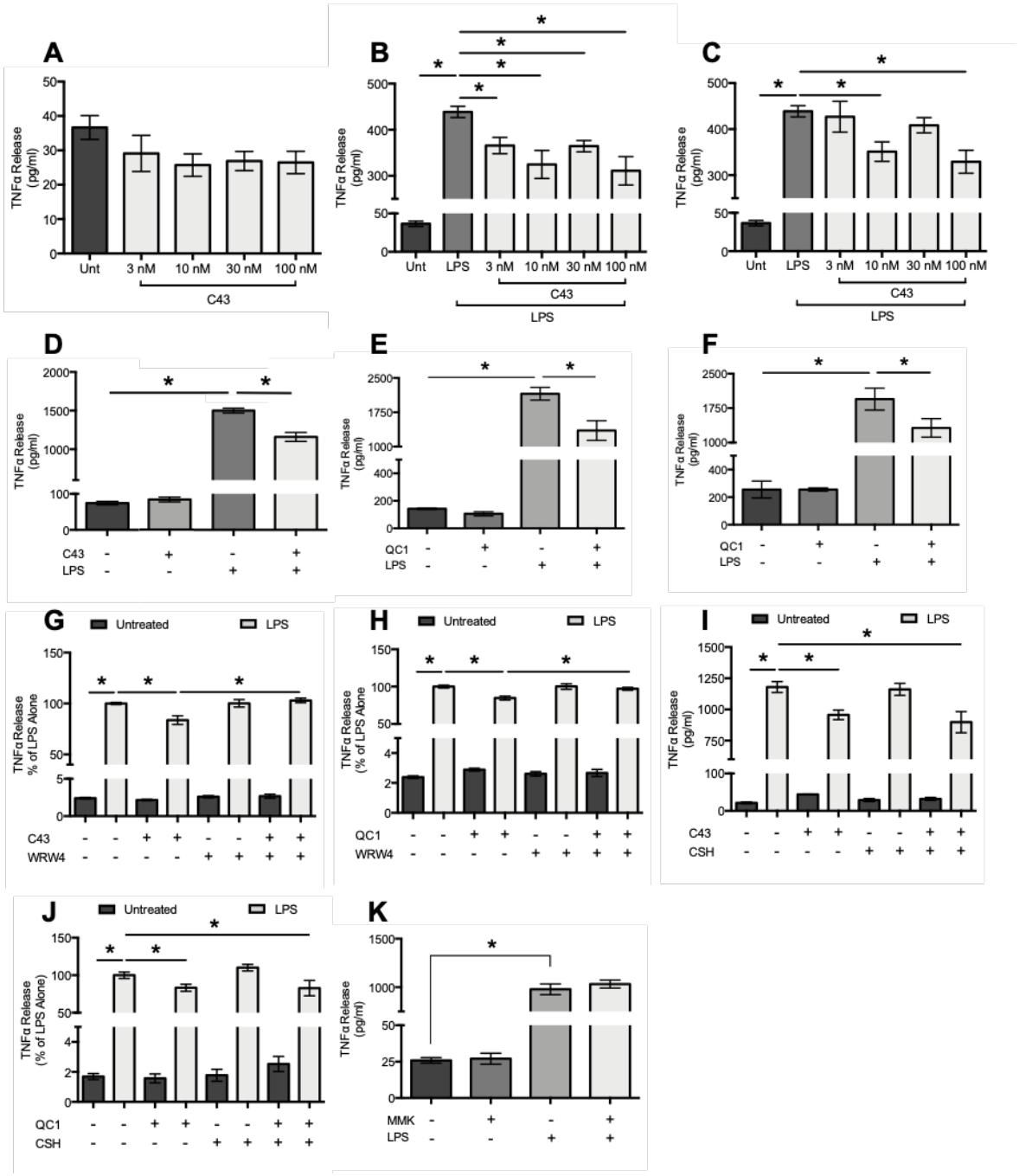

Figure 3.5 The effects of Fpr2/3 agonists and LPS on TNFα release in BV-2 microglia at 24 h and 48 h. A; the effects of varying C43 concentrations (3, 10, 30 and 100 nM) on TNFα release following 24 h exposure. **B**; TNFα release following 24 h LPS administration ± C43 1 h pre-treatment addition at varying concentrations. **C**; TNFα concentration measured at 24 h after LPS ± C43 1 h post-treatment. **D**; effects of 1 h post-treatment of 100 nM C43 on LPS-induced TNFα release following 48 h exposure to the endotoxin. **E** and **F**; effects of QC1 (100 nM) 1 h post-treatment on LPS-induced TNFα release at 24 h and 48 h post-LPS addition, respectively. **G** and **H**; effects of WRW_4 (10 μM) administration on TNFα at 48 h after LPS exposure, when administered 10 min prior to C43 and QC1 (and 50 min post-LPS), respectively. **I** and **J**; effects of CSH addition on TNFα at 48 h post-LPS, when administered 10 min before Fpr2/3 agonists and 50 min after LPS. For WRW_4 and CSH experiments, Fpr2/3 agonists were administered 1 h after LPS. **K**; the effects of 1 h post-administration of MMK-1 on TNFα production at 48 h following initial LPS exposure. Data are means ± SEM of 4-6 independent cultures in triplicate. **P* < 0.05.

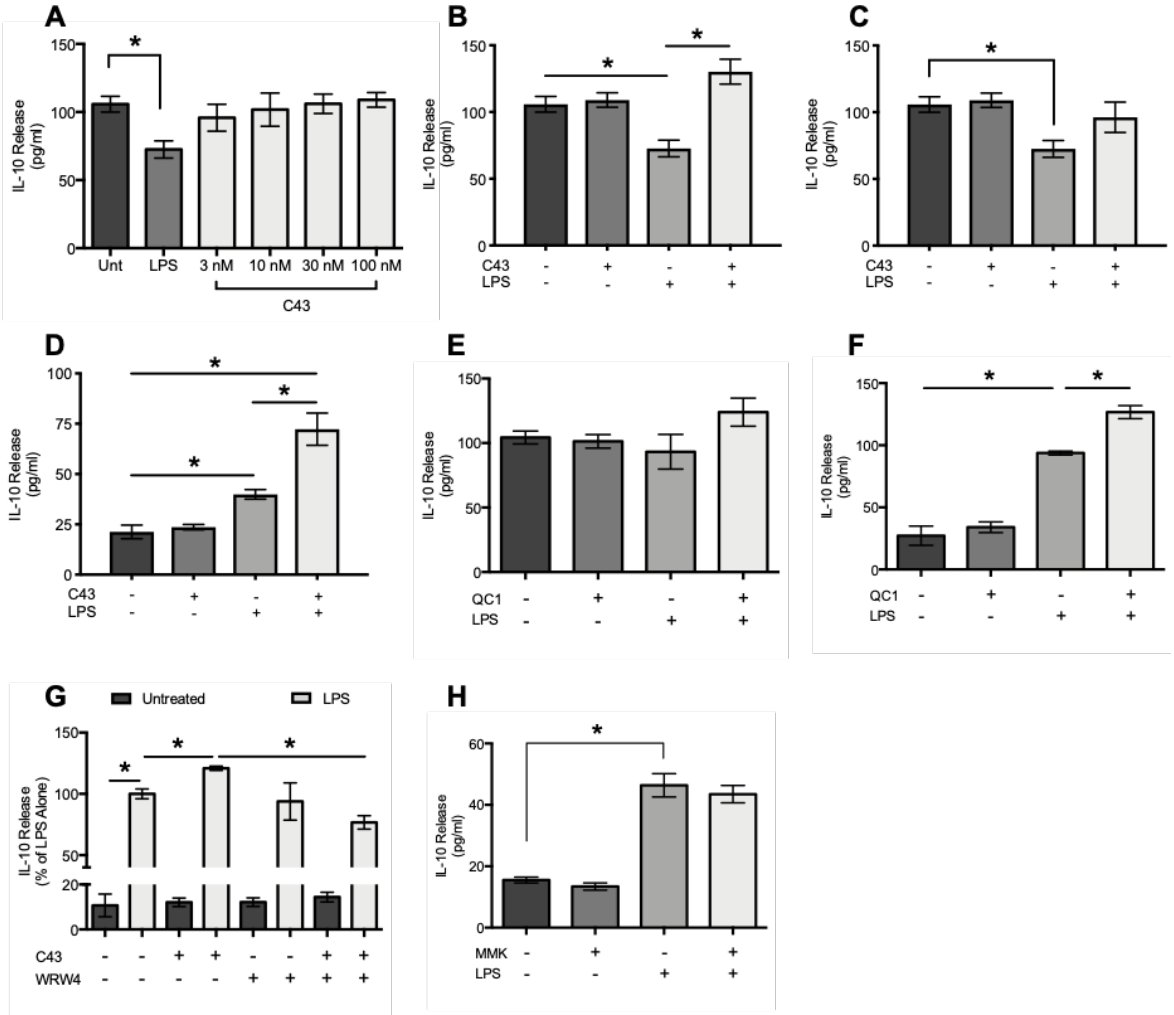

Figure 3.6 The effects of Fpr2/3 agonists and LPS on IL-10 production in BV-2 microglia at 24 h and 48 h. A; effect of LPS and varying concentrations of C43 alone on IL-10 production at 24 h, compared to untreated cells. **B**; effects of 1 h C43 (100 nM) pre-treatment on IL-10 production following LPS insult at 24 h. **C**; effect of 1 h C43 (100 nM) post-treatment on IL-10 production following LPS stimulation at 24 h. **D**; IL-10 release at 48 h, following LPS administration and C43 1 h post-treatment. **E** and **F**; effects of 1 h QC1 (100 nM) post-treatment on IL-10 production following LPS insult for 24 h and 48 h, respectively. **G**; the effects of WRW_4 on IL-10 production against C43 (100 nM) at 48 h. **H**; the effect of MMK-1 on IL-10 production at 48 h, added 1 h after LPS. Data are means ± SEM of 3-6 independent cultures in triplicate. **P* < 0.05.

3.4.4. The effects of Fpr2/3 are independent of AnxA1

Previous work by our group and others has shown that endogenous Fpr2/3 ligand AnxA1 has a key role in inflammatory resolution (Lima et al., 2017; Locatelli et al., 2014; McArthur et al., 2015) and IL-10 release (Sadani N Cooray et al., 2013; Souza et al., 2007). We therefore determined whether changes in cellular AnxA1 levels correlated with IL-10 production in BV-2 microglia. AnxA1 expression was not elevated by either C43 or QC1 (Figure 3.7A-D), nor were cytokine or NO responses to these agonists affected by AnxA1 knockdown through stable transfection with AnxA1 targeting shRNA, ShA1 (Figure 3.7E-J). Data provided here therefore suggests the effects of C43 and QC1 are independent of AnxA1.

3.4.5. Fpr2/3 agonists modulate BV-2 microglia cell surface marker expression

The relative expression of different cell surface markers provide insights into the inflammatory phenotype of microglia. To further characterise the pro-resolving effects of Fpr2/3 ligands, we examined the expression of a panel of microglial pro-inflammatory (CD11b, CD38, CD40, CD45, CD86) and pro-resolving (CD206) phenotypic markers at 48 h post-LPS treatment, with Fpr2/3 agonists given 24 h post-LPS to allow time for changes in protein synthesis. Neither administration of C43 nor QC1 alone had an effect on any of these CD molecules (Figure 3.8). With the exception of CD86, all pro-inflammatory markers were upregulated following LPS insult (Figure 3.8). Treatment with C43 post-LPS significantly reduced CD38 and CD40 expression (Figure 3.8C and 3.8E) but did not affect CD11b or CD45 (Figure 3.8A and 3.8G). Treatment with QC1 was less effective, significantly reducing LPS-induced CD38 expression (Figure 3.8D), but not affecting any of the other pro-inflammatory markers (Figure 3.8B, 3.8F, 3.8H and 3.8J). Expression of the anti-inflammatory, pro-resolution marker CD206 was not affected by either agonist alone but was significantly reduced by LPS treatment (Figure 3.8K and 3.8L). This reduction was reversed by C43 only, with QC1 being ineffective (Figure 3.8K and 3.8L). In summary, Fpr2/3 stimulation is able to successfully modulate the expression of several different inflammatory cell surface markers, holding promise to drive microglial cells towards a pro-resolving phenotype following insult with an inflammatory stimulus.

3.4.6. Fpr2/3 agonists and LPS increase BV-2 phagocytic capacity

A key behaviour of inflammatory microglia and macrophages is the phagocytosis of pathogenic material, such as Aβ and invading bacteria (Lucin et al., 2013), alongside the efferocytosis of damaged and dying cells (Chang et al., 2018). Pro-resolving microglia show a higher efferocytotic capacity than pro-inflammatory cells, and activation of Fpr2/3 has

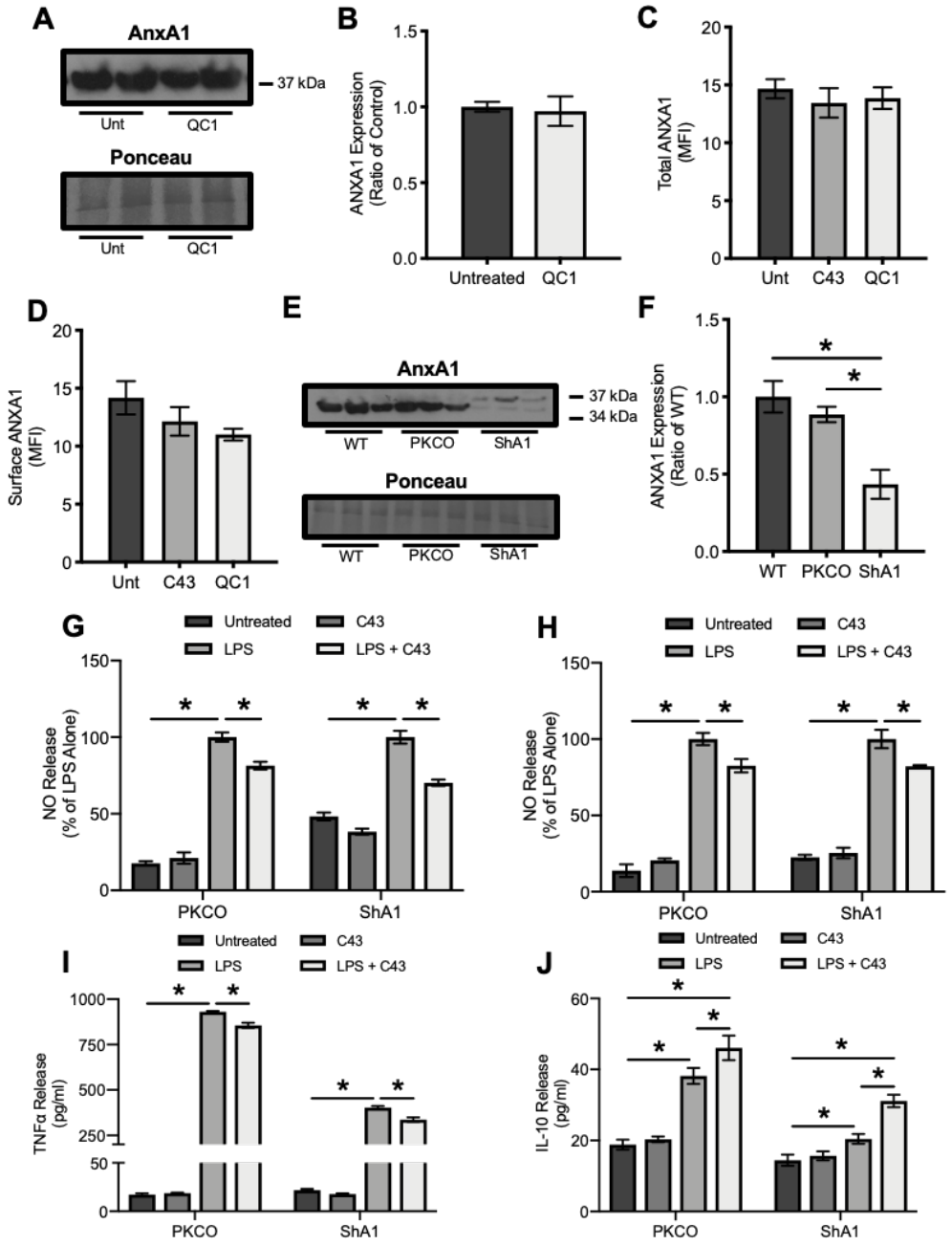

Figure 3.7 The expression and localisation of AnxA1 in BV-2 microglia, alongside the effects on pro-inflammatory mediator release following transfection-induced AnxA1 knockdown. Fpr2/3 agonists were both administered at 100 nM. **A**; western blot example highlighting AnxA1 expression following 24 h stimulation with QC1 alongside untreated cells. The Ponceau S stain was used as a loading control. **B**; relative AnxA1 expression ratios from western blot data. **C**; total AnxA1 expression at 24 h following Fpr2/3 agonist stimulation compared to untreated cells. **D**; relative surface expression levels of AnxA1 at 24 h following treatment with Fpr2/3 agonists compared to untreated cells. **E**; representative western blot highlighting the successful knockdown of AnxA1 in ShA1 plasmid treated BV-2 microglia compared to WT and plasmid control (PKCO) cells. The Ponceau S stain was used as a protein loading control. **F**; graphical representation of the relative AnxA1 ratio between WT, PKCO and ShA1 microglia. **G**; NO release as measured indirectly by nitrite production at 24 h in PKCO and ShA1 microglia. **H**; NO release at 48 h in PKCO and ShA1 cells. **I**; TNFα release at 24 h in PKCO and ShA1 cells. **J**; IL-10 release at 48 h in PKCO and ShA1 cells. For G-J, Fpr2/3 agonists were administered 1 h after LPS, with supernatant collected at 24 and 48 h post-LPS. Data are means ± SEM (*n* = 3-6 independent cultures in triplicate). **P* < 0.05.

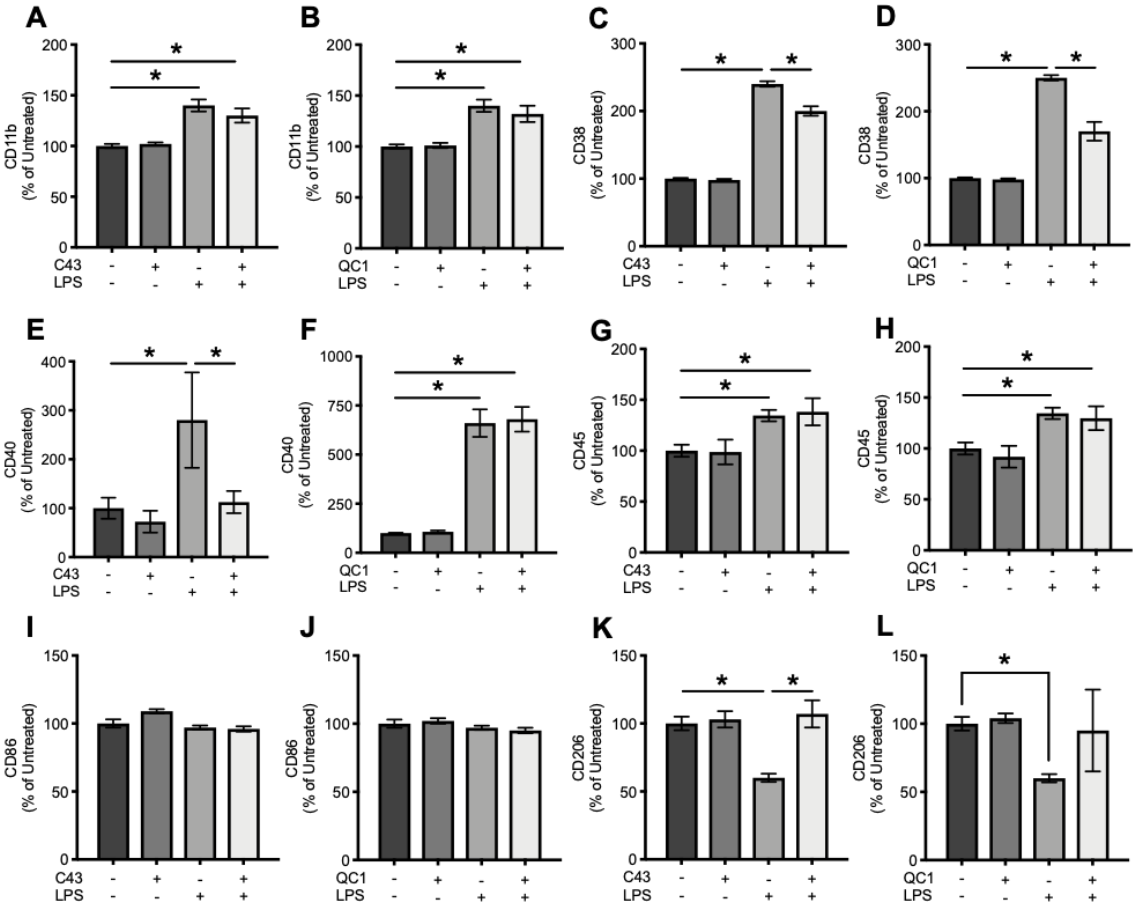

Figure 3.8 The median fluorescent intensities of a panel of CD microglial phenotypic markers. Cells were pre-treated with LPS for 24 h, before the addition of C43 or QC1 (100 nM). Marker expression was determined 48 h post-LPS. All marker expression levels are shown as percentage of untreated. **A** and **B**; relative expression levels of CD11b. **C** and **D**; expression levels of CD38. Both Fpr2/3 agonists significantly reversed the LPS-induced increase in CD38. **E** and **F**; CD40 expression in BV-2 cells. C43 but not QC1 significantly reduced CD40 expression post-LPS induction. **G** and **H**; CD45 expression levels. **I** and **J**; CD86 expression. No changes were observed for any of the treatment groups. **K** and **L**; expression of the pro-resolving CD206 was reduced by LPS and rescued by C43 addition. QC1 had no significant effect. LPS significantly affected the expression of all CD phenotypic markers examined, excluding CD86. Data are means ± SEM for 3-6 independent cultures in triplicate. **P* < 0.05.

been previously shown to regulate bacterial phagocytosis (Gobbetti et al., 2014; Lan et al., 2017; Zhang et al., 2017). We therefore examined the phagocytic capacity of BV-2 cells following LPS stimulation for 24 h and 48 h ± 1 h post-stimulation with Fpr2/3 agonists, using fluorescently labelled heat-killed *E. coli* bioparticles. At 24 h post-LPS treatment, whilst C43 and QC1 treatment alone had no effect on bacterial phagocytosis, both potentiated the pro-phagocytic effects of LPS pre-treatment (Figure 3.9A and 3.9B), an effect not seen with QC1 (Figure 3.9B). This effect of C43 was no longer apparent 48 h post-LPS treatment (Figure 3.9C and 3.9D). LPS alone significantly increased bacterial phagocytosis at 48 h only (Figure 3.9C and Figure 3.9D). Fpr2/3 agonists therefore appear to modulate microglial phenotype following an inflammatory insult, inducing an upregulation of phagocytosis which may contribute to the removal of pathogenic material and cellular debris.

3.4.7. Fpr2/3 activation reverses LPS-induced mitochondrial and NADPH oxidase-initiated ROS production in microglia

Beyond classical neuroinflammatory mediators such as cytokines and NO, the link between oxidative damage and AD has become clearer in recent years. Oxidised protein content is increased in the CSF of patients with both AD and MCI (Di Domenico et al., 2016), suggesting oxidative damage may begin many years before symptoms become apparent. Oxidised protein content is also found in the brain, where oxidative markers increase in a disease-dependent manner. This correlates with patient Mini-Mental Status Examination (MMSE) scores (Ansari and Scheff, 2010), a 30-point questionnaire widely used in clinical and research settings to determine patient cognition. LPS activation of TLR4 stimulates ROS production in immune cells (Kim et al., 2010). To determine whether LPS similarly triggered ROS production in BV-2 microglia and whether Fpr2/3 agonist treatment could reverse this, ROS production was assessed with the intracellular ROS tracer CM-H_2DCFDA. Stimulation with LPS significantly increased ROS production in BV-2 microglia over 1 h, with both C43 and QC1 (100 nM) completely reversing this when administered 10 min after LPS (Figure 3.10A-3.10D); neither C43 nor QC1 affected ROS production when administered alone.

Superoxide and NO can combine to produce the highly reactive ROS species peroxynitrite ($ONOO^-$; Radi, 2018). Thus, $ONOO^-$ (and hydroxyl radical; •OH) production after 1 h was examined using the hydroxyphenylfluorescein (HPF) tracer. Cells treated with C43 and QC1 10 min after LPS exposure exhibited significantly reduced •OH and $ONOO^-$ release compared to untreated cells, an effect absent when administered without LPS (Figure 3.10E and 3.10F). The production of H_2O_2 at 2 h was also determined, using the Promega ROS-Glo assay kit. However, none of the experimental groups produced detectable amounts of H_2O_2, as compared to the standard curve and positive control (data not shown).

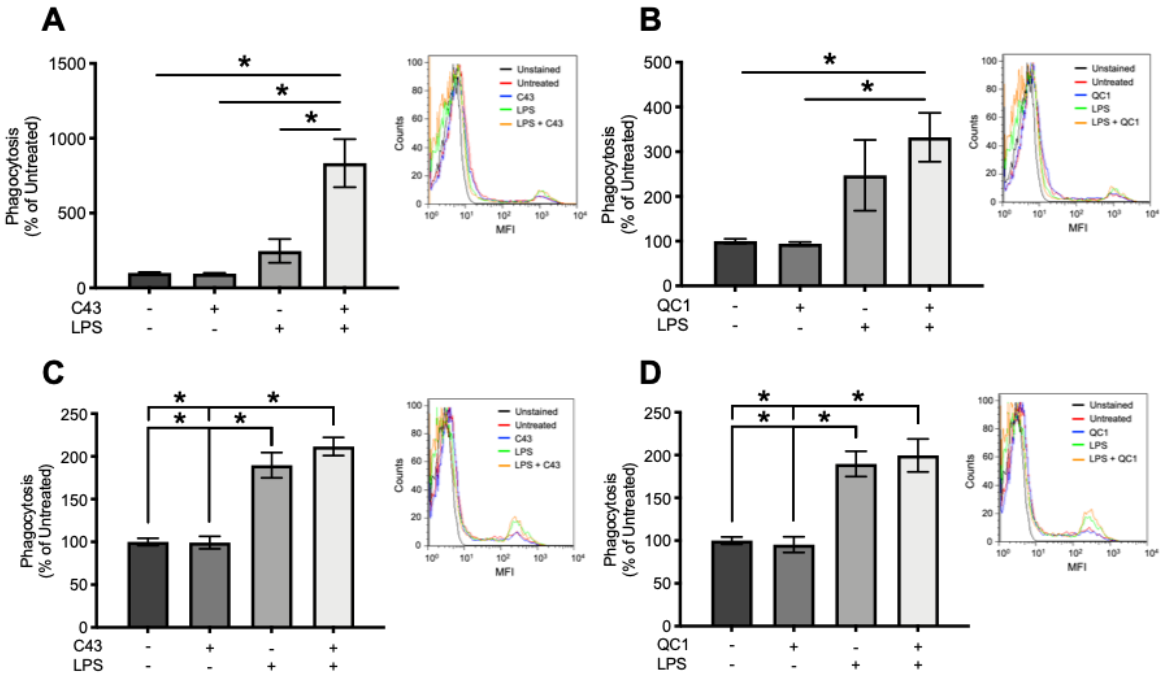

Figure 3.9 The phagocytic index of BV-2 microglia following LPS exposure for 24 h and 48 h. Fpr2/3 agonists (100 nM) were administered 1 h post-LPS. Microglial phagocytic capacity was identified by engulfment of fluorescent *E. coli* bioparticles and measured by flow cytometry. **A**; phagocytosis by BV-2 cells was increased following the combined treatment of LPS and C43 at 24 h. **B**; LPS and QC1 combined stimulation increased phagocytic index at 24 h. **C**; LPS significantly increased BV-2 phagocytic index at 48 h, whereby C43 did not contribute towards this effect. **D**; LPS upregulation of phagocytosis at 48 h is not affected by QC1. Data are means ± SEM of 3-4 independent cultures repeated in triplicate. **P* < 0.05.

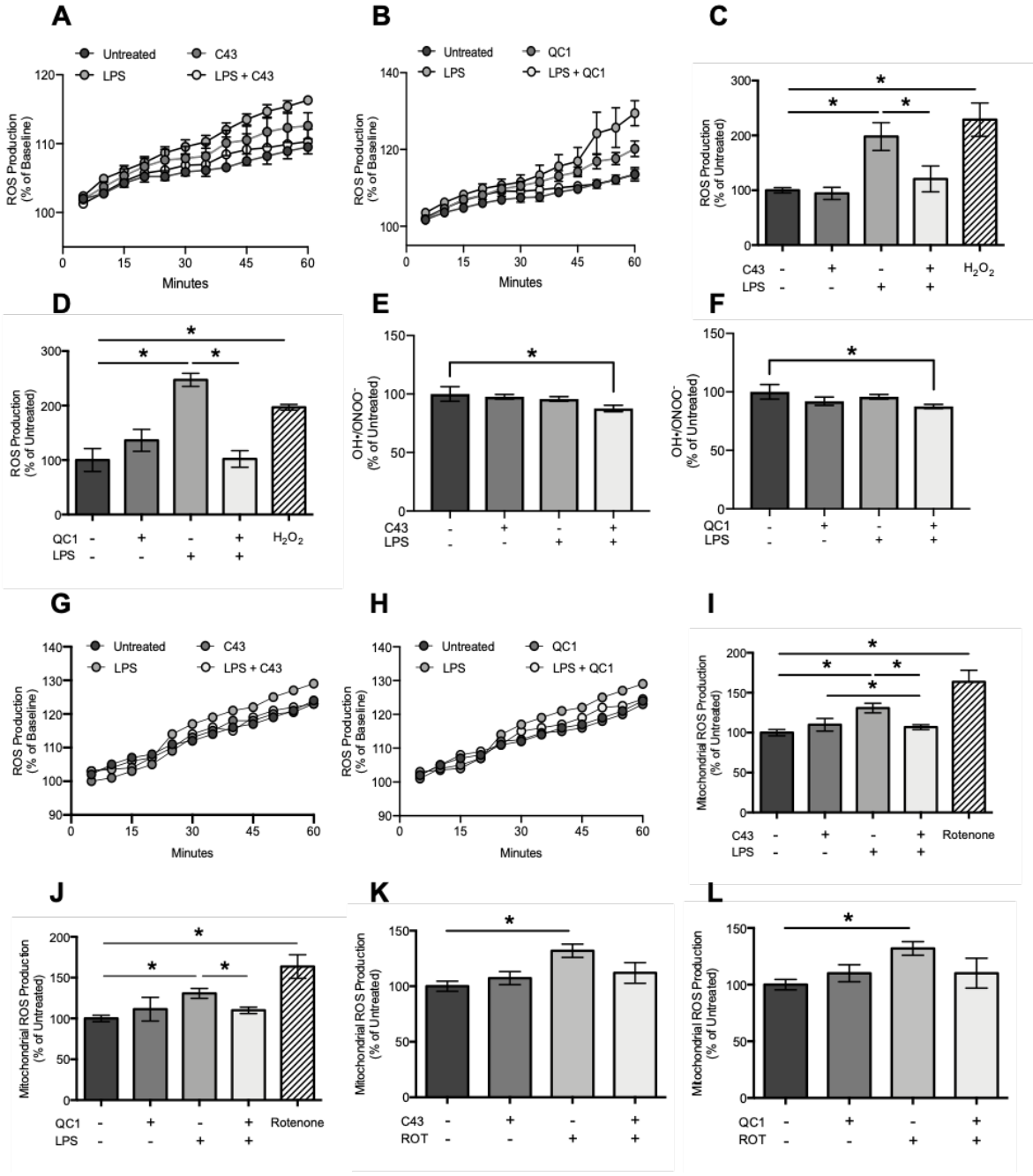

Figure 3.10 The effects of Fpr2/3 agonists and LPS on ROS production in BV-2 microglia. For all experiments, Fpr2/3 agonists were administered 10 min post-LPS. **A** and **B**; relative ROS production gradients following LPS and drug treatments, compared to untreated. Measurements were recorded every 5 min for 1 h. **C** and **D**; overall ROS production of each treatment group. H_2O_2 was included as a positive control for the assay. ROS was detected with CM-H_2DCFDA. **E** and **F**; $^{\bullet}OH$ and $ONOO^-$ production at 1 h following LPS and Fpr2/3 agonist stimulation. **G** and **H**; mitochondrial ROS (mtROS) gradients of different treatment groups compared to untreated cells over 1 h. **I** and **J**; mtROS production over a period of 1 h for different treatment groups. Rotenone was used as a positive control. **K** and **L**; the effects of C43 and QC1 on rotenone-induced mtROS production up to 2 h. Mitochondrial ROS production was detected with MitoSOX Red every 5 min for up to 2 h. Data are means ± SEM of 3-5 independent cultures in triplicate. **P* < 0.05.

Previous reports show that LPS can contribute to mitochondrial ROS production (Mills et al., 2016; Park et al., 2015). To decipher whether mitochondria contributed as a source of LPS-induced ROS production in our study, mitochondrial specific superoxide was examined using the MitoSOX fluorescent tracer, with Fpr2/3 agonists administered as for CM-H_2DCFDA. Interestingly, LPS increased mitochondrial ROS (mtROS) over a 2 h period, with both C43 and QC1 reversing this back towards untreated levels (Figure 3.10G-3.10J). However, neither FPR2 agonist prevented increased mtROS production initiated by the mitochondrial complex I inhibitor rotenone (Figure 3.10K and 3.10L).

LPS has also been shown to produce ROS via the activation of microglial NADPH oxidase (Yauger et al., 2019). The NADPH oxidase subtype NOX2 is found at highest levels in microglia (Hou et al., 2018), and is therefore a prime candidate to investigate ROS production. The NOX2 enzyme consists of multiple protein subunits, including the plasma membrane bound gp91phox and the cytosolic regulatory protein p67phox (Ma et al., 2017). When activated, p67phox is transported to the cell membrane and colocalises with gp91phox, in a pathway dependent on the small GTPase Rac1 (Haslund-Vinding et al., 2017). NADPH oxidase assembly was determined by confocal microscopic examination, with 30 min LPS ± 10 min post-C43 treatment before cell fixing, staining and visualisation. Compared to untreated cells, LPS increased the localisation of p67phox to the plasma membrane after 30 min exposure, supporting increased co-localisation with gp91phox (Figure 3.11A). Interestingly, whilst C43 did not impact localisation of these subunits when administered alone, addition 10 min post-LPS reversed p67phox mobilisation induced by this inflammogen (Figure 3.11A). These processes are shown with a distribution false-colour image for p67phox, displaying more clearly the relative levels and cellular distribution of p67phox (Figure 3.11A). A false-colour image was used for both gp91phox and p67phox co-localisation, highlighting strong peripheral co-localisation in LPS treated microglia, with C43 treatment reversing this effect (Figure 3.11B).

3.4.8. Fpr2/3 agonists do not modulate antioxidant pathways following LPS insult

Having shown Fpr2/3 agonists to abrogate LPS-induced ROS production, we investigated their mechanism of action, focussing firstly on antioxidant defences to examine whether receptor stimulation modified activities of several pathways. However, neither C43 nor QC1 post-treatments affected the ratio of oxidised glutathione disulfide (GSSG) to reduced glutathione (GSH:GSSG) after 2 h LPS exposure (Figure 3.12A), nor did they exert any effect on either superoxide dismutase-2 (SOD2; 24 h) or hemeoxygenase-1 (HO-1; 6 and 24 h; Figure 3.12B-3.12I). Thus, Fpr2/3 stimulation appears to reduce LPS-induced ROS production without modulating antioxidant systems.

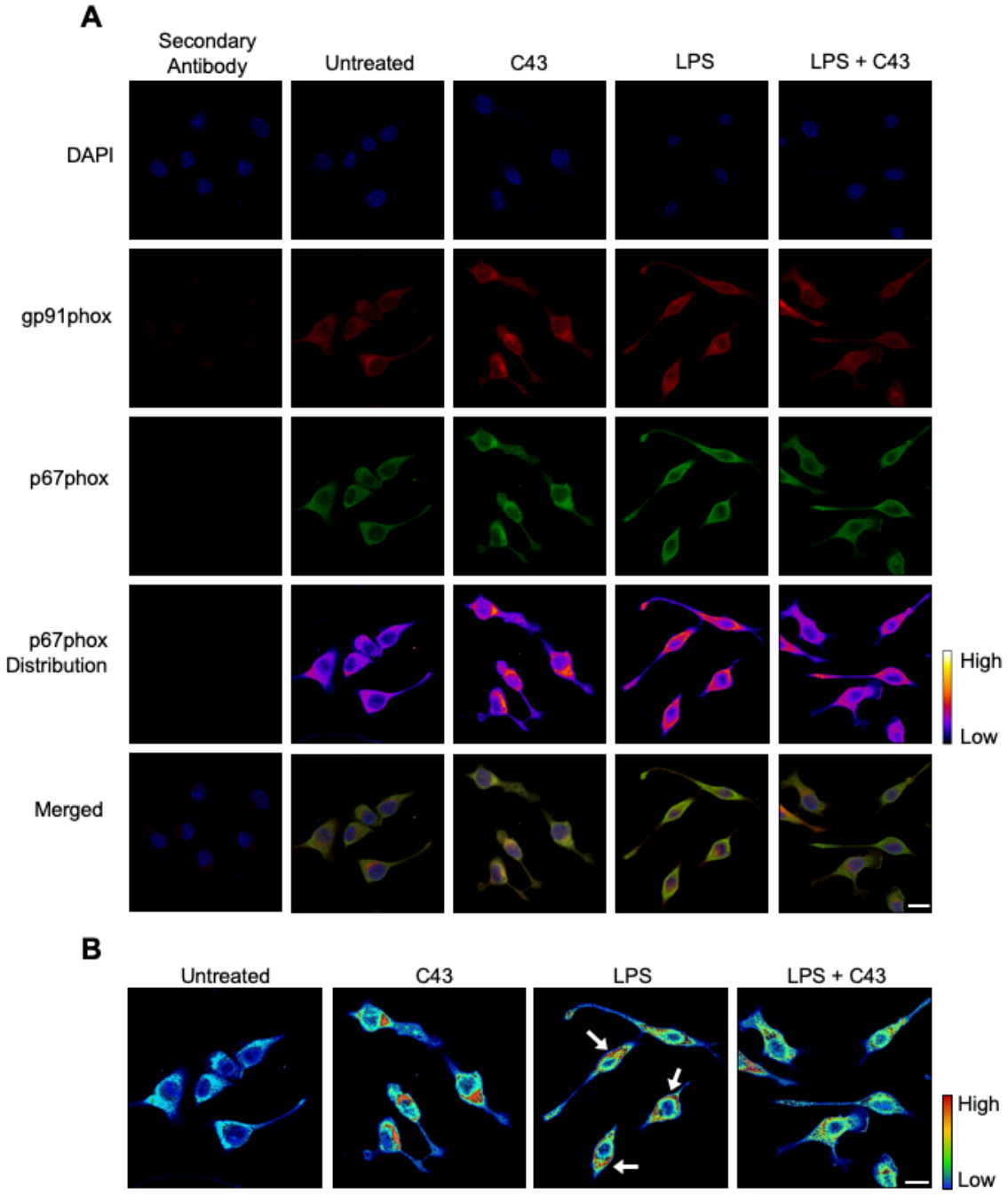

Figure 3.11 The effects of LPS ± C43 on NADPH oxidase subunit co-localisation as determined by confocal microscopy. Samples were fixed following 30 min treatment with LPS ± 10 min-post treatment with C43. **A**; immunostaining of gp91phox (red), p67phox (green), counterstained with DAPI (blue). Treatment with LPS induced the recruitment of p67phox from the cytosol towards the plasma membrane, as clearly represented in the false-colour distribution images. Post-treatment of C43 successfully reversed this. **B**; false-colour image for p67phox and gp91phox co-localisation further emphasising peripheral NADPH subunit co-localisation following LPS treatment alone, with C43 reversing this. Peripheral co-localisation is labelled via white arrows. Scale bar = 10 μm. Images are representative of 3 independent cultures.

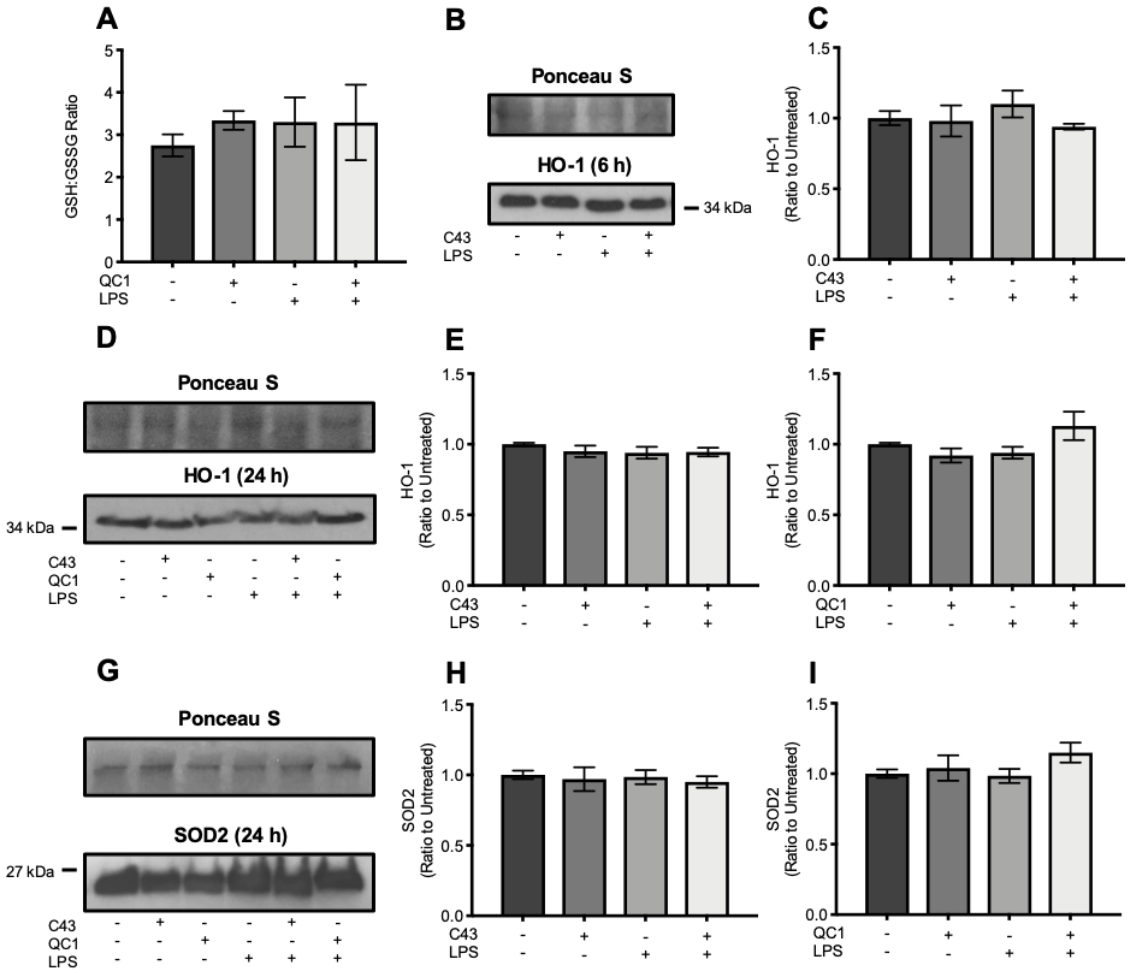

Figure 3.12 The effects of Fpr2/3 agonists and LPS on the reduced to oxidized glutathione ratio, alongside HO-1 and SOD2 expression. A; the relative ratio of reduced (GSH) to oxidized (GSSG) glutathione following 2 h pre-treatment with LPS ± QC1. QC1 was added 10 min after LPS. **B**; HO-1 expression at 6 h-post LPS. C43 was added 1 h after LPS. Ponceau S stain was used as the loading control. **C**; relative HO-1 ratio at 6 h, compared to untreated cells. **D**; HO-1 expression following 24 h LPS exposure ± Fpr2/3 agonist 1 h post-treatment. **E** and **F**; HO-1 expression ratio at 24 h compared to untreated cells for LPS ± C43 and QC1, respectively. **G**; SOD2 expression at after 24 h exposure to LPS ± Fpr2/3 agonist 1 h post-treatment. **H** and **I**; relative HO-1 expression ratio of C43 and QC1 treatment groups compared to untreated. Data are means ± SEM for 3-4 independent cultures in triplicate.

3.4.9. Fpr2/3 agonists reduce LPS-induced L-lactate production and glucose utilisation

Interaction between the control of metabolism and inflammatory phenotype in macrophage-lineage cells is increasingly evident, with a shift towards glycolysis and away from the Krebs cycle and fatty acid oxidation (FAO) being strongly associated with a pro-inflammatory macrophage phenotype (O'Neill and Hardie, 2013), whilst oxidative phosphorylation is more associated with a pro-resolving phenotype (Rodríguez-Prados et al., 2010). Whether something similar happens in CNS immune cells is not known. To investigate whether this occurs, we examined the end-stage glycolytic metabolite L-lactate in BV-2 culture medium following LPS and Fpr2/3 agonist treatments in serum-free high (4.5 g/L; 25 mM) and physiological (1 g/L; 5.6 mM) glucose levels. Initial studies confirmed that 24 h treatment with LPS significantly increased L-lactate release compared with untreated cells, an effect reversed by subsequent 1 h post-LPS treatment with either C43 or QC1 (100 nM), an observation similar for both high and physiological glucose conditions (Figure 3.13A-3.13D). Interestingly in high glucose medium, either C43 or QC1 administered alone stimulated a reduction in L-lactate levels at 24 h, but not 48 h (3.13A and 3.13B), an effect not seen in physiological glucose conditions (Figure 3.13C and 3.13D).

Upregulated aerobic glycolysis is associated with increased glucose uptake (Aït-Ali et al., 2015), hence we determined BV-2 cellular glucose usage at 24 h and 48 h post-LPS in both high and physiological glucose medium. In high glucose medium, treatment with LPS significantly decreased glucose concentration in the supernatant at both 24 h and 48 h, which was only reversed by Fpr2/3 agonists at 24 h when administered 1 h post-LPS (Figure 3.14A and 3.14B). A similar trend was observed in physiological glucose levels, but C43 significantly reversed LPS-induced reduction in supernatant glucose levels at both 24 h and 48 h (Figure 3.14C and 3.14D). When administered alone, neither of these Fpr2/3 ligands facilitated changes in glucose concentration (Figure 3.14A-3.14D). Thus, this data provides evidence that Fpr2/3 activation can reduce LPS-induced glycolysis.

3.4.10. Fpr2/3 stimulation with C43 phosphorylates p38 MAPK but not ERK1/2

Stimulation of human FPR2 has been associated with activation of both the p38 MAPK and ERK1/2 signalling pathways (Sadani N Cooray et al., 2013; Guo et al., 2016; He and Ye, 2017; McArthur et al., 2015); we therefore examined activation of these pathways in BV-2 cells in response to C43, the most potent of the two anti-LPS agonists. Initial western blotting suggested that C43 rapidly increased the phosphorylation of p38 MAPK (Figure 3.15A). an effect quantified and corroborated with the InstantOne (total/phospho) multispecies p38 ELISA kit (Figure 3.15B and 3.15C). In contrast, C43 did not appear to phosphorylate ERK1/2 at any of the time points tested (Figure 3.15D). To further validate

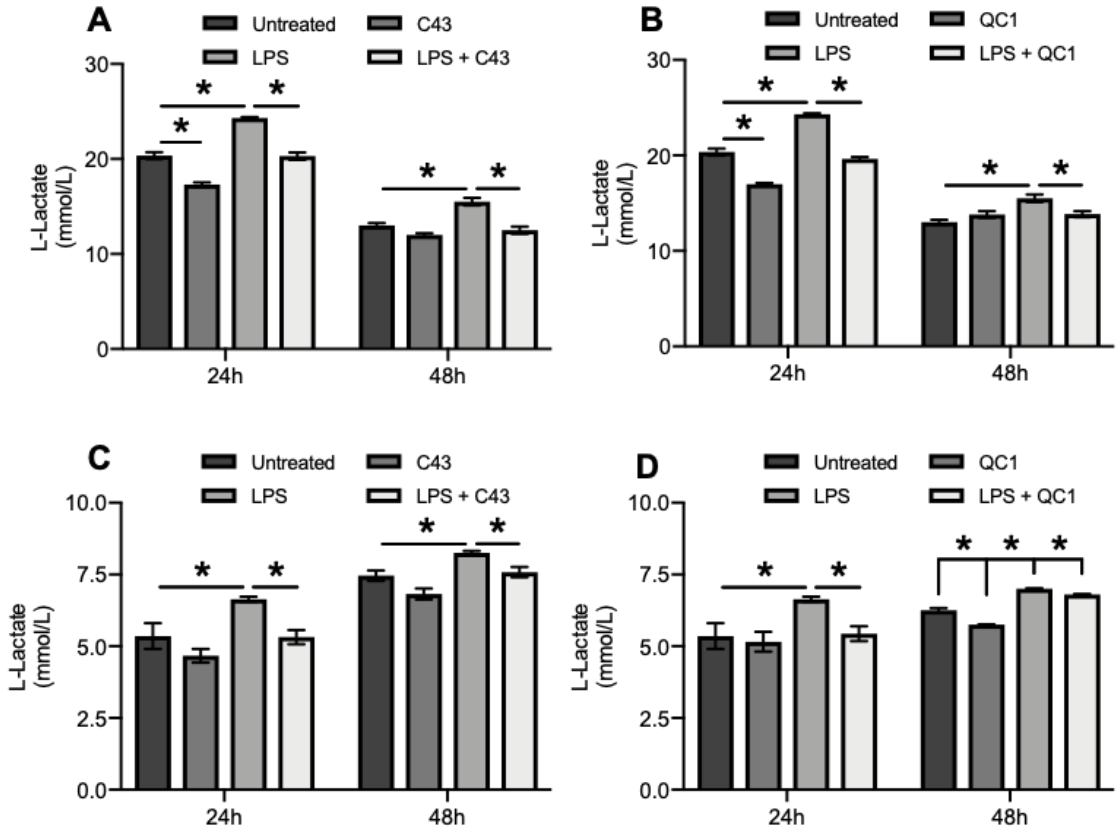

Figure 3.13 The effects of LPS and Fpr2/3 agonist treatment on the cellular production and secretion of L-lactate in high and physiological glucose conditions at 24 h and 48 h post-LPS exposure. In all experimental treatments, Fpr2/3 agonists (100 nM) were administered 1 h following LPS. **A** and **B**; L-lactate production at 24 h and 48 h in high glucose medium. Fpr2/3 agonists significantly reduced L-lactate when administered alone after 24 h. This effect was lost at 48 h, but the ability remained evident post-LPS at both time points. **C** and **D**; L-lactate levels at 24 h and 48 h in physiological glucose medium. C43 and QC1 reduced L-lactate production post-LPS at both 24 h and 48 h, whilst the effects of QC1 at 48 h were smaller compared to C43. However, QC1 also significantly reduced L-lactate production alone compared to untreated cells at 48 h. This was not observed for C43. Data are means ± SEM for 3-4 independent cultures plated in triplicate. *$P < 0.05$.

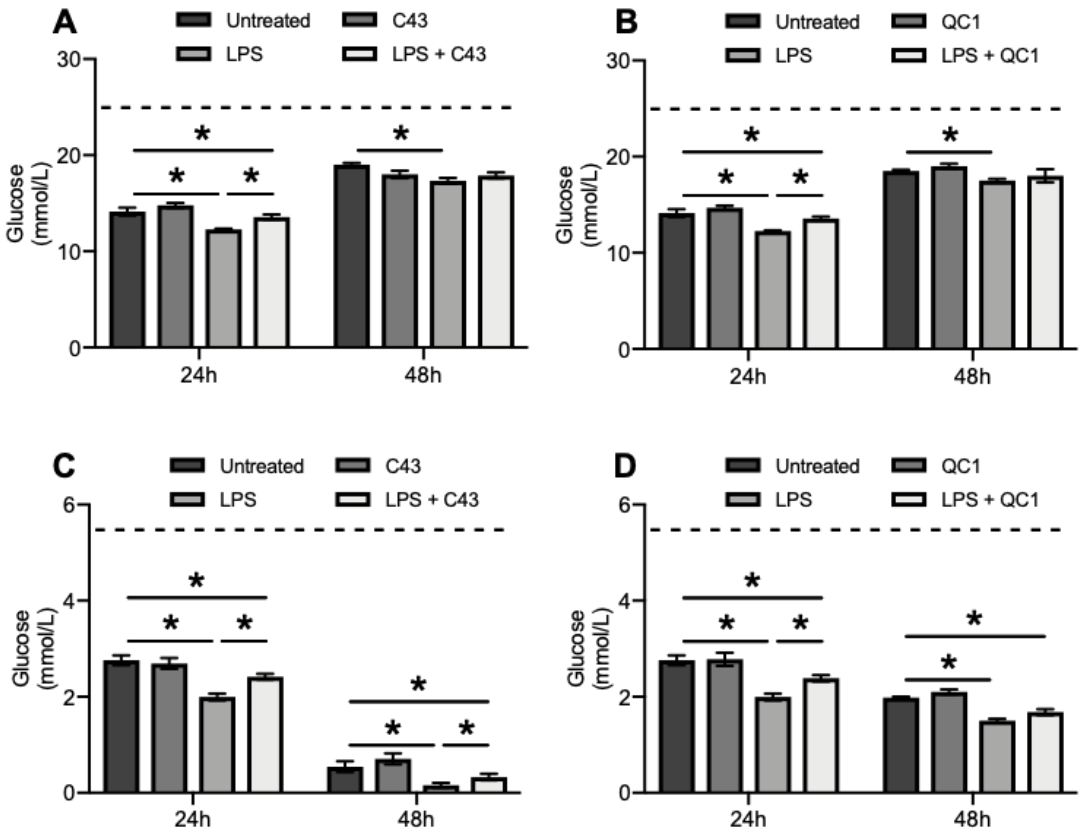

Figure 3.14 The effects of LPS and Fpr2/3 agonists on glucose usage of BV-2 microglia in high glucose and physiological glucose media at 24 h and 48 h post-LPS. Fpr2/3 agonists (100 nM) were administered 1 h following LPS insult. Graphs show glucose concentration in the cell supernatant, with reduced levels indicating increased cellular glucose usage. Dotted lines represent glucose concentration in respective physiological and high glucose medium in the absence of cells. **A** and **B**; glucose concentration in high glucose medium supernatant at 24 h and 48 h post-LPS. C43 and QC1 significantly reverse increased glucose utilisation induced by LPS at 24 h but not 48 h. **C** and **D**; glucose in physiological glucose medium after 24 h and 48 h LPS exposure. C43 successfully reverses increased glucose usage by microglia following 24 h and 48 h LPS exposure. This was only observed for QC1 at 24 h. Data are means ± SEM (n = 3-4 independent cultures in triplicate) *$P < 0.05$.

these findings, LPS-induced production of nitrite ± 1 h post-treatment with Fpr2/3 agonists at 24 h was determined in the presence of the p38 inhibitor SB203580 (2 μM) or the ERK1/2 inhibitor FR 180204 (10 μM), both administered 10 min prior to the Fpr2/3 agonist. Supporting our previous data, SB203580 inhibited the nitrite-reducing effects of C43 and QC1 (Figure 3.15E and 3.15F) but this effect was not seen for FR 180204 (Figure 3.15G and 3.15H).

3.4.11. C43 stimulated Fpr2/3 activation reverses LPS-induced NF-κB nuclear translocation via a p38 MAPK dependent mechanism

It is well established that LPS can increase cytokine release via activation of the transcription factor NF-κB (Park et al., 2016; Zusso et al., 2017). We therefore examined whether this process occurred in BV-2 cells, and if it could be modulated by Fpr2/3 agonists. To evaluate this, cells were stimulated with LPS for 30 min ± C43 treatment at 10 min post-LPS and intracellular localisation of the NF-κB p65 subunit was assessed by confocal microscopy. As expected, LPS treatment induced nuclear translocation of NF-κB, an effect markedly attenuated by subsequent C43 treatment (Figure 3.16A). Moreover, the mitigating effects of C43 were inhibited by the p38 MAPK inhibitor SB203580, further confirming the involvement of this pathway in Fpr2/3 signaling.

Nuclear translocation of NF-κB p65 is prevented by the presence of the inhibitor complex IκBα, which holds NF-κB in the cytoplasm, thus having a central role as a control system for NF-κB related gene transcription (Zhang et al., 2017). 30 min LPS treatment led to a significant reduction in IκBα expression, an effect prevented by C43 treatment 10 min post-LPS (Figure 3.16B and 3.16C).

3.5. Discussion

Whilst ignored for decades, the central contribution of neuroinflammation towards AD propagation is now widely acknowledged (Dunn et al., 2015; Heneka et al., 2015; Kreisl et al., 2013; Lucin et al., 2013); with some suggesting that it may contribute towards disease pathogenesis just as much or perhaps even more than Aβ and hyperphosphorylated tau protein aggregates (Zhang et al., 2013). Supporting this, the microglial inflammatory marker TSPO correlates with disease severity in humans (Kreisl et al., 2013), a finding which cannot be said for Aβ (Serrano-Pozo et al., 2011), which has been considered by many to be the primary cause of AD for over 25 years (Hardy and Higgins, 1992).

A role for inflammation in AD is supported by multiple genetic studies which have linked SNPs in innate immune genes to AD, implicating microglia in disease pathogenesis (Guerreiro et al., 2013; Jonsson et al., 2013; Mecca et al., 2018; Sims et al., 2017) alongside

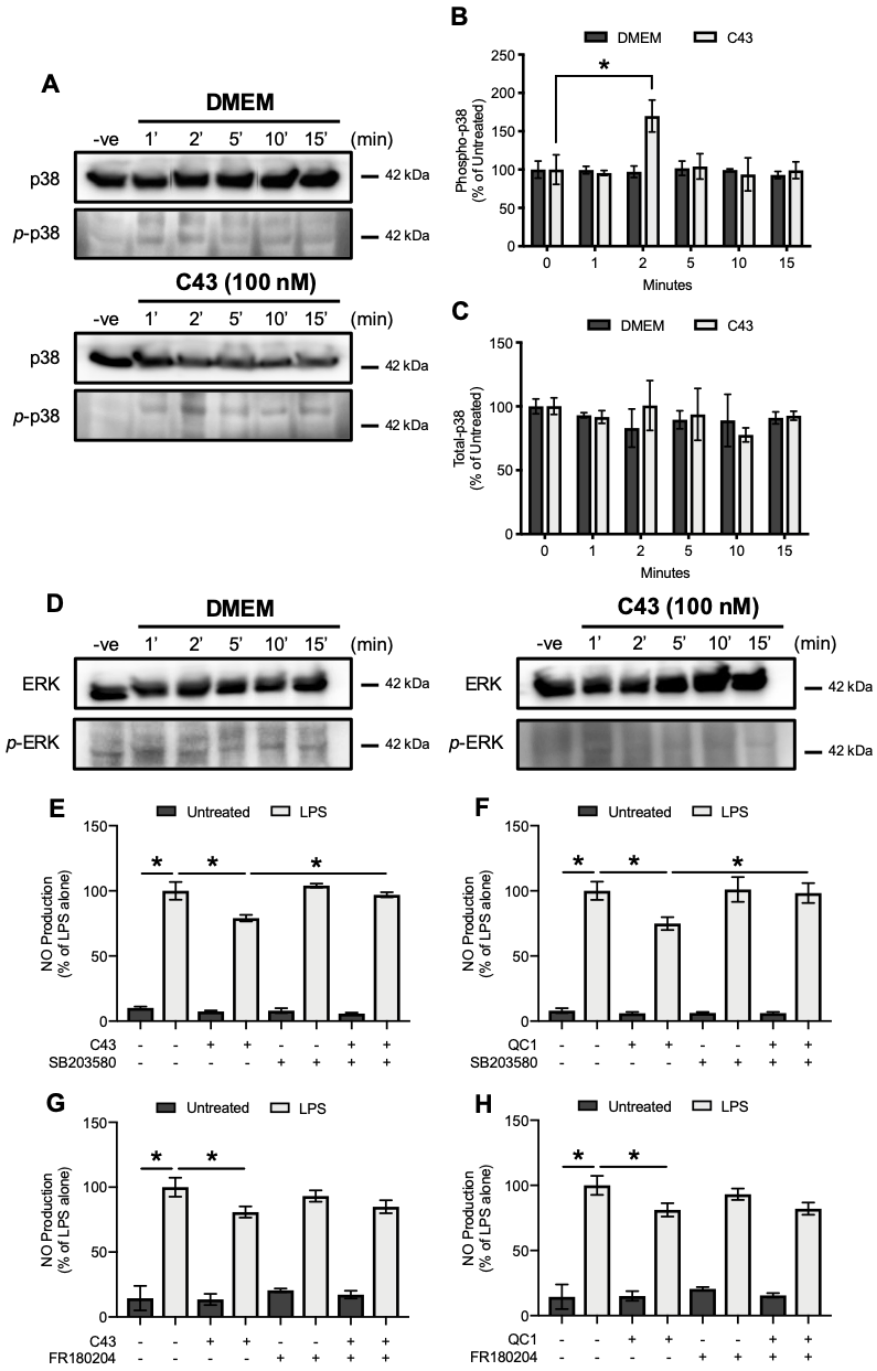

Figure 3.15 C43 stimulates p38 MAPK but not ERK1/2 phosphorylation. A; initial western blotting detected possible p38 MAPK phosphorylation (*p*-p38) by C43 following 2 min exposure to the Fpr2/3 agonist. DMEM treated cells were used as a negative control. Expression of *p*-p38 was compared to total protein levels. **B**; increased *p*-p38 by C43 after 2 min was confirmed by the InstantOne^{TM} (total/phospho) multispecies p38 ELISA kit. Vehicle was cells treated with DMEM. **C**; relative total p38 expression levels detected through ELISA. **D**; ERK1/2 expression as assessed via western blot. Phosphorylated ERK1/2 (*p*-ERK) was not affected by either DMEM or C43 addition. *p*-ERK was compared against total protein. **E** and **F**; nitrite production at 24 h post-LPS. Fpr2/3 agonists were administered 1 h after LPS addition. The p38 inhibitor SB203580 (2 μM) was administered 10 min prior to C43 and QC1. SB203580 significantly inhibited the nitrite reducing abilities of both agonists following LPS stimulation. **G** and **H**; nitrite levels were also determined at 24 h post-LPS with the inclusion of the ERK1/2 inhibitor FR 180204 (10 μM) 10 min prior to C43 and QC1. However, this inhibitor had no effect on nitrite production, nor did it inhibit the nitrite reduction capabilities of C43 or QC1. Data are means ± SEM of 3-6 independent cultures in triplicate. **P* < 0.05.

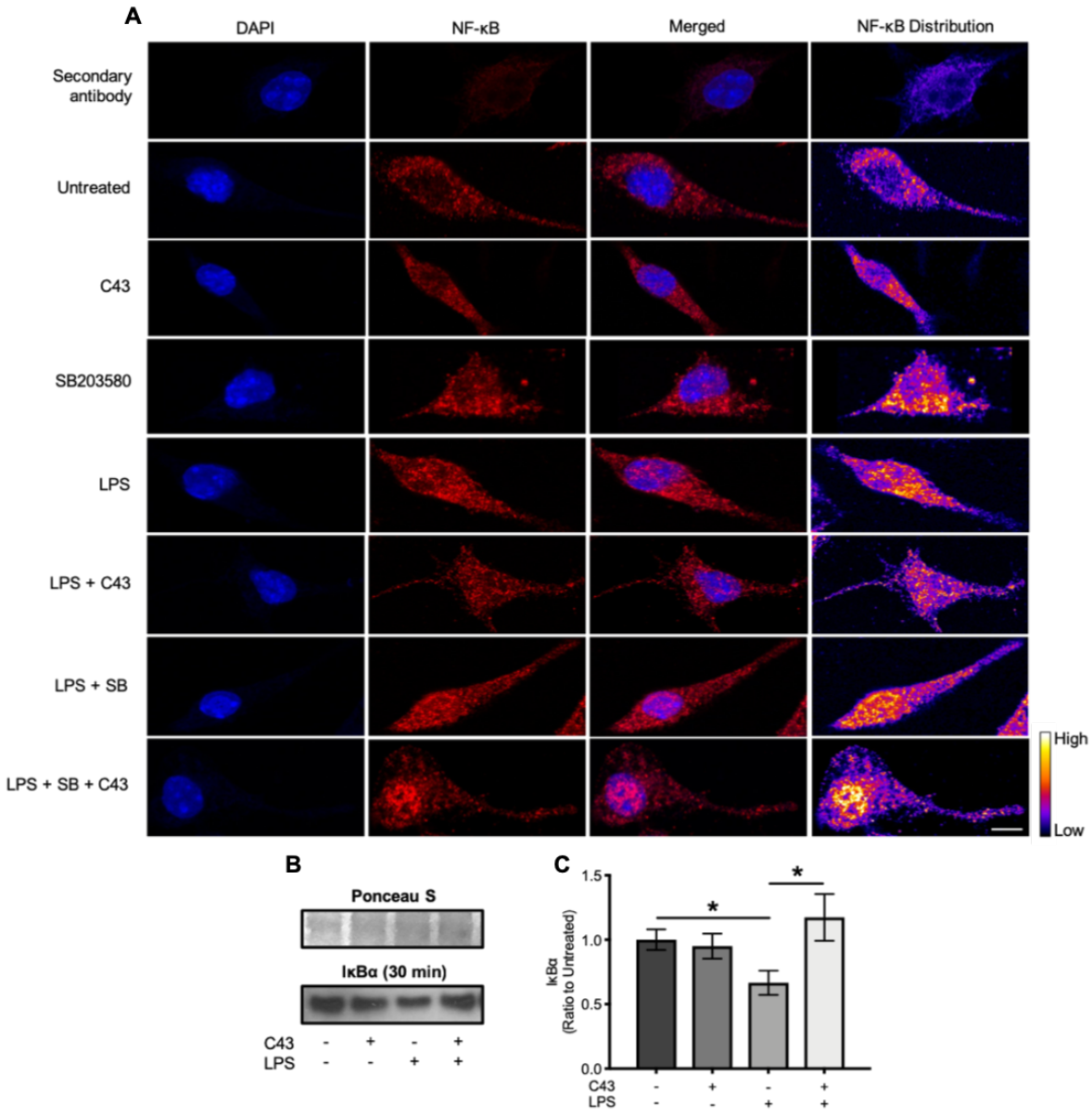

Figure 3.16 The effects of LPS and C43 on NF-κB p65 subunit translocation is modulated by IκBα. Cells were treated with LPS for 30 min ± 10-min C43 post-treatment. The p38 inhibitor SB203580 (SB; 2 μM) was administered 5 min prior to C43. Cells were fixed in 2% formalin at 30 min post-LPS for confocal imaging. **A**; cellular distribution of NF-κB p65 as determined by confocal microscopy. NF-κB p65 was identified with a rabbit monoclonal IgG primary and a polyclonal goat anti-rabbit Alexa Fluor™ 647 secondary antibody. DAPI was used to counterstain nuclei. For the false-colour distribution images, white/yellow represents high expression and blue/purple represent low expression of NF-κB p65, respectively. Images represent single optical sections and are representative of three independent experiments. Magnification is 63x. Scale bar = 10 μm. **B**; western blot analysis of IκBα following 30 min LPS stimulation ± C43 10 min post-treatment. Ponceau S stain was used as a protein loading control. **C**; ratio of IκBα expression of LPS and C43 treated cells compared to untreated. Images are representative of 3 independent cultures. Data graphically represented is means ± SEM of 3 independent cultures in triplicate. *P < 0.05.

post-mortem (Hopperton et al., 2018) and PET imaging studies (Kreisl et al., 2013; López-Picón et al., 2018) of AD. Brain inflammation accompanies Aβ deposition in the majority of MCI cases that convert to AD (Parbo et al., 2017). Innate inflammation may therefore contribute to the disease and targeting microglia may hold central importance for future research. Here we show that neuroinflammation can be successfully reduced through microglial Fpr2/3 activation and therefore emphasise that this receptor may provide a novel therapeutic approach for reducing the severity and onset of neuroinflammation in neurodegenerative diseases such as AD.

In an inflammatory response, the pro-inflammatory induction phase is essential to orchestrate an effective host defence. The resolution phase which follows is responsible for restoring tissue homeostasis once a danger signal has been eliminated (Buckley et al., 2013), but inhibition of this protective phase can lead to chronic inflammatory disease, with arthritis and colitis being clinical examples of peripheral resolution dysfunction (Nielsen and Ainsworth, 2013; Perretti et al., 2017a). This supports the complex nature of the immune system. Multiple studies bolster the opinion that this happens in the brains of AD patients (Fan et al., 2017, 2015; Hopperton et al., 2018; Kreisl et al., 2013; Parbo et al., 2017), thus pharmacologically encouraging inflammatory resolution may be a viable alternative therapeutic strategy to tackle neurodegenerative diseases with a considerable inflammatory component, including AD (Frigerio et al., 2018; Hopperton et al., 2018). In this study, we provide evidence that Fpr2/3 stimulation successfully shifts microglial phenotype from pro-inflammatory to one with pro-resolving characteristics, highlighted by shifts in cytokine production, phagocytosis and metabolism. We therefore underline that Fpr2/3 modulation not only reduces markers of neuroinflammation, but also actively shifts the microglial response towards one of active tissue protection and repair; a crucial alteration for neuronal protection in neurodegenerative disease.

Murine Fpr2/3 and human FPR2 have central roles in the resolution of peripheral inflammation (Sadani N Cooray et al., 2013; Dalli et al., 2012; Gobbetti et al., 2014; McArthur et al., 2015; Vital et al., 2016). Despite also being expressed in microglia (Chen et al., 2007; McArthur et al., 2010; Ries et al., 2016), little is known about its potential as an anti-neuroinflammatory target. We show evidence that post-LPS activation of Fpr2/3 with specific agonists successfully contribute to the reversal of LPS-induced inflammation in BV-2 microglia, supporting the exploitation of this receptor as a therapeutic, rather than a prophylactic. Fpr2/3 may therefore protect tissue from neuroinflammatory damage after it has already initiated. Our data highlights the facilitation of further research into the potential therapeutic capacity of exploiting these pro-resolving receptors for *in vivo* models of neuroinflammatory and neurodegenerative disease, including AD.

3.5.1. Fpr2/3 stimulation reduces key features of pro-inflammatory microglia

Chronically activated microglia are characterised by the release of pro-inflammatory mediators, including nitric oxide, cytokines such as TNFα, and chemokines alongside the production of different ROS (Heneka et al., 2014; Salter and Stevens, 2017). Here we emphasise a fundamental function for Fpr2/3 in regulating the oxidative stress response in microglia, wherein it successfully reversed the oxidative capacity of a strongly potent inflammogen, LPS, alongside modulating multiple aspects of the pro-inflammatory microglial response. Our data here highlight the clear pro-resolving actions of two independent Fpr2/3 agonists, C43 and QC1 when given prior to or after LPS, providing data on the potential to both prevent and reverse neuroinflammation. The importance of reducing neuroinflammation in neurodegenerative diseases cannot be ignored. In pre-clinical models, multiple lines of evidence emphasise that reducing neuroinflammation can contribute to a reduction in synaptic and axonal damage (Hong et al., 2016), neuronal death (Shi et al., 2017) and cognitive decline (d'Avila et al., 2018). Inhibition of microglial activation can also preserve hippocampal neurogenesis (Wadhwa et al., 2017), therefore suggesting the potential ability of Fpr2/3 stimulation to reduce the likelihood of neuronal damage and death as a consequence of neuroinflammation. Importantly, the anti-inflammatory observations made for these Fpr2/3 ligands were absent of any signs of microglial toxicity, as highlighted through cell cycle and cell viability analysis. This is important going forward, wherein tolerability and lack of toxicity is essential for *in vivo* research utilising these compounds. Previous murine work using these agonists in the periphery also showed no signs of toxicity (He et al., 2011; Kao et al., 2014).

Oxidative stress is an essential component of the immune response to destroy invading pathogens (Paiva and Bozza, 2014; Winterbourn and Kettle, 2013), but it also has a central role in cell signalling, wherein it regulates the inflammatory response (Latz et al., 2013; Singel and Segal, 2016). Despite this clear physiological importance, it can be a double-edged sword. The high energy consumption of the brain results in it being more vulnerable to oxidative damage than any other organ (Cobley et al., 2018; Magistretti and Allaman, 2015), due to high mitochondrial ROS production and modest endogenous antioxidant defences of neurones (Baxter and Hardingham, 2016; Bell et al., 2015). However, data presented here highlights that Fpr2/3 stimulation can reverse both mitochondrial and NADPH oxidase induced ROS production, underlining that select agonists for this receptor may provide neurones protection from rogue microglia and their associated ROS response. Increased ROS within immune cells can also lead to the hyperactivation of inflammatory responses through the activation of the inflammasome (Harijith et al., 2014) and transcription of pro-inflammatory genes triggered by NF-κB translocation (Dornas et al., 2017). This leads to tissue damage, pathology and cell death associated with chronic inflammation (Mittal et al., 2014). Whilst IL-1β was not released in our study, suggesting a

lack of inflammasome activation Fpr2/3 stimulation prevented the nuclear translocation of NF-κB, consequentially reducing the expression of several pro-inflammatory mediators. With ROS production appearing to be central contributors to microglial inflammation, Fpr2/3 induced reversal of NADPH oxidase and mitochondrial induced ROS production may hold significance for reducing neuroinflammation *in vivo*. This still holds pertinence even though activation of these ROS pathways here were bacterially (LPS) modulated, because they are both active and appear to contribute to neurodegeneration in AD (Wyssenbach et al., 2016)

ROS production which exceeds the scavenging capacity of neuronal antioxidant response systems can lead to the oxidation of proteins, lipids and nucleic acids, observed in the human brain (Ercegovac et al., 2010). This appears to be the case in AD, where oxidative markers increase in a disease-dependent manner, correlating with patient MMSE scores (Ansari and Scheff, 2010), with high ROS levels reported to increase Aβ pathology in transgenic mice (Han et al., 2015). For our study, as well stimulating cytokines, we confirmed that LPS is a potent stimulator of ROS production (Kim et al., 2010; Yauger et al., 2019). Here we show the novel finding that selective Fpr2/3 activation can completely reverse LPS-induced ROS production, including superoxide, without modulation of the antioxidant systems glutathione, HO-1 or SOD-2. Interestingly, LPS-induced mitochondrial and NADPH oxidase induced ROS production has been shown to promote the production of several pro-inflammatory cytokines, including TNFα (Bordt and Polster, 2014; Bulua et al., 2011). We observed here that both Fpr2/3 agonists significantly reduced ROS from both sources, alongside TNFα production, respectively. In addition, formylated peptides derived from bacteria and mitochondria are recognised to stimulate FPRs (Dorward et al., 2017; Gabl et al., 2018; Ye et al., 2009). Today, the origin of mitochondria remains speculative but many conjecture that their manifestation occurred through endosymbiosis, wherein these organelles originally manifested as primitive bacterial cells (Dyall et al., 2004; Pallen, 2011). FPRs may have therefore evolved alongside mitochondria, in part as damage recognition receptors. This again further supports that Fpr2/3 may have functions in regulating mitochondrial physiology, but current research on their role in mitochondrial function is lacking. Further research is therefore warranted to determine whether these pro-resolving receptors have any direct effects on the functioning of this organelle.

The production of free radicals is widely recognised to activate of NF-κB (Dornas et al., 2017; Hara-Chikuma et al., 2015; Ndengele et al., 2005), resulting in an inflammatory response (Nathan and Cunningham-Bussel, 2013; Wang et al., 2016). The combination of LPS-induced ROS production alongside IKK-induced IκBα degradation are both likely contributors towards the pathological observations presented in this study (Karin et al., 2004; Yang et al., 2003). For the first time, we show that Fpr2/3 activation reverses LPS-induced NF-κB translocation via p38 signaling and inhibition of IκBα degradation.

3.5.2. Fpr2/3 stimulation can promote a pro-resolving microglial phenotype

Clinical trials looking into the therapeutic potential of anti-inflammatory compounds in AD have not been successful. Importantly, the majority of these failed therapeutics have been NSAIDs, such as aspirin (AD Collaborative Group et al., 2008), rofecoxib (Reines et al., 2004) and naproxen (Meyer et al., 2019), and have been given at symptomatic stages of AD. However, anti-inflammatory drugs such as these primarily focus on the selective inhibition of particular inflammatory processes, preventing the production of specific inflammatory mediators. Utilisation of these inhibitory anti-inflammatory strategies may have a limited impact on the phenotypic nature of the resident microglial cells of the brain. We suggest that microglial phenotypic modulation is a key therapeutic target to facilitate endogenous tissue repair and neuronal protection, supplementing any additional anti-inflammatory pharmacological approaches.

Our study builds upon previous research exhibiting the crucial functions of murine Fpr2/3 and human FPR2 in the resolution of inflammation (Sadani N Cooray et al., 2013; Gobbetti et al., 2014; Kang and Lee, 2016; Petri et al., 2017; Trentin et al., 2015). We have highlighted that both C43 and QC1 can successfully modulate the expression of several characteristic features associated with pro-resolving microglia and tissue repair, which may hold premise for future research into several different CNS pathological situations wherein the resolution of inflammation is hindered.

First, IL-10 release was significantly upregulated by these two small molecules following LPS pre-treatment. This finding supports previous peripheral data, whereby Fpr2/3 activation increased IL-10 release (Sadani N Cooray et al., 2013; Fredman et al., 2015) via p38 activation (Sadani N Cooray et al., 2013; Saraiva and O'Garra, 2010), supporting our mechanistic findings in this study. However, these studies reported IL-10 release in the absence of a pro-inflammatory insult (Sadani N Cooray et al., 2013), or with Fpr2/3 agonist pre-treatment. Our study reports that Fpr2/3 increases IL-10 after exposure to an inflammatory challenge. This is of particular importance for therapeutic AD strategies, where neuroinflammation is extensive (Heneka et al., 2015). IL-10 is a pro-resolving cytokine centrally involved in the resolution of inflammation, reducing the production of pro-inflammatory mediators by both microglia and astrocytes (Cherry et al., 2014). Several lines of evidence place defective IL-10 production or signalling in both animal models of disease and AD patients (Di Bona et al., 2012; Kiyota et al., 2012). Whereas IL-10 production likely correlates with higher numbers of pro-resolving microglia, which appear to be neuroprotective (Tang and Le, 2016).

A second feature which is important for microglial modulation of brain tissue homeostasis is the engulfment and clearance of cellular debris by phagocytosis, a process modulated by several receptors including CD206 (Rajaram et al., 2017). Our data show that Fpr2/3

stimulation can both increase the rapidity of the microglial phagocytic response to bacterial bioparticles and reverse the LPS-induced reduction of CD206 expression. Fpr2/3 stimulation may therefore increase the phagocytic capacity of endogenous microglia. Previous research from our group has shown this to be true, wherein receptor knockout impairs peritoneal bacterial clearance in mice (Gobbetti et al., 2014), with Fpr2/3 stimulation increasing the capacity of primary microglia to efferocytose neurones (McArthur et al., 2010). Phagocytosis and efferocytosis are facilitated by distinct molecular mechanisms (Martin et al., 2014; Underhill and Goodridge, 2012), and our data presented here alongside previous reports highlight the broad potential for Fpr2/3 stimulation to modulate both of these processes. Interestingly, microglial phagocytosis and CD206 expression both appear to be decreased in several *in vitro* and *vivo* studies of AD (Orre et al., 2014; Porrini et al., 2015; Wendt et al., 2017; Zhang et al., 2019), and pro-inflammatory microglia are known to have a reduced phagocytic capacity in both non-diseased and AD states (Hellwig et al., 2015; Orihuela et al., 2016; Wolf et al., 2017). In AD, this reduction in phagocytosis likely leads to the pathological accumulation of toxic Aβ (Bradshaw et al., 2013; Fiala et al., 2005). Thus, increasing microglial phagocytosis may be of particular interest to minimise Aβ accumulation and neuronal damage.

Fpr2/3 was also shown to reduce the expression of two central pro-inflammatory phenotypic markers, CD38 and CD40, both of which are upregulated in the human AD brain (Akiyama and McGeer, 1990; Togo et al., 2000). These markers regulate calcium signalling and chemotaxis alongside ROS production, respectively (Ha et al., 2011; Partida-Sánchez et al., 2001). Thus, Fpr2/3 agonists hold the promise to modulate a diverse array of microglial immunological responses, and further research is required to determine its potential as a neuroinflammatory therapeutic.

The modulation of microglial phenotype through Fpr2/3 signalling is likely primarily associated with downstream p38 signalling. Aligning with previous research (Cooray et al., 2013), we report here that that Fpr2/3 stimulation can result in the downstream upregulation of IL-10 through p38. Whilst IL-10 is a central pro-resolving cytokine as described above, we cannot conclude that other pro-resolving molecules were not upregulated following Fpr2/3 activation. Other cytokines and growth factors associated with resolving pathways include IL-4, IL-13 and TGFβ (Salvi et al., 2017), thus further elucidation as to whether Fpr2/3 mediated p38 signalling, or alterative Fpr2/3 mediated signalling pathways are responsible for the upregulation of any of these additional pro-resolving mediators.

3.5.3. Fpr2/3 stimulation may modulate microglial metabolism

Increasing evidence has linked immune cell phenotype with metabolism, with glycolysis appearing to play a critical role in the pro-inflammatory activation of innate cells such as

macrophages and microglia (Gao et al., 2017; O'Neill and Pearce, 2016; Stienstra et al., 2017). This has been shown for macrophages exposed to LPS (Palsson-McDermott et al., 2015; Tan et al., 2015), emphasising the importance of aerobic glycolysis in these cells. This is similar to the Warburg effect in cancerous tissue whereby under aerobic conditions, cancer cells favour glycolytic metabolism over the oxidative phosphorylation pathway (Vander Heiden et al., 2009). The maintenance of this metabolic phenotype is seemingly counterintuitive given that aerobic glycolysis is far less efficient than oxidative phosphorylation in terms of ATP yield (Mookerjee et al., 2017). However, previous work suggests that a shift towards aerobic glycolysis may be more efficient when glucose uptake is increased (Vazquez et al., 2010), because glucose is the sole energy source for glycolysis (Kelly et al., 2015). For example, even dietary fructose is converted into glucose by the small intestine (Jang et al., 2018). In addition, glycolysis provides many intermediates which can be utilised for inflammatory mediator synthesis, many of which are not produced by the Krebs cycle (Ganeshan and Chawla, 2014). Our data confirm previous reports that LPS can reduce microglial ATP production (George et al., 2015), likely through a shift towards glycolysis, which our data supports.

Another effector associated with LPS stimulation may be mitochondrial ROS production, which appears to be central to the bactericidal activity of macrophages (West et al., 2011). Glycolysis may therefore compensate for this shift in mitochondrial metabolism away from ATP production and towards mtROS production by the electron transport chain (Palsson-McDermott and O'Neill, 2013). This may also be true for NO production, which has been primarily reported to inhibit mitochondrial ATP production in cardiac cells (Benamar et al., 2008; Brown and Borutaite, 2007). Our data highlight potential roles for these peripheral findings in activated microglia, wherein we observed that LPS significantly increased mtROS production, glucose uptake and utilisation, and extracellular L-lactate concentration in both high and physiological levels of glucose. These effects were reversed by the post-treatment with Fpr2/3 agonists C43 and QC1, further supporting the idea that selective Fpr2/3 stimulation may alter microglial metabolism in several disease states. We also show that Fpr2/3 activation can reverse LPS-induced NADPH oxidase activation, an enzyme crucially responsible for ROS production in microglia (Sorce et al., 2017; Vilhardt et al., 2017).

In terms of both inflammation and glycolysis, increased extracellular lactate is usually associated with a negative feedback loop, reducing the activities of both, including attenuating pro-inflammatory cytokine release (Dietl et al., 2010). However, due to neurones primarily utilising L-lactate as an energy source, supplied as a consequence of the astrocyte-neurone shuttle (Mächler et al., 2016), the accumulation of L-lactate we observed *in vitro* is unlikely to happen within the brain. Thus, further study is required to determine the effects of Fpr2/3 stimulation on immunometabolic phenotypes.

Peripheral research focusing on the inflammatory resolution capacity of murine Fpr2/3 and human FPR2 is ongoing (Sadani N Cooray et al., 2013; Gobbetti et al., 2014; Purvis et al., 2019; Qin et al., 2017), but this usually excludes investigation into metabolic changes. Our data on microglial inflammatory metabolic shifting associated with Fpr2/3 activation is the first of its kind, suggesting that human FPR2 facilitates similar functions, and could therefore be a beneficial therapeutic target not just for neuroinflammation in neurodegenerative disease, but also for changes in CNS metabolism; something that might be a key link between metabolic disorders such as insulin resistance and type 2 diabetes, and the increased risk of developing AD (Johnson et al., 2017; Moran et al., 2015).

3.5.4. Fpr2/3 agonist selection will be crucial for therapeutic potential

Murine Fpr2/3 and its human analogue FPR2 display crucial roles in inflammation and host defence (Ye et al., 2009), highlighted by selective agonists eliciting anti-inflammatory and pro-resolving effects. However, in our experiments, administration of the synthetic peptide agonist MMK-1 further increased nitric oxide production following LPS stimulation. This, alongside C43 and QC1 are only a few from a diverse range of ligands which exist for human FPR2, including bacterial and mitochondrial-derived formyl peptides, eicosanoids and small molecules (He and Ye, 2017). Some of these agonists include the pro-inflammatory serum amyloid A and $A\beta_{1\text{-}42}$ (Le et al., 2001; Tiffany et al., 2001; Wang et al., 2018a), but many are endogenous pro-resolving ligands, with species such as AnxA1, LXA4 and resolvin D1 shown to be expressed in the brain (Bisicchia et al., 2018; McArthur et al., 2010; Wang et al., 2015), and appear to be essential for BBB integrity (Cristante et al., 2013) and in reducing AD pathology (Dunn et al., 2015), including increasing Aβ phagocytosis (Mizwicki et al., 2013; Ries et al., 2016). Despite the clear benefits of utilising these named specialised pro-resolving mediators (SPMs), their therapeutic potential is reduced due to either their chemical instability and half-life (LXA4 and resolvin D1; Maderna and Godson, 2009; Mozurkewich et al., 2016; Skarke et al., 2015), or their large size (AnxA1, 37 kDa), likely inhibiting their ability to cross the BBB. These SPMs may also be non-specific to Fpr2/3, with AnxA1 binding to integrin α4β1 (Parente and Solito, 2004), with further suggestions that LXA4 and its analogues do not signal through human FPR2 (Forsman and Dahlgren, 2009). We wanted to utilise specific agonists to support the potential of the receptor as a viable therapeutic target.

3.5.5. Experimental limitations and improvements

The preliminary data gathered here emphasises Fpr2/3 involvement in inflammatory resolution and phenotypic shifting, further supporting the initial work which elucidated these functions. However, as with all *in vitro* experimental designs, limitations to our inflammatory

model are plentiful. Despite BV-2 microglia being a suitable cellular replacement for primary microglial cultures (Henn et al., 2009), single cell culture is not sufficient to correctly determine the overall effects of C43/QC1 in the neuroinflammatory environment of the AD brain. Besides their immunosurveillance and inflammatory roles, microglia are central in establishing synaptic networks and remodelling synapses through synaptic pruning (Paolicelli et al., 2011), emphasising the important role they possess in synaptic plasticity (Salter and Beggs, 2014). Our model is thus unable to determine whether these neuronal-modulating capabilities of microglia would be affected by Fpr2/3 activation.

Pro-inflammatory microglia are responsible for the activation of neurotoxic astrocytes, wherein their ability to promote neuronal survival and synaptogenesis is lost, contributing towards neuronal death (Liddelow et al., 2017; Shi et al., 2017; Yun et al., 2018). Whilst we clearly identified the pro-resolving capabilities of Fpr2/3 agonists in microglia, the knock-on consequences for astrocytic phenotype and neuronal survival is unknown. In terms of neurodegenerative disease, improving our model to include astrocytes in co-culture, followed by the further inclusion of neurones in a triple-culture model, or utilising brain slice culture techniques could elucidate the effects of different Fpr2/3 ligands on cellular communication responses and the consequences for neuronal survival, following exposure to LPS and neurodegenerative toxins such as $A\beta_{1-42}$. This is essential, as the communication responses between these three cell types may have significant contributions towards neuronal toxicity or repair processes.

The pro-resolving effects of Fpr2/3 stimulation in microglia are exciting for further neuroinflammatory research going forward. However, the microglial immune response is extraordinarily diverse and will vary depending on the pathogenic insult. Recent research has highlighted that at least nine transcriptionally distinct microglial states exist, with uniquely expressed gene sets (Hammond et al., 2019). Multiple reactive microglial subtypes were also found in demyelinating injury in mice (Hammond et al., 2019), suggesting that several complicated phenotypes may exist in neurodegenerative conditions, and these may fluctuate depending on the disease in question. This will be something to take into consideration going forward, emphasising that pro-resolving therapeutics need to be able to contribute towards a global shift in microglial phenotype to one that is neuroprotective, rather than a limited response in reducing pro-inflammatory mediator release. Sex also appears to have major effects on immune cell gene expression. In females, genes appeared to be enriched which are involved in PRR pathways (Schmiedel et al., 2018). Our group has also shown that oestradiol promotes pro-resolving microglial behaviour through AnxA1, providing evidence that the reduction in female oestrogen following menopause may contribute to increased inflammation and risk of AD development (Christensen and Pike, 2015; Loiola et al., 2019; Nadkarni and McArthur, 2013). This has implications for *in vitro* and *in vivo* model exploitation for both peripheral and neuroinflammatory disease.

Phagocytosis is an important microglial response to remove cellular debris and toxic Aβ peptides (Ries et al., 2016), whilst efferocytosis is essential to remove apoptotic cells (Chang et al., 2018). Our study highlighted that Fpr2/3 stimulation could increase the ability of microglia to phagocytosis *E. coli* bioparticles. Despite this providing a novel insight into the phagocytic response associated with Fpr2/3 activation in microglia, the relevance of this for neurodegeneration could be questioned. For example, it does not provide an indication of efferocytotic ability, which may contribute towards detrimental synaptic destruction; an unwanted characteristic previously reported (Hong et al., 2016). Looking into the microglial ability to phagocytose cellular debris and toxins relevant for neurodegenerative disease following Fpr2/3 stimulation will therefore be crucial to provide further therapeutic credit for these pro-resolving receptors.

Data also suggest that Fpr2/3 stimulation can modulate microglial metabolism. Our initial observations highlighting Fpr2/3 mediated changes in L-lactate production, glucose uptake and mtROS production support the premise that these pro-resolving receptors may have an important role in immunometabolism (Gao et al., 2017). Mitochondria (alongside NADPH oxidase enzymes) are the primary source of cellular superoxide production (Bordt and Polster, 2014; Brennan et al., 2009; Finkel and Holbrook, 2000). However, mitochondrial formation of free radicals via reversal of electron transport can inhibit mitochondrial ATP production (Scialò et al., 2017), shifting cellular reliance to alternative metabolic pathways, including aerobic glycolysis. Whilst the data presented here holds initial promise, it is important to note that myeloid cells such as microglia can display a wide variety of different phenotypes (Hammond et al., 2019), including several different complicated metabolic signatures which do not resemble the Warburg effect (Stienstra et al., 2017). Also, how these signatures are encoded mechanistically is currently unknown. It will be important to confirm these phenotypic changes following a neuroinflammatory stimulus *in* vivo, alongside distinguishing any associated metabolic changes. Thus, further investigation into different components of microglial metabolism following inflammatory insult is essential.

In terms of LPS, whilst it is a potent inflammogen, neuroinflammation is usually sterile in nature, and thus bacterial LPS is unlikely to be seen in neurodegenerative disease such as AD. However in some circumstances, bacterial infection associated with other diseases such as *Porphyromonas Gingivalis* periodontal infection has been shown to have consistent links with AD (Singhrao et al., 2015). However, as an initial proof of concept study, determining whether Fpr2/3 stimulation can modulate multiple pro-resolving pathways following LPS-associated microglial activation provided inciteful information before processing to more complex *in vitro* and *in vivo* models. The results displayed in Chapter 3 help us elucidate whether the peripheral pro-resolution pathways associated with Fpr2/3 activation could also be modulated within the CNS, to which we provide considerable evidence to support this.

Finally, the obvious limitation to any *in vitro* study is the validity for translational application of data. This research was primarily a proof of concept study to determine whether Fpr2/3 stimulation could successfully temper different aspects of the microglial neuroinflammatory response. Whilst this model is simplistic in comparison to the intricate detail and complexity of the brain, initial *in vitro* experiments are justified to reduce unnecessary usage and euthanisation of animals. As no licenced human microglia were available for purchase during this study, BV-2 cells were used instead, as the most extensively characterised murine microglial cell line available (Timmerman et al., 2018). Despite this, a shift towards a human *in vitro* system is desirable. Recent research has highlighted that while human and murine microglia do indeed have a lot in common, limited overlap was observed in microglial genes which were regulated during aging, suggesting human and murine microglial cells age differently (Galatro et al., 2017; Olah et al., 2018). Whether the transcriptional responses of BV-2 microglia to LPS are representative of primary murine microglia is being questioned (Das et al., 2016; He et al., 2018), and thus supplementary research is required to support our findings.

3.5.6. Future work

The primary data gathered and displayed in this chapter provides an overlook to what could be an exciting step forward in understanding the therapeutic potential of human FPR2 for neuroinflammatory disease. Nevertheless, further work will be important to accurately evaluate whether it can be a druggable receptor. An obvious factor to note is that microglia release a range of different pro-inflammatory and pro-resolving cytokines under different conditions (Heneka et al., 2014), whilst we only selected a few relevant ones for our investigations. In the brain, an important consideration must be made for chemokines, which are essential for microglial migration and peripheral blood cell recruitment to damaged tissue (Gyoneva and Ransohoff, 2015), with its release stimulated by Aβ (Heneka et al., 2015). Complement is the third component of the core pro-inflammatory triad which we did not analyse in this study. Complement has essential roles in regulating the host immune response to microbial invasion (Hajishengallis et al., 2017), but it also appears to be crucial for the neurotoxic communication between microglia and astrocytes (Liddelow et al., 2017) alongside the pathological microglial pruning of synapses in AD mouse models (Hong et al., 2016). With C1q, C3 and the microglial complement receptor CR3 being prime candidates for pathological synaptic degradation (Hong et al., 2016), these will be important components to consider for future investigation to differentiate Fpr2/3 activation from typical anti-inflammatory therapies that have previously failed in clinical trials for AD (Meyer et al., 2019), including NSAIDs which only inhibit the release of one or a small number of pro-inflammatory mediators.

Here we highlight that Fpr2/3 activation can upregulate IL-10, a central pro-resolving cytokine (Sica and Mantovani, 2012). Production of IL-10 reduces the inflammatory response through STAT3 phosphorylation (Lobo-Silva et al., 2016), thus our future work could determine whether Fpr2/3 activation can directly effect this. Alongside IL-10, we highlighted that CD206 expression was upregulated when LPS administered cells were then treated with C43. This is one of several pro-resolving phenotypic markers which are expressed in myeloid cells, also including arginase 1 (Arg), FIZZ1, Ym1 and TREM2 (Lan et al., 2017). We also identified that Fpr2/3 stimulation could reduce LPS-induced NO production without reducing iNOS expression. Further study into the microglial expression profile of Arg1 may therefore be warranted, as this enzyme is responsible for the production of urea and L-ornithine from L-arginine, preventing iNOS utilising the latter to produce the reactive nitrogen species (Lisi et al., 2017).

We also observed LPS-increased microglial glycolysis and L-lactate production, both of which were reduced by Fpr2/3 stimulation. Glucose uptake is controlled by a group of membrane proteins called GLUTs, (Yan, 2017), which facilitate glucose transport across the plasma membrane. Microglia express a particular subtype, termed GLUT5 (Sasaki et al., 2004). Because Fpr2/3 activation modulated microglial glucose usage, further work looking into the relative expression of GLUT5 following Fpr2/3 activation may provide more incite regarding potential immunometabolic functioning of these pro-resolving receptors. Further, the increase in glycolysis observed following LPS stimulation is likely due to pyruvate kinase M2, an essential enzyme necessary for the shift in cellular metabolism towards glycolysis (Palsson-McDermott et al., 2015). Because both C43 and QC1 reduced L-lactate release when administered post-LPS, identifying whether these agonists modulate pyruvate kinase M2 expression will provide further insights into potential mechanisms Fpr2/3 can modulate metabolism. This is also true for the monocarboxylate transporter 4 (MCT4), a plasma membrane protein required for exporting L-lactate from the cytoplasm into the extracellular environment (Kaushik et al., 2019).

Identifying all the mechanisms by which Fpr2/3 facilitates its effects is essential. One of the ways LPS enables its inflammatory response in phagocytes is through the kinase activities of IKK, tagging IκBα for proteasome degradation and consequentially freeing NF-κB for nuclear translocation (Newton and Dixit, 2012). This is what we observed here, with Fpr2/3 stimulation preventing this. However, further investigation of the pathway is possible. For example, looking specifically at both IKK phosphorylation and real-time movement of phosphorylated IκBα towards the proteasome with immunostaining techniques. Whilst our data suggest that this may be p38 mediated, inclusion of an inhibitor for this kinase for all of these aforementioned techniques would confirm its importance in this Fpr2/3 mediated anti-inflammatory pathway. Alongside this, whilst IL-10 is recognised to be transcriptionally regulated by p38, this is not the only anti-inflammatory cytokine localised in microglia, with

others such as IL-4 also reducing LPS induced pro-inflammatory cytokine production (Woodward et al., 2010). Another consideration is that anti-inflammatory effects can also be mediated by AMPK and STAT3 signalling (Zhu et al., 2015), and previous research by our group has shown Fpr2/3 can activate AMPK signalling, contributing towards a macrophage pro-resolving phenotype in mice (McArthur et al., 2018).

Investigation of AMPK signalling is of particular relevance for immunometabolism, wherein this kinase is a metabolic sensor (Kelly et al., 2015). It also appears to negatively regulate pyruvate kinase M2 expression (Huang et al., 2018), and thus AMPK activation is likely to block the metabolic gateway towards aerobic glycolysis. Because this metabolic shift towards glycolysis can fuel inflammatory mediator production and increased glucose utilisation, we propose that alongside p38, AMPK regulation may be of critical importance for the anti-inflammatory and immunometabolic consequences of Fpr2/3 stimulation. Future work will therefore expand on whether Fpr2/3 activation has consequential effects on metabolic pathways associated with inflammatory modulation, and determine the therapeutic relevance of this modulation for neuroinflammatory disease.

3.5.7. Chapter summary

Here we show evidence that activation of the pro-resolving receptors Fpr2/3 with specific agonists successfully contributes to reversing LPS-induced inflammation in BV-2 microglia. Reduced production of pro-inflammatory mediators, ROS, NO and L-lactate alongside observable increases in phagocytosis and IL-10 production following Fpr2/3 stimulation all support the notion that Fpr2/3 activation can promote a pro-resolving phenotype when administered after a microglial inflammatory insult. We also report that Fpr2/3 can reverse LPS-induced mitochondrial and NADPH oxidase induced ROS production. This chapter thus highlights that FPR2 may be of therapeutic benefit for neurodegenerative diseases which have a considerable neuroinflammatory component, but *in vivo* work will be crucial to confirm these phenotypic changes do not only occur *in vitro*.

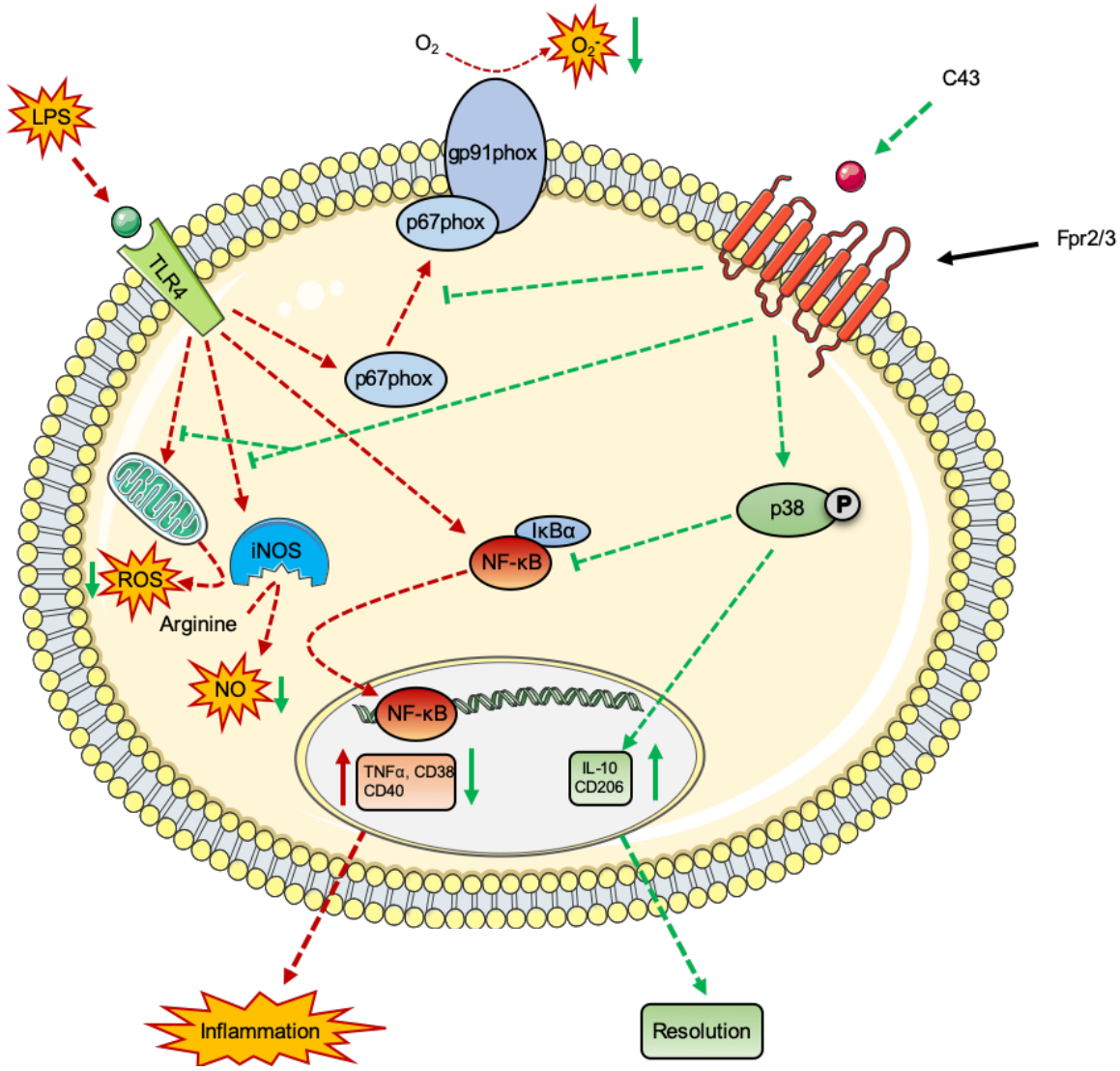

Figure 3.17 Summary diagram for Chapter 3, detailing the effects of LPS and C43 on BV-2 microglia. Mechanism pathways are presented with the dashed arrows and inhibitory lines. Solid arrows represent overall changes. Red lines represent LPS stimulated responses, whereas green lines represent C43 and Fpr2/3 mediated effects. LPS increased both mitochondrial and NADPH oxidase induced ROS production, alongside increasing NO and TNFα production, CD pro-inflammatory phenotypic marker expression and NF-κB nuclear translocation. C43-induced Fpr2/3 activation was able to reverse these effects, alongside upregulating IL-10 production, CD206 expression, and phagocytosis. These processes were partly p38 MAPK dependent.

Chapter 4: The effects of Fpr2/3 agonists and oAβ on ROS Production and Metabolism

4.1. Overview of the Chapter

Despite the central role proposed for Aβ in AD clinical trials targeted towards amyloid continue to fail, and have done for over 16 years (Panza et al., 2019). Immunotherapy for Aβ specifically targets the accumulation of extracellular plaques, but these may not be responsible for driving AD pathology (Benilova et al., 2012; Ferreira et al., 2015; Müller-Schiffmann et al., 2016; Walsh et al., 2002). This is likely why utilising Aβ immunotherapy to remove plaques does not rescue patients from cognitive decline (Holmes et al., 2008; Panza et al., 2019). However, Aβ is not only present in plaques, and the role of oligomeric forms has not been fully assessed.

Whilst Aβ has been used at high concentrations (5-25 μM) *in vitro* to activate microglial inflammation (Caldeira et al., 2017; Wang et al., 2018), its effects at more pathophysiologically appropriate concentrations (Van Helmond et al., 2010) have not been investigated. To avoid repeating widely available *in vitro* research focusing on high concentrations of oAβ, this chapter was primed to determine novel findings; how disease relevant concentrations of oAβ effect microglial function, alongside understanding whether Fpr2/3 agonists can mitigate these actions. In doing so, we will establish the proof-of-principle for targeting of Fpr2/3 as a potential therapeutic strategy to control microglial behaviour in AD. If microglial inflammation could be stimulated by oAβ in our model system, then Fpr2/3 may prove to be a beneficial receptor to exploit as a potential therapeutic to reduce chronic inflammation and neuronal damage in AD. However, despite not focusing on tau pathology in this study, we do emphasise the importance of hyperphosphorylated tau in the development and progression of AD, alongside its direct association with microglial activation (Hopp et al., 2018; Maphis et al., 2015; Yoshiyama et al., 2007). The findings of this Chapter will hopefully provide a proof of concept for the therapeutic efficacy for Fpr2/3 agonists in AD research, priming future study looking into the effects of select agonists on the primary triad of pathologies associated with the disease: neuroinflammation, Aβ aggregation and exacerbated tau hyperphosphorylation.

4.2. Aim and hypothesis

We hypothesised that a disease relevant concentration of oAβ would trigger microglial inflammation *in vitro*, and that Fpr2/3 agonists will restore cellular homeostasis. The first aim of the chapter was thus to establish the effects of oAβ upon BV-2 microglia. The second aim was to confirm whether select Fpr2/3 agonist post-treatment could reverse this oAβ-induced microglial activation, to highlight the potential of Fpr2/3 as an AD therapeutic.

4.3. Experimental design

Several different experimental approaches were used to interrogate these hypotheses. This included cytokine and nitrite detection, ROS production analysis and antioxidant changes. The concentration of oAβ used in this work is representative of measured levels in the brains of AD patients post-mortem (Van Helmond et al., 2010), this is markedly lower than concentrations used in previous *in vitro* studies (Caldeira et al., 2017; Wang et al., 2018), but may more closely reflect processes occurring at earlier stages in AD that might be more amenable to intervention.

Following assessment of inflammatory parameters in BV-2 microglia exposed to oAβ, with or without Fpr2/3 ligand treatment, we analysed the metabolic changes that occur in these cells, given the increasingly apparent links between metabolism and immunophenotype. This included changes in glucose uptake and utilisation, L-lactate production, pentose phosphate pathway activity and mitochondrial function. Finally, we assessed the ability of Fpr2/3 ligands to exert functional protection against oAβ-induced microglial toxicity through the use of co-cultures between BV-2 microglia and differentiated human neuroblastoma SH-SY5Y neurones (Figure 2.1 and Figure 2.2). For experimental timings, oAβ was administered 10 min or 1h prior to C43/QC1 for acute assays (2 h or less) or 24 h/48 h designs, respectively. Summary designs of different experimental procedures, including SH-SY5Y differentiation and co-culturing are presented in Figure 4.1. Different treatment designs were determined as previously described in Section 3.3.

4.4. Results

4.4.1. oAβ does not affect BV-2 cell cycle or cell viability

Initial studies investigated the potential for oAβ to be directly toxic for microglia, either alone or in combination with Fpr2/3 agonist treatment. The effect of oAβ upon cell survival was established using a range of pathophysiologically relevant oAβ concentrations (30, 100, 300 and 1000 nM) as detected by the Prestoblue reagent, with actinomycin D (1 μg/ml) and H_2O_2 (200 μM) treatment used as positive controls. No significant changes in cell survival

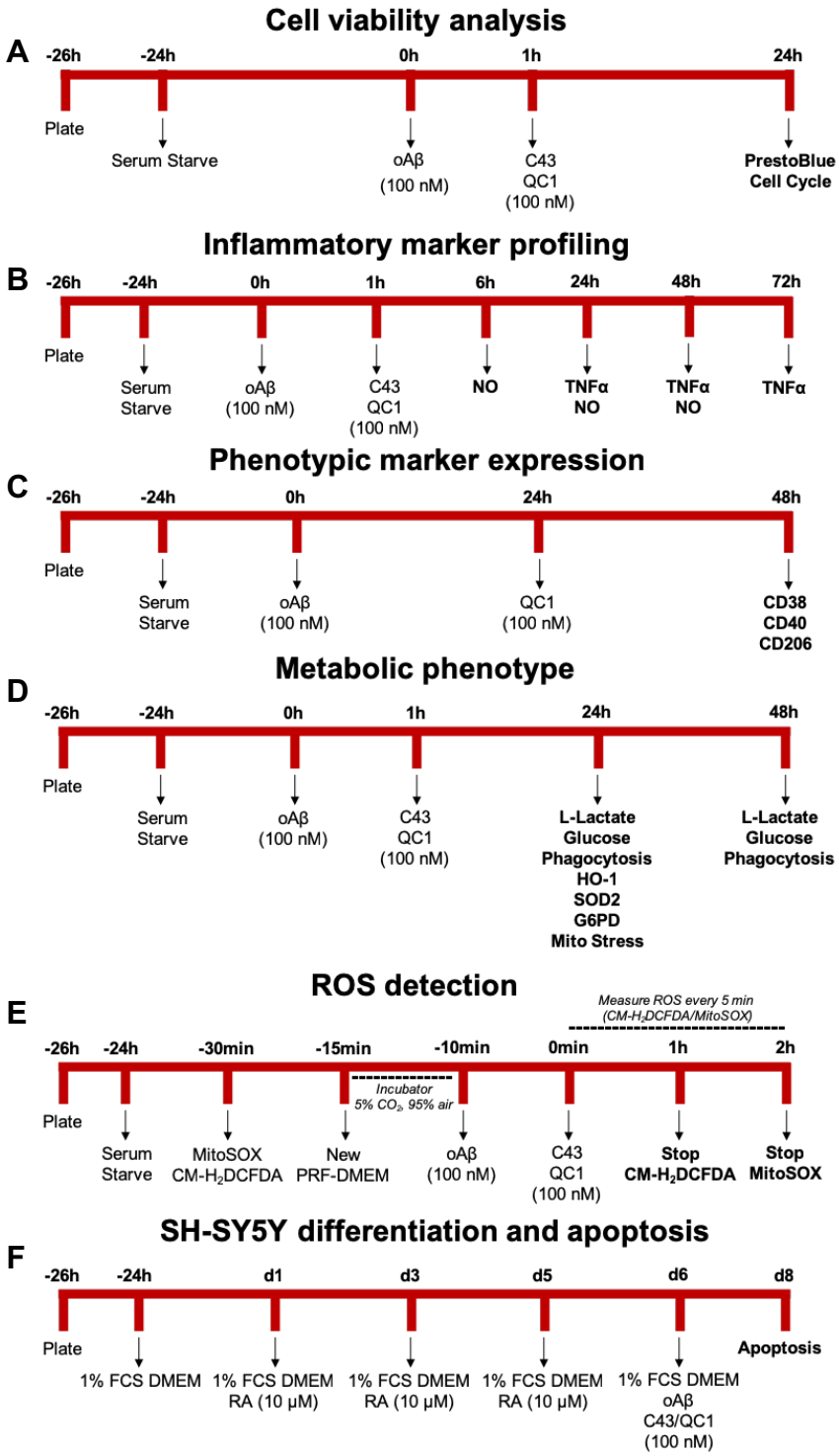

Figure 4.1 Summary of different experimental protocols in Chapter 4. A; cell viability analysis, with 24 h oAβ exposure ± 1 h C43/QC1 post-treatment. **B**; inflammatory marker profiling. oAβ was administered 1 h prior to C43 and QC1. **C**; expression of phenotypic markers in both BV-2 and primary murine microglia, carried out 48 h post-oAβ. **D**; for metabolic phenotype profiling, including phagocytosis capacity and mitochondrial stress analysis, cells were treated as for inflammatory marker profiling. **E**; ROS detection occurred every 5 min for 1 h (CM-H_2DCFDA) and 1 h (MitoSOX Red). •OH and $ONOO^-$ production was measured 1 h and H_2O_2 at 2 h post-oAβ, respectively. **F**; SH-SY5Y differentiation and apoptosis protocol. Cells were plated with *trans*-retinoic acid (tRA; 10 μM in 1% hiFCS DMEM) for 5 days (d1-5), which was replaced with fresh medium on day 3. On day 6, tRA media was removed and new 1% FCS DMEM (without tRA) was added before 48 h oAβ exposure ± 1 h C43/QC1 post-treatment.

were identified for any of the oAβ concentrations tested (Figure 4.2A). As mentioned in Chapter 3.4.1, the PrestoBlue reagent cannot readily distinguish between survival and proliferation. Thus, cell cycle progression was analysed by flow cytometry with the DNA-binding tracer DAPI. Confirming preliminary PrestoBlue data, no changes in Sub-G_0/G_1, apoptotic/necrotic cells were observed (Figure 4.2B). Moreover, with the exception of a reduction in G_2/M phase cells seen with combined oAβ + QC1 treatment, neither oAβ nor Fpr2/3 ligands affected BV-2 cell cycle stage distribution (Figure 4.2B and 4.2C). In summary, oAβ did not display any microglial toxicity, but Fpr2/3 activation following exposure to different toxins may contribute to small shifts in cell cycle progression.

4.4.2. QC1 and oAβ modulate pro-inflammatory markers in primary but not BV-2 microglia

Initial experiments investigated whether oAβ modulated the production of the soluble inflammatory markers nitrite, TNFα and IL-1β, or expression of the surface marker CD40. For nitrite, the Griess reagent did not detect any changes at either 6 h or 24 h (data not shown). A more sensitive method, 2-3-diaminoaphthalene (DAN), highlighted a small but significant increase of NO production compared to untreated cells at 6 h only (Figure 4.3A). However, microglia release large quantities of NO when activated, so the importance of this in terms of a cellular response is debatable (Hall and Garthwaite, 2009). No differences were observed between untreated and oAβ administered cells with regards to TNFα release at 24 h, 48 h or 72 h, as measured by ELISA (Figure 4.3B), and IL-1β was non-detectable at all times tested (data not shown). No change was observed for CD40 at 24 h (Figure 4.3C).

Next, the effects of oAβ on isolated primary microglia from wildtype (WT) C57Bl/6 mice was determined. Unlike BV-2 microglia, at 48 h, oAβ successfully increased the expression of the pro-inflammatory marker CD38 in WT cells (Figure 4.4A and 4.4B). Addition of QC1 was able to completely reverse this when administered 24 h post-oAβ. This Fpr2/3 ligand was also able to increase the expression of CD206, both alone and following oAβ stimulation (Figure 4.4C and 4.4D). Importantly, the effects of oAβ and QC1 on CD38 and CD206 were completely ablated in primary microglia from Fpr2/3 knockout (KO) mice (Figure 4.4E and 4.4F), confirming the central role of this receptor in the actions of both compounds upon microglia.

4.4.3. C43 but not QC1 increases BV-2 phagocytosis following oAβ insult

Microglia destroy pathogenic material, including bacteria through phagocytosis (Lucin et al., 2013). The effects of oAβ and Fpr2/3 agonists on BV-2 phagocytic capacity were therefore determined at 24 h and 48 h post-oAβ insult. 1 h post-treatment with C43 significantly

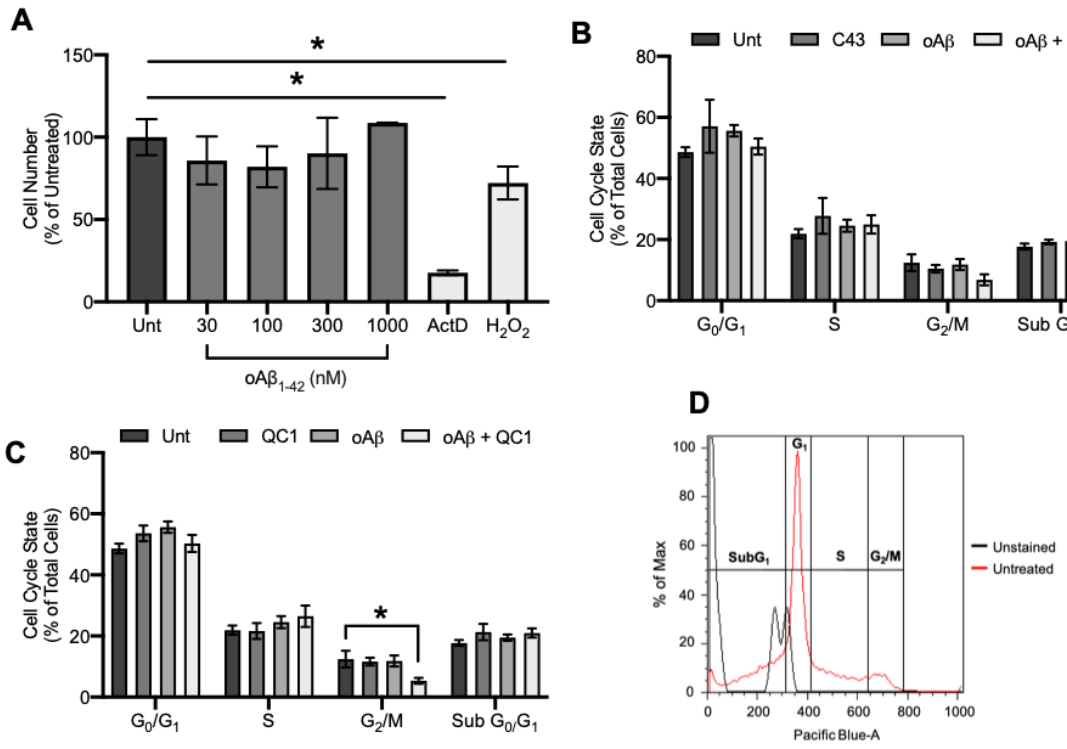

Figure 4.2 The effects of C43, QC1 and oAβ (100 nM) on BV-2 cell viability and cell cycle phase, measured by the PrestoBlue cell viability assay and DAPI flow cytometry analysis, respectively. oAβ was administered 1 h prior to Fpr2/3 ligands. Measurements are 24 h post-oAβ. **A**; cell viability at 24 h as measured through cell number, compared to untreated. Actinomycin (1 µg/ml) and H_2O_2 (200 µM) were used as positive controls. **B**; cell cycle analysis at 24 h following oAβ treatment, with 1 h post-addition of C43. No significant differences were observed. **C**; cell cycle analysis at 24 h for oAβ and QC1. A significant reduction in the G_2/M phase was identified in cells treated with both oAβ and QC1. No other changes were observed. **D**; representative histogram of DAPI cell cycle analysis. Data are means ± SEM. 3-4 independent cultures were used in triplicate. **P* < 0.05.

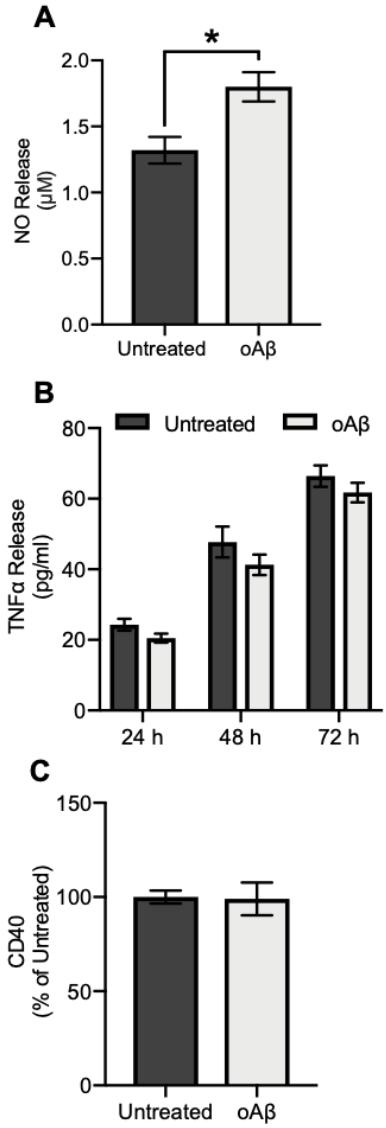

Figure 4.3 The effects of oAβ on inflammatory marker expression in BV-2 microglia. **A**; NO release at 6 h following oAβ insult, as detected with DAN. **B**; oAβ did not affect TNFα release at 24 h, 48 h or 72 h when compared to untreated. **C**; no difference in CD40 expression was observed at 24 h post-oAβ, determined by flow cytometry. Data are means ± SEM of 3-6 independent cultures in triplicate. *$P < 0.05$.

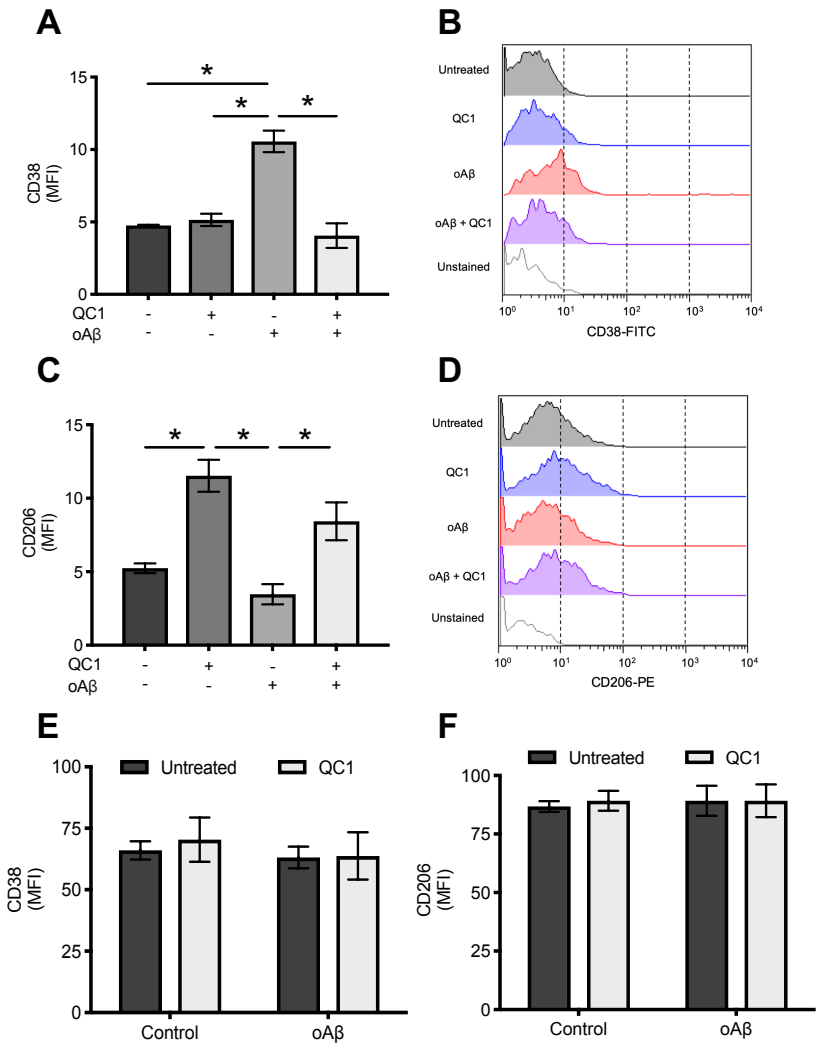

Figure 4.4 The effects of oAβ on CD38 and CD206 inflammatory marker expression in primary murine microglia from C57Bl/6 wildtype (WT) and Fpr2/3 knockout (KO) mice. Measurement times are all post-oAβ. QC1 was administered 24 h after oAβ. **A**; QC1 significantly reduced oAβ upregulation of CD38 in WT primary microglia at 48 h, when administered 24 h post amyloid. **B**; representative histogram of WT CD38 expression. **C**; QC1 significantly increased CD206 expression in WT microglia at 48 h, both when administered alone and 24 h post-oAβ insult. **D**; representative histogram tracer for WT CD206 expression. **E**; no difference was observed in CD38 expression in Fpr2/3 KO primary microglia following 48 h oAβ treatment. **F**; no differences were observed for CD206 expression after 48 h exposure to oAβ in Fpr2/3 KO primary microglia. Data are means ± SEM of 3 independent mice. *$P < 0.05$.

increased cellular phagocytosis of *E. coli* particles at 24 h following oAβ stimulation (Figure 4.5A), but this effect was lost at 48 h (Figure 4.5B). Conversely, neither QC1 or oAβ significantly affected phagocytosis at either 24 h or 48 h (Figure 4.5).

4.4.4. oAβ-Fpr2/3 stimulated ROS production is reversed by QC1 and C43

Production of ROS is a key response of microglia to inflammatory stimuli, primarily as an antimicrobial defence (Liu et al., 2010; Spooner and Yilmaz, 2011). However, markers of oxidative stress are present in AD (Nunomura et al., 2001), and ROS may be a driver of neuronal apoptosis (Zhang et al., 2017). We investigated microglial ROS every 5 min using the general ROS production tracer CM-H_2DCFDA. ROS was increased after 20 minutes exposure to oAβ, remaining higher than untreated throughout the entire 1 h detection time (Figure 4.6A). This was successfully reversed by both C43 and QC1, which were administered 10 min after oAβ (Figure 4.6B and 4.6C).

Similarly, analysis of H_2O_2, a product of superoxide dismutase activity (Wang et al., 2018), revealed that whilst baseline H_2O_2 release was undetectable, appreciable quantities were released upon 2 h exposure to oAβ, and this was significantly reversed by QC1 treatment 10 min post-oAβ (Figure 4.6D). As discussed in Section 3.4.7, superoxide and NO can combine to produce the highly reactive ROS species $ONOO^-$ (Radi, 2018). However, no detectable changes in $ONOO^-$ were observed for any of the treatment groups after 1 h (Figure 4.6E and 4.6F).

To confirm the effects of QC1 were initiated through Fpr2/3 activation, general ROS production was again analysed but with the inclusion of WRW_4 10 min prior to QC1, which successfully blocked the ROS-reducing capacity of this ligand (Figure 4.6G). Interestingly, WRW_4 also attenuated the ROS producing capabilities of oAβ when administered.

To further determine whether oAβ can elicit microglial responses through Fpr2/3 activation, CM-H_2DCFDA was used to determine ROS production following 1 h oAβ insult in WT and Fpr2/3 KO primary microglia from C57Bl/6 mice and examined by flow cytometry. Similarly to BV-2 cells, oAβ successfully increased ROS production in WT primary microglia, when compared to untreated (Figure 4.7). However, Fpr2/3 KO inhibited ROS production when compared to WT. Interestingly, Fpr2/3 KO also appeared to decrease the overall ROS produced by primary microglia, as shown by the overall reduced MFI.

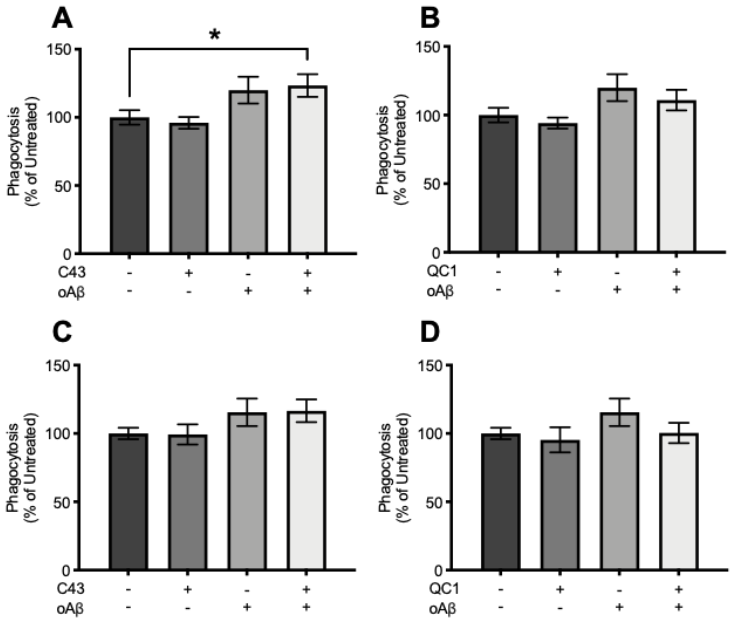

Figure 4.5 The effects of C43, QC1 and oAβ on BV-2 phagocytic capacity at 24 h and 48 h post-oAβ. Data are percentages of mean fluorescent intensities normalised to untreated cells. Measurements of phagocytosis are determined by cellular engulfment of fluorescently labelled *E. coli* bioparticles. C43 and QC1 were administered 1 h after oAβ. **A** and **B**; phagocytosis following 24 h administration with oAβ ± C43 or QC1, respectively. **C** and **D**; phagocytic capacity following 48 h exposure to oAβ ± c43 OR QC1. Data are means ± SEM of 3-4 independent cultures in triplicate. **P* < 0.05.

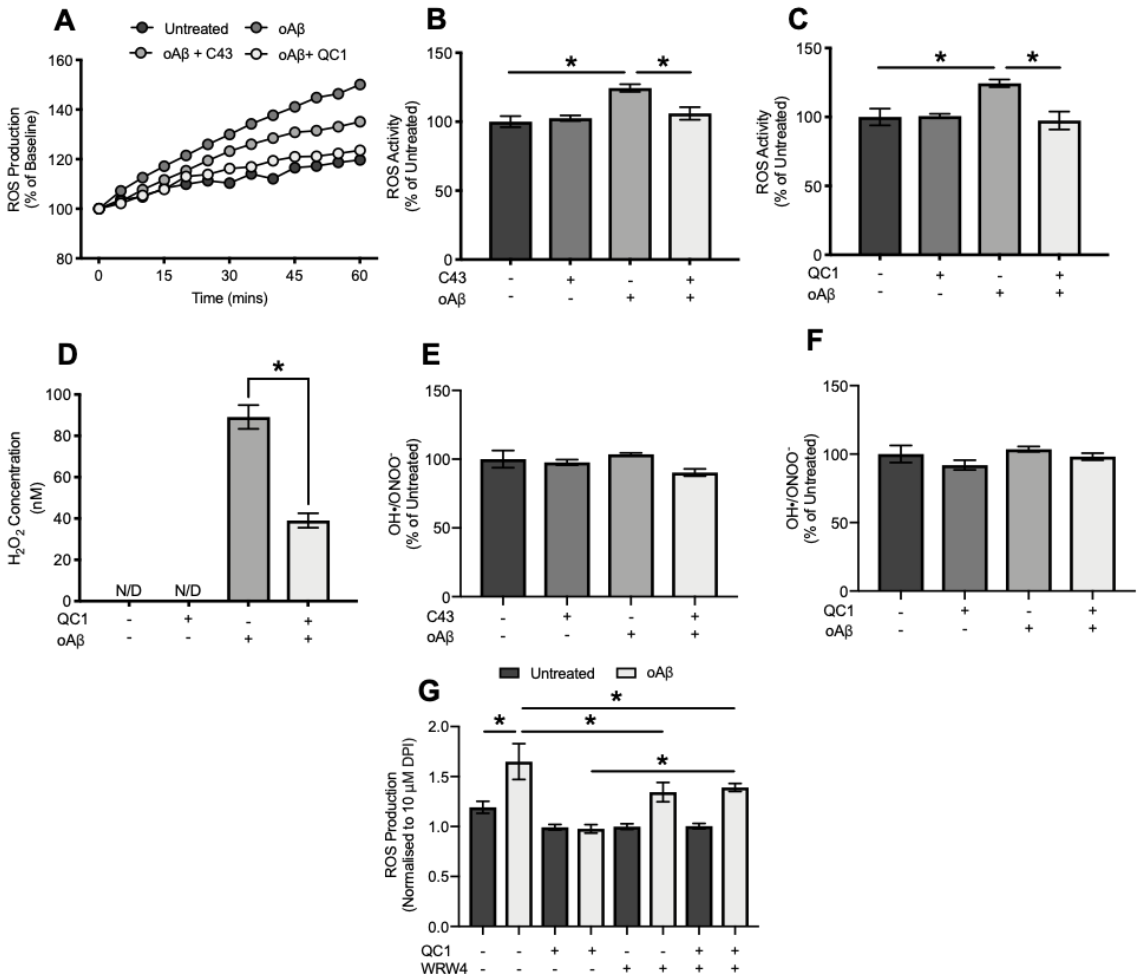

Figure 4.6 The effects of Fpr2/3 stimulation on ROS production in BV-2 microglia. For all experiments, C43/QC1 were added to cells 10 min post-oAβ. WRW_4 (10 μM) was added 5 min prior to QC1. Average rate of ROS production was normalised to untreated cells. **A**; ROS production over 1 h for C43, QC1 and oAβ in BV-2 microglia as measured by CM-H_2DCFDA. **B** and **C**; ROS gradient percentage values for oAβ and C43 or QC1 administered BV-2 microglia, respectively. **D**; H_2O_2 production after 2 h oAβ exposure, as detected by the Promega ROS-Glo assay. QC1 successfully reduced oAβ-induced H_2O_2 production. Untreated and cells administered with QC1 alone did not produce detectable levels of H_2O_2. **E** and **F**; •OH and $ONOO^-$ production at 1 h post oAβ ± C43 or QC1, respectively. No significant differences were observed for any of the substances. **G**; WRW_4 inhibits the anti-oxidative capacity of QC1. WRW_4 was also shown to inhibit the ROS producing ability of oAβ, as detected with CM-H_2DCFDA. WRW_4 was added 5 min post-oAβ. ROS was observed for 1 h and normalised to cells treated with the NADPH oxidase inhibitor DPI (10 μM). Data are means ± SEM (n = 3-6 independent cultures). *P < 0.05.

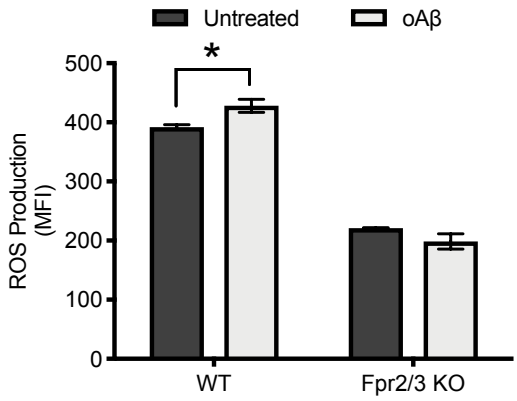

Figure 4.7 oAβ-induced ROS production in primary microglia is Fpr2/3 mediated. Microglia were isolated from the brains of WT and Fpr2/3 KO C57Bl/6 mice and cultured. ROS production was detected 1 h post-oAβ stimulation by CM-H_2DCFDA and flow cytometry. oAβ significantly increased ROS release in primary murine microglia cultured from WT mice. However, microglia harvested from Fpr2/3 KO mice did not produce an oAβ-mediated ROS response. Further, total ROS production in untreated KO cells was considerably smaller than that observed in the WT. Data are means ± SEM of three independent cultures. Three mice were used per group. *$P < 0.05$.

4.4.5. oAβ induces NADPH oxidase mediated ROS production without affecting mitochondrial ROS, a response attenuated by Fpr2/3 stimulation

A major source of cellular ROS is the mitochondria (Finkel and Holbrook, 2000), hence ROS production localised to this organelle was determined using the MitoSOX tracer and the mitochondrial complex I inhibitor rotenone, as previously described (Section 3.4.7). However, no increase in mitochondrial superoxide production was seen with oAβ or QC1 over treatment times in which CM-H_2DCFDA detected a clear ROS response (Figure 4.8A and 4.8B).

Previous research has shown that ROS produced by NADPH oxidase may contribute to neuronal damage in neurodegenerative disease, including in AD (Ma et al., 2017). Microglial NOX2 is therefore a prime candidate to investigate ROS production initiated by oAβ. Thus, the induction of ROS production by oAβ was determined with CM-H_2DCFDA following 10 min pre-incubation with the NADPH oxidase inhibitor diphenyleneiodonium (DPI; 1 μM).

oAβ-induced ROS production was sensitive to this NOX2 inhibitor (Figure 4.8C). Supporting a role for NADPH oxidase in oAβ-induced ROS production. 5 min pre-treatment with the Rac1 inhibitor NSC 23766 (50 μM) also ablated oAβ-induced ROS production (Figure 4.8D). Together, these experiments indicate a clear involvement of NADPH oxidase in oAβ-induced oxidative stress.

Construction of the NADPH oxidase assembly was determined by confocal microscopic examination. Compared to untreated cells, oAβ significantly increased the localisation of p67phox to the plasma membrane after 30 min exposure, indicating increased colocalization with gp91phox (Figure 4.9A). Whilst QC1 had no impact on the localisation of these NOX2 components alone, its administration 10 min after oAβ reversed the mobilisation of p67phox (Figure 4.9A). This process is shown with a distribution false-colour image for p67phox, highlighting more clearly the relative levels of this subunit in different cellular locations following drug treatment (Figure 4.9A). This is also shown in the orthogonal projects in Figure 4.9B. A false-colour image for both gp91phox and p67phox staining highlights co-localisation evident for samples treated with oAβ only (Figure 4.9C).

4.4.6. QC1 and C43 do not modulate antioxidant pathways following oAβ insult

Beyond effects upon NADPH oxidase activity, a component of the anti-ROS effects of Fpr2/3 may be due to modification of intracellular antioxidant defences (Vilhardt et al., 2017). We investigated the effects of Fpr2/3 stimulation upon three key antioxidant systems; glutathione, HO-1 and SOD-2. No differences were observed in GSH:GSSG ratio 2 h post-oAβ addition, nor when QC1 was administered 10 min after oAβ (Figure 4.10A).

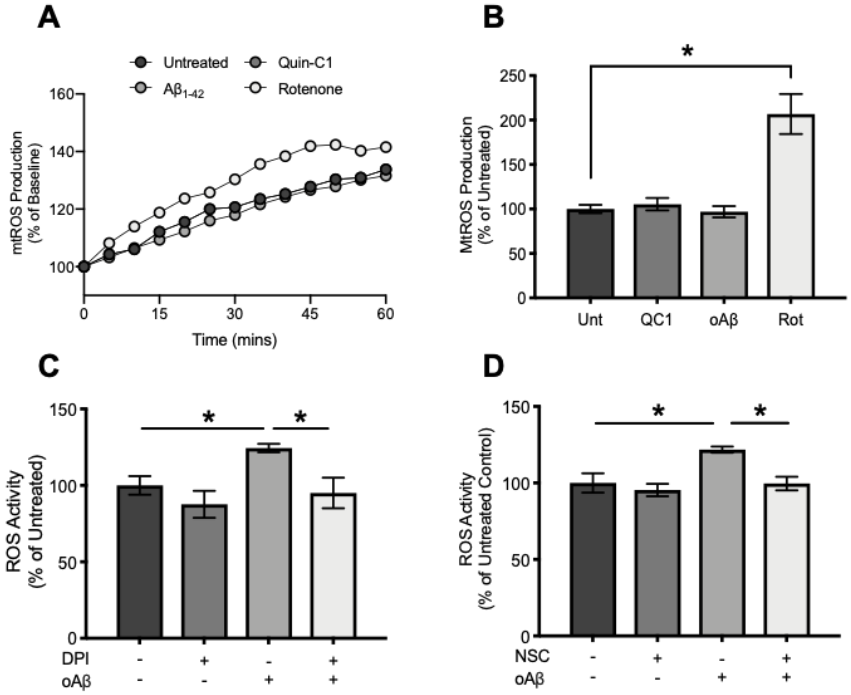

Figure 4.8 oAβ stimulates NADPH oxidase induced-ROS production in BV-2 microglia without stimulating mtROS. QCI was administered 10 min post-oAβ, whilst the NADPH oxidase inhibitor DPI (1 μM) and the Rac1 inhibitor NSC 23766 (50 μM) were added 10 min prior to oAβ. ROS detection with MitoSOX Red and CM-H_2DCFDA was measured every 5 min for 1 h following oAβ treatment. 1 h rotenone treatment was employed as a positive control for mtROS detection. **A** and **B**; oAβ failed to induce mtROS production as examined using the MitoSOX tracer. **C**; oAβ induced ROS production, as detected by CM-H_2DCFDA, was inhibited by DPI. **D**; ROS induced by oAβ was also inhibited by NSC 23766, as detected with CM-H_2DCFDA. Data are means ± SEM (n = 3-6 independent cultures). *P < 0.05.

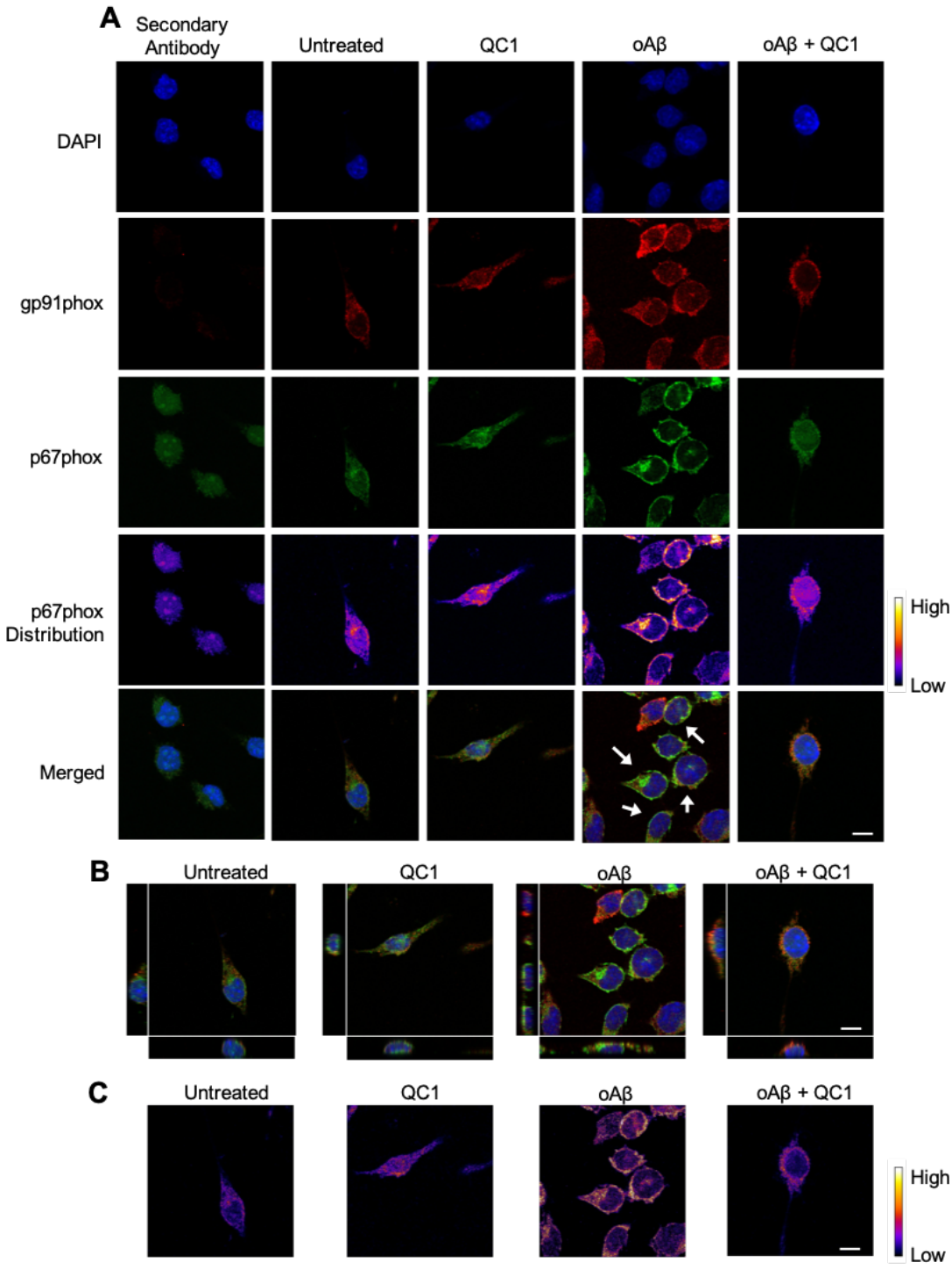

Figure 4.9 The effects of oAβ ± QC1 (100 nM) on NADPH oxidase subunit colocalization as determined by confocal microscopy. Samples were fixed following 30 min exposure to oAβ ± 10 min post-treatment of QC1. Cells treated with the secondary antibody alone are also shown to display any non-specific binding. **A**; immunostaining for two NOX2 subunits, gp91phox (red), p67phox (green), counterstained with DAPI (blue). Treatment with oAβ induced the recruitment of p67phox to the plasma membrane, with QC1 administration reversing this. The p67phox distribution false-colour images clarifies the relative localisation of p67phox under different treatment conditions. QC1 had no effect on p67phox or gp91phox alone. Co-localisation has been depicted for oAβ treated cells with the white arrows. **B**; Orthogonal projections of confocal Z-stack images of gp91phox and p67 immunostaining. C; false-colour images for gp91phox and p67phox highlights co-localisation between red and green pixels from A. Scale bar = 10 µm. Images represent 3-4 independent cultures. Magnification is 63x with an oil immersion lens.

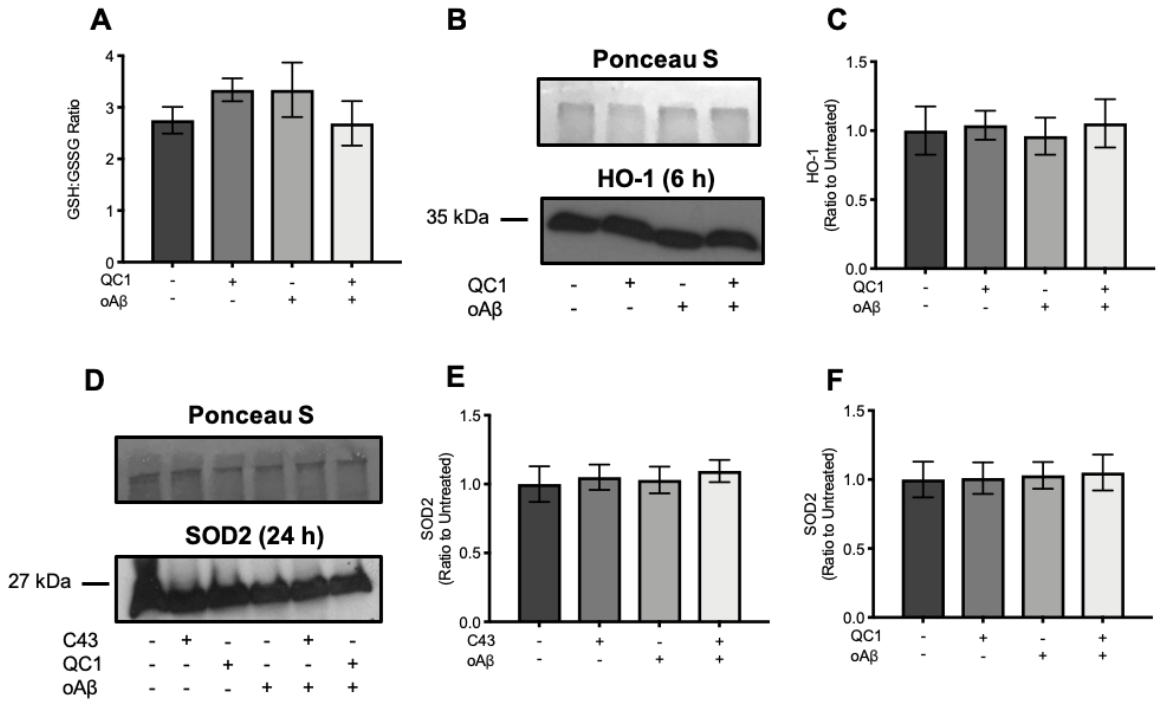

Figure 4.10 The relative ratio of reduced to oxidised glutathione peptide (GSH:GSSG) and antioxidant enzyme expression in BV-2 microglia. For GSH/GSSG, cells were administered with oAβ for 2 h, with QC1 added 10 min post-toxin. For antioxidant enzymes, QC1 was added 1 h post-oAβ, with timings for all experiments post-oAβ treatment. **A**; no significant differences were observed in GSH:GSSG ratio after 2 h treatment with oAβ ± QC1. **B**; representative western blot showing HO-1 expression at 6 h, with Ponceau S staining used as a loading control. **C**; HO-1 expression was not affected by either oAβ or QC1, at 6 h administration when compared to untreated cells. **D**; representative western blot showing SOD2 expression 24 h post oAβ insult. Ponceau S staining was used as the loading control. **E** and **F**; the relative expression of SOD2 was not affected by any of the treatment groups, showing similar expression levels to untreated BV-2 microglia. Data are means ± SEM of 3 independent cultures in triplicate.

No consequential changes in either HO-1 or SOD-2 expression were observed (6 h and 24 h post-oAβ, respectively) for any treatment group, with timings based on previous BV-2 microglial work (Figure 4.10B-F; Bozic et al., 2015; Kwon et al., 2017). In summary, Fpr2/3 ligands can successfully reverse oAβ induced ROS production via preventing NADPH oxidase activation, without effecting the GSH, HO-1 or SOD-2 antioxidant defence systems.

4.4.7. oAβ reduces L-lactate production but increases glucose uptake and utilisation in microglia

NADPH oxidase activation and ROS production is an energy intensive process; hence we examined the impact of oAβ on glucose utilisation and L-lactate production, measuring their concentration. Initially, cells were incubated in high glucose media (4.5 g/L) and exposed to a range of pathologically relevant concentrations of oAβ (30, 100, 300 or 1000 nM). After 24 h exposure, oAβ exposure (excluding 100 nM) significantly increased glucose usage compared to untreated (Figure 4.11A), without altering L-lactate production (4.11B).

Next, we utilised BV-2 microglia cultured in medium with physiological concentrations of glucose (1 g/L; Danaei et al., 2011), and looked at changes in both glucose and L-lactate after 24 h and 48 h oAβ (100 nM) exposure ± C43/QC1 1 h post-treatment. Glucose utilisation was increased by oAβ at both 24 h and 48 h, with both Fpr2/3 agonists reversing this at 48 h (Figure 4.11C and 4.11D). No observable changes were noted for Fpr2/3 ligands administered alone. oAβ significantly reduced L-lactate concentration at both 24 h and 48 h, which neither C43 nor QC1 could rescue (Figure 4.11E and 4.11F). These Fpr2/3 ligands had no direct effect on L-lactate production when administered to cells alone (Figure 4.11E and 4.11F). In summary, data here suggests that oAβ can significantly reduce glycolysis, whilst also increasing glucose utilisation, the latter of which Fpr2/3 ligands can successfully reverse.

4.4.8. oAβ reduces basal mitochondrial respiration and ATP production

Following confirmation that oAβ modulates glucose uptake and lactate production, the effects of oAβ on glycolysis and mitochondrial function were determined through the use of the Agilent Seahorse XF Cell Mito Stress Test. Following 24 h stimulation with oAβ in DMEM (1 g/L glucose), mitochondrial respiration was determined, with summary graphs of oxygen consumption rate (OCR) and extracellular acidification rate (ECAR) per minute for each treatment group displayed in Figure 4.12A and 4.12B. Both basal respiration and ATP production were significantly reduced by 24 h exposure to oAβ, correlating with a reduction in proton leak (Figure 4.12C, 4.12D and 4.12E), supporting an overall reduction in mitochondrial respiration. However, neither the maximal respiration capacity, spare respiratory capacity or coupling efficiency of mitochondria were affected (Figure 4.12F,

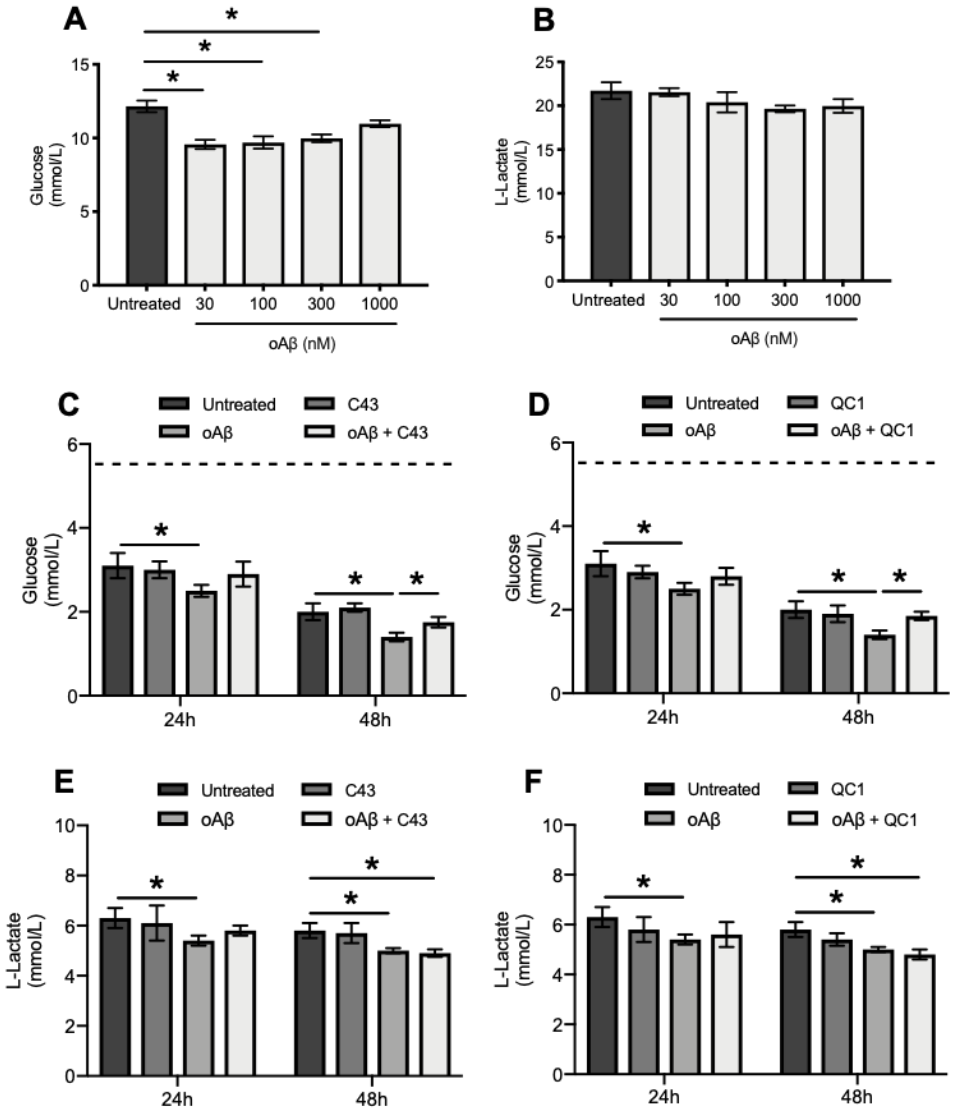

Figure 4.11 The effects of oAβ on BV-2 glucose utilisation and L-lactate production in high glucose (4.5 g/L) and physiological glucose concentration (1 g/L) medium. Glucose and L-lactate measurements were made at 24 h and 48 h post-oAβ ± C43/QC1 (100 nM), administered 1 h after the toxin. Glucose usage and L-lactate production were measured by concentration in cellular supernatant, using a YSI 2300 Stat Plus. **A**; concentration-response curve (30, 100, 300 or 1000 nM) of oAβ on glucose concentration in high glucose containing medium at 24 h. **B**; concentration-response curve (30, 100, 300 or 1000 nM) of oAβ on L-lactate production in high glucose containing medium at 24 h. **C** and **D**; glucose concentration in physiological glucose containing media at 24 h and 48 h post-oAβ. Both C43 and QC1 were able to reverse this, but at 48 h only. **E** and **F**; oAβ significantly decreased L-lactate production in physiological glucose containing medium at both 24 h and 48 h. Neither C43 nor QC1 reversed this. Data are means ± SEM for 3-4 independent cultures in triplicate. **P* < 0.05.

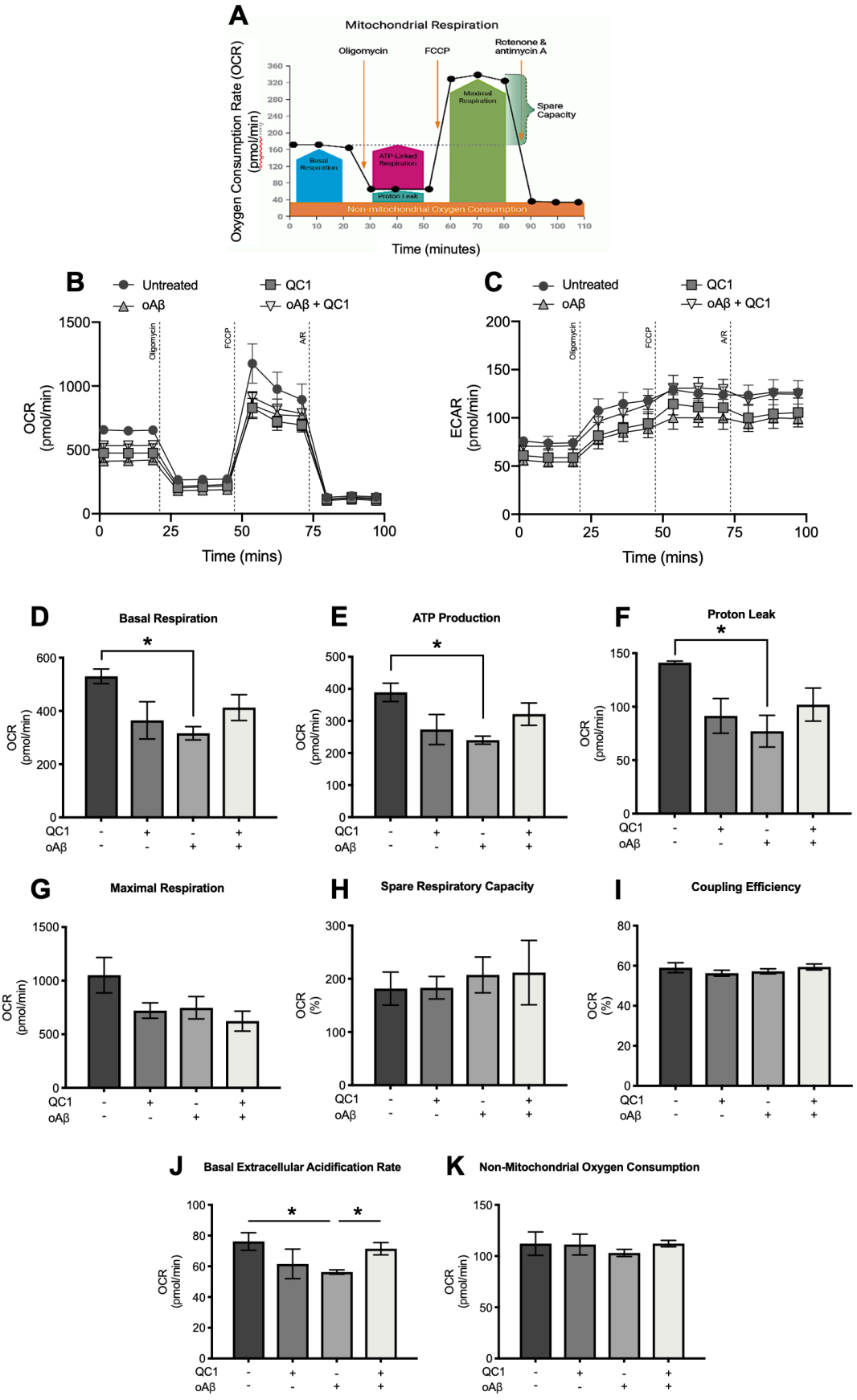
A
Mitochondrial Respiration
Oligomycin
FCCP
Rotenone & antimycin A
Maximal Respiration
Spare Capacity
ATP-Linked Respiration
Basal Respiration
Proton Leak
Non-mitochondrial Oxygen Consumption
Oxygen Consumption Rate (OCR) (pmol/min)
Time (minutes)
B
Untreated
oAβ
QC1
oAβ + QC1
OCR (pmol/min)
Time (mins)
C
ECAR (pmol/min)
D
Basal Respiration
E
ATP Production
F
Proton Leak
G
Maximal Respiration
H
Spare Respiratory Capacity
I
Coupling Efficiency
J
Basal Extracellular Acidification Rate
K
Non-Mitochondrial Oxygen Consumption

Figure 4.12 The effects of 24 h microglial exposure to oAβ on mitochondrial and non-mitochondrial respiration rate. Addition of QC1 was 1 h post-oAβ. **A**; a labelled diagram of a Agilent seahorse XF Cell Mito Stress Test profile, showing how key parameters of mitochondrial function are calculated. **B**; the oxygen consumption rate (OCR) profile of BV-2 microglia treated with either oAβ, QC1 or both, alongside that for untreated cells. **C**; the extracellular acidification rate (ECAR) profile for cells treated as described in A. The injection points for oligomycin (4 μM), FCCP (0.6 μM) and rotenone with antimycin A (1 μM) are included in graphs A and B. **D**; basal mitochondrial respiration rate was significantly reduced by oAβ. **E**; ATP production was also significantly reduced by oAβ. **F**; Proton leak represents basal respiration not coupled to ATP production. 24 h incubation with oAβ significantly reduced mitochondrial proton leak. QC1 did not affect any of these components of mitochondrial respiration. **G**; maximal respiration was unaffected by any of the cellular treatments. **H**; cellular spare respiratory capacity does not change upon cellular treatment with oAβ or QC1. **I**; cellular coupling efficiency for untreated cells was approximately 60% but was not affected following oAβ and QC1 treatments. Coupling efficiency is the percentage of basal respiration that is used for ATP production. **J**; administration of oAβ significantly reduced basal ECAR, which QC1 reversed towards levels comparable to that of untreated cells. **K**; the rate of non-mitochondrial oxygen consumption was not affected by cell treatment. Data are means ± SEM for 3-5 independent cultures in triplicate. *P < 0.05.

4.12G and 4.12H). Addition of QC1 had no effect on any of these components, either when administered alone or 1 h post-oAβ insult (Figure 4.12C-H). oAβ also significantly reduced basal ECAR, measured before the serial injection of oligomycin, FCCP and rotenone/antimycin A (Figure 4.12I). QC1 was able to significantly reverse this back towards untreated levels, suggesting QC1-induced Fpr2/3 activation modulates glycolysis without affecting mitochondrial respiration. In addition, whilst ECAR measurements were altered upon drug treatment, the overall non-mitochondrial oxygen consumption rate was neither affected by oAβ nor QC1 (Figure 4.12J), supporting that other processes are using increased oxygen concentrations despite reductions in both mitochondrial and glycolytic respiration following oAβ stimulation.

To quantify intracellular rates of glycolytic and oxidative ATP production, data was analysed as described previously (Mookerjee et al., 2017). Basal ATP production rates were based upon OCR and ECAR prior to serial injections. Maximal ATP production was calculated via OCR and ECAR rates following FCCP injection. In comparison to untreated cells, basal oAβ treatment reduced ATP production from oxidative phosphorylation (Figure 4.13A), an effect reversed by administration of QC1 1 h post-oAβ (Figure 4.13A). However, QC1 had no effect when administered alone. No differences were observed for maximal cellular ATP production via oxidative mechanisms (Figure 4.13A). Further, basal ATP production from glycolysis was reduced by oAβ when compared to untreated cells, but this observation was not significant. Despite this, QC1 significantly increased this oAβ-induced reduction to levels similar to that of untreated cells (Figure 4.13B). The differences between ATP production via both sources is summarised in Figure 4.13C.

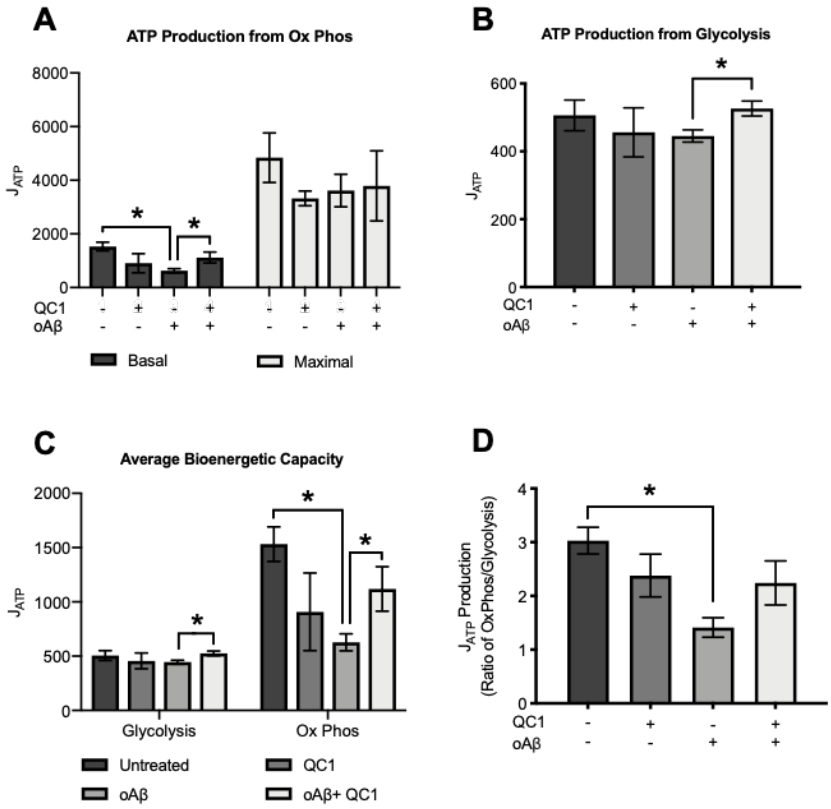

Figure 4.13 The effects of 24 h exposure of BV-2 microglia to oAβ ± QC1 on ATP production via glycolysis and oxidative phosphorylation. QC1 was administered 10 min-post oAβ. Data shows joules of ATP production. **A**; ATP production from oxidative phosphorylation under basal and maximal respiratory conditions. Values following FCCP inclusion were used to determine maximal ATP production. oAβ significantly decreased $_{J}$ATP production under basal conditions compared to untreated. QC1 successfully reversed this, increasing $_{J}$ATP to levels comparable to untreated cells. No differences were observed for maximal ATP production. **B**; ATP production from glycolysis following cellular treatments of oAβ and QC1 compared to untreated under basal conditions. No changes were observed compared to untreated, but QC1 significantly increased the oAβ-induced reduction in $_{J}$ATP observed. **C**; comparison of average bioenergetic capacity of ATP production from glycolysis and oxidative phosphorylation from A and B. **D**; the ratio of ATP production from oxidative phosphorylation and glycolysis. oAβ significantly reduced this ratio, whilst no other changes were observed. Data are means ± SEM of 3-5 independent cultures in triplicate. *P < 0.05.

The overall ratio of ATP produced via oxidative phosphorylation compared to glycolysis was then determined. Following oAβ insult, cellular reliance on oxidative phosphorylation for ATP production decreases significantly, due to an almost two-fold reduction in $_J$ATP production ratio (Figure 4.13D). Therefore, this data supports that oAβ induces a reduction in oxidative phosphorylation, ATP production and glycolytic L-lactate production (Figure 4.12 and 4.13), possibly due to metabolic intermediates being utilised for other cellular processes.

4.4.9. QC1 reverses oAβ increased G6PD activity

Activation of NADPH oxidases can only produce superoxide radicals for as long as a supply of NADPH is available (Ma et al., 2017). As shown in Figure 4.14A**,** glucose 6-phosphate (G6P) lies at the beginning of two major metabolic pathways: glycolysis and the pentose phosphate pathway (PPP; Grant, 2008), which maintains cellular levels of NADPH. Glucose 6-phosphate dehydrogenase (G6PD) is the rate limiting enzyme in the PPP, and thus the primary regulator of the pathway (Grant, 2008). Upregulation of the PPP can therefore divert G6P towards NADPH production, meaning less will be available for glycolysis and oxidative phosphorylation. It is therefore possible that increased G6PD activity is responsible for the reduction in L-lactate and mitochondrial respiration observed following oAβ treatment in Sections 4.4.7 and 4.4.8. Further, increases in oAβ-induced glucose utilisation may be due to increased cellular demand for NADPH as a consequence of NADPH oxidase activation. Thus, to determine whether oAβ-induced ROS production drives NADPH depletion and activates the PPP, microglial G6PD activity was determined at 24 h post-oAβ in DMEM (1g/L glucose). Stimulation with oAβ significantly increased G6PD activity compared to untreated cells (Figure 4.14B). This was reversed by the administration of QC1 1 h post-oAβ, restoring G6PD activity to that of untreated cells (Figure 4.14B). Treatment with QC1 alone did not affect G6PD activity, suggesting the reversal of an oAβ triggered process rather than a direct effect upon the enzyme.

4.4.10. C43 and QC1 prevent oAβ-induced nuclear translocation of NF-κB

ROS production is known to instigate nuclear translocation of the ubiquitous transcription factor NF-κB, particularly H_2O_2 (Hara-Chikuma et al., 2015; Henríquez-Olguín et al., 2015). This ROS species was increased following oAβ addition, but successfully reduced by QC1 post-treatment (Figure 4.6D). NOX2 activation has been suggested to upregulate NF-κB activity (Fan et al., 2017; Li et al., 2018; Vara et al., 2018), which in turn increases the transcription of the NOX2 component gp91phox (Anrather et al., 2006; H. Li et al., 2018; Mariappan et al., 2010). Despite a lack of inflammation observed in this study, oAβ is well established to activate NF-κB (Liu et al., 2015b; Zhao et al., 2018; Zhou et al., 2014), and

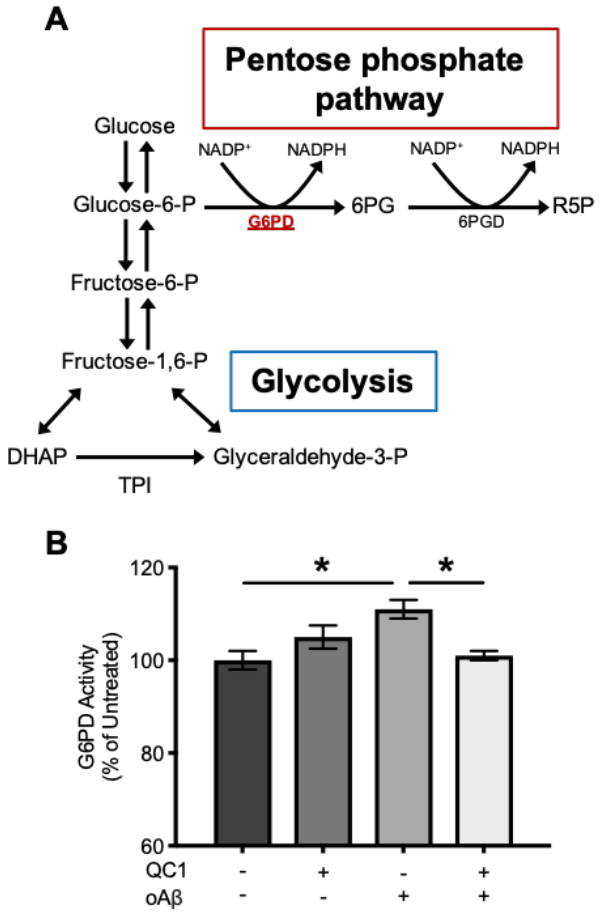

Figure 4.14 G6PD activity in BV-2 microglia following 24 h insult with oAβ. Administration of QC1 was 1 h post-oAβ. **A**; a simplified diagram representation of the link between the pentose phosphate and glycolytic pathways. If glucose 6-phosphate is oxidised, it enters the PPP pathway. If it is instead isomerised to fructose 6-phosphate, it moves through glycolysis. Diagram adapted from Grant, 2008. **B**; G6PD activity at 24 h following oAβ and QC1 stimulation. Administration of oAβ significantly increased G6PD activity compared to untreated cells. QC1 successfully reversed this. However, QC1 had no impact on G6PD when administered alone. Abbreviations: 6PG, 6-phosphogluconate; 6PGD, 6-phosphogluconate dehydrogenase; DHAP, dihydroxyacetone phosphate; G6PD, glucose 6-phosphate dehydrogenase; $NADP^+$, nicotinamide adenine dinucleotide phosphate; NADPH, reduced nicotinamide adenine dinucleotide phosphate; P, phosphate; R5P, ribulose 5-phosphate; TPI, triosephosphate isomerase. Data are means ± SEM for 3-4 independent cultures in triplicate. *$P < 0.05$.

chronic oAβ-induced microglial ROS production may be responsible for NF-κB-triggered neuroinflammation observed in AD (Heneka et al., 2015; Hou et al., 2017; Qin and Crews, 2012). Because of this, we immunofluorescently examined whether oAβ-induced NOX2 activation increases NF-κB nuclear translocation following 30 min oAβ stimulation ± C43/QC1 10 min post-treatment. Cells were fixed with 2% formaldehyde, stained for NF-κB and counterstained for DAPI, respectively. It was identified that oAβ successfully stimulated the nuclear translocation of NF-κB, which is most clearly highlighted in the false-colour distribution images in Figure 4.15. More interestingly, both C43 and QC1 successfully reversed oAβ-induced NF-κB nuclear translocation, as highlighted by the lack of preferential nuclear distribution observed when compared to cells treated with oAβ alone (Figure 4.15). This links with the successful prevention of NADPH activation and reduction in H_2O_2 observed following Fpr2/3 activation.

4.4.11. QC1 protects differentiated SH-SY5Y cells from oAβ-induced apoptosis in a BV-2 microglial co-culture system

Microglial ROS production causes neuronal dysfunction (Sorce et al., 2017), likely through direct oxidative damage (Wu et al., 2012; Yauger et al., 2019). To determine whether oAβ-induced NADPH oxidase activation and metabolic modulation could lead to apoptosis of neuronal-like cultures *in vitro*, human derived SH-SY5Y neuroblastoma cells were co-cultured with BV-2 microglia. SH-SY5Y cells were initially differentiated with tRA for 5 days (Kovalevich and Langford, 2013). Next, differentiated cells were analysed to determine the expression of both CD200 and FPR2, with cells expected to express the former, which is a neuronal marker, but not the latter due to no literature being available to support FPR2 expression on neurones; this was determined to be the case (Figure 4.16A and 4.16B).

Initial experiments determined that exposure of SH-SY5Y cells to oAβ for 48 h had no effect on cell survival, with or without cell differentiation (Figure 4.16). For co-culture experiments, SH-SY5Y cells were isolated using CD200 and the microglial marker CD11b (Figure 17A). Interestingly, in the presence of BV-2 cells, differentiated SH-SY5Y cells displayed a significant increase in apoptosis following 48 h oAβ treatment compared to untreated cells (Figure 4.17B). QC1 administered 1 h post-oAβ successfully reversed this, but QC1 did not elicit any effects on SH-SY5Y apoptosis when administered alone (Figure 4.17B). To understand whether microglia have to be present for increased neuronal apoptosis, SH-SY5Y cells in single culture were treated for 48 h with conditioned medium from BV-2 microglia exposed to oAβ for 24 h. Interestingly, SH-SY5Y cells did not undergo apoptosis under this protocol (Figure 4.17C), suggested that microglia have to be present to facilitate oAβ-induced apoptosis.

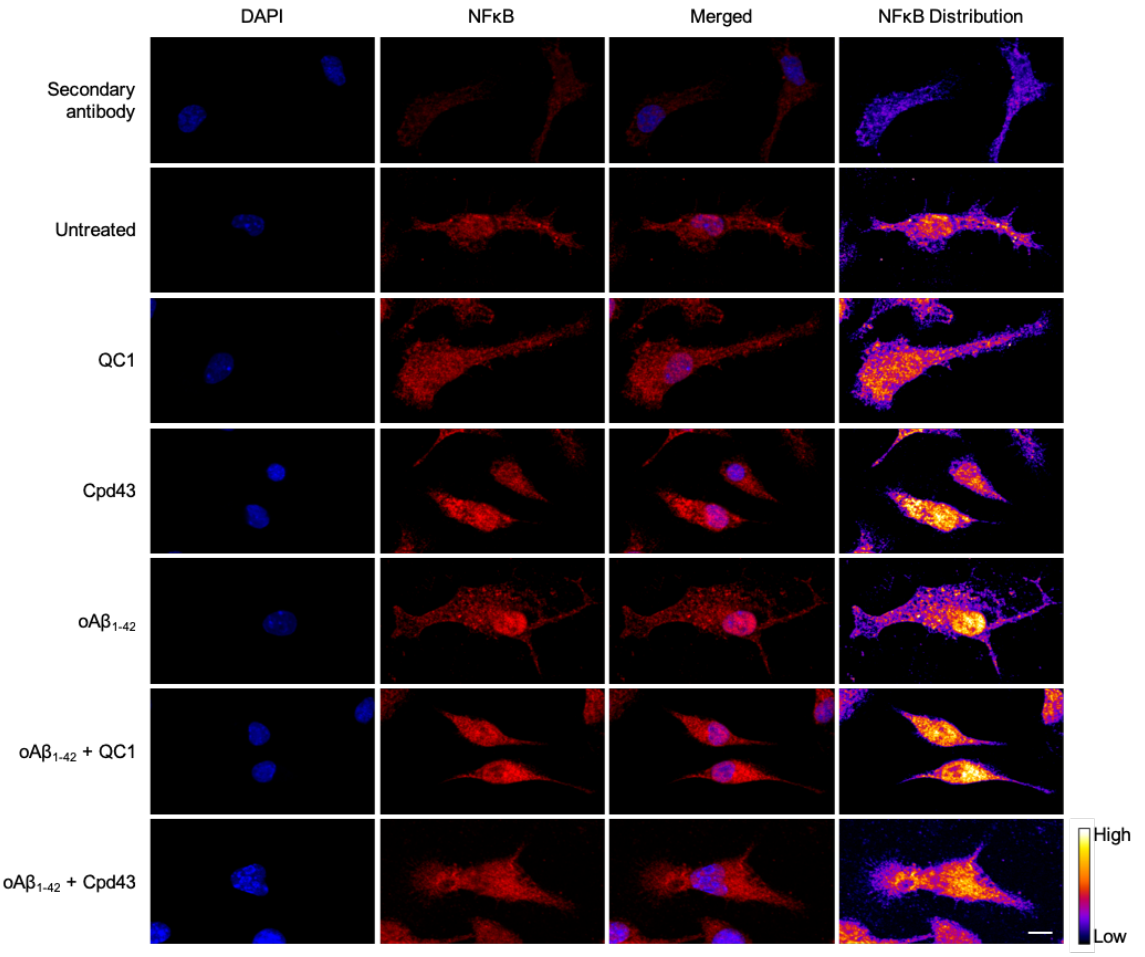

Figure 4.15 The effects of oAβ, C43 and QC1 on the cellular distribution of NF-κB. Cells were treated with oAβ for 30 minutes before being fixed. C43 or QC1 were added 10 minutes after oAβ. Cells were stained for NF-κB (red) and counterstained with DAPI (blue). Staining for NF-κB secondary antibody alone is also shown to identify any non-specific antibody binding. Unlike C43 and QC1, oAβ resulted in the nuclear translocation of NF-κB, which is highlighted most clearly in the NF-κB false-colour distribution images. C43 and QC1 both successfully prevented this process. For NF-kB distribution images, white/yellow and dark blue/purple represent high and low expression, respectively. Scale bar = 10 μm. Images represent 3 independent cultures.

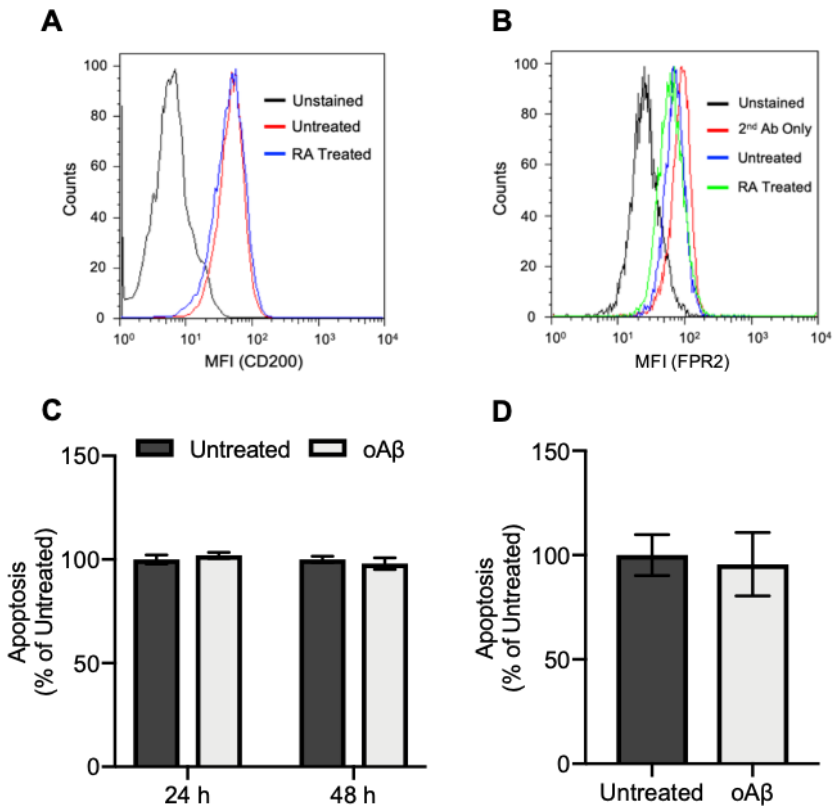

Figure 4.16 Apoptosis of naïve and differentiated SH-SY5Y cells in single culture, as determined with flow cytometry. All measurements are 24 h or 48 h post-oAβ exposure. **A** and **B**; differentiated SH-SY5Y expression of CD200 and FPR2, respectively. Median fluorescence intensity was compared against unstained and secondary antibody alone (FPR2 only). **C**; exposure to oAβ for 24 h and 48 h did not stimulate apoptosis in naïve SH-SY5Y cells in single culture. **D**; 48 h treatment with oAβ did not result in apoptosis of differentiated SH-SY5Y cells. Data presented are means ± SEM (*n* = 3-6 independent cultures in triplicate.

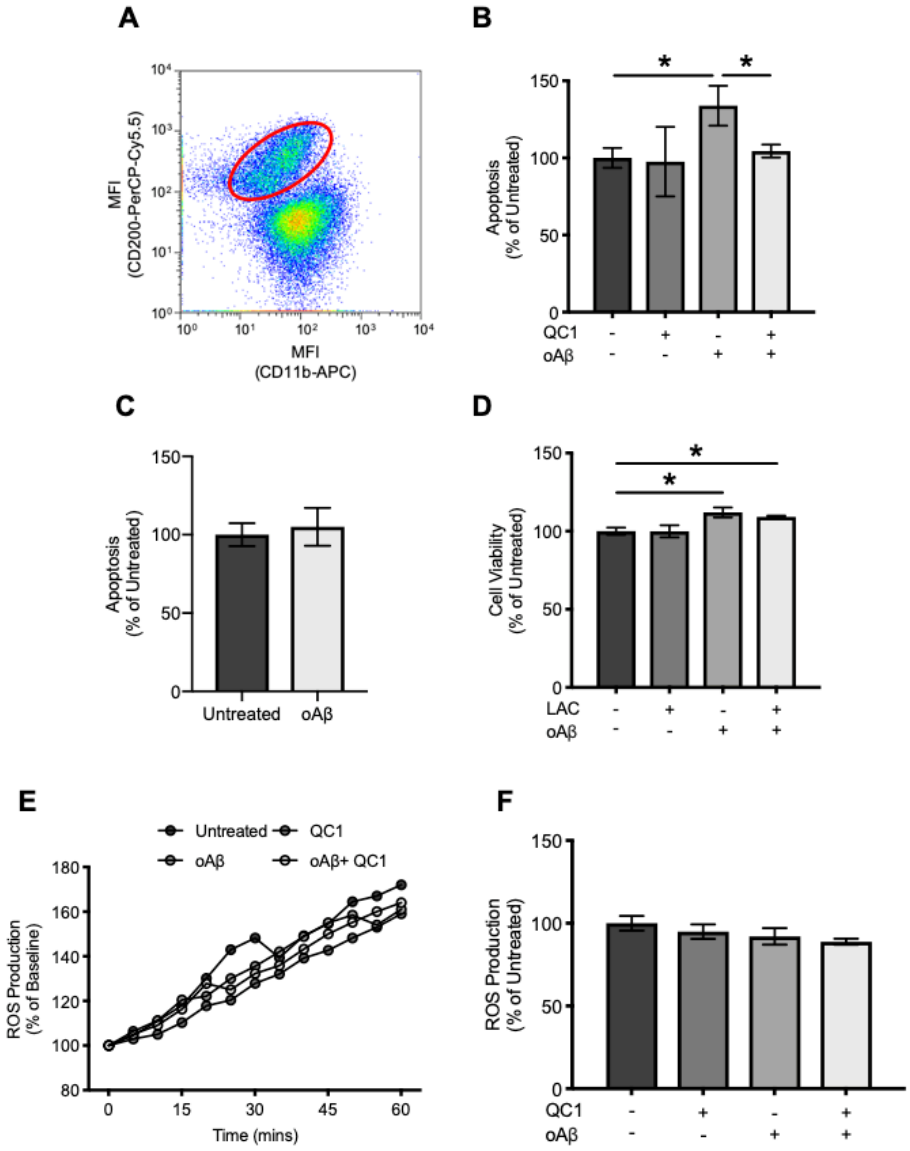

Figure 4.17 SH-SY5Y apoptosis analysis in co-culture with BV-2 microglia. Microglia were added to 5-day differentiated SH-SY5Y cells, and co-cultures were administered with oAβ the following day, with apoptosis of SH-SY5Y cells determined via flow cytometry at 48 hour post-oAβ. Addition of QC1 and L-Lactate was 1 h after oAβ. Cells were separated for analysis with fluorescently conjugated rat monoclonal CD200 (PerCP/Cy5.5) and rat monoclonal CD11b (APC) antibodies, markers for neurones and microglia, respectively. For ROS detection in SH-SY5Y cells, oAβ was administered 10 min prior to QC1. ROS was then measured every 5 min for 1 h. **A**; cell gating for SH-SY5Y isolation on a logarithmic scale. **B**; oAβ increased SH-SY5Y apoptosis following 48 h exposure. QC1 significantly reversed this effect but facilitated no change when administered alone. **C**; pre-conditioned media from microglia exposed to oAβ for 24 h failed to increase cellular apoptosis of differentiated SH-SY5Y cells following 48 h culturing. **D**; L-lactate (100 μM) failed to protect differentiated SH-SY5Y cells from oAβ-induced apoptosis in co-culture at 48 h. **E**; exposure of single culture differentiated SH-SY5Y cells to oAβ for 1 h did not increase cellular ROS production when compared to untreated cells. QC1 also failed to elicit an effect when administered 10 min post-oAβ. **F**; bar graph representation of the different ROS gradients represented in E. Data presented are means ± SEM of 3-6 independent cultures in triplicate. *$P < 0.05$.

Interstitial lactate is known to be present in the brain despite there being adequate oxygen availability, a phenomenon which occurs through aerobic glycolysis. Astrocytes are known to harvest a reservoir of L-lactate (Sotelo-Hitschfeld et al., 2015), acting as a neuronal supply for this organic compound, in a process coined the 'astrocyte-to-neuron lactate shuttle', releasing it into the extracellular space, before being subsequently taken up by neurones to be used as an energy substrate (Choi et al., 2012; Mächler et al., 2016). *In vivo*, neurones prefer to utilise lactate over glucose (Fünfschilling et al., 2012; Wyss et al., 2011). As a consequence of oAβ reducing L-lactate concentration in single cultured BV-2 cells, the effects of administrating additional L-lactate (100 μM) on apoptosis was also sought, but this did not inhibit the apoptotic ability of oAβ (Figure 4.17D). Analysis of ROS using CM-H_2DCFDA did however confirm that oAβ does not upregulate ROS in differentiated SH-SY5Y single culture (Figure 4.17E and 4.17F), implicating increased phagocytosis and microglial ROS production in the apoptosis of this neuronal-like cell line in BV-2 co-culture.

4.5. Discussion

The amyloid hypothesis of AD was first proposed in 1992 (Hardy and Higgins, 1992). Work published later emphasised the importance of Aβ accumulation in the progressive neurodegeneration that characterises this disease (Bernstein et al., 2009; Busciglio et al., 1995; Mawuenyega et al., 2010). Despite this, therapeutics targeted towards Aβ continue to fail in a clinical setting (Panza et al., 2019). This is also true for tau (Gauthier et al., 2016), the other primary pathological feature of AD (Shi et al., 2017). Following these consistent failures, disease focus has shifted towards a previously ignored pathological candidate: the immune response. Multiple research groups have deciphered which genes and polymorphisms are associated with an increased LOAD risk, many of which have central roles in the innate immune system (Jansen et al., 2019; Kunkle et al., 2019; Yokoyama et al., 2016). Deciphering cellular communication patterns alongside microglial-Aβ/tau pathological mechanisms is therefore crucial.

Many chronic disorders are associated with an overactive and uncontrolled inflammatory response, including periodontitis (Kinane et al., 2017) and T2DM (Donath and Shoelson, 2011), both of which increase AD risk (Leira et al., 2017; Moreno-Gonzalez et al., 2017). Peripheral inflammation in midlife is associated with increased cognitive decline over a 20-year period (Walker et al., 2019), suggesting that pre-clinical inflammation hold importance in the development of disease symptoms.

The link between peripheral inflammatory and metabolic diseases and AD risk is likely associated with the metabolic control of immune cells, referred to as immunometabolism

(O'Neill et al., 2016). As discussed in Chapter 3, pro-inflammatory innate cells such as microglia adopt a metabolic profile reliant on glycolysis, whilst pro-resolving cells harness oxidative phosphorylation (O'Neill and Pearce, 2016; Orihuela et al., 2016; Stienstra et al., 2017). This shift towards glycolysis is important for the production of intermediates utilised for inflammatory mediator synthesis, many of which are not produced by the Krebs cycle (Ganeshan and Chawla, 2014). This may explain why we observed pro-inflammatory mediator release in Chapter 3, but not in this Chapter. In our previous study, LPS treatment resulted in the increase in L-lactate production, an indirect measure of glycolysis. At the same time, multiple markers of neuroinflammation were also increased. However, here we provide evidence that oAβ exposure reduces L-lactate production and glycolysis, whilst no inflammatory response was observed, further supporting the importance of the microglial metabolic profile in facilitating an inflammatory response.

In AD, a chronic neuroinflammatory environment manifests (Heneka et al., 2015). We propose that this is associated with an unresolved neuroinflammatory response, perhaps initiated by unresolved ROS production, leading to long-lasting glycolytic reliance of microglia and continual inflammatory damage. Due to the inefficiency of ATP production by glycolysis, the microglial demand for glucose would likely increase, facilitated by augmented glucose uptake (Wang et al., 2019). Here we observe increased microglial glucose demand following oAβ treatment.

In vitro studies have shown that high concentrations of Aβ (2-25 μM) can activate microglial inflammation (Caldeira et al., 2017; Liu et al., 2015; Urrutia et al., 2017; Wang et al., 2018; Yang et al., 2017). However, the effects of pathophysiological relevant concentrations of Aβ (Van Helmond et al., 2010) have not been investigated. In our study, we have used a concentration of oAβ based on AD patient brain autopsy data (Van Helmond et al., 2010), and wanted to determine whether Fpr2/3 stimulation could modulate the effects manifested by microglial oAβ exposure.

In Chapter 3, we underlined the importance of murine Fpr2/3 and human FPR2 receptors in the resolution of inflammation (Sadani N Cooray et al., 2013; Gobbetti et al., 2014; McArthur et al., 2015; Vital et al., 2016). Previous research has highlighted that several endogenous FPR2 ligands are expressed in the brain (Bisicchia et al., 2018; McArthur et al., 2010; Wang et al., 2015), but become significantly reduced in AD patients (Wang et al., 2015). In this Chapter, we hypothesised that pharmacological activation of Fpr2/3 post-oAβ administration would successfully reverse microglial inflammation, protecting neurones from apoptosis. This would potentiate interest in human FPR2 as a neuroinflammatory therapeutic target for AD.

4.5.1. Treatment with oAβ facilitates ROS production without triggering an inflammatory response

Chronic neuroinflammation is a central pathology in the progression of AD (Heneka et al., 2015; Hong et al., 2016; Yin et al., 2017), with increased pro-inflammatory cytokine levels measured in both the CSF and blood of patients (Brosseron et al., 2014; Popp et al., 2017). The reason often proposed for inflammatory involvement associates with continual oAβ stimulation of microglia, alongside unsuccessful removal of these toxic peptides (Ferretti et al., 2012; Yin et al., 2017). This supports why reduced function variants of TREM2 are associated with an increased risk of AD development in patients (Guerreiro et al., 2013; Jonsson et al., 2013; Sims et al., 2017). However, oxidative stress is the more immediate response, with ROS species often produced within seconds (Granger and Kvietys, 2015) compared to cytokines and other inflammatory mediators which undergo transcription (Newton and Dixit, 2012; Shih et al., 2015). Further, as ROS production has been proposed to act as second messengers for pro-inflammatory cytokine responses (Bordt and Polster, 2014; Choi et al., 2012; Haddad and Land, 2002), wherein it regulates the inflammatory response (Latz et al., 2013; Singel and Segal, 2016), ROS production associated with microglial activation might be a central confounding factor in the progression of oxidative damage and neurodegeneration. This idea is something we want to emphasise, especially when carrying out *in vitro* work. We highlight that treatment with a pathologically relevant concentration of oAβ (Van Helmond et al., 2010) can stimulate microglial ROS production without the initiation of an inflammatory response. We propose that oAβ-microglial-ROS communication may be a primary instigator associated with microglial dysfunction, but this also underlines the importance of using appropriate concentrations of Aβ for *in vitro* neuroinflammatory research. Multiple groups have published data highlighting the neuroinflammatory effects of Aβ exposure to microglia, but the concentration is often up to 250 times higher than observed in AD patients (Caldeira et al., 2017; Liu et al., 2015; Urrutia et al., 2017; Van Helmond et al., 2010; Wang et al., 2018; Yang et al., 2017).

As discussed in Chapter 3, ROS are an essential component of the immune response, destroying invading pathogens (Paiva and Bozza, 2014; Winterbourn and Kettle, 2013). The destructive nature of ROS supports our notion that when pathologically produced, it can consequentially result in extensive endogenous damage. Support for this is widespread in AD, with oxidative markers identified to increase in a disease-dependent manner, correlating with patient MMSE scores (Ansari and Scheff, 2010), with even oxidative biomarkers observed in the CSF of patients before clinical AD manifests (Di Domenico et al., 2016). It is not surprising then that ROS production and oxidative damage has been proposed to be one of the earliest events in the disease (Nunomura et al., 2001). In animal studies, knockout of one allele of SOD-2 significantly increased brain Aβ levels and plaque burden in Tg19959 mice (Li et al., 2004), whilst mitochondrially targeted catalase, an

antioxidant which catalyses the decomposition of H_2O_2 to water and oxygen, was shown to reduce brain levels of Aβ, BACE1, APP and oxidative DNA damage in AβPP mice, increasing their life span (Mao et al., 2012).

In Chapter 3, we discussed our novel finding that Fpr2/3 stimulation can successfully reverse ROS production by the well-established potent inflammogen, LPS. In this Chapter we present original data underlining that Fpr2/3 agonist post-treatment can significantly reverse oAβ-induced microglial ROS production in the absence of an inflammatory response. This occurred without any modulation of the antioxidant systems glutathione, HO-1 or SOD-2. Previous pre-clinical data has emphasised that neurones excrete Aβ as a consequence of aging, whereby peroxynitrite and HNE associated lipid peroxidation could increase the amyloidogenic activity of γ-secretase, increasing $Aβ_{1-42}$ production (Guix et al., 2012; Gwon et al., 2012). In our study, we identified that Aβ could stimulate superoxide induction in the absence of NO. Because both of these oxidative species are required to form peroxynitrite, the absence of this latter cytotoxic oxidative species is unsurprising. However, iNOS expression has been shown to increase microglial activation in AD-like mice (Nathan et al., 2005), alongside being upregulated in human AD brain (Lüth et al., 2001); so the potential importance of this reactive species in disease progression cannot be ignored. Further, despite not providing evidence to suggest that Fpr2/3 stimulation modulates iNOS expression, we have shown that specified ligands can significantly reduce NO production (Chapter 3). We therefore suggest that modulation of this receptor could potentially decrease peroxynitrite production via the direct prevention of both NO and superoxide production.

The production of ROS has long been proposed to be associated with oAβ pathology (Giraldo et al., 2014; Han et al., 2015; Huang et al., 1999; Ojala and Sutinen, 2017; Wilkinson et al., 2012), appearing to contribute towards further Aβ deposition and memory deficits (Hernández-Zimbrón and Rivas-Arancibia, 2015; Kanamaru et al., 2015). This is likely why a diet high in antioxidants may reduce AD risk (Berti et al., 2018; Gu et al., 2010; Singh et al., 2014). Fpr2/3 stimulation may also contribute to this through not only the ability to reduce ROS production, but also indirectly prevent further ROS-associated amyloidogenic APP processing and Aβ production.

4.5.2. Aβ-induced ROS production via NADPH oxidase and the PPP pathway is reversed by Fpr2/3 stimulation

Here we provide the novel findings that Fpr2/3 activation can successfully reverse oAβ-induced ROS production by inhibiting activation of NADPH oxidase; likely due to the inhibition of co-localisation between NADPH subunits p67phox and gp91phox. When active, cytosolic regulatory components of the enzyme including p67phox and the small GTPase

Rac1 translocate to the membrane bound gp91phox complex, which is necessary for NADPH oxidase activation (Haslund-Vinding et al., 2017). Fpr2/3 activation reverses this translocation when administered after oAβ exposure. Whether Rac1 is modulated to prevent NADPH oxidase activation needs further elucidation. Previous research in our group highlighted that Fpr2/3 can signal through this GTPase (Cristante et al., 2013; McArthur et al., 2015), but because oAβ can signal through Rac1 to activate NADPH oxidase (Wyssenbach et al., 2016), some of the effects of Fpr2/3 stimulation on NADPH oxidase are difficult to interpret. However, AnxA1 can signal through ROCK and RhoA via Fpr2/3 (McArthur et al., 2009; Purvis et al., 2019), a signalling pathway which negatively regulates Rac1 (Byrne et al., 2016). Thus, further research into Fpr2/3-RhoA/Rac1 mediated NADPH oxidase modulation is warranted. However, we did not observe Aβ-induced mtROS production, despite this occurring in neurones (Du et al., 2008; SanMartín et al., 2017). Thus, our data emphasises that in microglia, Aβ-induced ROS production may primarily be associated with NADPH oxidases.

Free radicals are widely recognised to activate NF-κB (Dornas et al., 2017; Ndengele et al., 2005), with particular emphasis on H_2O_2 (Hara-Chikuma et al., 2015; Henríquez-Olguín et al., 2015; Ho et al., 2011), which may upregulate the transcription of several NF-κB-dependent pro-inflammatory genes (de Oliveira-Marques et al., 2007). Here we underline that oAβ-induced H_2O_2 production, likely spontaneously from NADPH oxidase produced superoxide (Mander et al., 2006), was significantly reduced by Fpr2/3 stimulation. Interestingly, oAβ exposure induced NF-κB nuclear translocation, with Fpr2/3 successfully reversing this, all in the absence of an inflammatory response. We suggest that NADPH oxidase activation may be important for a microglial priming response. It has been proposed that microglia respond to both peripheral and CNS damage by adopting an activated state, a process referred to as cellular priming (Perry and Holmes, 2014; Wendeln et al., 2018). Remaining in this relatively active phenotypic state, microglial exposure to a secondary inflammatory stimulus at a later point results in an exaggerated inflammatory response not seen in stimulus-naïve microglia. This priming effect has been linked to neurodegenerative disease development, including AD (Li et al., 2018). However, it is unlikely that an *in vitro* model will appropriately recapture *in vivo* priming mechanisms. Thus, our observations only provide a potential insight into this proposed process, with further elucidation warranted.

Activation of NADPH oxidase is an energy intensive process, wherein G6PD activity is central for NADPH formation and consequent superoxide production (Haslund-Vinding et al., 2017; Wang et al., 2014). G6PD is also the rate-limiting enzyme for the PPP (Grant, 2008). Thus, we propose that G6PD activation increases NADPH production to fuel NADPH oxidase function associated with oAβ stimulation. Our data supports this, with oAβ increasing the activity of G6PD. Strikingly, this increased activity was reversed by Fpr2/3 stimulation post-oAβ. Work in mice highlights that activation of the PPP can stimulate

macrophage ROS production and cytokine secretion (Baardman et al., 2018), emphasising that this pathway may be an primary perpetrator associated with induction of the microglial inflammatory response seen in AD. However, we did not observe an inflammatory response here. As previously mentioned, NADPH oxidase activation may be responsible for a microglial priming response for exacerbated neuroinflammation, and previous work supports this, wherein murine deficiency of p47phox and gp91phox promoted a pro-resolving microglial phenotype in response to Aβ challenge (Choi et al., 2012). However, cellular priming is difficult to model *in vitro*. Nevertheless, Fpr2/3 stimulation is a promising therapeutic target to modulate both NADPH oxidase induced ROS production and G6PD activity in microglia.

4.5.3. Fpr2/3 activation can modulate metabolic changes associated with G6PD activation

G6PD has knock-on consequences for microglial metabolism. G6P lies at the beginning of two major metabolic pathways: glycolysis and the PPP (Grant, 2008). The activation of the PPP pathway results in less glucose being available for glycolysis. Interestingly, aerobic glycolysis correlates with memory performance in WT but not APP/PS1 mice (Harris et al., 2016), suggesting that glycolysis may link to the manifestation of clinical symptoms in AD. Lactate shuttled to neurones induces the expression of genes associates with synaptic plasticity, alongside being required for long-term memory formation (Suzuki et al., 2011; Yang et al., 2014). Thus, early stage disease may result in reduced glycolysis and impairment of these processes. However, in APP/PS1 mice, inflammatory microglia are primarily glycolytic (Holland et al., 2018), emphasising a biphasic metabolic response may occur during disease progression, with glycolysis only being upregulated upon the onset of neuroinflammation. Data therefore suggests a double-edged role exists for microglia glycolysis, despite the current lack of human data establishing temporal progression of microglial metabolic changes. Nevertheless, determination of serum metabolomic profiles showed upregulation of the PPP in patients who later progressed to AD (Orešič et al., 2011), arguing that this metabolic pathway may have a critical role in the early stages of disease manifestation. Data provided here supports that Fpr2/3 stimulation can reverse oAβ-induced reduction of glycolysis, returning levels to that of untreated cells, likely due to the downregulation of ROS production and the PPP.

The reduction of glycolysis can also diminish pyruvate production, thus decreasing the Krebs cycle and oxidative phosphorylation (Compan et al., 2015; O'Neill et al., 2016). In microglia, reduced oxidative phosphorylation is associated with the development of a pro-inflammatory phenotype (Holland et al., 2018; Orihuela et al., 2016). However, here we identify that oAβ can significantly reduce mitochondrial respiration and ATP production in the absence of inflammation, again suggesting that this metabolic shift may act as a priming

response to initiate microglial inflammation associated with extended exposure to oAβ. However, our study uses an acute *in vitro* model, and thus this assumption must be further quantified. Nevertheless, these findings may be of particular relevance for pathological pathways associated with AD (Felsky et al., 2019). This shines a light on the importance of glucose hypometabolism, which is observed in the brains of AD patients, and correlates with Aβ pathology (Pascoal et al., 2019). Thus, the Fpr2/3 initiated reversal of Aβ-induced NADPH oxidase and G6PD activation alongside glycolysis reduction may have far reaching benefits for AD which require further investigation. However, Whilst Fpr2/3 stimulation by QC1 did not significantly alter mitochondrial metabolism, a trend in the reduction of maximal respiratory capacity was observed, and thus further experimentation into the mitochondrial effects of Fpr2/3 stimulation may be warranted. Nevertheless, we display novel microglial metabolic effects of both oAβ and Fpr2/3 stimulation, wherein the latter may hold promise to modulate metabolism and oxidative stress before the initiation of an oAβ-induced microglial inflammatory phenotypic switch, touted to be essential for disease progression (Serrano-Pozo et al., 2013).

4.5.4. Microglial activation is the key perpetrator of neuronal death

Considerable support exists underpinning the importance of neuroinflammation in AD progression (Felsky et al., 2019; Guerreiro et al., 2013; Heneka et al., 2015; Shi and Holtzman, 2018; Yin et al., 2017), with microglia established to contribute towards both direct and indirect neuronal death (Floden et al., 2005; Liddelow et al., 2017; Park et al., 2018; Yun et al., 2018). Whilst we observed no signs of oAβ-induced microglial inflammation in our study, previous work supports a link between oxidative stress, myelin and synaptic damage and consequent axonopathy in motor neurones (Fischer et al., 2012). Failed CNS myelin generation is also prevented by necroptosis of pro-inflammatory microglia, preceded by the repopulation of pro-regenerative microglia (Lloyd et al., 2019). In addition, neurone death can be both ROS and microglial phagocytosis mediated (Floden et al., 2005; Neher et al., 2011). Here we provide evidence that oAβ-induced apoptosis of differentiated SH-SY5Y cells is mediated through microglial activation, in the absence of an inflammatory response. This observation appears to be due to direct microglial-SH-SY5Y communication, because co-culturing is essential for this apoptotic effect, with microglial conditioned medium exposed to oAβ having no effect on cellular apoptosis. We report for the first time that microglial Fpr2/3 stimulation can successfully prevent neuronal apoptosis induced by oAβ. Alongside this, Fpr2/3 activation elicits wide-ranging pro-resolving and protective effects, including well established pro-resolving inflammatory functions (Bisicchia et al., 2018; Gobbetti et al., 2014; McArthur et al., 2018), and the newly reported anti-oxidant and metabolic modulation functions. Thus, pharmacological supplementation to modulate Fpr2/3 may yet provide therapeutic efficacy through a multi-pronged mechanistic approach.

Previous research reports that oAβ elicited direct neuronal toxicity (Akhter et al., 2018; Guivernau et al., 2016; Izuo et al., 2013; Tanokashira et al., 2017; Xing et al., 2013), but the concentration administered in these studies ranged from 10 to 1,000 times higher than that observed in human AD brain (Van Helmond et al., 2010). Additionally, several of these studies analysed neuronal toxicity through the MTT assay (Guivernau et al., 2016; Izuo et al., 2013), which measures metabolic activity. As we show here, oAβ can significantly reduce microglial metabolism without inducing toxicity, suggesting these studies may be reporting changes in neuronal metabolic profile rather than cellular damage. It is therefore crucial that appropriate oAβ concentrations are selected for *in vitro* study to represent cellular responses likely to occur in clinical disease. However, as a result of the data presented here, we suggest that Fpr2/3 stimulation may hold substantial promise to help reduce ROS production, microglial inflammation and neuronal death if administered during early *in vivo* stages of disease.

4.5.5. Experimental limitations and improvements

The novel data presented here underline that Fpr2/3 activation can prevent microglial induced SH-SY5Y apoptosis associated with oAβ stimulation. Limitations of the study do exist, however. Firstly, this study was carried out *in vitro*. Whilst the data presented here provide novel insights into the functions of Fpr2/3 following oAβ insult, the importance of determining whether this pro-resolving receptor can prevent neuronal apoptosis *in vivo* is paramount. This will elucidate whether therapeutics designed towards Fpr2/3 hold promise for neurodegenerative disease research going forward. Second, it is important to note that BV-2 microglia and SH-SY5Y are from murine and human origin, respectively. The use of the newly identified and ATCC verified human microglial HMC3 cell line will be important for future clarification of our murine observations (Dello Russo et al., 2018). We also proposed that Fpr2/3 stimulation directly prevents the activation of NADPH oxidase, thus reversing the production of ROS species such as superoxide and H_2O_2. Whilst we identified that Fpr2/3 stimulation did not affect the antioxidant systems GSH, HO-1 or SOD-2, the effects on other antioxidant systems such as catalase, thioredoxins, peroxiredoxins and Nrf2 (Vilhardt et al., 2017) were not determined and need to be considered going forward.
For any AD research, it is important to consider that tau pathology correlates with dementia status (Brier et al., 2016). Differentiated SH-SY5Y cells can express phosphorylated tau under certain conditions (Greco et al., 2009; Majd et al., 2018), thus it could be possible that microglial ROS production is associated with SH-SY5Y tau pathology. Whilst no visually observable changes were noted in the neuronal processes of differentiated SH-SY5Y cells, this does not necessarily mean intracellular pathology has not accumulated.

Despite the co-culture studies providing a means for microglial-neuronal communication, astrocytes were not included here. Because microglia can stimulate astrocytic neurotoxicity and inflammation (Kirkley et al., 2017; Liddelow et al., 2017), alongside oAβ inducing direct pro-oxidant and pro-inflammatory astrocytic responses (Urrutia et al., 2017; Wang et al., 2013), astrocytes may contribute to oAβ-induced neuronal apoptosis. It is therefore important to determine whether Fpr2/3 stimulation can still protect neurones from apoptosis in the presence of an astrocytic response. However, because no evidence suggests Fpr2/3 is expressed in astrocytes (He and Ye, 2017), any astrocytic changes will likely be mediated indirectly via microglial Fpr2/3 activation. A triple culture incorporating both glial cells and neurones is therefore warranted. In addition to 2D tri-culture systems, advanced 3D human triculture systems are now available, which recapitulate intracellular interactions, Aβ and tau pathology, neuroinflammation and neurotoxicity (Park et al., 2018). Brain-slice cultures would be a greater advancement to determine the cell-cell communication effects *ex-vivo* on neuronal apoptosis following oAβ treatment and Fpr2/3 activation.

The data here also shows that oAβ reduces microglial oxidative phosphorylation. However, the effects of oAβ-induced microglial modulation on SH-SY5Y was not determined. This was primarily due to the fact that SH-SY5Y cells are of neuroblastoma origin. Due to variations in metabolism associated with cancer cells (Vander Heiden et al., 2009), shifts in SH-SY5Y metabolic profiles may not represent that present in neurones. This further emphasises the importance to determine the effects of microglial Fpr2/3 activation on the apoptosis of primary neurones exposed to oAβ.

4.5.6. Future work

Alongside the pro-resolving effects of Fpr2/3 stimulation in Chapter 3, the novel data provided here suggest that modulation of these receptors may become a new therapeutic approach in AD research. Despite this, further work establishing the roles of Fpr2/3 in AD models is critical. An important point to note is that mature SH-SY5Y cells are known to express synaptic related proteins, including post-synaptic material 95 and synaptophysin (Chamniansawat and Chongthammakun, 2009; Oe et al., 2005). Because microglia have important roles in both synaptic pruning and plasticity (Paolicelli et al., 2011; Salter and Beggs, 2014), it would be interesting to determine whether oAβ treatment and Fpr2/3 activation modulate the expression of these proteins, alongside analysing how this may relate to the physical appearance of the neuritic structures which develop in these mature cells. Fpr2/3-mediated modulation to these proteins would suggest that this pro-resolving pathway may have an important role in the synapse, potentially implicating Fpr2/3 in microglial mediated pruning and synaptic plasticity. In addition, the effects of Fpr2/3 stimulation on synaptic transmission could be determined via electrophysiological analysis

in primary neurones (Gu et al., 2016), potentially facilitating interest as to whether Fpr2/3 activation can conserve neuronal communication. LTP of hippocampal neurones both *in vitro* (Gartner and Staiger, 2002) and in hippocampal brain slices (Paci et al., 2017) could also provide insights as to whether microglial Fpr2/3 modulation could have knock-on consequences for memory, providing further justification for *in vivo* work.

Whilst we looked at the ability of microglia to phagocytosis *E.coli* bioparticles, this does not provide any indication as to whether Fpr2/3 stimulation with C43/QC1 can contribute towards phagocytosis of oAβ. Previous research shows that AnxA1 induced Fpr2/3 stimulation can increase Aβ clearance and degradation via microglial phagocytosis and neprilysin activity in N2a neuronal cells (Ries et al., 2016). Future work could investigate this via incorporating fluorescently labelled oAβ (Pan et al., 2011), similar to the BODIPY FL labelled bioparticles used in our study. However, because microglia express a range of oAβ degrading proteases including neprilysin (Ries and Sastre, 2016), determining whether Fpr2/3 stimulation can modulate the activity of these will be of particular interest to combat Aβ accumulation in early stage disease.

Because our data suggests that oAβ-induced ROS production is Fpr2/3 mediated, further studies are required to determine whether modulation of Rac1 recruitment between oAβ and pro-resolving ligands are responsible for the reversal of NADPH oxidase activation. AnxA1-induced Fpr2/3 activation upregulates ROCK/RhoA signalling (Cristante et al., 2013; Purvis et al., 2019), which often inhibits Rac1 (Byrne et al., 2016). Thus, signalling analysis between NADPH oxidase, Fpr2/3 and Rac1/RhoA will be crucial to further elucidate the anti-oxidative mechanism associated with this pro-resolving receptor.

The importance of *in vivo* work in AD research is also clear. The consequential effects of our findings on pathology, memory and behaviour in transgenic animal models will be crucial to determine whether modulation of Fpr2/3 holds promise for not only AD, but other neurodegenerative conditions. Incorporating knockout mouse strains, such as Fpr2/3$^{-/-}$ (McArthur et al., 2015) and gp91phox$^{-/-}$ (Dohi et al., 2010) alongside G6PD inhibition models (Mele et al., 2018) will help elucidate the importance of the interactions we have observed *in vitro* in terms in murine disease. Parallel supplementation experiments with siRNA for these proteins *in vitro* will further support the mechanistic association between Fpr2/3 stimulation and PPP-induced NADPH oxidase activation.

4.5.7. Chapter Summary

In this chapter we provide data supporting the pathology of oligomeric 42 kDa amyloid beta in microglia involves NADPH oxidase-mediated ROS production, consequently modulating

metabolism. We show this happens in the absence of an inflammatory response (Figure 4.18). The consequences of this for neuronal survival were investigated through the development of a BV-2 microglia SH-SY5Y co-culture model, wherein oAβ increased differentiated SH-SY5Y apoptosis, but only in the presence of BV-2 microglia. We also observed that microglial expression of the pro-resolving receptor Fpr2/3 protects differentiated SH-SY5Y from this increase in cellular apoptosis. We report that this protective mechanism is related to the newly identified antioxidant and metabolic modulating capabilities of Fpr2/3.

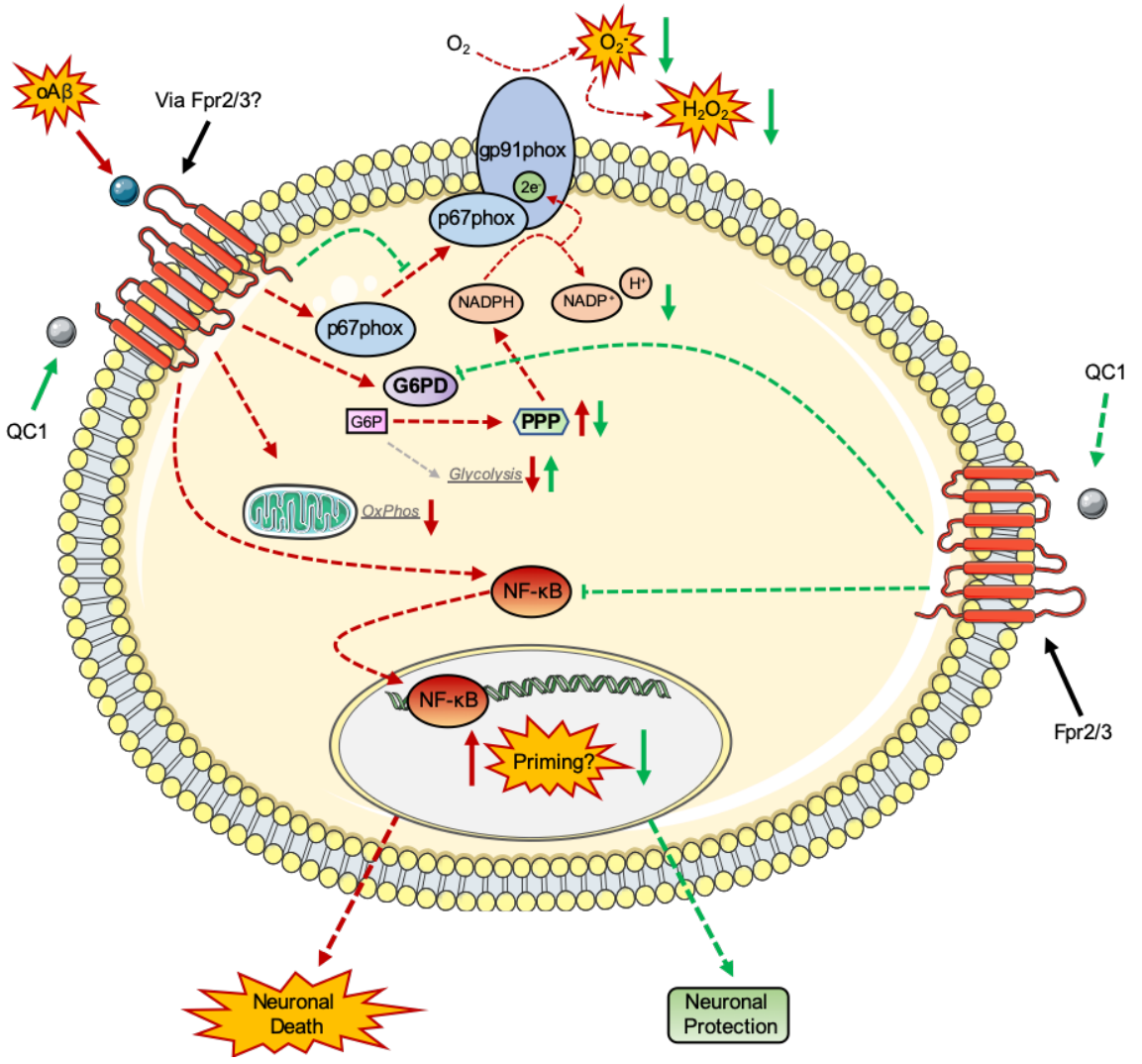

Figure 4.18 Summary diagram for Chapter 4, detailing the effects of oAβ and QC1 on BV-2 microglia. Mechanism pathways are represented with dashed arrows and inhibitory lines. Solid arrows represent overall changes. Red lines represent oAβ stimulated responses, whereas green lines represent QC1 mediated effects. oAβ treatment resulted in NADPH oxidase-induced ROS production. This resulted in metabolic effects, reducing both oxidative phosphorylation (OxPhos) and glycolysis. Instead, increased glucose 6-phosphate dehydrogenase (G6PD) activity shifted glucose 6-phosphate towards the pentose phosphate pathway (PPP) to produce more NADPH for ROS production. Data presented in this thesis suggest these effects might be partially mediated by Fpr2/3. oAβ also triggered NF-κB nuclear translocation in the absence of an inflammatory response. Whether this is associated with microglial priming needs further investigation. QC1 treatment prevented NADPH oxidase activation and ROS production, resulting in a reduction in G6PD activity and increased glycolysis. It also prevented NF-κB activation. However, no differences were observed for OxPhos following QC1 treatment.

Chapter 5: Summary and Future Directions

5.1. Summary

The central research question of this thesis is whether Fpr2/3 is a good therapeutic candidate for neurodegenerative disease. The aims were to identify whether Fpr2/3 stimulation could suppress both LPS and oAβ induced microglial activation through promotion of a pro-resolving phenotype, associated tissue repair and cell conservation (McArthur et al., 2018; Orihuela et al., 2016). Both LPS and oAβ are recognised to stimulate ROS production (Kim et al., 2010; Urrutia et al., 2017), and we determined whether Fpr2/3 activation modulated this response, analysing the mechanisms involved. Previous research highlighted that innate immune cells modulate their metabolic profile, with pro-inflammatory and pro-resolving phagocytes utilising aerobic glycolysis and oxidative phosphorylation for energy, respectively (O'Neill and Hardie, 2013; Rodríguez-Prados et al., 2010). We therefore determined whether metabolic shifts would be associated with LPS and oAβ induced inflammation, and whether Fpr2/3 stimulation had any metabolic modulating capacity. Our final aim was to establish whether resolution effects of Fpr2/3 post-oAβ administration could protect the neuronal cell line SH-SY5Y from oAβ-induced apoptosis. Multiple studies emphasise direct neuronal toxicity of oAβ (Akhter et al., 2018; Guivernau et al., 2016; Izuo et al., 2013; Tanokashira et al., 2017; Xing et al., 2013), whilst others underline the importance of microglia (Floden et al., 2005; Liddelow et al., 2017; Yun et al., 2018), we aimed to determine whether microglia presence in co-culture was pivotal for toxicity.

Our results highlight for the first time that Fpr2/3 stimulation can not only promote a pro-resolving phenotype following LPS stimulation, but also reverse ROS production from two independent sources: the mitochondria and NADPH oxidases. Interestingly, and despite our assumptions, oAβ did not trigger an inflammatory response in our study. It did however initiate NADPH oxidase-induced ROS, resulting in changes to microglial metabolism, which appeared to be essential to facilitate oAβ-induced SH-SY5Y apoptosis, with cell death only occurring in BV-2 SH-SY5Y co-cultures. Strikingly, Fpr2/3 activation with QC1 successfully prevented this apoptotic response. In summary, our data highlights several novel functions for Fpr2/3 stimulation in microglia: preventing both NADPH oxidase and mitochondrial induced ROS production, consequentially modulating microglial metabolism, and preventing microglial-induced neuronal death.

Our data highlighting the pro-resolution role of Fpr2/3 in microglia following LPS exposure was not surprising. However, we report here for the first time Fpr2/3 activation can reverse

mitochondrial and NADPH oxidase induced ROS production in microglia. Previous reports have suggested that Fpr2/3 activation can stimulate ROS production and cellular differentiation in murine stem cells (Zhang et al., 2017), alongside triggering ROS in murine granulocytes (Filina et al., 2014). However, we did not observe ROS-production associated with our ligands of interest. Supporting these previous findings.

Here we report new metabolic parameters associated with ROS production and reversal by Fpr2/3. Extensive research underlines the importance of microglia in neuronal degeneration in neuroinflammatory disorders (Crotti and Glass, 2015; Heneka et al., 2014; Lan et al., 2017; Walker and Lue, 2015; Wang et al., 2015). In AD, the extent of inflammation appears to correlate with cognitive symptoms more closely than Aβ accumulation (Farrell et al., 2017; Kreisl et al., 2013; Serrano-Pozo et al., 2011). Our data also highlight that microglia can cause neuronal apoptosis, and that ROS production and metabolic dysfunction may be contributing factors towards this process (Fan et al., 2015; Floden et al., 2005; Ma et al., 2017).

5.2. Experimental discrepancies

Strong emphasis surrounds the use of pathologically relevant toxin concentrations for *in vitro* neurodegenerative research. Multiple studies support direct neuronal toxicity of oAβ (Akhter et al., 2018; Guivernau et al., 2016; Izuo et al., 2013; Tanokashira et al., 2017; Xing et al., 2013), but we did not observe this. The concentration used in our study was selected based on observed oAβ levels in human AD brain (Van Helmond et al., 2010), whereas concentrations utilised by previous studies ranged between 10 to 1,000 times higher. Thus, these observed *in vitro* toxic effects are unlikely to represent the *in vivo* condition.

In this thesis, we report that Fpr2/3 can both downregulate and increase glycolysis following LPS and oAβ exposure, respectively, novel findings that may initially appear to contradict each other. However, we propose that these shifts in glycolysis are directly linked to the pro-resolving and ROS-lowering capacity of Fpr2/3 stimulation. Following inflammatory stimulation, innate immune cells adopt a glycolytic metabolic profile to produce cytokines and other pro-inflammatory mediators (Ganeshan and Chawla, 2014; O'Neill and Hardie, 2013), often resulting in ROS production (Bordt and Polster, 2014; Yauger et al., 2019).

The pro-resolving effects of Fpr2/3 are directly associated with a decrease in glycolysis, as pro-resolving immune cells rely upon oxidative phosphorylation for metabolism (O'Neill et al., 2016). Following oAβ exposure however, NADPH oxidase-induced ROS production and subsequent reductions in intracellular NADPH stimulated the PPP, resulting in less glucose availability for glycolysis. We show that Fpr2/3 stimulation can reverse NADPH oxidase induced ROS production, which consequentially reduces activity of the PPP, returning glycolysis to a rate similar to untreated cells. This emphasises that Fpr2/3 stimulation may

hold differing effects during neuroinflammatory disease, depending on the stage of microglial activation.

5.3. Research limitations

Our work used the immortalised murine BV-2 microglial line; the most extensively characterised murine microglial line available (Timmerman et al., 2018), and often used as a substitute for primary microglia. Whilst we did implement some primary microglial experiments for key findings, this was limited due to time, cost, availability and handling ability. BV-2 microglia were also produced via the inclusion of an oncogene carrying retrovirus (Blasi et al., 1990). Whether these cells can mimic primary microglia or the *in vivo* situation with high fidelity has been called into question (Horvath et al., 2008). Despite this, we believed it was an appropriate first-line model to determine the therapeutic efficacy of Fpr2/3.

The importance of using human microglia is clearly evident, however. Recent research highlights that while human and murine microglia overlap considerably, this is limited for genes regulated during aging, supporting the notion that human and murine cells age differently (Galatro et al., 2017; Olah et al., 2018). This is something to take into consideration for both *in vitro* and *in vivo* murine research going forward. Nevertheless, the human microglial cell line HMC3 has been made commercially available (Dello Russo et al., 2018), with these being the preferred choice for future investigations.

Possibly the most significant limitation of this research in terms of clinical AD is the lack of data surrounding tau hyperphosphorylation. Whilst neuronally expressed tau has physiological functions in synaptic plasticity, learning and memory (Biundo et al., 2018), hyperphosphorylated tau is a key pathological feature in the development and progression of AD (Bejanin et al., 2017). Further, multiple pro-inflammatory cytokines elevated in AD, including TNFα, are associated with increased tau pathology (Domingues et al., 2017; Shi et al., 2011). Microglial activation also appears to occur prior to synaptic loss and tau pathology (Yoshiyama et al., 2007), suggesting that microglia may be directly associated with neuronal damage through tau hyperphosphorylation. This is supported by recent research reporting that activated microglia dramatically promote tau propagation and associated neurotoxicity (Asai et al., 2015), alongside directly contributing to tau pathology spread (Hopp et al., 2018).

The above results therefore suggest that inflamed microglia are crucially connected to the progression of pathological tau. Thus, the interaction between tau and microglia is a central component of AD research which should be excluded with caution. Whilst we did indeed exclude tau pathology in this work, the characterisation of microglial activation on neuronal apoptosis was only determined at the very end of this piece of work. As a whole, this thesis

was a proof of concept study, primarily focusing on the effects of Fpr2/3 activation on microglial activation, modulation and phenotype, and determining the therapeutic potential of this receptor for more complicated neurodegenerative disease models. These include priming future research studies in animal models, but also with complicated 3D in vitro systems which include not only oAβ and microglial activation, but also hyperphosphorylated tau pathology (Park et al., 2018).

Whilst we provide novel data supporting the benefits of Fpr2/3 modulation for neuroinflammatory research, this study did manifest some practical limitations. Our main technical experimental limitation was that of western blotting. The initial loading control we planned to consistently utilise was β-actin, but the banding pattern of this was affected by LPS (Figure 3.4). Determined to understand why, we were unable to find any previous literature reporting such an occurrence. However, because the endogenous Fpr2/3 agonist ANXA1 has been reported to mobilize the actin cytoskeleton in human blood monocytes (McArthur et al., 2015), administration of our ligands may have modulated actin expression regardless. Total kinase expression, for example ERK1/2 could have also been a potential option, due to their activity being associated with phosphorylation rather than upregulation. However, we deemed Ponceau S staining as suitable for our study due to previous research highlighting comparable densitometric analyses between β-actin and Ponceau S (Romero-Calvo et al., 2010).

5.4. Fpr2/3 agonists may hold promise for several central nervous system diseases

Whilst our research interest is centrally focused on discovering an alternative therapeutic strategy to tackle the chronic neurodegenerative environment established in the brains of AD patients, our data highlights that activation of human FPR2 may be of therapeutic benefit for several different neurological and neurodegenerative diseases, which have a considerable neuroinflammatory component. For example, alongside AD, neuroinflammation and oxidative damage are extensive in many CNS disorders including Parkinson's disease (Abeliovich and Gitler, 2016), stroke (Chamorro et al., 2016), multiple sclerosis (Kallaur et al., 2017), traumatic brain injury (Karve et al., 2016) and epilepsy (Vezzani et al., 2011). Thus, the therapeutic scope for human FPR2 modulation is enticing, and something which has stimulated our interest.

5.5. Future work

In this study we highlight that microglial ROS production appears to be a crucial contributor towards neuronal apoptosis. ROS production has also been linked towards tau pathology (Giraldo et al., 2014), with the latter being a critical determinant of neuronal dysfunction

(Hoover et al., 2010; Shi et al., 2017; Spires-Jones and Hyman, 2014). Reactive microglia appear to be a driver of tau pathological spread in the brain (Maphis et al., 2015). Further, in preclinical and symptomatic stages of AD, lower aerobic glycolysis is associated with higher tau deposition (Vlassenko et al., 2018). Thus, it is highly likely that that pro-resolving and newly described antioxidative and immunological functions of Fpr2/3 activation could prevent the hyperphosphorylation of tau in neurones. Further research will be essential to confirm this both *in vitro* and *in vivo*, but it could hold significant benefit for AD research going forward.

Whether Fpr2/3 activation can preserve neuronal health in a 3D culture model of AD which includes not just neurones and microglia, but also astrocytes (Park et al., 2018) will be beneficial, due to neuronal toxicity associated with microglial-astrocytic communication (Kirkley et al., 2017; Liddelow et al., 2017). Microglial inflammation can shift astrocytes into a neurotoxic phenotype, resulting in them losing the ability to promote neuronal survival, synaptogenesis and neural outgrowth, contributing instead to neuronal death (Liddelow et al., 2017). Interestingly, inhibiting this microglial-induced conversion of astrocytes is neuroprotective in Parkinson's disease models (Yun et al., 2018). Determining whether the microglial effects of Fpr2/3 activation could modulate astrocyte toxicity and neuronal health will provide further insight into the therapeutic potential of this pro-resolving receptor.

Brain slice cultures will provide an *ex vivo* approach to investigate neuronal damage following inflammogen exposure in Fpr2/3$^{-/-}$ animals, so we can determine the importance of this pro-resolving receptor in limiting neurodegenerative damage. This could also be supplemented with WT Fpr2/3 animals and exogenous administration of Fpr2/3 ligands, allowing for neurodegenerative marker comparisons to hopefully further emphasise that Fpr2/3 stimulation can provide neurones with protection from inflammatory and AD related toxic insults.

5.6. Closing remarks

AD is the most common cause of dementia in the aging population, affecting approximately 4% of all individuals over the age of 65 (Hebert et al., 2013; Prince et al., 2013). As of July 2015, the global disease burden is estimated to be around 37 million people (United Nations, 2015), but numbers are expected to rise exponentially to 78 million by 2050 (Prince et al., 2015). In comparison to other diseases such as HIV, heart disease and breast cancer, where death rates have steadily decreased in recent history, AD associated death continues to rise (James et al., 2014; Lehman et al., 2012; Murphy et al., 2013), with the disease being a clear public health crisis.

The peripheral pro-resolving properties of murine Fpr2/3 and human FPR2 during inflammation are clear (Sadani N Cooray et al., 2013; Gobbetti et al., 2014; McArthur et al., 2018, 2015). Interestingly, several endogenous FPR2 ligands are expressed in the brain (Bisicchia et al., 2018; McArthur et al., 2010; Wang et al., 2015), and are reduced in the hippocampus, entorhinal cortex and CSF of AD patients (Wang et al., 2015; Zhu et al., 2016). With both of these aforementioned brain regions highly affected by AD pathology, evidence supports the importance of pro-resolving systems such as FPR2 in protecting neurones from extensive microglial activation and neuroinflammatory damage. Despite this, research into the therapeutic potential of FPR2 agonists for AD is relatively sparse. Here we show for the first time that microglial Fpr2/3 stimulation can rescue neuronal cells from Aβ-induced, microglial facilitated apoptosis. However, we also provide evidence that Fpr2/3 activation can stimulate a pro-resolving microglial phenotype following LPS exposure, suggesting that select ligands for this diverse receptor may be suitable for research into an entire host of different neuroinflammatory and neurodegenerative conditions.

AD patients are in desperate need for new therapeutics, with clinical trial failures all too apparent and devastating (Gauthier et al., 2016; Panza et al., 2019, 2016). Pursuing pro-resolving approaches will provide novel insights into the importance of aberrant microglial activation, metabolism and neuroinflammation in specific aspects of AD. We believe, based on previous literature and the data presented here, that Fpr2/3 is an appropriate receptor to target in future investigations not only for AD, but multiple neuroinflammatory and neurodegenerative diseases.

Bibliography

Abeliovich, A., Gitler, A.D., 2016. Defects in trafficking bridge Parkinson's disease pathology and genetics. Nature 539, 207–216. doi:10.1038/nature20414

AD Collaborative Group, Bentham, P., Gray, R., Sellwood, E., Hills, R., Crome, P., Raftery, J., 2008. Aspirin in Alzheimer's disease (AD2000): a randomised open-label trial. Lancet Neurol. 7, 41–49. doi:10.1016/S1474-4422(07)70293-4

Agrawal, S.M., Williamson, J., Sharma, R., Kebir, H., Patel, K., Prat, A., Yong, V.W., 2013. Extracellular matrix metalloproteinase inducer shows active perivascular cuffs in multiple sclerosis. Brain 136, 1760–1777. doi:10.1093/brain/awt093

Aït-Ali, N., Fridlich, R., Millet-Puel, G., Clérin, E., Delalande, F., Jaillard, C., Blond, F., Perrocheau, L., Reichman, S., Byrne, L.C., Olivier-Bandini, A., Bellalou, J., Moyse, E., Bouillaud, F., Nicol, X., Dalkara, D., van Dorsselaer, A., Sahel, J.-A., Léveillard, T., 2015. Rod-Derived Cone Viability Factor Promotes Cone Survival by Stimulating Aerobic Glycolysis. Cell 161, 817–832. doi:10.1016/j.cell.2015.03.023

Akhter, R., Saleem, S., Saha, A., Biswas, S.C., 2018. The pro-apoptotic protein Bmf co-operates with Bim and Puma in neuron death induced by β-amyloid or NGF deprivation. Mol. Cell. Neurosci. 88, 249–257. doi:10.1016/j.mcn.2018.02.011

Akira, S., Hemmi, H., 2003. Recognition of pathogen-associated molecular patterns by TLR family. Immunol. Lett. 85, 85–95.

Akiyama, H., Barger, S., Barnum, S., Bradt, B., Bauer, J., Cole, G.M., Cooper, N.R., Eikelenboom, P., Emmerling, M., Fiebich, B.L., Finch, C.E., Frautschy, S., Griffin, W.S., Hampel, H., Hull, M., Landreth, G., Lue, L., Mrak, R., Mackenzie, I.R., McGeer, P.L., O'Banion, M.K., Pachter, J., Pasinetti, G., Plata-Salaman, C., Rogers, J., Rydel, R., Shen, Y., Streit, W., Strohmeyer, R., Tooyoma, I., Van Muiswinkel, F.L., Veerhuis, R., Walker, D., Webster, S., Wegrzyniak, B., Wenk, G., Wyss-Coray, T., 2000. Inflammation and Alzheimer's disease. Neurobiol. Aging 21, 383–421.

Akiyama, H., McGeer, P.L., 1990. Brain microglia constitutively express beta-2 integrins. J. Neuroimmunol. 30, 81–93.

Al-Madol, M.A., Shaqura, M., John, T., Likar, R., Ebied, R.S., Schäfer, M., Mousa, S.A., 2017. Comparative Expression Analyses of Pro- versus Anti-Inflammatory Mediators within Synovium of Patients with Joint Trauma, Osteoarthritis, and Rheumatoid Arthritis. Mediators Inflamm. 2017, 1–11. doi:10.1155/2017/9243736

Albuquerque, E., Pereira, E., Alkondon, M., Rogers, S., 2009. Mammalian Nicotinic Acetylcholine Receptors: From Structure to Function. Physiol. Rev. 89, 73–120. doi:10.1152/physrev.00015.2008.Mammalian

Aldini, G., Vistoli, G., Stefek, M., Chondrogianni, N., Grune, T., Sereikaite, J., Sadowska-Bartosz, I., Bartosz, G., 2013. Molecular strategies to prevent, inhibit, and degrade advanced glycoxidation and advanced lipoxidation end products. Free Radic. Res. 47, 93–137. doi:10.3109/10715762.2013.792926

Alexander, G.E., Ryan, L., Bowers, D., Foster, T.C., Bizon, J.L., Geldmacher, D.S., Glisky, E.L., 2012. Characterizing cognitive aging in humans with links to animal models. Front. Aging Neurosci. 4, 21. doi:10.3389/fnagi.2012.00021

Andrews, N.W., Almeida, P.E., Corrotte, M., 2014. Damage control: cellular mechanisms of plasma membrane repair. Trends Cell Biol. 24, 734–42. doi:10.1016/j.tcb.2014.07.008

Anrather, J., Racchumi, G., Iadecola, C., 2006. NF-kappaB regulates phagocytic NADPH oxidase by inducing the expression of gp91phox. J. Biol. Chem. 281, 5657–67. doi:10.1074/jbc.M506172200

Ansari, M.A., Scheff, S.W., 2010. Oxidative stress in the progression of Alzheimer disease in the frontal cortex. J. Neuropathol. Exp. Neurol. 69, 155–67. doi:10.1097/NEN.0b013e3181cb5af4

Apelt, J., Schliebs, R., 2001. Beta-amyloid-induced glial expression of both pro- and anti-inflammatory cytokines in cerebral cortex of aged transgenic Tg2576 mice with Alzheimer plaque pathology. Brain Res. 894, 21–30.

Arriagada, P. V, Growdon, J.H., Hedley-Whyte, E.T., Hyman, B.T., 1992. Neurofibrillary tangles but not senile plaques parallel duration and severity of Alzheimer's disease. Neurology 42, 631–9.

Asai, H., Ikezu, S., Tsunoda, S., Medalla, M., Luebke, J., Haydar, T., Wolozin, B., Butovsky, O., Kügler, S., Ikezu, T., 2015. Depletion of microglia and inhibition of exosome synthesis halt tau propagation. Nat. Neurosci. 18, 1584–93. doi:10.1038/nn.4132

Baardman, J., Verberk, S.G.S., Prange, K.H.M., van Weeghel, M., van der Velden, S., Ryan, D.G., Wüst, R.C.I., Neele, A.E., Speijer, D., Denis, S.W., Witte, M.E., Houtkooper, R.H., O'neill, L.A., Knatko, E. V., Dinkova-Kostova, A.T., Lutgens, E., de Winther, M.P.J., Van den Bossche, J., 2018. A Defective Pentose Phosphate Pathway Reduces Inflammatory Macrophage Responses during Hypercholesterolemia. Cell Rep. 25, 2044-2052.e5. doi:10.1016/j.celrep.2018.10.092

Bachmeier, C., Paris, D., Beaulieu-Abdelahad, D., Mouzon, B., Mullan, M., Crawford, F., 2013. A multifaceted role for apoE in the clearance of beta-amyloid across the blood-brain barrier. Neurodegener. Dis. 11, 13–21. doi:10.1159/000337231

Bagyinszky, E., Giau, V. Van, Shim, K., Suk, K., An, S.S.A., Kim, S., 2017. Role of inflammatory molecules in the Alzheimer's disease progression and diagnosis. J. Neurol. Sci. 376, 242–254. doi:10.1016/j.jns.2017.03.031

Bai, X., Yan, C., Yang, G., Lu, P., Ma, D., Sun, L., Zhou, R., Scheres, S.H.W., Shi, Y., 2015. An atomic structure of human γ-secretase. Nature 525, 212–7. doi:10.1038/nature14892

Balasingam, V., Yong, V.W., 1996. Attenuation of astroglial reactivity by interleukin-10. J. Neurosci. 16, 2945–55.

Balducci, C., Frasca, A., Zotti, M., La Vitola, P., Mhillaj, E., Grigoli, E., Iacobellis, M., Grandi, F., Messa, M., Colombo, L., Molteni, M., Trabace, L., Rossetti, C., Salmona, M., Forloni, G., 2017. Toll-like receptor 4-dependent glial cell activation mediates the impairment in memory establishment induced by β-amyloid oligomers in an acute mouse model of Alzheimer's disease. Brain. Behav. Immun. 60, 188–197. doi:10.1016/j.bbi.2016.10.012

Bales, K.R., Liu, F., Wu, S., Lin, S., Koger, D., DeLong, C., Hansen, J.C., Sullivan, P.M., Paul, S.M., 2009. Human APOE Isoform-Dependent Effects on Brain -Amyloid Levels in PDAPP Transgenic Mice. J. Neurosci. 29, 6771–6779. doi:10.1523/JNEUROSCI.0887-09.2009

Bales, K.R., O'Neill, S.M., Pozdnyakov, N., Pan, F., Caouette, D., Pi, Y., Wood, K.M., Volfson, D., Cirrito, J.R., Han, B.-H., Johnson, A.W., Zipfel, G.J., Samad, T.A., 2016. Passive immunotherapy targeting amyloid-β reduces cerebral amyloid angiopathy and improves vascular reactivity. Brain 139, 563–577. doi:10.1093/brain/awv313

Barnwal, B., Karlberg, H., Mirazimi, A., Tan, Y.-J., 2016. The Non-structural Protein of Crimean-Congo Hemorrhagic Fever Virus Disrupts the Mitochondrial Membrane Potential and Induces Apoptosis. J. Biol. Chem. 291, 582–592. doi:10.1074/jbc.M115.667436

Barone, E., Cenini, G., Sultana, R., Di Domenico, F., Fiorini, A., Perluigi, M., Noel, T., Wang, C., Mancuso, C., St. Clair, D.K., Butterfield, D.A., 2012. Lack of p53 Decreases Basal Oxidative Stress Levels in the Brain Through Upregulation of Thioredoxin-1, Biliverdin Reductase-A, Manganese Superoxide Dismutase, and Nuclear Factor Kappa-B. Antioxid. Redox Signal. 16, 1407–1420. doi:10.1089/ars.2011.4124

Bate, C., Kempster, S., Last, V., Williams, A., 2006. Interferon-gamma increases neuronal death in response to amyloid-beta1-42. J. Neuroinflammation 3, 7. doi:10.1186/1742-2094-3-7

Bateman, R.J., Xiong, C., Benzinger, T.L.S., Fagan, A.M., Goate, A., Fox, N.C., Marcus, D.S., Cairns, N.J., Xie, X., Blazey, T.M., Holtzman, D.M., Santacruz, A., Buckles, V., Oliver, A., Moulder, K., Aisen, P.S., Ghetti, B., Klunk, W.E., McDade, E., Martins, R.N., Masters, C.L., Mayeux, R., Ringman, J.M., Rossor, M.N., Schofield, P.R., Sperling, R.A., Salloway, S., Morris, J.C., Dominantly Inherited Alzheimer Network, 2012. Clinical and Biomarker Changes in Dominantly Inherited Alzheimer's Disease. N. Engl. J. Med. 367, 795–804. doi:10.1056/NEJMoa1202753

Baxter, P.S., Hardingham, G.E., 2016. Adaptive regulation of the brain's antioxidant defences by neurons and astrocytes. Free Radic. Biol. Med. 100, 147–152. doi:10.1016/j.freeradbiomed.2016.06.027

Beecham, G.W., Hamilton, K., Naj, A.C., Martin, E.R., Huentelman, M., Myers, A.J., Corneveaux, J.J., Hardy, J., Vonsattel, J.-P., Younkin, S.G., Bennett, D.A., De Jager, P.L., Larson, E.B., Crane, P.K., Kamboh, M.I., Kofler, J.K., Mash, D.C., Duque, L., Gilbert, J.R., Gwirtsman, H., Buxbaum, J.D., Kramer, P., Dickson, D.W., Farrer, L.A., Frosch, M.P., Ghetti, B., Haines, J.L., Hyman, B.T., Kukull, W.A., Mayeux, R.P., Pericak-Vance, M.A., Schneider, J.A., Trojanowski, J.Q., Reiman, E.M., Schellenberg, G.D., Montine, T.J., 2014. Genome-wide association meta-analysis of neuropathologic features of Alzheimer's disease and related dementias. PLoS Genet. 10, e1004606. doi:10.1371/journal.pgen.1004606

Bejanin, A., Schonhaut, D.R., La Joie, R., Kramer, J.H., Baker, S.L., Sosa, N., Ayakta, N., Cantwell, A., Janabi, M., Lauriola, M., O'Neil, J.P., Gorno-Tempini, M.L., Miller, Z.A., Rosen, H.J., Miller, B.L., Jagust, W.J., Rabinovici, G.D., 2017. Tau pathology and neurodegeneration contribute to cognitive impairment in Alzheimer's disease. Brain 140, 3286–3300. doi:10.1093/brain/awx243

Bell, K.F.S., Al-Mubarak, B., Martel, M.-A., McKay, S., Wheelan, N., Hasel, P., Márkus, N.M., Baxter, P., Deighton, R.F., Serio, A., Bilican, B., Chowdhry, S., Meakin, P.J., Ashford, M.L.J., Wyllie, D.J.A., Scannevin, R.H., Chandran, S., Hayes, J.D., Hardingham, G.E., 2015. Neuronal development is promoted by weakened intrinsic antioxidant defences due to epigenetic repression of Nrf2. Nat. Commun. 6, 7066. doi:10.1038/ncomms8066

Bell, R.D., Sagare, A.P., Friedman, A.E., Bedi, G.S., Holtzman, D.M., Deane, R., Zlokovic, B. V, 2006. Transport pathways for clearance of human Alzheimer's amyloid β-peptide and apolipoproteins E and J in the mouse central nervous system. J. Cereb. Blood Flow Metab. 27, 909–18. doi:10.1038/sj.jcbfm.9600419

Benamar, A., Rolletschek, H., Borisjuk, L., Avelange-Macherel, M.-H., Curien, G., Mostefai, H.A., Andriantsitohaina, R., Macherel, D., 2008. Nitrite–nitric oxide control of mitochondrial respiration at the frontier of anoxia. Biochim. Biophys. Acta - Bioenerg. Bioenerg. 1777, 1268–1275. doi:10.1016/j.bbabio.2008.06.002

Benilova, I., Karran, E., De Strooper, B., 2012. The toxic Aβ oligomer and Alzheimer's disease: an emperor in need of clothes. Nat. Neurosci. 15, 349–357. doi:10.1038/nn.3028

Berger, Z., Roder, H., Hanna, A., Carlson, A., Rangachari, V., Yue, M., Wszolek, Z., Ashe, K., Knight, J., Dickson, D., Andorfer, C., Rosenberry, T.L., Lewis, J., Hutton, M., Janus, C., 2007. Accumulation of Pathological Tau Species and Memory Loss in a Conditional Model of Tauopathy. J. Neurosci. 27, 3650–3662. doi:10.1523/JNEUROSCI.0587-07.2007

Bergström, P., Agholme, L., Nazir, F.H., Satir, T.M., Toombs, J., Wellington, H., Strandberg, J., Bontell, T.O., Kvartsberg, H., Holmström, M., Boreström, C., Simonsson, S., Kunath, T., Lindahl, A., Blennow, K., Hanse, E., Portelius, E., Wray, S., Zetterberg, H., 2016. Amyloid precursor protein expression and processing are differentially regulated during cortical neuron differentiation. Sci. Rep. 6, 29200. doi:10.1038/srep29200

Bernstein, S.L., Dupuis, N.F., Lazo, N.D., Wyttenbach, T., Condron, M.M., Bitan, G., Teplow, D.B., Shea, J.-E., Ruotolo, B.T., Robinson, C. V., Bowers, M.T., 2009. Amyloid-β protein oligomerization and the importance of tetramers and dodecamers

in the aetiology of Alzheimer's disease. Nat. Chem. 1, 326–331. doi:10.1038/nchem.247

Berti, V., Walters, M., Sterling, J., Quinn, C.G., Logue, M., Andrews, R., Matthews, D.C., Osorio, R.S., Pupi, A., Vallabhajosula, S., Isaacson, R.S., de Leon, M.J., Mosconi, L., 2018. Mediterranean diet and 3-year Alzheimer brain biomarker changes in middle-aged adults. Neurology 90, e1789–e1798. doi:10.1212/WNL.0000000000005527

Beutler, B., Jiang, Z., Georgel, P., Crozat, K., Croker, B., Rutschmann, S., Du, X., Hoebe, K., 2006. Genetic Analysis Of Host Resistance: Toll-Like Receptor Signaling and Immunity at Large. Annu. Rev. Immunol. 24, 353–389. doi:10.1146/annurev.immunol.24.021605.090552

Bierhaus, A., Schiekofer, S., Schwaninger, M., Andrassy, M., Humpert, P.M., Chen, J., Hong, M., Luther, T., Henle, T., Klöting, I., Morcos, M., Hofmann, M., Tritschler, H., Weigle, B., Kasper, M., Smith, M., Perry, G., Schmidt, A.M., Stern, D.M., Häring, H.U., Schleicher, E., Nawroth, P.P., 2001. Diabetes-associated sustained activation of the transcription factor nuclear factor-kappaB. Diabetes 50, 2792–808.

Bisicchia, E., Sasso, V., Catanzaro, G., Leuti, A., Besharat, Z.M., Chiacchiarini, M., Molinari, M., Ferretti, E., Viscomi, M.T., Chiurchiù, V., 2018. Resolvin D1 Halts Remote Neuroinflammation and Improves Functional Recovery after Focal Brain Damage Via ALX/FPR2 Receptor-Regulated MicroRNAs. Mol. Neurobiol. 55, 6894–6905. doi:10.1007/s12035-018-0889-z

Biundo, F., Del Prete, D., Zhang, H., Arancio, O., D'Adamio, L., 2018. A role for tau in learning, memory and synaptic plasticity. Sci. Rep. 8, 3184. doi:10.1038/s41598-018-21596-3

Blasi, E., Barluzzi, R., Bocchini, V., Mazzolla, R., Bistoni, F., 1990. Immortalization of murine microglial cells by a v-raf/v-myc carrying retrovirus. J. Neuroimmunol. 27, 229–37.

Blessed, G., Tomlinson, B., Roth, M., 1968. The association between quantitative measures of dementia and of senile change in the cerebral grey matter of elderly subjects. Br. J. Psychiatry 114, 797–811. doi:10.1007/s13398-014-0173-7.2

Bliss, T. V, Lomo, T., 1973. Long-lasting potentiation of synaptic transmission in the dentate area of the anaesthetized rabbit following stimulation of the perforant path. J. Physiol. 232, 331–56.

Boche, D., Perry, V.H., Nicoll, J.A.R., 2013. Review: Activation patterns of microglia and their identification in the human brain. Neuropathol. Appl. Neurobiol. 39, 3–18. doi:10.1111/nan.12011

Boncler, M., Różalski, M., Krajewska, U., Podsędek, A., Watala, C., 2014. Comparison of PrestoBlue and MTT assays of cellular viability in the assessment of anti-proliferative effects of plant extracts on human endothelial cells. J. Pharmacol. Toxicol. Methods 69, 9–16. doi:10.1016/j.vascn.2013.09.003

Bordt, E.A., Polster, B.M., 2014. NADPH oxidase- and mitochondria-derived reactive oxygen species in proinflammatory microglial activation: a bipartisan affair? Free Radic. Biol. Med. 76, 34–46. doi:10.1016/j.freeradbiomed.2014.07.033

Borger, E., Aitken, L., Du, H., Zhang, W., Gunn-Moore, F.J., Yan, S.S. Du, 2013. Is amyloid binding alcohol dehydrogenase a drug target for treating Alzheimer's disease? Curr. Alzheimer Res. 10, 21–9.

Boumezbeur, F., Petersen, K.F., Cline, G.W., Mason, G.F., Behar, K.L., Shulman, G.I., Rothman, D.L., 2010. The contribution of blood lactate to brain energy metabolism in humans measured by dynamic 13C nuclear magnetic resonance spectroscopy. J. Neurosci. 30, 13983–91. doi:10.1523/JNEUROSCI.2040-10.2010

Bours, M.J.L., Swennen, E.L.R., Di Virgilio, F., Cronstein, B.N., Dagnelie, P.C., 2006. Adenosine 5′-triphosphate and adenosine as endogenous signaling molecules in immunity and inflammation. Pharmacol. Ther. 112, 358–404. doi:10.1016/j.pharmthera.2005.04.013

Bouvier, D.S., Murai, K.K., 2015. Synergistic actions of microglia and astrocytes in the progression of Alzheimer's disease. J. Alzheimers. Dis. 45, 1001–14. doi:10.3233/JAD-143156

Bouzier-Sore, A.-K., Voisin, P., Bouchaud, V., Bezancon, E., Franconi, J.-M., Pellerin, L., 2006. Competition between glucose and lactate as oxidative energy substrates in both neurons and astrocytes: a comparative NMR study. Eur. J. Neurosci. 24, 1687–94. doi:10.1111/j.1460-9568.2006.05056.x

Bozic, I., Savic, D., Stevanovic, I., Pekovic, S., Nedeljkovic, N., Lavrnja, I., 2015. Benfotiamine upregulates antioxidative system in activated BV-2 microglia cells. Front. Cell. Neurosci. 9, 351. doi:10.3389/fncel.2015.00351

Braak, H., Braak, E., 1991. Neuropathological stageing of Alzheimer-related changes. Acta Neuropathol. 82, 239–59.

Bradshaw, E.M., Chibnik, L.B., Keenan, B.T., Ottoboni, L., Raj, T., Tang, A., Rosenkrantz, L.L., Imboywa, S., Lee, M., Von Korff, A., Morris, M.C., Evans, D.A., Johnson, K., Sperling, R.A., Schneider, J.A., Bennett, D.A., De Jager, P.L., De Jager, P.L., 2013. CD33 Alzheimer's disease locus: altered monocyte function and amyloid biology. Nat. Neurosci. 16, 848–850. doi:10.1038/nn.3435

Braun, M.C., Wang, J.M., Lahey, E., Rabin, R.L., Kelsall, B.L., 2001. Activation of the formyl peptide receptor by the HIV-derived peptide T-20 suppresses interleukin-12 p70 production by human monocytes. Blood 97, 3531–6.

Brennan, A.M., Suh, S.W., Won, S.J., Narasimhan, P., Kauppinen, T.M., Lee, H., Edling, Y., Chan, P.H., Swanson, R.A., 2009. NADPH oxidase is the primary source of superoxide induced by NMDA receptor activation. Nat. Neurosci. 12, 857–63. doi:10.1038/nn.2334

Brier, M.R., Hassenstab, J., Cairns, N.J., Holtzman, D.M., Fagan, A.M., Morris, J.C., Ances, B.M., Gordon, B., Friedrichsen, K., Christensen, J., Owen, C., Aldea, P., Su, Y., Benzinger, T.L.S., McCarthy, J., Stern, A., 2016. Tau and Aβ imaging, CSF measures, and cognition in Alzheimer's disease. Sci. Transl. Med. 8. doi:10.1126/scitranslmed.aaf2362

Broersen, K., Jonckheere, W., Rozenski, J., Vandersteen, A., Pauwels, K., Pastore, A., Rousseau, F., Schymkowitz, J., 2011. A standardized and biocompatible preparation of aggregate-free amyloid beta peptide for biophysical and biological studies of Alzheimer's disease. Protein Eng. Des. Sel. 24, 743–50. doi:10.1093/protein/gzr020

Brogden, R.N., 1986. Pyrazolone derivatives. Drugs 32 Suppl 4, 60–70. doi:10.2165/00003495-198600324-00006

Brooks, S.W., Dykes, A.C., Schreurs, B.G., 2017. A High-Cholesterol Diet Increases 27-Hydroxycholesterol and Modifies Estrogen Receptor Expression and Neurodegeneration in Rabbit Hippocampus. J. Alzheimer's Dis. 56, 185–196. doi:10.3233/JAD-160725

Brosseron, F., Krauthausen, M., Kummer, M., Heneka, M.T., 2014. Body Fluid Cytokine Levels in Mild Cognitive Impairment and Alzheimer's Disease: a Comparative Overview. Mol. Neurobiol. 50, 534–544. doi:10.1007/s12035-014-8657-1

Brown, G., Borutaite, V., 2007. Nitric oxide and mitochondrial respiration in the heart. Cardiovasc. Res. 75, 283–290. doi:10.1016/j.cardiores.2007.03.022

Bruttger, J., Karram, K., Wörtge, S., Regen, T., Marini, F., Hoppmann, N., Klein, M., Blank, T., Yona, S., Wolf, Y., Mack, M., Pinteaux, E., Müller, W., Zipp, F., Binder, H., Bopp, T., Prinz, M., Jung, S., Waisman, A., 2015. Genetic Cell Ablation Reveals Clusters of Local Self-Renewing Microglia in the Mammalian Central Nervous System. Immunity 43, 92–106. doi:10.1016/j.immuni.2015.06.012

Bryan, N.S., Grisham, M.B., 2007. Methods to detect nitric oxide and its metabolites in biological samples. Free Radic. Biol. Med. 43, 645–57. doi:10.1016/j.freeradbiomed.2007.04.026

Buckley, C.D., Gilroy, D.W., Serhan, C.N., Stockinger, B., Tak, P.P., 2013. The resolution

of inflammation. Nat. Rev. Immunol. 13, 59–66. doi:10.1038/nri3362

Bulua, A.C., Simon, A., Maddipati, R., Pelletier, M., Park, H., Kim, K.-Y., Sack, M.N., Kastner, D.L., Siegel, R.M., 2011. Mitochondrial reactive oxygen species promote production of proinflammatory cytokines and are elevated in TNFR1-associated periodic syndrome (TRAPS). J. Exp. Med. 208, 519–533. doi:10.1084/jem.20102049

Bürli, R.W., Xu, H., Zou, X., Muller, K., Golden, J., Frohn, M., Adlam, M., Plant, M.H., Wong, M., McElvain, M., Regal, K., Viswanadhan, V.N., Tagari, P., Hungate, R., 2006. Potent hFPRL1 (ALXR) agonists as potential anti-inflammatory agents. Bioorg. Med. Chem. Lett. 16, 3713–8. doi:10.1016/j.bmcl.2006.04.068

Busche, M.A., Grienberger, C., Keskin, A.D., Song, B., Neumann, U., Staufenbiel, M., Förstl, H., Konnerth, A., 2015. Decreased amyloid-β and increased neuronal hyperactivity by immunotherapy in Alzheimer's models. Nat. Neurosci. 18, 1725–1727. doi:10.1038/nn.4163

Busciglio, J., Lorenzo, A., Yeh, J., Yankner, B.A., 1995. β-Amyloid fibrils induce tau phosphorylation and loss of microtubule binding. Neuron 14, 879–888. doi:10.1016/0896-6273(95)90232-5

Bush, A.I., Tanzi, R.E., 2008. Therapeutics for Alzheimer's disease based on the metal hypothesis. Neurotherapeutics 5, 421–32. doi:10.1016/j.nurt.2008.05.001

Butterfield, D.A., Swomley, A.M., Sultana, R., 2013. Amyloid β-peptide (1-42)-induced oxidative stress in Alzheimer disease: importance in disease pathogenesis and progression. Antioxid. Redox Signal. 19, 823–35. doi:10.1089/ars.2012.5027

Byrne, K.M., Monsefi, N., Dawson, J.C., Degasperi, A., Bukowski-Wills, J.-C., Volinsky, N., Dobrzyński, M., Birtwistle, M.R., Tsyganov, M.A., Kiyatkin, A., Kida, K., Finch, A.J., Carragher, N.O., Kolch, W., Nguyen, L.K., von Kriegsheim, A., Kholodenko, B.N., 2016. Bistability in the Rac1, PAK, and RhoA Signaling Network Drives Actin Cytoskeleton Dynamics and Cell Motility Switches. Cell Syst. 2, 38–48. doi:10.1016/j.cels.2016.01.003

Cagnin, A., Brooks, D.J., Kennedy, A.M., Gunn, R.N., Myers, R., Turkheimer, F.E., Jones, T., Banati, R.B., 2001. In-vivo measurement of activated microglia in dementia. Lancet 358, 461–467. doi:10.1016/S0140-6736(01)05625-2

Cahill, L., 2006. Why sex matters for neuroscience. Nat. Rev. Neurosci. 7, 477–484. doi:10.1038/nrn1909

Cai, Q., Li, Y., Pei, G., 2017. Polysaccharides from Ganoderma lucidum attenuate microglia-mediated neuroinflammation and modulate microglial phagocytosis and behavioural response. J. Neuroinflammation 14, 63. doi:10.1186/s12974-017-0839-0

Cai, Z., Liu, N., Wang, C., Qin, B., Zhou, Y., Xiao, M., Chang, L., Yan, L.-J., Zhao, B., 2016. Role of RAGE in Alzheimer's Disease. Cell. Mol. Neurobiol. 36, 483–495. doi:10.1007/s10571-015-0233-3

Caldeira, C., Cunha, C., Vaz, A.R., Falcão, A.S., Barateiro, A., Seixas, E., Fernandes, A., Brites, D., 2017. Key Aging-Associated Alterations in Primary Microglia Response to Beta-Amyloid Stimulation. Front. Aging Neurosci. 9, 277. doi:10.3389/fnagi.2017.00277

Calderón-Garcidueñas, L., Reynoso-Robles, R., Vargas- Martínez, J., Gómez-Maqueo-Chew, A., Pérez-Guillé, B., Mukherjee, P.S., Torres-Jardón, R., Perry, G., Gónzalez-Maciel, A., 2016. Prefrontal white matter pathology in air pollution exposed Mexico City young urbanites and their potential impact on neurovascular unit dysfunction and the development of Alzheimer's disease. Environ. Res. 146, 404–417. doi:10.1016/j.envres.2015.12.031

Castellano, J.M., Kim, J., Stewart, F.R., Jiang, H., DeMattos, R.B., Patterson, B.W., Fagan, A.M., Morris, J.C., Mawuenyega, K.G., Cruchaga, C., Goate, A.M., Bales, K.R., Paul, S.M., Bateman, R.J., Holtzman, D.M., 2011. Human apoE isoforms differentially regulate brain amyloid-β peptide clearance. Sci. Transl. Med. 3, 89ra57. doi:10.1126/scitranslmed.3002156

Castelli, V., Benedetti, E., Antonosante, A., Catanesi, M., Pitari, G., Ippoliti, R., Cimini, A., d'Angelo, M., 2019. Neuronal Cells Rearrangement During Aging and Neurodegenerative Disease: Metabolism, Oxidative Stress and Organelles Dynamic. Front. Mol. Neurosci. 12, 132. doi:10.3389/fnmol.2019.00132

Cerajewska, T.L., Davies, M., West, N.X., 2015. Periodontitis: a potential risk factor for Alzheimer's disease. BDJ 218, 29–34. doi:10.1038/sj.bdj.2014.1137

Cermakova, P., Eriksdotter, M., Lund, L.H., Winblad, B., Religa, P., Religa, D., 2015. Heart failure and Alzheimer's disease. J. Intern. Med. 277, 406–425. doi:10.1111/joim.12287

Chachlaki, K., Garthwaite, J., Prevot, V., 2017. The gentle art of saying NO: how nitric oxide gets things done in the hypothalamus. Nat. Rev. Endocrinol. 13, 521–535. doi:10.1038/nrendo.2017.69

Chamniansawat, S., Chongthammakun, S., 2009. Estrogen stimulates activity-regulated cytoskeleton associated protein (Arc) expression via the MAPK- and PI-3K-dependent pathways in SH-SY5Y cells. Neurosci. Lett. 452, 130–135. doi:10.1016/j.neulet.2009.01.010

Chamorro, Á., Dirnagl, U., Urra, X., Planas, A.M., 2016. Neuroprotection in acute stroke: targeting excitotoxicity, oxidative and nitrosative stress, and inflammation. Lancet Neurol. 15, 869–881. doi:10.1016/S1474-4422(16)00114-9

Chan, G., White, C.C., Winn, P.A., Cimpean, M., Replogle, J.M., Glick, L.R., Cuerdon, N.E., Ryan, K.J., Johnson, K.A., Schneider, J.A., Bennett, D.A., Chibnik, L.B., Sperling, R.A., Bradshaw, E.M., De Jager, P.L., 2015. CD33 modulates TREM2: convergence of Alzheimer loci. Nat. Neurosci. 18, 1556–1558. doi:10.1038/nn.4126

Chang, C.-F., Goods, B.A., Askenase, M.H., Hammond, M.D., Renfroe, S.C., Steinschneider, A.F., Landreneau, M.J., Ai, Y., Beatty, H.E., da Costa, L.H.A., Mack, M., Sheth, K.N., Greer, D.M., Huttner, A., Coman, D., Hyder, F., Ghosh, S., Rothlin, C. V, Love, J.C., Sansing, L.H., 2018. Erythrocyte efferocytosis modulates macrophages towards recovery after intracerebral hemorrhage. J. Clin. Invest. 128, 607–624. doi:10.1172/JCI95612

Chang, C.-F., Wan, J., Li, Q., Renfroe, S.C., Heller, N.M., Wang, J., 2017. Alternative activation-skewed microglia/macrophages promote hematoma resolution in experimental intracerebral hemorrhage. Neurobiol. Dis. 103, 54–69. doi:10.1016/j.nbd.2017.03.016

Chasseigneaux, S., Allinquant, B., 2012. Functions of Aβ, sAPPα and sAPPβ: Similarities and differences. J. Neurochem. 120, 99–108. doi:10.1111/j.1471-4159.2011.07584.x

Chen, C.T., Green, J.T., Orr, S.K., Bazinet, R.P., 2008. Regulation of brain polyunsaturated fatty acid uptake and turnover. Prostaglandins. Leukot. Essent. Fatty Acids 79, 85–91. doi:10.1016/j.plefa.2008.09.003

Chen, K., Iribarren, P., Huang, J., Zhang, L., Gong, W., Cho, E.H., Lockett, S., Dunlop, N.M., Wang, J.M., 2007. Induction of the Formyl Peptide Receptor 2 in Microglia by IFN- and Synergy with CD40 Ligand. J. Immunol. 178, 1759–1766. doi:10.4049/jimmunol.178.3.1759

Chen, L., Na, R., Boldt, E., Ran, Q., 2015. NLRP3 inflammasome activation by mitochondrial reactive oxygen species plays a key role in long-term cognitive impairment induced by paraquat exposure. Neurobiol. Aging 36, 2533–2543. doi:10.1016/j.neurobiolaging.2015.05.018

Chen, T.-J., Chen, S.-S., Wang, D.-C., Hung, H.-S., 2016. The Cholinergic Signaling Responsible for the Expression of a Memory-Related Protein in Primary Rat Cortical Neurons. J. Cell. Physiol. 2428–2438. doi:10.1002/jcp.25347

Cheng, Y., Bai, F., 2018. The Association of Tau With Mitochondrial Dysfunction in Alzheimer's Disease. Front. Neurosci. 12, 163. doi:10.3389/fnins.2018.00163

Cherry, J.D., Olschowka, J.A., O'Banion, M., 2014. Neuroinflammation and M2 microglia: the good, the bad, and the inflamed. J. Neuroinflammation 11, 98. doi:10.1186/1742-

2094-11-98

Chiasseu, M., Alarcon-Martinez, L., Belforte, N., Quintero, H., Dotigny, F., Destroismaisons, L., Velde, C. Vande, Panayi, F., Louis, C., Polo, A. Di, 2017. Tau accumulation in the retina promotes early neuronal dysfunction and precedes brain pathology in a mouse model of Alzheimer's disease. Mol. Neurodegener. 12. doi:10.1186/s13024-017-0199-3

Chiurchiù, V., Orlacchio, A., Maccarrone, M., 2016. Is Modulation of Oxidative Stress an Answer? The State of the Art of Redox Therapeutic Actions in Neurodegenerative Diseases. Oxid. Med. Cell. Longev. 2016, 7909380. doi:10.1155/2016/7909380

Choi, H.B., Gordon, G.R.J., Zhou, N., Tai, C., Rungta, R.L., Martinez, J., Milner, T.A., Ryu, J.K., McLarnon, J.G., Tresguerres, M., Levin, L.R., Buck, J., MacVicar, B.A., 2012. Metabolic Communication between Astrocytes and Neurons via Bicarbonate-Responsive Soluble Adenylyl Cyclase. Neuron 75, 1094–1104. doi:10.1016/j.neuron.2012.08.032

Choi, I.-Y., Lim, J.-H., Kim, C., Song, H.Y., Ju, C., Kim, W.-K., 2013. 4-hydroxy-2(E)-Nonenal facilitates NMDA-Induced Neurotoxicity via Triggering Mitochondrial Permeability Transition Pore Opening and Mitochondrial Calcium Overload. Exp. Neurobiol. 22, 200–7. doi:10.5607/en.2013.22.3.200

Choi, S.-H., Aid, S., Kim, H.-W., Jackson, S.H., Bosetti, F., 2012. Inhibition of NADPH oxidase promotes alternative and anti-inflammatory microglial activation during neuroinflammation. J. Neurochem. 120, 292–301. doi:10.1111/j.1471-4159.2011.07572.x

Chondrogianni, N., Petropoulos, I., Grimm, S., Georgila, K., Catalgol, B., Friguet, B., Grune, T., Gonos, E.S., 2014. Protein damage, repair and proteolysis. Mol. Aspects Med. 35, 1–71. doi:10.1016/j.mam.2012.09.001

Christensen, A., Pike, C.J., 2015. Menopause, obesity and inflammation: interactive risk factors for Alzheimer's disease. Front. Aging Neurosci. 7, 130. doi:10.3389/fnagi.2015.00130

Clark, I.A., Vissel, B., 2015. Amyloid β: one of three danger-associated molecules that are secondary inducers of the proinflammatory cytokines that mediate Alzheimer's disease. Br. J. Pharmacol. 172, 3714–27. doi:10.1111/bph.13181

Cobley, J.N., Fiorello, M.L., Bailey, D.M., 2018. 13 reasons why the brain is susceptible to oxidative stress. Redox Biol. 15, 490–503. doi:10.1016/j.redox.2018.01.008

Colombo, A., Wang, H., Kuhn, P.-H., Page, R., Kremmer, E., Dempsey, P.J., Crawford, H.C., Lichtenthaler, S.F., 2013. Constitutive α- and β-secretase cleavages of the amyloid precursor protein are partially coupled in neurons, but not in frequently used cell lines. Neurobiol. Dis. 49, 137–147. doi:10.1016/j.nbd.2012.08.011

Colombo, E., Farina, C., 2016. Astrocytes: Key Regulators of Neuroinflammation. Trends Immunol. 37, 608–620. doi:10.1016/j.it.2016.06.006

Compan, V., Pierredon, S., Vanderperre, B., Krznar, P., Marchiq, I., Zamboni, N., Pouyssegur, J., Martinou, J.-C., 2015. Monitoring Mitochondrial Pyruvate Carrier Activity in Real Time Using a BRET-Based Biosensor: Investigation of the Warburg Effect. Mol. Cell 59, 491–501. doi:10.1016/j.molcel.2015.06.035

Cooray, Sadani N., Gobbetti, T., Montero-Melendez, T., McArthur, S., Thompson, D., Clark, A.J.L., Flower, R.J., Perretti, M., 2013. Ligand-specific conformational change of the G-protein-coupled receptor ALX/FPR2 determines proresolving functional responses. Proc. Natl. Acad. Sci. U. S. A. 110, 18232–18237. doi:10.1073/pnas.1308253110

Cooray, Sadani N, Gobbetti, T., Montero-Melendez, T., McArthur, S., Thompson, D., Clark, A.J.L., Flower, R.J., Perretti, M., 2013. Ligand-specific conformational change of the G-protein-coupled receptor ALX/FPR2 determines proresolving functional responses. Proc. Natl. Acad. Sci. U. S. A. 110, 18232–7. doi:10.1073/pnas.1308253110

Corminboeuf, O., Leroy, X., 2015. FPR2/ALXR Agonists and the Resolution of Inflammation. J. Med. Chem. 58, 537–559. doi:10.1021/jm501051x

Crawford, F.C., Wood, M., Ferguson, S., Mathura, V.S., Faza, B., Wilson, S., Fan, T., O'Steen, B., Ait-Ghezala, G., Hayes, R., Mullan, M.J., 2007. Genomic analysis of response to traumatic brain injury in a mouse model of Alzheimer's disease (APPsw). Brain Res. 1185, 45–58. doi:10.1016/J.BRAINRES.2007.09.042

Crescenzi, O., Tomaselli, S., Guerrini, R., Salvadori, S., D'Ursi, A.M., Temussi, P.A., Picone, D., 2002. Solution structure of the Alzheimer amyloid beta-peptide (1-42) in an apolar microenvironment. Similarity with a virus fusion domain. Eur. J. Biochem. 269, 5642–8.

Cristante, E., McArthur, S., Mauro, C., Maggioli, E., Romero, I.A., Wylezinska-Arridge, M., Couraud, P.O., Lopez-Tremoleda, J., Christian, H.C., Weksler, B.B., Malaspina, A., Solito, E., 2013. Identification of an essential endogenous regulator of blood-brain barrier integrity, and its pathological and therapeutic implications. Proc. Natl. Acad. Sci. 110, 832–841. doi:10.1073/pnas.1209362110

Crotti, A., Glass, C.K., 2015. The choreography of neuroinflammation in Huntington's disease. Trends Immunol. 36, 364–373. doi:10.1016/j.it.2015.04.007

Croxson, P.L., Browning, P.G.F., Gaffan, D., Baxter, M.G., 2012. Acetylcholine Facilitates Recovery of Episodic Memory after Brain Damage. J. Neurosci. 32, 13787–13795. doi:10.1523/JNEUROSCI.2947-12.2012

Cui, Y.H., Le, Y., Gong, W., Proost, P., Van Damme, J., Murphy, W.J., Wang, J.M., 2002a. Bacterial lipopolysaccharide selectively up-regulates the function of the chemotactic peptide receptor formyl peptide receptor 2 in murine microglial cells. J. Immunol. 168, 434–42. doi:10.4049/jimmunol.168.1.434

Cui, Y.H., Le, Y., Zhang, X., Gong, W., Abe, K., Sun, R., Van Damme, J., Proost, P., Wang, J.M., 2002b. Up-regulation of FPR2, a chemotactic receptor for amyloid beta 1-42 (A beta 42), in murine microglial cells by TNF alpha. Neurobiol. Dis. 10, 366–77.

Cummings, B.J., Pike, C.J., Shankle, R., Cotman, C.W., 1996. Beta-amyloid deposition and other measures of neuropathology predict cognitive status in Alzheimer's disease. Neurobiol. Aging 17, 921–33.

d'Avila, J.C., Siqueira, L.D., Mazeraud, A., Azevedo, E.P., Foguel, D., Castro-Faria-Neto, H.C., Sharshar, T., Chrétien, F., Bozza, F.A., 2018. Age-related cognitive impairment is associated with long-term neuroinflammation and oxidative stress in a mouse model of episodic systemic inflammation. J. Neuroinflammation 15, 28. doi:10.1186/s12974-018-1059-y

Dalli, J., Montero-Melendez, T., McArthur, S., Perretti, M., 2012. Annexin A1 N-Terminal Derived Peptide Ac2-26 Exerts Chemokinetic Effects on Human Neutrophils. Front. Pharmacol. 3, 28. doi:10.3389/fphar.2012.00028

Danaei, G., Finucane, M.M., Lu, Y., Singh, G.M., Cowan, M.J., Paciorek, C.J., Lin, J.K., Farzadfar, F., Khang, Y.-H., Stevens, G.A., Rao, M., Ali, M.K., Riley, L.M., Robinson, C.A., Ezzati, M., Global Burden of Metabolic Risk Factors of Chronic Diseases Collaborating Group (Blood Glucose), 2011. National, regional, and global trends in fasting plasma glucose and diabetes prevalence since 1980: systematic analysis of health examination surveys and epidemiological studies with 370 country-years and 2·7 million participants. Lancet 378, 31–40. doi:10.1016/S0140-6736(11)60679-X

DaRocha-Souto, B., Scotton, T.C., Coma, M., Serrano-Pozo, A., Hashimoto, T., Serenó, L., Rodríguez, M., Sánchez, B., Hyman, B.T., Gómez-Isla, T., 2011. Brain oligomeric β-amyloid but not total amyloid plaque burden correlates with neuronal loss and astrocyte inflammatory response in amyloid precursor protein/tau transgenic mice. J. Neuropathol. Exp. Neurol. 70, 360–376. doi:10.1097/NEN.0b013e318217a118

Das, A., Kim, S.H., Arifuzzaman, S., Yoon, T., Chai, J.C., Lee, Y.S., Park, K.S., Jung, K.H., Chai, Y.G., 2016. Transcriptome sequencing reveals that LPS-triggered transcriptional responses in established microglia BV2 cell lines are poorly representative of primary microglia. J. Neuroinflammation 13, 182.

doi:10.1186/s12974-016-0644-1

Das, U., Wang, L., Ganguly, A., Saikia, J.M., Wagner, S.L., Koo, E.H., Roy, S., 2016. Visualizing APP and BACE-1 approximation in neurons yields insight into the amyloidogenic pathway. Nat. Neurosci. 19, 55–64. doi:10.1038/nn.4188

Davis, B.M., Salinas-Navarro, M., Cordeiro, M.F., Moons, L., De Groef, L., 2017. Characterizing microglia activation: a spatial statistics approach to maximize information extraction. Sci. Rep. 7, 1576. doi:10.1038/s41598-017-01747-8

De Felice, F.G., Ferreira, S.T., 2014. Inflammation, Defective Insulin Signaling, and Mitochondrial Dysfunction as Common Molecular Denominators Connecting Type 2 Diabetes to Alzheimer Disease. Diabetes 63, 2262–2272. doi:10.2337/db13-1954

De Haas, A.H., Boddeke, H.W.G.M., Brouwer, N., Biber, K., 2007. Optimized isolation enables ex vivo analysis of microglia from various central nervous system regions. Glia 55, 1374–1384. doi:10.1002/glia.20554

de Oliveira-Marques, V., Cyrne, L., Marinho, H.S., Antunes, F., 2007. A Quantitative Study of NF-κB Activation by H2 O2: Relevance in Inflammation and Synergy with TNF-α. J. Immunol. 178, 3893–3902. doi:10.4049/jimmunol.178.6.3893

de Oliveira, J.R., da Silva, P.R., Rogério, A. de P., 2017. AT-RvD1 modulates the activation of bronchial epithelial cells induced by lipopolysaccharide and Dermatophagoides pteronyssinus. Eur. J. Pharmacol. doi:10.1016/j.ejphar.2017.03.029

de Rivero Vaccari, J.P., Dietrich, W.D., Keane, R.W., 2014. Activation and regulation of cellular inflammasomes: gaps in our knowledge for central nervous system injury. J. Cereb. Blood Flow Metab. 34, 369–75. doi:10.1038/jcbfm.2013.227

De Strooper, B., Iwatsubo, T., Wolfe, M.S., 2012. Presenilins and γ-secretase: structure, function, and role in Alzheimer Disease. Cold Spring Harb. Perspect. Med. 2, a006304. doi:10.1101/cshperspect.a006304

Della Bianca, V., Dusi, S., Bianchini, E., Dal Prà, I., Rossi, F., 1999. β-amyloid activates the O2·- forming NADPH oxidase in microglia, monocytes, and neutrophils. A possible inflammatory mechanism of neuronal damage in Alzheimer's disease. J. Biol. Chem. 274, 15493–15499. doi:10.1074/jbc.274.22.15493

Dello Russo, C., Cappoli, N., Coletta, I., Mezzogori, D., Paciello, F., Pozzoli, G., Navarra, P., Battaglia, A., 2018. The human microglial HMC3 cell line: where do we stand? A systematic literature review. J. Neuroinflammation 15, 259. doi:10.1186/s12974-018-1288-0

Di Bona, D., Rizzo, C., Bonaventura, G., Candore, G., Caruso, C., 2012. Association Between Interleukin-10 Polymorphisms and Alzheimer's Disease: A Systematic Review and Meta-Analysis. J. Alzheimer's Dis. 29, 751–759. doi:10.3233/JAD-2012-111838

Di Domenico, F., Pupo, G., Giraldo, E., Badìa, M.-C., Monllor, P., Lloret, A., Eugenia Schininà, M., Giorgi, A., Cini, C., Tramutola, A., Butterfield, D.A., Viña, J., Perluigi, M., 2016. Oxidative signature of cerebrospinal fluid from mild cognitive impairment and Alzheimer disease patients. Free Radic. Biol. Med. 91, 1–9. doi:10.1016/j.freeradbiomed.2015.12.004

Di, J., Cohen, L.S., Corbo, C.P., Phillips, G.R., El Idrissi, A., Alonso, A.D., 2016. Abnormal tau induces cognitive impairment through two different mechanisms: synaptic dysfunction and neuronal loss. Sci. Rep. 6, 20833. doi:10.1038/srep20833

Di Scala, C., Chahinian, H., Yahi, N., Garmy, N., Fantini, J., 2014. Interaction of Alzheimer's β-Amyloid Peptides with Cholesterol: Mechanistic Insights into Amyloid Pore Formation. Biochemistry 53, 4489–4502. doi:10.1021/bi500373k

Dietl, K., Renner, K., Dettmer, K., Timischl, B., Eberhart, K., Dorn, C., Hellerbrand, C., Kastenberger, M., Kunz-Schughart, L.A., Oefner, P.J., Andreesen, R., Gottfried, E., Kreutz, M.P., 2010. Lactic Acid and Acidification Inhibit TNF Secretion and Glycolysis of Human Monocytes. J. Immunol. 184, 1200–1209. doi:10.4049/jimmunol.0902584

Ding, Y., Flores, J., Klebe, D., Li, P., McBride, D.W., Tang, J., Zhang, J.H., 2019. Annexin A1 attenuates neuroinflammation through FPR2/p38/COX-2 pathway after intracerebral hemorrhage in male mice. J. Neurosci. Res. jnr.24478. doi:10.1002/jnr.24478

Dohi, K., Ohtaki, H., Nakamachi, T., Yofu, S., Satoh, K., Miyamoto, K., Song, D., Tsunawaki, S., Shioda, S., Aruga, T., 2010. Gp91phox (NOX2) in classically activated microglia exacerbates traumatic brain injury. J. Neuroinflammation 7, 41. doi:10.1186/1742-2094-7-41

Domingues, C., da Cruz E Silva, O.A.B., Henriques, A.G., 2017. Impact of Cytokines and Chemokines on Alzheimer's Disease Neuropathological Hallmarks. Curr. Alzheimer Res. 14, 870–882. doi:10.2174/1567205014666170317113606

Donath, M.Y., Shoelson, S.E., 2011. Type 2 diabetes as an inflammatory disease. Nat. Rev. Immunol. 11, 98–107. doi:10.1038/nri2925

Dornas, W.C., Cardoso, L.M., Silva, M., Machado, N.L.S., Chianca, D.A., Alzamora, A.C., Lima, W.G., Lagente, V., Silva, M.E., 2017. Oxidative stress causes hypertension and activation of nuclear factor-κB after high-fructose and salt treatments. Sci. Rep. 7, 46051. doi:10.1038/srep46051

Dorostkar, M.M., Burgold, S., Filser, S., Barghorn, S., Schmidt, B., Anumala, U.R., Hillen, H., Klein, C., Herms, J., 2014. Immunotherapy alleviates amyloid-associated synaptic pathology in an Alzheimer's disease mouse model. Brain 137, 3319–3326. doi:10.1093/brain/awu280

Dorward, D.A., Lucas, C.D., Chapman, G.B., Haslett, C., Dhaliwal, K., Rossi, A.G., 2015. The Role of Formylated Peptides and Formyl Peptide Receptor 1 in Governing Neutrophil Function during Acute Inflammation. Am. J. Pathol. 185, 1172–1184. doi:10.1016/j.ajpath.2015.01.020

Dorward, D.A., Lucas, C.D., Doherty, M.K., Chapman, G.B., Scholefield, E.J., Conway Morris, A., Felton, J.M., Kipari, T., Humphries, D.C., Robb, C.T., Simpson, A.J., Whitfield, P.D., Haslett, C., Dhaliwal, K., Rossi, A.G., 2017. Novel role for endogenous mitochondrial formylated peptide-driven formyl peptide receptor 1 signalling in acute respiratory distress syndrome. Thorax 72, 928–936. doi:10.1136/thoraxjnl-2017-210030

Drachman, D.A., 2014. The amyloid hypothesis, time to move on: Amyloid is the downstream result, not cause, of Alzheimer's disease. Alzheimer's Dement. 10, 372–380. doi:10.1016/j.jalz.2013.11.003

Drechsler, M., de Jong, R., Rossaint, J., Viola, J.R., Leoni, G., Wang, J.M., Grommes, J., Hinkel, R., Kupatt, C., Weber, C., Döring, Y., Zarbock, A., Soehnlein, O., 2015. Annexin A1 counteracts chemokine-induced arterial myeloid cell recruitment. Circ. Res. 116, 827–35. doi:10.1161/CIRCRESAHA.116.305825

Dronse, J., Fliessbach, K., Bischof, G.N., von Reutern, B., Faber, J., Hammes, J., Kuhnert, G., Neumaier, B., Onur, O.A., Kukolja, J., van Eimeren, T., Jessen, F., Fink, G.R., Klockgether, T., Drzezga, A., 2016. In vivo Patterns of Tau Pathology, Amyloid-β Burden, and Neuronal Dysfunction in Clinical Variants of Alzheimer's Disease. J. Alzheimer's Dis. 55, 465–471. doi:10.3233/JAD-160316

Du, C., Wang, Y., Zhang, F., Yan, S., Guan, Y., Gong, X., Zhang, T., Cui, X., Wang, X., Zhang, C.X., 2017. Synaptotagmin-11 inhibits cytokine secretion and phagocytosis in microglia. Glia 65, 1656–1667. doi:10.1002/glia.23186

Du, H., Guo, L., Fang, F., Chen, D., A Sosunov, A., M McKhann, G., Yan, Y., Wang, C., Zhang, H., Molkentin, J.D., Gunn-Moore, F.J., Vonsattel, J.P., Arancio, O., Chen, J.X., Yan, S. Du, 2008. Cyclophilin D deficiency attenuates mitochondrial and neuronal perturbation and ameliorates learning and memory in Alzheimer's disease. Nat. Med. 14, 1097–1105. doi:10.1038/nm.1868

Du, H., Yan, S.S., 2010. Mitochondrial permeability transition pore in Alzheimer's disease: Cyclophilin D and amyloid beta. Biochim. Biophys. Acta - Mol. Basis Dis. 1802, 198–204. doi:10.1016/j.bbadis.2009.07.005

Dufton, N., Hannon, R., Brancaleone, V., Dalli, J., Patel, H.B., Gray, M., D'Acquisto, F., Buckingham, J.C., Perretti, M., Flower, R.J., 2010. Anti-inflammatory role of the murine formyl-peptide receptor 2: ligand-specific effects on leukocyte responses and experimental inflammation. J. Immunol. 184, 2611–9. doi:10.4049/jimmunol.0903526

Dunn, H.C., Ager, R.R., Baglietto-Vargas, D., Cheng, D., Kitazawa, M., Cribbs, D.H., Medeiros, R., 2015. Restoration of lipoxin A4 signaling reduces Alzheimer's disease-like pathology in the 3xTg-AD mouse model. J. Alzheimers. Dis. 43, 893–903. doi:10.3233/JAD-141335

Durazzo, T.C., Mattsson, N., Weiner, M.W., Alzheimer's Disease Neuroimaging Initiative, 2014. Smoking and increased Alzheimer's disease risk: a review of potential mechanisms. Alzheimers. Dement. 10, S122-45. doi:10.1016/j.jalz.2014.04.009

Dyall, S.D., Brown, M.T., Johnson, P.J., 2004. Ancient invasions: from endosymbionts to organelles. Science 304, 253–7. doi:10.1126/science.1094884

Dykiert, D., Der, G., Starr, J.M., Deary, I.J., 2012. Age Differences in Intra-Individual Variability in Simple and Choice Reaction Time: Systematic Review and Meta-Analysis. PLoS One 7, e45759. doi:10.1371/journal.pone.0045759

Eikelenboom, P., van Exel, E., Hoozemans, J.J.M., Veerhuis, R., Rozemuller, A.J.M., van Gool, W.A., 2010. Neuroinflammation – An Early Event in Both the History and Pathogenesis of Alzheimer's Disease. Neurodegener. Dis. 7, 38–41. doi:10.1159/000283480

Elkamhawy, A., Park, J., Hassan, A.H.E., Ra, H., Pae, A.N., Lee, J., Park, B.-G., Moon, B., Park, H.-M., Roh, E.J., 2017. Discovery of 1-(3-(benzyloxy)pyridin-2-yl)-3-(2-(piperazin-1-yl)ethyl)urea: A new modulator for amyloid beta-induced mitochondrial dysfunction. Eur. J. Med. Chem. 128, 56–69. doi:10.1016/j.ejmech.2016.12.057

Ercegovac, M., Jovic, N., Simic, T., Beslac-Bumbasirevic, L., Sokic, D., Djukic, T., Savic-Radojevic, A., Matic, M., Mimic-Oka, J., Pljesa-Ercegovac, M., 2010. Byproducts of protein, lipid and DNA oxidative damage and antioxidant enzyme activities in seizure. Seizure 19, 205–210. doi:10.1016/J.SEIZURE.2010.02.002

Erten-Lyons, D., Dodge, H.H., Woltjer, R., Silbert, L.C., Howieson, D.B., Kramer, P., Kaye, J.A., 2013. Neuropathologic Basis of Age-Associated Brain Atrophy. JAMA Neurol. 70, 616. doi:10.1001/jamaneurol.2013.1957

Ettinger, A., Wittmann, T., 2014. Fluorescence live cell imaging. Methods Cell Biol. 123, 77–94. doi:10.1016/B978-0-12-420138-5.00005-7

Fá, M., Puzzo, D., Piacentini, R., Staniszewski, A., Zhang, H., Baltrons, M.A., Li Puma, D.D., Chatterjee, I., Li, J., Saeed, F., Berman, H.L., Ripoli, C., Gulisano, W., Gonzalez, J., Tian, H., Costa, J.A., Lopez, P., Davidowitz, E., Yu, W.H., Haroutunian, V., Brown, L.M., Palmeri, A., Sigurdsson, E.M., Duff, K.E., Teich, A.F., Honig, L.S., Sierks, M., Moe, J.G., D'Adamio, L., Grassi, C., Kanaan, N.M., Fraser, P.E., Arancio, O., 2016. Extracellular Tau Oligomers Produce An Immediate Impairment of LTP and Memory. Sci. Rep. 6, 19393. doi:10.1038/srep19393

Fan, B., Wang, B.-F., Che, L., Sun, Y.-J., Liu, S.-Y., Li, G.-Y., 2017. Blockage of NOX2/MAPK/NF-κB Pathway Protects Photoreceptors against Glucose Deprivation-Induced Cell Death. Oxid. Med. Cell. Longev. 2017, 1–14. doi:10.1155/2017/5093473

Fan, R., DeFilippis, K., Van Nostrand, W.E., 2007. Induction of complement proteins in a mouse model for cerebral microvascular A beta deposition. J. Neuroinflammation 4, 22. doi:10.1186/1742-2094-4-22

Fan, Z., Brooks, D.J., Okello, A., Edison, P., 2017. An early and late peak in microglial activation in Alzheimer's disease trajectory. Brain 140, 792–803. doi:10.1093/brain/aww349

Fan, Z., Okello, A.A., Brooks, D.J., Edison, P., 2015. Longitudinal influence of microglial activation and amyloid on neuronal function in Alzheimer's disease. Brain 138, 3685–3698. doi:10.1093/brain/awv288

Fang, F., Lue, L.-F., Yan, Shiqiang, Xu, H., Luddy, J.S., Chen, D., Walker, D.G., Stern, D.M., Yan, Shifang, Schmidt, A.M., Chen, J.X., Yan, S.S., 2010. RAGE-dependent signaling in microglia contributes to neuroinflammation, Abeta accumulation, and impaired learning/memory in a mouse model of Alzheimer's disease. FASEB J. 24, 1043–55. doi:10.1096/fj.09-139634

Farkas, A.M., Kilgore, T.M., Lotze, M.T., 2007. Detecting DNA: getting and begetting cancer. Curr. Opin. Investig. drugs 8, 981–6.

Farrell, M.E., Kennedy, K.M., Rodrigue, K.M., Wig, G., Bischof, G.N., Rieck, J.R., Chen, X., Festini, S.B., Devous, M.D., Park, D.C., Park, D.C., 2017. Association of Longitudinal Cognitive Decline With Amyloid Burden in Middle-aged and Older Adults: Evidence for a Dose-Response Relationship. JAMA Neurol. 74, 830–838. doi:10.1001/jamaneurol.2017.0892

Farrer, L.A., Cupples, L.A., Haines, J.L., Hyman, B., Kukull, W.A., Mayeux, R., Myers, R.H., Pericak-Vance, M.A., Risch, N., van Duijn, C.M., 1997. Effects of age, sex, and ethnicity on the association between apolipoprotein E genotype and Alzheimer disease. A meta-analysis. APOE and Alzheimer Disease Meta Analysis Consortium. JAMA J. Am. Med. Assoc. 278, 1349–1356. doi:10.1001/jama.278.16.1349

Farris, W., Mansourian, S., Chang, Y., Lindsley, L., Eckman, E.A., Frosch, M.P., Eckman, C.B., Tanzi, R.E., Selkoe, D.J., Guenette, S., 2003. Insulin-degrading enzyme regulates the levels of insulin, amyloid beta-protein, and the beta-amyloid precursor protein intracellular domain in vivo. Proc. Natl. Acad. Sci. U. S. A. 100, 4162–7. doi:10.1073/pnas.0230450100

Felsky, D., Roostaei, T., Nho, K., Risacher, S.L., Bradshaw, E.M., Petyuk, V., Schneider, J.A., Saykin, A., Bennett, D.A., De Jager, P.L., 2019. Neuropathological correlates and genetic architecture of microglial activation in elderly human brain. Nat. Commun. 10, 409. doi:10.1038/s41467-018-08279-3

Fernandez-Perez, E.J., Peters, C., Aguayo, L.G., 2016. Membrane Damage Induced by Amyloid Beta and a Potential Link with Neuroinflammation. Curr. Pharm. Des. 22, 1295–304.

Ferrari, C., Macchiarulo, A., Costantino, G., Pellicciari, R., 2006. Pharmacophore model for bile acids recognition by the FPR receptor. J. Comput. Aided. Mol. Des. 20, 295–303. doi:10.1007/s10822-006-9055-1

Ferreira, S.T., Lourenco, M. V, Oliveira, M.M., De Felice, F.G., 2015. Soluble amyloid-β oligomers as synaptotoxins leading to cognitive impairment in Alzheimer's disease. Front. Cell. Neurosci. 9, 191. doi:10.3389/fncel.2015.00191

Ferretti, M.T., Bruno, M.A., Ducatenzeiler, A., Klein, W.L., Cuello, A.C., 2012. Intracellular Aβ-oligomers and early inflammation in a model of Alzheimer's disease. Neurobiol. Aging 33, 1329–1342. doi:10.1016/j.neurobiolaging.2011.01.007

Fiala, M., Lin, J., Ringman, J., Kermani-Arab, V., Tsao, G., Patel, A., Lossinsky, A.S., Graves, M.C., Gustavson, A., Sayre, J., Sofroni, E., Suarez, T., Chiappelli, F., Bernard, G., 2005. Ineffective phagocytosis of amyloid-beta by macrophages of Alzheimer's disease patients. J. Alzheimers. Dis. 7, 221–32; discussion 255-62.

Figley, C.R., Stroman, P.W., 2011. The role(s) of astrocytes and astrocyte activity in neurometabolism, neurovascular coupling, and the production of functional neuroimaging signals. Eur. J. Neurosci. 33, 577–88. doi:10.1111/j.1460-9568.2010.07584.x

Filina, J. V., Gabdoulkhakova, A.G., Safronova, V.G., 2014. RhoA/ROCK downregulates FPR2-mediated NADPH oxidase activation in mouse bone marrow granulocytes. Cell. Signal. 26, 2138–2146. doi:10.1016/j.cellsig.2014.05.017

Finkel, T., Holbrook, N.J., 2000. Oxidants, oxidative stress and the biology of ageing. Nature 408, 239–247. doi:10.1038/35041687

Fischer, L.R., Li, Y., Asress, S.A., Jones, D.P., Glass, J.D., 2012. Absence of SOD1 leads to oxidative stress in peripheral nerve and causes a progressive distal motor axonopathy. Exp. Neurol. 233, 163–71. doi:10.1016/j.expneurol.2011.09.020

Floden, A.M., Combs, C.K., 2011. Microglia demonstrate age-dependent interaction with amyloid-β fibrils. J. Alzheimers. Dis. 25, 279–93. doi:10.3233/JAD-2011-101014

Floden, A.M., Li, S., Combs, C.K., 2005. Beta-amyloid-stimulated microglia induce neuron death via synergistic stimulation of tumor necrosis factor alpha and NMDA receptors. J. Neurosci. 25, 2566–75. doi:10.1523/JNEUROSCI.4998-04.2005

Fontaine, D.A., Davis, D.B., 2016. Attention to Background Strain Is Essential for Metabolic Research: C57BL/6 and the International Knockout Mouse Consortium. Diabetes 65, 25–33. doi:10.2337/db15-0982

Forsman, H., Dahlgren, C., 2009. Lipoxin A $_4$ Metabolites/Analogues from Two Commercial Sources have No Effects on TNF-α-mediated Priming or Activation through the Neutrophil Formyl Peptide Receptors. Scand. J. Immunol. 70, 396–402. doi:10.1111/j.1365-3083.2009.02311.x

Frautschy, S.A., Yang, F., Irrizarry, M., Hyman, B., Saido, T.C., Hsiao, K., Cole, G.M., 1998. Microglial response to amyloid plaques in APPsw transgenic mice. Am. J. Pathol. 152, 307–17.

Fredman, G., Kamaly, N., Spolitu, S., Milton, J., Ghorpade, D., Chiasson, R., Kuriakose, G., Perretti, M., Farokhzad, O., Tabas, I., 2015. Targeted nanoparticles containing the proresolving peptide Ac2-26 protect against advanced atherosclerosis in hypercholesterolemic mice. Sci. Transl. Med. 7, 275ra20-275ra20. doi:10.1126/scitranslmed.aaa1065

Frigerio, F., Pasqualini, G., Craparotta, I., Marchini, S., van Vliet, E.A., Foerch, P., Vandenplas, C., Leclercq, K., Aronica, E., Porcu, L., Pistorius, K., Colas, R.A., Hansen, T. V, Perretti, M., Kaminski, R.M., Dalli, J., Vezzani, A., 2018. n-3 Docosapentaenoic acid-derived protectin D1 promotes resolution of neuroinflammation and arrests epileptogenesis. Brain 141, 3130–3143. doi:10.1093/brain/awy247

Fu, Z., Aucoin, D., Davis, J., Van Nostrand, W.E., Smith, S.O., 2015. Mechanism of Nucleated Conformational Conversion of Aβ42. Biochemistry 54, 4197–4207. doi:10.1021/acs.biochem.5b00467

Füger, P., Hefendehl, J.K., Veeraraghavalu, K., Wendeln, A.-C., Schlosser, C., Obermüller, U., Wegenast-Braun, B.M., Neher, J.J., Martus, P., Kohsaka, S., Thunemann, M., Feil, R., Sisodia, S.S., Skodras, A., Jucker, M., 2017. Microglia turnover with aging and in an Alzheimer's model via long-term in vivo single-cell imaging. Nat. Neurosci. 20, 1371–1376. doi:10.1038/nn.4631

Fünfschilling, U., Supplie, L.M., Mahad, D., Boretius, S., Saab, A.S., Edgar, J., Brinkmann, B.G., Kassmann, C.M., Tzvetanova, I.D., Möbius, W., Diaz, F., Meijer, D., Suter, U., Hamprecht, B., Sereda, M.W., Moraes, C.T., Frahm, J., Goebbels, S., Nave, K.-A., 2012. Glycolytic oligodendrocytes maintain myelin and long-term axonal integrity. Nature 485, 517–521. doi:10.1038/nature11007

Furtado, M., Katzman, M.A., 2015. Examining the role of neuroinflammation in major depression. Psychiatry Res. 229, 27–36. doi:10.1016/j.psychres.2015.06.009

Gabl, M., Sundqvist, M., Holdfeldt, A., Lind, S., Mårtensson, J., Christenson, K., Marutani, T., Dahlgren, C., Mukai, H., Forsman, H., 2018. Mitocryptides from Human Mitochondrial DNA-Encoded Proteins Activate Neutrophil Formyl Peptide Receptors: Receptor Preference and Signaling Properties. J. Immunol. 200, 3269–3282. doi:10.4049/jimmunol.1701719

Galatro, T.F., Holtman, I.R., Lerario, A.M., Vainchtein, I.D., Brouwer, N., Sola, P.R., Veras, M.M., Pereira, T.F., Leite, R.E.P., Möller, T., Wes, P.D., Sogayar, M.C., Laman, J.D., den Dunnen, W., Pasqualucci, C.A., Oba-Shinjo, S.M., Boddeke, E.W.G.M., Marie, S.K.N., Eggen, B.J.L., 2017. Transcriptomic analysis of purified human cortical microglia reveals age-associated changes. Nat. Neurosci. 20, 1162–1171. doi:10.1038/nn.4597

Ganeshan, K., Chawla, A., 2014. Metabolic regulation of immune responses. Annu. Rev. Immunol. 32, 609–34. doi:10.1146/annurev-immunol-032713-120236

Gao, J.-L., Chen, H., Filie, J.D., Kozak, C.A., Murphy, P.M., 1998. Differential Expansion of the N-Formylpeptide Receptor Gene Cluster in Human and Mouse. Genomics 51, 270–276. doi:10.1006/geno.1998.5376

Gao, Y., Vidal-Itriago, A., Kalsbeek, M.J., Layritz, C., García-Cáceres, C., Tom, R.Z., Eichmann, T.O., Vaz, F.M., Houtkooper, R.H., van der Wel, N., Verhoeven, A.J., Yan, J., Kalsbeek, A., Eckel, R.H., Hofmann, S.M., Yi, C.-X., 2017. Lipoprotein Lipase Maintains Microglial Innate Immunity in Obesity. Cell Rep. 20, 3034–3042. doi:10.1016/j.celrep.2017.09.008

Gartner, A., Staiger, V., 2002. Neurotrophin secretion from hippocampal neurons evoked by long-term-potentiation-inducing electrical stimulation patterns. Proc. Natl. Acad. Sci. 99, 6386–6391. doi:10.1073/pnas.092129699

Gauthier, S., Feldman, H.H., Schneider, L.S., Wilcock, G.K., Frisoni, G.B., Hardlund, J.H., Moebius, H.J., Bentham, P., Kook, K.A., Wischik, D.J., Schelter, B.O., Davis, C.S., Staff, R.T., Bracoud, L., Shamsi, K., Storey, J.M.D., Harrington, C.R., Wischik, C.M., 2016. Efficacy and safety of tau-aggregation inhibitor therapy in patients with mild or moderate Alzheimer's disease: a randomised, controlled, double-blind, parallel-arm, phase 3 trial. Lancet 388, 2873–2884. doi:10.1016/S0140-6736(16)31275-2

Gemma, C., Bachstetter, A.D., 2013. The role of microglia in adult hippocampal neurogenesis. Front. Cell. Neurosci. 7, 229. doi:10.3389/fncel.2013.00229

George, J., Gonçalves, F.Q., Cristóvão, G., Rodrigues, L., Meyer Fernandes, J.R., Gonçalves, T., Cunha, R.A., Gomes, C.A., 2015. Different danger signals differently impact on microglial proliferation through alterations of ATP release and extracellular metabolism. Glia 63, 1636–45. doi:10.1002/glia.22833

Gilman, S., Koller, M., Black, R.S., Jenkins, L., Griffith, S.G., Fox, N.C., Eisner, L., Kirby, L., Rovira, M.B., Forette, F., Orgogozo, J.-M., 2005. Clinical effects of Abeta immunization (AN1792) in patients with AD in an interrupted trial. Neurology 64, 1553–62. doi:10.1212/01.WNL.0000159740.16984.3C

Ginhoux, F., Jung, S., 2014. Monocytes and macrophages: developmental pathways and tissue homeostasis. Nat. Rev. Immunol. 14, 392–404. doi:10.1038/nri3671

Ginhoux, F., Lim, S., Hoeffel, G., Low, D., Huber, T., 2013. Origin and differentiation of microglia. Front. Cell. Neurosci. 7, 45. doi:10.3389/fncel.2013.00045

Giovannini, M.G., Lana, D., Pepeu, G., 2015. The integrated role of ACh, ERK and mTOR in the mechanisms of hippocampal inhibitory avoidance memory. Neurobiol. Learn. Mem. 119, 18–33. doi:10.1016/j.nlm.2014.12.014

Giraldo, E., Lloret, A., Fuchsberger, T., Viña, J., 2014. Aβ and tau toxicities in Alzheimer's are linked via oxidative stress-induced p38 activation: Protective role of vitamin E. Redox Biol. 2, 873–877. doi:10.1016/j.redox.2014.03.002

Goate, A., Chartier-Harlin, M.C., Mullan, M., Brown, J., Crawford, F., Fidani, L., Giuffra, L., Haynes, A., Irving, N., James, L., 1991. Segregation of a missense mutation in the amyloid precursor protein gene with familial Alzheimer's disease. Nature 349, 704–706. doi:10.1038/349704a0

Gobbetti, T., Coldewey, S.M., Chen, J., McArthur, S., le Faouder, P., Cenac, N., Flower, R.J., Thiemermann, C., Perretti, M., 2014. Nonredundant protective properties of FPR2/ALX in polymicrobial murine sepsis. Proc. Natl. Acad. Sci. U. S. A. 111, 18685–90. doi:10.1073/pnas.1410938111

Goetzl, E.J., Miller, B.L., 2017. Multicellular hypothesis for the pathogenesis of Alzheimer's disease. FASEB J. 31, 1792–1795. doi:10.1096/fj.201601221R

Gomez-Nicola, D., Boche, D., 2015. Post-mortem analysis of neuroinflammatory changes in human Alzheimer's disease. Alzheimers. Res. Ther. 7, 42. doi:10.1186/s13195-015-0126-1

Gomez-Nicola, D., Perry, V.H., 2016. Analysis of microglial proliferation in Alzheimer's disease. Methods Mol. Biol. 1303, 185–193. doi:10.1007/978-1-4939-2627-5_10

Gosselin, D., Link, V.M., Romanoski, C.E., Fonseca, G.J., Eichenfield, D.Z., Spann, N.J.,

Stender, J.D., Chun, H.B., Garner, H., Geissmann, F., Glass, C.K., 2014. Environment drives selection and function of enhancers controlling tissue-specific macrophage identities. Cell 159, 1327–40. doi:10.1016/j.cell.2014.11.023

Goyal, M.S., Hawrylycz, M., Miller, J.A., Snyder, A.Z., Raichle, M.E., 2014. Aerobic Glycolysis in the Human Brain Is Associated with Development and Neotenous Gene Expression. Cell Metab. 19, 49–57. doi:10.1016/j.cmet.2013.11.020

Goyal, M.S., Vlassenko, A.G., Blazey, T.M., Su, Y., Couture, L.E., Durbin, T.J., Bateman, R.J., Benzinger, T.L.-S., Morris, J.C., Raichle, M.E., 2017. Loss of Brain Aerobic Glycolysis in Normal Human Aging. Cell Metab. 26, 353-360.e3. doi:10.1016/j.cmet.2017.07.010

Granger, D.N., Kvietys, P.R., 2015. Reperfusion injury and reactive oxygen species: The evolution of a concept. Redox Biol. 6, 524–551. doi:10.1016/j.redox.2015.08.020

Grant, C.M., 2008. Metabolic reconfiguration is a regulated response to oxidative stress. J. Biol. doi:10.1186/jbiol63

Greco, S.J., Sarkar, S., Casadesus, G., Zhu, X., Smith, M.A., Ashford, J.W., Johnston, J.M., Tezapsidis, N., 2009. Leptin inhibits glycogen synthase kinase-3β to prevent tau phosphorylation in neuronal cells. Neurosci. Lett. 455, 191–194. doi:10.1016/j.neulet.2009.03.066

Gregor, M.F., Hotamisligil, G.S., 2011. Inflammatory mechanisms in obesity. Annu. Rev. Immunol. 29, 415–45. doi:10.1146/annurev-immunol-031210-101322

Grutzendler, J., Morris, J.C., 2001. Cholinesterase inhibitors for Alzheimer's disease. Drugs. doi:10.2165/00003495-200161010-00005

Gu, X., Mao, X., Lussier, M.P., Hutchison, M.A., Zhou, L., Hamra, F.K., Roche, K.W., Lu, W., 2016. GSG1L suppresses AMPA receptor-mediated synaptic transmission and uniquely modulates AMPA receptor kinetics in hippocampal neurons. Nat. Commun. 7, 10873. doi:10.1038/ncomms10873

Gu, Y., Luchsinger, J.A., Stern, Y., Scarmeas, N., 2010. Mediterranean Diet, Inflammatory and Metabolic Biomarkers, and Risk of Alzheimer's Disease. J. Alzheimer's Dis. 22, 483–492. doi:10.3233/JAD-2010-100897

Guerreiro, R., Bras, J., 2015. The age factor in Alzheimer's disease. Genome Med. 7, 1–3. doi:10.1186/s13073-015-0232-5

Guerreiro, R., Wojtas, A., Bras, J., Carrasquillo, M., Rogaeva, E., Majounie, E., Cruchaga, C., Sassi, C., Kauwe, J.S.K., Younkin, S., Hazrati, L., Collinge, J., Pocock, J., Lashley, T., Williams, J., Lambert, J.-C., Amouyel, P., Goate, A., Rademakers, R., Morgan, K., Powell, J., St. George-Hyslop, P., Singleton, A., Hardy, J., Alzheimer Genetic Analysis Group, 2013. *TREM2* Variants in Alzheimer's Disease. N. Engl. J. Med. 368, 117–127. doi:10.1056/NEJMoa1211851

Guerrero-Muñoz, M.J., Gerson, J., Castillo-Carranza, D.L., 2015. Tau Oligomers: The Toxic Player at Synapses in Alzheimer's Disease. Front. Cell. Neurosci. 9, 464. doi:10.3389/fncel.2015.00464

Guivernau, B., Bonet, J., Valls-Comamala, V., Bosch-Morató, M., Godoy, J.A., Inestrosa, N.C., Perálvarez-Marín, A., Fernández-Busquets, X., Andreu, D., Oliva, B., Muñoz, F.J., 2016. Amyloid-β Peptide Nitrotyrosination Stabilizes Oligomers and Enhances NMDAR-Mediated Toxicity. J. Neurosci. 36, 11693–11703. doi:10.1523/JNEUROSCI.1081-16.2016

Guix, F.X., Wahle, T., Vennekens, K., Snellinx, A., Chávez-Gutiérrez, L., Ill-Raga, G., Ramos-Fernandez, E., Guardia-Laguarta, C., Lleó, A., Arimon, M., Berezovska, O., Muñoz, F.J., Dotti, C.G., De Strooper, B., 2012. Modification of γ-secretase by nitrosative stress links neuronal ageing to sporadic Alzheimer's disease. EMBO Mol. Med. 4, 660–673. doi:10.1002/emmm.201200243

Guo, Z., Hu, Q., Xu, L., Guo, Z.-N., Ou, Y., He, Y., Yin, C., Sun, X., Tang, J., Zhang, J.H., 2016. Lipoxin A4 Reduces Inflammation Through Formyl Peptide Receptor 2/p38 MAPK Signaling Pathway in Subarachnoid Hemorrhage Rats. Stroke 47, 490–7.

doi:10.1161/STROKEAHA.115.011223

Gupta, R., Sen, N., 2015. Traumatic brain injury: a risk factor for neurodegenerative diseases. Rev. Neurosci. 27, 93–100. doi:10.1515/revneuro-2015-0017

Gutiérrez-Aguilar, M., Baines, C.P., 2015. Structural mechanisms of cyclophilin D-dependent control of the mitochondrial permeability transition pore. Biochim. Biophys. Acta - Gen. Subj. 1850, 2041–2047. doi:10.1016/j.bbagen.2014.11.009

Gwon, A.R., Park, J.S., Arumugam, T. V., Kwon, Y.K., Chan, S.L., Kim, S.H., Baik, S.H., Yang, S., Yun, Y.K., Choi, Y., Kim, S., Tang, S.C., Hyun, D.H., Cheng, A., Dann, C.E., Bernier, M., Lee, J., Markesbery, W.R., Mattson, M.P., Jo, D.G., 2012. Oxidative lipid modification of nicastrin enhances amyloidogenic γ-secretase activity in Alzheimer's disease. Aging Cell 11, 559–568. doi:10.1111/j.1474-9726.2012.00817.x

Gyoneva, S., Ransohoff, R.M., 2015. Inflammatory reaction after traumatic brain injury: therapeutic potential of targeting cell–cell communication by chemokines. Trends Pharmacol. Sci. 36, 471–480. doi:10.1016/j.tips.2015.04.003

Ha, Y.J., Seul, H.J., Lee, J.R., 2011. Ligation of CD40 receptor in human B lymphocytes triggers the 5-lipoxygenase pathway to produce reactive oxygen species and activate p38 MAPK. Exp. Mol. Med. 43, 101. doi:10.3858/emm.2011.43.2.012

Haddad, J.J., Land, S.C., 2002. Redox/ROS regulation of lipopolysaccharide-induced mitogen-activated protein kinase (MAPK) activation and MAPK-mediated TNF-α biosynthesis. Br. J. Pharmacol. 135, 520–536. doi:10.1038/sj.bjp.0704467

Hajishengallis, G., Reis, E.S., Mastellos, D.C., Ricklin, D., Lambris, J.D., 2017. Novel mechanisms and functions of complement. Nat. Immunol. 18, 1288–1298. doi:10.1038/ni.3858

Hall, C.N., Garthwaite, J., 2009. What is the real physiological NO concentration in vivo? Nitric oxide Biol. Chem. 21, 92–103. doi:10.1016/j.niox.2009.07.002

Halliwell, B., Gutteridge, J.M.C., 1992. Biologically relevant metal ion-dependent An update hydroxyl radical generation. FEBS Lett. 307, 108–112. doi:10.1016/0014-5793(92)80911-Y

Hamelin, L., Lagarde, J., Dorothée, G., Leroy, C., Labit, M., Comley, R.A., de Souza, L.C., Corne, H., Dauphinot, L., Bertoux, M., Dubois, B., Gervais, P., Colliot, O., Potier, M.C., Bottlaender, M., Sarazin, M., Clinical IMABio3 team, 2016. Early and protective microglial activation in Alzheimer's disease: a prospective study using 18F-DPA-714 PET imaging. Brain 139, 1252–64. doi:10.1093/brain/aww017

Hammond, T.R., Dufort, C., Dissing-Olesen, L., Giera, S., Young, A., Wysoker, A., Walker, A.J., Gergits, F., Segel, M., Nemesh, J., Marsh, S.E., Saunders, A., Macosko, E., Ginhoux, F., Chen, J., Franklin, R.J.M., Piao, X., McCarroll, S.A., Stevens, B., 2019. Single-Cell RNA Sequencing of Microglia throughout the Mouse Lifespan and in the Injured Brain Reveals Complex Cell-State Changes. Immunity 50, 253-271.e6. doi:10.1016/j.immuni.2018.11.004

Han, B.H., Zhou, M.-L., Johnson, A.W., Singh, I., Liao, F., Vellimana, A.K., Nelson, J.W., Milner, E., Cirrito, J.R., Basak, J., Yoo, M., Dietrich, H.H., Holtzman, D.M., Zipfel, G.J., 2015. Contribution of reactive oxygen species to cerebral amyloid angiopathy, vasomotor dysfunction, and microhemorrhage in aged Tg2576 mice. Proc. Natl. Acad. Sci. U. S. A. 112, E881-90. doi:10.1073/pnas.1414930112

Hanna, A., Iremonger, K., Das, P., Dickson, D., Golde, T., Janus, C., 2012. Age-related increase in amyloid plaque burden is associated with impairment in conditioned fear memory in CRND8 mouse model of amyloidosis. Alzheimers. Res. Ther. 4, 21. doi:10.1186/alzrt124

Hansen, D. V., Hanson, J.E., Sheng, M., 2018. Microglia in Alzheimer's disease. J. Cell Biol. 217, 459–472. doi:10.1083/jcb.201709069

Hansson Petersen, C.A., Alikhani, N., Behbahani, H., Wiehager, B., Pavlov, P.F., Alafuzoff, I., Leinonen, V., Ito, A., Winblad, B., Glaser, E., Ankarcrona, M., 2008. The

amyloid beta-peptide is imported into mitochondria via the TOM import machinery and localized to mitochondrial cristae. Proc. Natl. Acad. Sci. U. S. A. 105, 13145–50. doi:10.1073/pnas.0806192105

Hara-Chikuma, M., Satooka, H., Watanabe, S., Honda, T., Miyachi, Y., Watanabe, T., Verkman, A.S., 2015. Aquaporin-3-mediated hydrogen peroxide transport is required for NF-κB signalling in keratinocytes and development of psoriasis. Nat. Commun. 6, 7454. doi:10.1038/ncomms8454

Hardy, J.A., Higgins, G.A., 1992. Alzheimer's disease: the amyloid cascade hypothesis. Science 256, 184–5.

Harijith, A., Ebenezer, D.L., Natarajan, V., 2014. Reactive oxygen species at the crossroads of inflammasome and inflammation. Front. Physiol. 5, 352. doi:10.3389/fphys.2014.00352

Harlow, E., Lane, D., 2006. Mounting Samples in Gelvatol or Mowiol. Cold Spring Harb. Protoc. 2006, pdb.prot4461. doi:10.1101/pdb.prot4461

Harris, R.A., Tindale, L., Lone, A., Singh, O., Macauley, S.L., Stanley, M., Holtzman, D.M., Bartha, R., Cumming, R.C., 2016. Aerobic Glycolysis in the Frontal Cortex Correlates with Memory Performance in Wild-Type Mice But Not the APP/PS1 Mouse Model of Cerebral Amyloidosis. J. Neurosci. 36, 1871–8. doi:10.1523/JNEUROSCI.3131-15.2016

Haslund-Vinding, J., McBean, G., Jaquet, V., Vilhardt, F., 2017. NADPH oxidases in oxidant production by microglia: activating receptors, pharmacology and association with disease. Br. J. Pharmacol. 174, 1733–1749. doi:10.1111/bph.13425

He, H.-Q., Troksa, E.L., Caltabiano, G., Pardo, L., Ye, R.D., 2014. Structural Determinants for the Interaction of Formyl Peptide Receptor 2 with Peptide Ligands. J. Biol. Chem. 289, 2295–2306. doi:10.1074/jbc.M113.509216

He, H.-Q., Ye, R.D., 2017. The Formyl Peptide Receptors: Diversity of Ligands and Mechanism for Recognition. Molecules 22, 455. doi:10.3390/molecules22030455

He, M., Cheng, N., Gao, W., Zhang, M., Zhang, Y., Ye, R.D., Wang, M., 2011. Characterization of Quin-C1 for its anti-inflammatory property in a mouse model of bleomycin-induced lung injury. Acta Pharmacol. Sin. 32, 601–10. doi:10.1038/aps.2011.4

He, Y., Yao, X., Taylor, N., Bai, Y., Lovenberg, T., Bhattacharya, A., 2018. RNA sequencing analysis reveals quiescent microglia isolation methods from postnatal mouse brains and limitations of BV2 cells. J. Neuroinflammation 15, 153. doi:10.1186/s12974-018-1195-4

Hebert, L.E., Weuve, J., Scherr, P.A., Evans, D.A., 2013. Alzheimer disease in the United States (2010-2050) estimated using the 2010 census. Neurology 80, 1778–1783. doi:10.1212/WNL.0b013e31828726f5

Hellwig, S., Masuch, A., Nestel, S., Katzmarski, N., Meyer-Luehmann, M., Biber, K., 2015. Forebrain microglia from wild-type but not adult 5xFAD mice prevent amyloid-β plaque formation in organotypic hippocampal slice cultures. Sci. Rep. 5, 14624. doi:10.1038/srep14624

Heneka, Michael T., Carson, M.J., Khoury, J. El, Landreth, G.E., Brosseron, F., Feinstein, D.L., Jacobs, A.H., Wyss-Coray, T., Vitorica, J., Ransohoff, R.M., Herrup, K., Frautschy, S.A., Finsen, B., Brown, G.C., Verkhratsky, A., Yamanaka, K., Koistinaho, J., Latz, E., Halle, A., Petzold, G.C., Town, T., Morgan, D., Shinohara, M.L., Perry, V.H., Holmes, C., Bazan, N.G., Brooks, D.J., Hunot, S., Joseph, B., Deigendesch, N., Garaschuk, O., Boddeke, E., Dinarello, C.A., Breitner, J.C., Cole, G.M., Golenbock, D.T., Kummer, M.P., 2015. Neuroinflammation in Alzheimer's disease. Lancet Neurol. 14, 388–405. doi:10.1016/S1474-4422(15)70016-5

Heneka, Michael T, Golenbock, D.T., Latz, E., 2015. Innate immunity in Alzheimer's disease. Nat. Immunol. 16, 229–36. doi:10.1038/ni.3102

Heneka, M.T., Kummer, M.P., Latz, E., 2014. Innate immune activation in

neurodegenerative disease. Nat. Publ. Gr. 14. doi:10.1038/nri3705

Heneka, M.T., Wiesinger, H., Dumitrescu-Ozimek, L., Riederer, P., Feinstein, D.L., Klockgether, T., 2001. Neuronal and glial coexpression of argininosuccinate synthetase and inducible nitric oxide synthase in Alzheimer disease. J. Neuropathol. Exp. Neurol. 60, 906–16.

Henn, A., Lund, S., Hedtjärn, M., Schrattenholz, A., Pörzgen, P., Leist, M., 2009. The suitability of BV2 cells as alternative model system for primary microglia cultures or for animal experiments examining brain inflammation. ALTEX 26, 83–94.

Henríquez-Olguín, C., Altamirano, F., Valladares, D., López, J.R., Allen, P.D., Jaimovich, E., 2015. Altered ROS production, NF-κB activation and interleukin-6 gene expression induced by electrical stimulation in dystrophic mdx skeletal muscle cells. Biochim. Biophys. Acta - Mol. Basis Dis. 1852, 1410–1419. doi:10.1016/j.bbadis.2015.03.012

Heo, S.C., Kwon, Y.W., Jang, I.H., Jeong, G.O., Lee, T.W., Yoon, J.W., Shin, H.J., Jeong, H.C., Ahn, Y., Ko, T.H., Lee, S.C., Han, J., Kim, J.H., 2017. Formyl Peptide Receptor 2 Is Involved in Cardiac Repair After Myocardial Infarction Through Mobilization of Circulating Angiogenic Cells. Stem Cells 35, 654–665. doi:10.1002/stem.2535

Herbst-Robinson, K.J., Liu, L., James, M., Yao, Y., Xie, S.X., Brunden, K.R., 2016. Inflammatory Eicosanoids Increase Amyloid Precursor Protein Expression via Activation of Multiple Neuronal Receptors. Sci. Rep. 5, 18286. doi:10.1038/srep18286

Hernández-Zimbrón, L.F., Rivas-Arancibia, S., 2015. Oxidative stress caused by ozone exposure induces β-amyloid 1–42 overproduction and mitochondrial accumulation by activating the amyloidogenic pathway. Neuroscience 304, 340–348. doi:10.1016/j.neuroscience.2015.07.011

Herrup, K., 2015. The case for rejecting the amyloid cascade hypothesis. Nat. Neurosci. 18, 794–799. doi:10.1038/nn.4017

Heymsfield, S.B., Chirachariyavej, T., Rhyu, I.J., Roongpisuthipong, C., Heo, M., Pietrobelli, A., 2009. Differences between brain mass and body weight scaling to height: potential mechanism of reduced mass-specific resting energy expenditure of taller adults. J. Appl. Physiol. 106, 40–8. doi:10.1152/japplphysiol.91123.2008

Hippius, H., Neundörfer, G., 2003. The discovery of Alzheimer's disease. Dialogues Clin. Neurosci. 5, 101–8.

Ho, J.Q., Asagiri, M., Hoffmann, A., Ghosh, G., 2011. Nf-κB potentiates caspase independent hydrogen peroxide induced cell death. PLoS One 6, e16815. doi:10.1371/journal.pone.0016815

Hock, B.J., Lamb, B.T., 2001. Transgenic mouse models of Alzheimer's disease. Trends Genet. 17, S7-12.

Holland, R., McIntosh, A.L., Finucane, O.M., Mela, V., Rubio-Araiz, A., Timmons, G., McCarthy, S.A., Gun'ko, Y.K., Lynch, M.A., 2018. Inflammatory microglia are glycolytic and iron retentive and typify the microglia in APP/PS1 mice. Brain. Behav. Immun. 68, 183–196. doi:10.1016/j.bbi.2017.10.017

Hollingworth, P., Harold, D., Sims, R., Gerrish, A., Lambert, J.-C., Carrasquillo, M.M., Abraham, R., Hamshere, M.L., Pahwa, J.S., Moskvina, V., Dowzell, K., Jones, N., Stretton, A., Thomas, C., Richards, A., Ivanov, D., Widdowson, C., Chapman, J., Lovestone, S., Powell, J., Proitsi, P., Lupton, M.K., Brayne, C., Rubinsztein, D.C., Gill, M., Lawlor, B., Lynch, A., Brown, K.S., Passmore, P.A., Craig, D., McGuinness, B., Todd, S., Holmes, C., Mann, D., Smith, A.D., Beaumont, H., Warden, D., Wilcock, G., Love, S., Kehoe, P.G., Hooper, N.M., Vardy, E.R.L.C., Hardy, J., Mead, S., Fox, N.C., Rossor, M., Collinge, J., Maier, W., Jessen, F., Rüther, E., Schürmann, B., Heun, R., Kölsch, H., van den Bussche, H., Heuser, I., Kornhuber, J., Wiltfang, J., Dichgans, M., Frölich, L., Hampel, H., Gallacher, J., Hüll, M., Rujescu, D., Giegling, I., Goate, A.M., Kauwe, J.S.K., Cruchaga, C., Nowotny, P., Morris, J.C., Mayo, K., Sleegers, K., Bettens, K., Engelborghs, S., De Deyn, P.P., Van Broeckhoven, C.,

Livingston, G., Bass, N.J., Gurling, H., McQuillin, A., Gwilliam, R., Deloukas, P., Al-Chalabi, A., Shaw, C.E., Tsolaki, M., Singleton, A.B., Guerreiro, R., Mühleisen, T.W., Nöthen, M.M., Moebus, S., Jöckel, K.-H., Klopp, N., Wichmann, H.-E., Pankratz, V.S., Sando, S.B., Aasly, J.O., Barcikowska, M., Wszolek, Z.K., Dickson, D.W., Graff-Radford, N.R., Petersen, R.C., van Duijn, C.M., Breteler, M.M.B., Ikram, M.A., DeStefano, A.L., Fitzpatrick, A.L., Lopez, O., Launer, L.J., Seshadri, S., Berr, C., Campion, D., Epelbaum, J., Dartigues, J.-F., Tzourio, C., Alpérovitch, A., Lathrop, M., Feulner, T.M., Friedrich, P., Riehle, C., Krawczak, M., Schreiber, S., Mayhaus, M., Nicolhaus, S., Wagenpfeil, S., Steinberg, S., Stefansson, H., Stefansson, K., Snædal, J., Björnsson, S., Jonsson, P. V, Chouraki, V., Genier-Boley, B., Hiltunen, M., Soininen, H., Combarros, O., Zelenika, D., Delepine, M., Bullido, M.J., Pasquier, F., Mateo, I., Frank-Garcia, A., Porcellini, E., Hanon, O., Coto, E., Alvarez, V., Bosco, P., Siciliano, G., Mancuso, M., Panza, F., Solfrizzi, V., Nacmias, B., Sorbi, S., Bossù, P., Piccardi, P., Arosio, B., Annoni, G., Seripa, D., Pilotto, A., Scarpini, E., Galimberti, D., Brice, A., Hannequin, D., Licastro, F., Jones, L., Holmans, P.A., Jonsson, T., Riemenschneider, M., Morgan, K., Younkin, S.G., Owen, M.J., O'Donovan, M., Amouyel, P., Williams, J., O'Donovan, M., Amouyel, P., Williams, J., 2011. Common variants at ABCA7, MS4A6A/MS4A4E, EPHA1, CD33 and CD2AP are associated with Alzheimer's disease. Nat. Genet. 43, 429–435. doi:10.1038/ng.803

Holmes, C., Boche, D., Wilkinson, D., Yadegarfar, G., Hopkins, V., Bayer, A., Jones, R.W., Bullock, R., Love, S., Neal, J.W., Zotova, E., Nicoll, J.A.R., 2008. Long-term effects of Abeta42 immunisation in Alzheimer's disease: follow-up of a randomised, placebo-controlled phase I trial. Lancet (London, England) 372, 216–23. doi:10.1016/S0140-6736(08)61075-2

Hong, S., Beja-Glasser, V.F., Nfonoyim, B.M., Frouin, A., Li, S., Ramakrishnan, S., Merry, K.M., Shi, Q., Rosenthal, A., Barres, B.A., Lemere, C.A., Selkoe, D.J., Stevens, B., 2016. Complement and microglia mediate early synapse loss in Alzheimer mouse models. Science (80-.). 352, 712–716. doi:10.1126/science.aad8373

Hong, Y., Shen, C., Yin, Q., Sun, M., Ma, Y., Liu, X., 2016. Effects of RAGE-Specific Inhibitor FPS-ZM1 on Amyloid-β Metabolism and AGEs-Induced Inflammation and Oxidative Stress in Rat Hippocampus. Neurochem. Res. 41, 1192–1199. doi:10.1007/s11064-015-1814-8

Hong, Y.G., Roh, S., Paik, D., Jeong, S., 2017. Development of a Reporter System for In Vivo Monitoring of γ-Secretase Activity in Drosophila. Mol. Cells 40, 73–81. doi:10.14348/molcells.2017.2294

Honig, L.S., Vellas, B., Woodward, M., Boada, M., Bullock, R., Borrie, M., Hager, K., Andreasen, N., Scarpini, E., Liu-Seifert, H., Case, M., Dean, R.A., Hake, A., Sundell, K., Poole Hoffmann, V., Carlson, C., Khanna, R., Mintun, M., DeMattos, R., Selzler, K.J., Siemers, E., 2018. Trial of Solanezumab for Mild Dementia Due to Alzheimer's Disease. N. Engl. J. Med. 378, 321–330. doi:10.1056/NEJMoa1705971

Hoover, B.R., Reed, M.N., Su, J., Penrod, R.D., Kotilinek, L.A., Grant, M.K., Pitstick, R., Carlson, G.A., Lanier, L.M., Yuan, L.-L., Ashe, K.H., Liao, D., 2010. Tau Mislocalization to Dendritic Spines Mediates Synaptic Dysfunction Independently of Neurodegeneration. Neuron 68, 1067–1081. doi:10.1016/j.neuron.2010.11.030

Hopp, S.C., Lin, Y., Oakley, D., Roe, A.D., Devos, S.L., Hanlon, D., Hyman, B.T., 2018. The role of microglia in processing and spreading of bioactive tau seeds in Alzheimer's disease. J. Neuroinflammation 15, 269. doi:10.1186/s12974-018-1309-z

Hopperton, K E, Mohammad, D., Trépanier, M.O., Giuliano, V., Bazinet, R.P., 2018. Markers of microglia in post-mortem brain samples from patients with Alzheimer's disease: a systematic review. Mol. Psychiatry 23, 177–198. doi:10.1038/mp.2017.246

Hopperton, Kathryn E., Trépanier, M.-O., James, N.C.E., Chouinard-Watkins, R., Bazinet, R.P., 2018. Fish oil feeding attenuates neuroinflammatory gene expression without concomitant changes in brain eicosanoids and docosanoids in a mouse model of Alzheimer's disease. Brain. Behav. Immun. 69, 74–90. doi:10.1016/j.bbi.2017.11.002

Horvath, R.J., Nutile-McMenemy, N., Alkaitis, M.S., DeLeo, J.A., 2008. Differential migration, LPS-induced cytokine, chemokine, and NO expression in immortalized BV-2 and HAPI cell lines and primary microglial cultures. J. Neurochem. 107, 557–569. doi:10.1111/j.1471-4159.2008.05633.x

Hou, L., Bao, X., Zang, C., Yang, H., Sun, F., Che, Y., Wu, X., Li, S., Zhang, D., Wang, Q., 2018. Integrin CD11b mediates α-synuclein-induced activation of NADPH oxidase through a Rho-dependent pathway. Redox Biol. 14, 600–608. doi:10.1016/j.redox.2017.11.010

Hou, L., Zhang, C., Wang, K., Liu, X., Wang, H., Che, Y., Sun, F., Zhou, X., Zhao, X., Wang, Q., 2017. Paraquat and maneb co-exposure induces noradrenergic locus coeruleus neurodegeneration through NADPH oxidase-mediated microglial activation. Toxicology 380, 1–10. doi:10.1016/j.tox.2017.02.009

Howard, R., McShane, R., Lindesay, J., Ritchie, C., Baldwin, A., Barber, R., Burns, A., Dening, T., Findlay, D., Holmes, C., Jones, Robert, Jones, Roy, McKeith, I., Macharouthu, A., O'Brien, J., Sheehan, B., Juszczak, E., Katona, C., Hills, R., Knapp, M., Ballard, C., Brown, R.G., Banerjee, S., Adams, J., Johnson, T., Bentham, P., Phillips, P.P.J., 2015. Nursing home placement in the Donepezil and Memantine in Moderate to Severe Alzheimer's Disease (DOMINO-AD) trial: secondary and post-hoc analyses. Lancet Neurol. 14, 1171–1181. doi:10.1016/S1474-4422(15)00258-6

Hu, J.Y., Le, Y., Dunlop, N.M., Wang, J.M., Gong, W., Gao, J.L., Murphy, P.M., 2001. Synthetic peptide MMK-1 is a highly specific chemotactic agonist for leukocyte FPRL1. J. Leukoc. Biol. 70, 155–161. doi:10.1189/jlb.70.1.155

Hu, Y.S., Xin, J., Hu, Y., Zhang, L., Wang, J., 2017. Analyzing the genes related to Alzheimer's disease via a network and pathway-based approach. Alzheimer's Res. Ther. 9, 29. doi:10.1186/s13195-017-0252-z

Huang, J., Liu, K., Zhu, S., Xie, M., Kang, R., Cao, L., Tang, D., 2018. AMPK regulates immunometabolism in sepsis. Brain. Behav. Immun. 72, 89–100. doi:10.1016/j.bbi.2017.11.003

Huang, X., Atwood, C.S., Hartshorn, M.A., Multhaup, G., Goldstein, L.E., Scarpa, R.C., Cuajungco, M.P., Gray, D.N., Lim, J., Moir, R.D., Tanzi, R.E., Bush, A.I., 1999. The Abeta peptide of Alzheimer's disease directly produces hydrogen peroxide through metal ion reduction. Biochemistry 38, 7609–7616. doi:10.1021/bi990438f

Huang, Y., 2011. Roles of apolipoprotein E4 (ApoE4) in the pathogenesis of Alzheimer's disease: lessons from ApoE mouse models. Biochem. Soc. Trans. 39, 924–932. doi:10.1042/BST0390924

Hughes, E.L., Becker, F., Flower, R.J., Buckingham, J.C., Gavins, F.N.E., 2017. Mast Cells Mediate Early Neutrophil Recruitment and Exhibit Anti-Inflammatory Properties via FPR2/ALX. Br. J. Pharmacol. doi:10.1111/bph.13847

Imtiaz, B., Tolppanen, A.-M., Kivipelto, M., Soininen, H., 2014. Future directions in Alzheimer's disease from risk factors to prevention. Biochem. Pharmacol. 88, 661–670. doi:10.1016/j.bcp.2014.01.003

Izuo, N., Murakami, K., Sato, M., Iwasaki, M., Izumi, Y., Shimizu, T., Akaike, A., Irie, K., Kume, T., 2013. Non-toxic conformer of amyloid β may suppress amyloid β-induced toxicity in rat primary neurons: Implications for a novel therapeutic strategy for Alzheimer's disease. Biochem. Biophys. Res. Commun. 438, 1–5. doi:10.1016/j.bbrc.2013.05.106

Jafari, E., Khajouei, M.R., Hassanzadeh, F., Hakimelahi, G.H., Khodarahmi, G.A., 2016. Quinazolinone and quinazoline derivatives: recent structures with potent antimicrobial and cytotoxic activities. Res. Pharm. Sci. 11, 1–14.

Jain, V., Langham, M.C., Wehrli, F.W., 2010. MRI estimation of global brain oxygen consumption rate. J. Cereb. Blood Flow Metab. 30, 1598–607. doi:10.1038/jcbfm.2010.49

James, B.D., Leurgans, S.E., Hebert, L.E., Scherr, P.A., Yaffe, K., Bennett, D.A., 2014. Contribution of Alzheimer disease to mortality in the United States. Neurology 82,

1045–50. doi:10.1212/WNL.0000000000000240

Jang, C., Hui, S., Lu, W., Cowan, A.J., Morscher, R.J., Lee, G., Liu, W., Tesz, G.J., Birnbaum, M.J., Rabinowitz, J.D., 2018. The Small Intestine Converts Dietary Fructose into Glucose and Organic Acids. Cell Metab. 27, 351-361.e3. doi:10.1016/j.cmet.2017.12.016

Jansen, I.E., Savage, J.E., Watanabe, K., Bryois, J., Williams, D.M., Steinberg, S., Sealock, J., Karlsson, I.K., Hägg, S., Athanasiu, L., Voyle, N., Proitsi, P., Witoelar, A., Stringer, S., Aarsland, D., Almdahl, I.S., Andersen, F., Bergh, S., Bettella, F., Bjornsson, S., Brækhus, A., Bråthen, G., de Leeuw, C., Desikan, R.S., Djurovic, S., Dumitrescu, L., Fladby, T., Hohman, T.J., Jonsson, P. V., Kiddle, S.J., Rongve, A., Saltvedt, I., Sando, S.B., Selbæk, G., Shoai, M., Skene, N.G., Snaedal, J., Stordal, E., Ulstein, I.D., Wang, Y., White, L.R., Hardy, J., Hjerling-Leffler, J., Sullivan, P.F., van der Flier, W.M., Dobson, R., Davis, L.K., Stefansson, H., Stefansson, K., Pedersen, N.L., Ripke, S., Andreassen, O.A., Posthuma, D., 2019. Genome-wide meta-analysis identifies new loci and functional pathways influencing Alzheimer's disease risk. Nat. Genet. 51, 404–413. doi:10.1038/s41588-018-0311-9

Jiang, S., Bhaskar, K., 2017. Dynamics of the Complement, Cytokine, and Chemokine Systems in the Regulation of Synaptic Function and Dysfunction Relevant to Alzheimer's Disease. J. Alzheimer's Dis. 57, 1123–1135. doi:10.3233/JAD-161123

Johnson, L.A., Torres, E.R.S., Impey, S., Stevens, J.F., Raber, J., 2017. Apolipoprotein E4 and Insulin Resistance Interact to Impair Cognition and Alter the Epigenome and Metabolome. Sci. Rep. 7, 43701. doi:10.1038/srep43701

Johnston, J.A., Liu, W.W., Todd, S.A., Coulson, D.T., Murphy, S., Irvine, G.B., Passmore, A.P., 2005. Expression and activity of beta-site amyloid precursor protein cleaving enzyme in Alzheimer's disease. Biochem. Soc. Trans. 33, 1096–100. doi:10.1042/BST20051096

Jonsson, T., Stefansson, H., Steinberg, S., Jonsdottir, I., Jonsson, P. V., Snaedal, J., Bjornsson, S., Huttenlocher, J., Levey, A.I., Lah, J.J., Rujescu, D., Hampel, H., Giegling, I., Andreassen, O.A., Engedal, K., Ulstein, I., Djurovic, S., Ibrahim-Verbaas, C., Hofman, A., Ikram, M.A., van Duijn, C.M., Thorsteinsdottir, U., Kong, A., Stefansson, K., 2013. Variant of *TREM2* Associated with the Risk of Alzheimer's Disease. N. Engl. J. Med. 368, 107–116. doi:10.1056/NEJMoa1211103

Joshi, A.U., Minhas, P.S., Liddelow, S.A., Haileselassie, B., Andreasson, K.I., Ii, G.W.D., Mochly-rosen, D., 2019. Fragmented mitochondria released from microglia trigger A1 astrocytic response and propagate inflammatory neurodegeneration 22.

Jucker, M., Walker, L.C., 2013. Self-propagation of pathogenic protein aggregates in neurodegenerative diseases. Nature 501, 45–51. doi:10.1038/nature12481

Jung, C., Lin, Y., Hwang, B., 2015. Ozone, Particulate Matter, and Newly Diagnosed Alzheimer's Disease: A Population-Based Cohort Study in Taiwan. J. Alzheimer's Dis. 44, 573–84.

Kain, V., Jadapalli, J.K., Tourki, B., Halade, G. V, 2019. Inhibition of FPR2 impaired leukocytes recruitment and elicited non-resolving inflammation in acute heart failure. Pharmacol. Res. 146, 104295. doi:10.1016/j.phrs.2019.104295

Kakizawa, S., Yamazawa, T., Chen, Y., Ito, A., Murayama, T., Oyamada, H., Kurebayashi, N., Sato, O., Watanabe, M., Mori, N., Oguchi, K., Sakurai, T., Takeshima, H., Saito, N., Iino, M., 2012. Nitric oxide-induced calcium release via ryanodine receptors regulates neuronal function. EMBO J. 31, 417–428. doi:10.1038/emboj.2011.386

Kallaur, A.P., Reiche, E.M.V., Oliveira, S.R., Simão, A.N.C., Pereira, W.L. de C.J., Alfieri, D.F., Flauzino, T., Proença, C. de M., Lozovoy, M.A.B., Kaimen-Maciel, D.R., Maes, M., 2017. Genetic, Immune-Inflammatory, and Oxidative Stress Biomarkers as Predictors for Disability and Disease Progression in Multiple Sclerosis. Mol. Neurobiol. 54, 31–44. doi:10.1007/s12035-015-9648-6

Kanamaru, T., Kamimura, N., Yokota, T., Iuchi, K., Nishimaki, K., Takami, S., Akashiba, H., Shitaka, Y., Katsura, K., Kimura, K., Ohta, S., 2015. Oxidative stress accelerates

amyloid deposition and memory impairment in a double-transgenic mouse model of Alzheimer's disease. Neurosci. Lett. 587, 126–131. doi:10.1016/j.neulet.2014.12.033

Kang, J.-W., Lee, S.-M., 2016. Resolvin D1 protects the liver from ischemia/reperfusion injury by enhancing M2 macrophage polarization and efferocytosis. Biochim. Biophys. Acta - Mol. Cell Biol. Lipids 1861, 1025–1035. doi:10.1016/j.bbalip.2016.06.002

Kao, W., Gu, R., Jia, Y., Wei, X., Fan, H., Harris, J., Zhang, Z., Quinn, J., Morand, E.F., Yang, Y.H., 2014. A formyl peptide receptor agonist suppresses inflammation and bone damage in arthritis. Br. J. Pharmacol. 171, 4087–96. doi:10.1111/bph.12768

Karin, M., Yamamoto, Y., Wang, Q.M., 2004. The IKK NF-κB system: a treasure trove for drug development. Nat. Rev. Drug Discov. 3, 17–26. doi:10.1038/nrd1279

Karve, I.P., Taylor, J.M., Crack, P.J., 2016. The contribution of astrocytes and microglia to traumatic brain injury. Br. J. Pharmacol. 173, 692–702. doi:10.1111/bph.13125

Kaushik, D.K., Bhattacharya, A., Mirzaei, R., Rawji, K.S., Ahn, Y., Rho, J.M., Yong, V.W., 2019. Enhanced glycolytic metabolism supports transmigration of brain-infiltrating macrophages in multiple sclerosis. J. Clin. Invest. 130. doi:10.1172/JCI124012

Kauwe, J.S.K., Bailey, M.H., Ridge, P.G., Perry, R., Wadsworth, M.E., Hoyt, K.L., Staley, L.A., Karch, C.M., Harari, O., Cruchaga, C., Ainscough, B.J., Bales, K., Pickering, E.H., Bertelsen, S., Fagan, A.M., Holtzman, D.M., Morris, J.C., Goate, A.M., Goate, A.M., 2014. Genome-Wide Association Study of CSF Levels of 59 Alzheimer's Disease Candidate Proteins: Significant Associations with Proteins Involved in Amyloid Processing and Inflammation. PLoS Genet. 10, e1004758. doi:10.1371/journal.pgen.1004758

Kelley, A.S., McGarry, K., Gorges, R., Skinner, J.S., 2015. The burden of health care costs for patients with dementia in the last 5 years of life. Ann. Intern. Med. 163, 729–736. doi:10.7326/M15-0381

Kelly, B., Aj, L., Neill, O.', 2015. Metabolic reprogramming in macrophages and dendritic cells in innate immunity. Nat. Publ. Gr. 25. doi:10.1038/cr.2015.68

Khaddaj-Mallat, R., Sirois, C., Sirois, M., Rizcallah, E., Marouan, S., Morin, C., Rousseau, É., 2016. Pro-Resolving Effects of Resolvin D2 in LTD4 and TNF-α Pre-Treated Human Bronchi. PLoS One 11, e0167058. doi:10.1371/journal.pone.0167058

Khan, M.A., Farahvash, A., Douda, D.N., Licht, J.-C., Grasemann, H., Sweezey, N., Palaniyar, N., 2017. JNK Activation Turns on LPS- and Gram-Negative Bacteria-Induced NADPH Oxidase-Dependent Suicidal NETosis. Sci. Rep. 7, 3409. doi:10.1038/s41598-017-03257-z

Kierdorf, K., Erny, D., Goldmann, T., Sander, V., Schulz, C., Perdiguero, E.G., Wieghofer, P., Heinrich, A., Riemke, P., Hölscher, C., Müller, D.N., Luckow, B., Brocker, T., Debowski, K., Fritz, G., Opdenakker, G., Diefenbach, A., Biber, K., Heikenwalder, M., Geissmann, F., Rosenbauer, F., Prinz, M., 2013. Microglia emerge from erythromyeloid precursors via Pu.1- and Irf8-dependent pathways. Nat. Neurosci. 16, 273–280. doi:10.1038/nn.3318

Kierdorf, K., Fritz, G., 2013. RAGE regulation and signaling in inflammation and beyond. J. Leukoc. Biol. 94, 55–68. doi:10.1189/jlb.1012519

Kim, J., Yang, Y., Song, S.S., Na, J.-H., Oh, K.J., Jeong, C., Yu, Y.G., Shin, Y.-K., 2014. Beta-amyloid oligomers activate apoptotic BAK pore for cytochrome c release. Biophys. J. 107, 1601–8. doi:10.1016/j.bpj.2014.07.074

Kim, S.-Y., Lee, J.-G., Cho, W.-S., Cho, K.-H., Sakong, J., Kim, J.-R., Chin, B.-R., Baek, S.-H., 2010. Role of NADPH oxidase-2 in lipopolysaccharide-induced matrix metalloproteinase expression and cell migration. Immunol. Cell Biol. 88, 197–204. doi:10.1038/icb.2009.87

Kinane, D.F., Stathopoulou, P.G., Papapanou, P.N., 2017. Periodontal diseases. Nat. Rev. Dis. Prim. 3, 17038. doi:10.1038/nrdp.2017.38

Kirkley, K.S., Popichak, K.A., Afzali, M.F., Legare, M.E., Tjalkens, R.B., 2017. Microglia

amplify inflammatory activation of astrocytes in manganese neurotoxicity. J. Neuroinflammation 14, 99. doi:10.1186/s12974-017-0871-0

Kishore, U., Reid, K.B., 2000. C1q: structure, function, and receptors. Immunopharmacology 49, 159–70.

Kiyota, T., Ingraham, K.L., Swan, R.J., Jacobsen, M.T., Andrews, S.J., Ikezu, T., 2012. AAV serotype 2/1-mediated gene delivery of anti-inflammatory interleukin-10 enhances neurogenesis and cognitive function in APP+PS1 mice. Gene Ther. 19, 724–733. doi:10.1038/gt.2011.126

Klevanski, M., Herrmann, U., Weyer, S.W., Fol, R., Cartier, N., Wolfer, D.P., Caldwell, J.H., Korte, M., Muller, U.C., 2015. The APP Intracellular Domain Is Required for Normal Synaptic Morphology, Synaptic Plasticity, and Hippocampus-Dependent Behavior. J. Neurosci. 35, 16018–16033. doi:10.1523/JNEUROSCI.2009-15.2015

Knoll, M., Ruska, E., 1932. Das Elektronenmikroskop. Zeitschrift für Phys. 78, 318–339. doi:10.1007/BF01342199

Kobayashi, D., Zeller, M., Cole, T., Buttini, M., McConlogue, L., Sinha, S., Freedman, S., Morris, R.G.M., Chen, K.S., 2008. BACE1 gene deletion: Impact on behavioral function in a model of Alzheimer's disease. Neurobiol. Aging 29, 861–873. doi:10.1016/j.neurobiolaging.2007.01.002

Koellhoffer, E.C., McCullough, L.D., Ritzel, R.M., 2017. Old Maids: Aging and Its Impact on Microglia Function. Int. J. Mol. Sci. 18. doi:10.3390/ijms18040769

Kopeikina, K.J., Hyman, B.T., Spires-Jones, T.L., 2012. Soluble forms of tau are toxic in Alzheimer's disease. Transl. Neurosci. 3, 223–233. doi:10.2478/s13380-012-0032-y

Kovalevich, J., Langford, D., 2013. Considerations for the use of SH-SY5Y neuroblastoma cells in neurobiology. Methods Mol. Biol. 1078, 9–21. doi:10.1007/978-1-62703-640-5_2

Kreisl, W.C., Lyoo, C.H., McGwier, M., Snow, J., Jenko, K.J., Kimura, N., Corona, W., Morse, C.L., Zoghbi, S.S., Pike, V.W., McMahon, F.J., Turner, R.S., Innis, R.B., Biomarkers Consortium PET Radioligand Project Team, 2013. In vivo radioligand binding to translocator protein correlates with severity of Alzheimer's disease. Brain 136, 2228–2238. doi:10.1093/brain/awt145

Krstic, D., Madhusudan, A., Doehner, J., Vogel, P., Notter, T., Imhof, C., Manalastas, A., Hilfiker, M., Pfister, S., Schwerdel, C., Riether, C., Meyer, U., Knuesel, I., 2012. Systemic immune challenges trigger and drive Alzheimer-like neuropathology in mice. J. Neuroinflammation 9, 151. doi:10.1186/1742-2094-9-151

Kunkle, B.W., Grenier-Boley, B., Sims, R., Bis, J.C., Damotte, V., Naj, A.C., Boland, A., Vronskaya, M., van der Lee, S.J., Amlie-Wolf, A., Bellenguez, C., Frizatti, A., Chouraki, V., Martin, E.R., Sleegers, K., Badarinarayan, N., Jakobsdottir, J., Hamilton-Nelson, K.L., Moreno-Grau, S., Olaso, R., Raybould, R., Chen, Y., Kuzma, A.B., Hiltunen, M., Morgan, T., Ahmad, S., Vardarajan, B.N., Epelbaum, J., Hoffmann, P., Boada, M., Beecham, G.W., Garnier, J.-G., Harold, D., Fitzpatrick, A.L., Valladares, O., Moutet, M.-L., Gerrish, A., Smith, A. V., Qu, L., Bacq, D., Denning, N., Jian, X., Zhao, Y., Del Zompo, M., Fox, N.C., Choi, S.-H., Mateo, I., Hughes, J.T., Adams, H.H., Malamon, J., Sanchez-Garcia, F., Patel, Y., Brody, J.A., Dombroski, B.A., Naranjo, M.C.D., Daniilidou, M., Eiriksdottir, G., Mukherjee, S., Wallon, D., Uphill, J., Aspelund, T., Cantwell, L.B., Garzia, F., Galimberti, D., Hofer, E., Butkiewicz, M., Fin, B., Scarpini, E., Sarnowski, C., Bush, W.S., Meslage, S., Kornhuber, J., White, C.C., Song, Y., Barber, R.C., Engelborghs, S., Sordon, S., Voijnovic, D., Adams, P.M., Vandenberghe, R., Mayhaus, M., Cupples, L.A., Albert, M.S., De Deyn, P.P., Gu, W., Himali, J.J., Beekly, D., Squassina, A., Hartmann, A.M., Orellana, A., Blacker, D., Rodriguez-Rodriguez, E., Lovestone, S., Garcia, M.E., Doody, R.S., Munoz-Fernadez, C., Sussams, R., Lin, H., Fairchild, T.J., Benito, Y.A., Holmes, C., Karamujić-Čomić, H., Frosch, M.P., Thonberg, H., Maier, W., Roschupkin, G., Ghetti, B., Giedraitis, V., Kawalia, A., Li, S., Huebinger, R.M., Kilander, L., Moebus, S., Hernández, I., Kamboh, M.I., Brundin, R., Turton, J., Yang, Q., Katz, M.J., Concari, L., Lord, J., Beiser, A.S., Keene, C.D., Helisalmi, S.,

Kloszewska, I., Kukull, W.A., Koivisto, A.M., Lynch, A., Tarraga, L., Larson, E.B., Haapasalo, A., Lawlor, B., Mosley, T.H., Lipton, R.B., Solfrizzi, V., Gill, M., Longstreth, W.T., Montine, T.J., Frisardi, V., Diez-Fairen, M., Rivadeneira, F., Petersen, R.C., Deramecourt, V., Alvarez, I., Salani, F., Ciaramella, A., Boerwinkle, E., Reiman, E.M., Fievet, N., Rotter, J.I., Reisch, J.S., Hanon, O., Cupidi, C., Andre Uitterlinden, A.G., Royall, D.R., Dufouil, C., Maletta, R.G., de Rojas, I., Sano, M., Brice, A., Cecchetti, R., George-Hyslop, P.S., Ritchie, K., Tsolaki, M., Tsuang, D.W., Dubois, B., Craig, D., Wu, C.-K., Soininen, H., Avramidou, D., Albin, R.L., Fratiglioni, L., Germanou, A., Apostolova, L.G., Keller, L., Koutroumani, M., Arnold, S.E., Panza, F., Gkatzima, O., Asthana, S., Hannequin, D., Whitehead, P., Atwood, C.S., Caffarra, P., Hampel, H., Quintela, I., Carracedo, Á., Lannfelt, L., Rubinsztein, D.C., Barnes, L.L., Pasquier, F., Frölich, L., Barral, S., McGuinness, B., Beach, T.G., Johnston, J.A., Becker, J.T., Passmore, P., Bigio, E.H., Schott, J.M., Bird, T.D., Warren, J.D., Boeve, B.F., Lupton, M.K., Bowen, J.D., Proitsi, P., Boxer, A., Powell, J.F., Burke, J.R., Kauwe, J.S.K., Burns, J.M., Mancuso, M., Buxbaum, J.D., Bonuccelli, U., Cairns, N.J., McQuillin, A., Cao, C., Livingston, G., Carlson, C.S., Bass, N.J., Carlsson, C.M., Hardy, J., Carney, R.M., Bras, J., Carrasquillo, M.M., Guerreiro, R., Allen, M., Chui, H.C., Fisher, E., Masullo, C., Crocco, E.A., DeCarli, C., Bisceglio, G., Dick, M., Ma, L., Duara, R., Graff-Radford, N.R., Evans, D.A., Hodges, A., Faber, K.M., Scherer, M., Fallon, K.B., Riemenschneider, M., Fardo, D.W., Heun, R., Farlow, M.R., Kölsch, H., Ferris, S., Leber, M., Foroud, T.M., Heuser, I., Galasko, D.R., Giegling, I., Gearing, M., Hüll, M., Geschwind, D.H., Gilbert, J.R., Morris, J., Green, R.C., Mayo, K., Growdon, J.H., Feulner, T., Hamilton, R.L., Harrell, L.E., Drichel, D., Honig, L.S., Cushion, T.D., Huentelman, M.J., Hollingworth, P., Hulette, C.M., Hyman, B.T., Marshall, R., Jarvik, G.P., Meggy, A., Abner, E., Menzies, G.E., Jin, L.-W., Leonenko, G., Real, L.M., Jun, G.R., Baldwin, C.T., Grozeva, D., Karydas, A., Russo, G., Kaye, J.A., Kim, R., Jessen, F., Kowall, N.W., Vellas, B., Kramer, J.H., Vardy, E., LaFerla, F.M., Jöckel, K.-H., Lah, J.J., Dichgans, M., Leverenz, J.B., Mann, D., Levey, A.I., Pickering-Brown, S., Lieberman, A.P., Klopp, N., Lunetta, K.L., Wichmann, H.-E., Lyketsos, C.G., Morgan, K., Marson, D.C., Brown, K., Martiniuk, F., Medway, C., Mash, D.C., Nöthen, M.M., Masliah, E., Hooper, N.M., McCormick, W.C., Daniele, A., McCurry, S.M., Bayer, A., McDavid, A.N., Gallacher, J., McKee, A.C., van den Bussche, H., Mesulam, M., Brayne, C., Miller, B.L., Riedel-Heller, S., Miller, C.A., Miller, J.W., Al-Chalabi, A., Morris, J.C., Shaw, C.E., Myers, A.J., Wiltfang, J., O'Bryant, S., Olichney, J.M., Alvarez, V., Parisi, J.E., Singleton, A.B., Paulson, H.L., Collinge, J., Perry, W.R., Mead, S., Peskind, E., Cribbs, D.H., Rossor, M., Pierce, A., Ryan, N.S., Poon, W.W., Nacmias, B., Potter, H., Sorbi, S., Quinn, J.F., Sacchinelli, E., Raj, A., Spalletta, G., Raskind, M., Caltagirone, C., Bossù, P., Orfei, M.D., Reisberg, B., Clarke, R., Reitz, C., Smith, A.D., Ringman, J.M., Warden, D., Roberson, E.D., Wilcock, G., Rogaeva, E., Bruni, A.C., Rosen, H.J., Gallo, M., Rosenberg, R.N., Ben-Shlomo, Y., Sager, M.A., Mecocci, P., Saykin, A.J., Pastor, P., Cuccaro, M.L., Vance, J.M., Schneider, J.A., Schneider, L.S., Slifer, S., Seeley, W.W., Smith, A.G., Sonnen, J.A., Spina, S., Stern, R.A., Swerdlow, R.H., Tang, M., Tanzi, R.E., Trojanowski, J.Q., Troncoso, J.C., Van Deerlin, V.M., Van Eldik, L.J., Vinters, H. V., Vonsattel, J.P., Weintraub, S., Welsh-Bohmer, K.A., Wilhelmsen, K.C., Williamson, J., Wingo, T.S., Woltjer, R.L., Wright, C.B., Yu, C.-E., Yu, L., Saba, Y., Pilotto, A., Bullido, M.J., Peters, O., Crane, P.K., Bennett, D., Bosco, P., Coto, E., Boccardi, V., De Jager, P.L., Lleo, A., Warner, N., Lopez, O.L., Ingelsson, M., Deloukas, P., Cruchaga, C., Graff, C., Gwilliam, R., Fornage, M., Goate, A.M., Sanchez-Juan, P., Kehoe, P.G., Amin, N., Ertekin-Taner, N., Berr, C., Debette, S., Love, S., Launer, L.J., Younkin, S.G., Dartigues, J.-F., Corcoran, C., Ikram, M.A., Dickson, D.W., Nicolas, G., Campion, D., Tschanz, J., Schmidt, H., Hakonarson, H., Clarimon, J., Munger, R., Schmidt, R., Farrer, L.A., Van Broeckhoven, C., C. O'Donovan, M., DeStefano, A.L., Jones, L., Haines, J.L., Deleuze, J.-F., Owen, M.J., Gudnason, V., Mayeux, R., Escott-Price, V., Psaty, B.M., Ramirez, A., Wang, L.-S., Ruiz, A., van Duijn, C.M., Holmans, P.A., Seshadri, S., Williams, J., Amouyel, P., Schellenberg, G.D., Lambert, J.-C., Pericak-Vance, M.A., Amouyel, P., Schellenberg, G.D., Lambert, J.-C., Pericak-Vance, M.A., 2019. Genetic meta-analysis of diagnosed Alzheimer's disease identifies new risk loci and implicates Aβ, tau,

immunity and lipid processing. Nat. Genet. 51, 414–430. doi:10.1038/s41588-019-0358-2

Kwon, Y.-W., Cheon, S.Y., Park, S.Y., Song, J., Lee, J.-H., 2017. Tryptanthrin Suppresses the Activation of the LPS-Treated BV2 Microglial Cell Line via Nrf2/HO-1 Antioxidant Signaling. Front. Cell. Neurosci. 11, 18. doi:10.3389/fncel.2017.00018

Lambert, J.-C., Heath, S., Even, G., Campion, D., Sleegers, K., Hiltunen, M., Combarros, O., Zelenika, D., Bullido, M.J., Tavernier, B., Letenneur, L., Bettens, K., Berr, C., Pasquier, F., Fiévet, N., Barberger-Gateau, P., Engelborghs, S., De Deyn, P., Mateo, I., Franck, A., Helisalmi, S., Porcellini, E., Hanon, O., de Pancorbo, M.M., Lendon, C., Dufouil, C., Jaillard, C., Leveillard, T., Alvarez, V., Bosco, P., Mancuso, M., Panza, F., Nacmias, B., Bossù, P., Piccardi, P., Annoni, G., Seripa, D., Galimberti, D., Hannequin, D., Licastro, F., Soininen, H., Ritchie, K., Blanché, H., Dartigues, J.-F., Tzourio, C., Gut, I., Van Broeckhoven, C., Alpérovitch, A., Lathrop, M., Amouyel, P., 2009. Genome-wide association study identifies variants at CLU and CR1 associated with Alzheimer's disease. Nat. Genet. 41, 1094–9. doi:10.1038/ng.439

Lan, X., Han, X., Li, Q., Yang, Q.-W., Wang, J., 2017. Modulators of microglial activation and polarization after intracerebral haemorrhage. Nat. Rev. Neurol. 13, 420–433. doi:10.1038/nrneurol.2017.69

Latta, C.H., Brothers, H.M., Wilcock, D.M., 2015. Neuroinflammation in Alzheimer's disease; A source of heterogeneity and target for personalized therapy. Neuroscience 302, 103–11. doi:10.1016/j.neuroscience.2014.09.061

Latz, E., Xiao, T.S., Stutz, A., 2013. Activation and regulation of the inflammasomes. Nat. Rev. Immunol. 13, 397–411. doi:10.1038/nri3452

Le, Y., Gong, W., Tiffany, H.L., Tumanov, A., Nedospasov, S., Shen, W., Dunlop, N.M., Gao, J.L., Murphy, P.M., Oppenheim, J.J., Wang, J.M., 2001. Amyloid (beta)42 activates a G-protein-coupled chemoattractant receptor, FPR-like-1. J. Neurosci. 21, RC123.

Le, Y., Murphy, P.M., Wang, J.M., 2002. Formyl-peptide receptors revisited. Trends Immunol. 23, 541–8.

Lecca, D., Janda, E., Mulas, G., Diana, A., Martino, C., Angius, F., Spolitu, S., Casu, M.A., Simbula, G., Boi, L., Batetta, B., Spiga, S., Carta, A.R., 2018. Boosting phagocytosis and anti-inflammatory phenotype in microglia mediates neuroprotection by PPARγ agonist MDG548 in Parkinson's disease models. Br. J. Pharmacol. 175, 3298–3314. doi:10.1111/bph.14214

Lee, J., Culyba, E.K., Powers, E.T., Kelly, J.W., 2011. Amyloid-β forms fibrils by nucleated conformational conversion of oligomers. Nat. Chem. Biol. 7, 602–9. doi:10.1038/nchembio.624

Lee, Y.B., Nagai, A., Kim, S.U., 2002. Cytokines, chemokines, and cytokine receptors in human microglia. J. Neurosci. Res. 69, 94–103. doi:10.1002/jnr.10253

Lehman, E.J., Hein, M.J., Baron, S.L., Gersic, C.M., 2012. Neurodegenerative causes of death among retired National Football League players. Neurology 79, 1970–4. doi:10.1212/WNL.0b013e31826daf50

Leira, Y., Domínguez, C., Seoane, J., Seoane-Romero, J., Pías-Peleteiro, J.M., Takkouche, B., Blanco, J., Aldrey, J.M., 2017. Is Periodontal Disease Associated with Alzheimer's Disease? A Systematic Review with Meta-Analysis. Neuroepidemiology 48, 21–31. doi:10.1159/000458411

Leriche, G., Chen, A.C., Kim, S., Selkoe, D.J., Yang, J., 2016. Fluorescent Analogue of Batimastat Enables Imaging of α-Secretase in Living Cells. ACS Chem. Neurosci. 7, 40–45. doi:10.1021/acschemneuro.5b00283

Lesné, S., Koh, M.T., Kotilinek, L., Kayed, R., Glabe, C.G., Yang, A., Gallagher, M., Ashe, K.H., 2006. A specific amyloid-β protein assembly in the brain impairs memory. Nature 440, 352–357. doi:10.1038/nature04533

Leszek, J., Barreto, G.E., Gąsiorowski, K., Koutsouraki, E., Ávila-Rodrigues, M., Aliev, G.,

2016. Inflammatory Mechanisms and Oxidative Stress as Key Factors Responsible for Progression of Neurodegeneration: Role of Brain Innate Immune System. CNS Neurol. Disord. Drug Targets 15, 329–36.

Li, F., Calingasan, N.Y., Yu, F., Mauck, W.M., Toidze, M., Almeida, C.G., Takahashi, R.H., Carlson, G.A., Flint Beal, M., Lin, M.T., Gouras, G.K., 2004. Increased plaque burden in brains of APP mutant MnSOD heterozygous knockout mice. J. Neurochem. 89, 1308–1312. doi:10.1111/j.1471-4159.2004.02455.x

Li, H., Luo, Y.F., Wang, Y.S., Yang, Q., Xiao, Y.L., Cai, H.R., Xie, C.M., 2018. Using ROS as a Second Messenger, NADPH Oxidase 2 Mediates Macrophage Senescence via Interaction with NF-κB during Pseudomonas aeruginosa Infection. Oxid. Med. Cell. Longev. 2018, 9741838. doi:10.1155/2018/9741838

Li, J.-W., Zong, Y., Cao, X.-P., Tan, Lin, Tan, Lan, 2018. Microglial priming in Alzheimer's disease. Ann. Transl. Med. 6, 176. doi:10.21037/atm.2018.04.22

Li, Q., Cui, J., Fang, C., Liu, M., Min, G., Li, L., 2017. S-Adenosylmethionine Attenuates Oxidative Stress and Neuroinflammation Induced by Amyloid-β Through Modulation of Glutathione Metabolism. J. Alzheimer's Dis. 58, 549–558. doi:10.3233/JAD-170177

Li, T., Braunstein, K.E., Zhang, J., Lau, A., Sibener, L., Deeble, C., Wong, P.C., 2016. The neuritic plaque facilitates pathological conversion of tau in an Alzheimer's disease mouse model. Nat. Commun. 7, 12082. doi:10.1038/ncomms12082

Li, W., 2013. Phagocyte dysfunction, tissue aging and degeneration. Ageing Res. Rev. 12, 1005–1012. doi:10.1016/j.arr.2013.05.006

Li, W., Huang, E., 2016. An Update on Type 2 Diabetes Mellitus as a Risk Factor for Dementia. J. Alzheimers. Dis. doi:10.3233/JAD-160114

Lichtenthaler, S.F., 2006. Ectodomain Shedding of the Amyloid Precursor Protein: Cellular Control Mechanisms and Novel Modifiers. Neurodegener. Dis. 3, 262–269. doi:10.1159/000095265

Liddelow, S.A., Guttenplan, K.A., Clarke, L.E., Bennett, F.C., Bohlen, C.J., Schirmer, L., Bennett, M.L., Münch, A.E., Chung, W.-S., Peterson, T.C., Wilton, D.K., Frouin, A., Napier, B.A., Panicker, N., Kumar, M., Buckwalter, M.S., Rowitch, D.H., Dawson, V.L., Dawson, T.M., Stevens, B., Barres, B.A., 2017. Neurotoxic reactive astrocytes are induced by activated microglia. Nature 541, 481–487. doi:10.1038/nature21029

Lima, K.M., Vago, J.P., Caux, T.R., Negreiros-Lima, G.L., Sugimoto, M.A., Tavares, L.P., Arribada, R.G., Carmo, A.A.F., Galvão, I., Costa, B.R.C., Soriani, F.M., Pinho, V., Solito, E., Perretti, M., Teixeira, M.M., Sousa, L.P., 2017. The resolution of acute inflammation induced by cyclic AMP is dependent on annexin A1. J. Biol. Chem. 292, 13758–13773. doi:10.1074/jbc.M117.800391

Lisi, L., Pizzoferrato, M., Miscioscia, F.T., Topai, A., Navarra, P., 2017. Interactions between integrase inhibitors and human arginase 1. J. Neurochem. 142, 153–159. doi:10.1111/jnc.14039

Liu, C.-C., Hu, J., Tsai, C.-W., Yue, M., Melrose, H.L., Kanekiyo, T., Bu, G., 2015. Neuronal LRP1 Regulates Glucose Metabolism and Insulin Signaling in the Brain. J. Neurosci. 35, 5851–5859. doi:10.1523/JNEUROSCI.5180-14.2015

Liu, Chia-Chen, Liu, Chia-Chan, Kanekiyo, T., Xu, H., Bu, G., 2013. Apolipoprotein E and Alzheimer disease: risk, mechanisms and therapy. Nat. Rev. Neurol. 9, 106–18. doi:10.1038/nrneurol.2012.263

Liu, H., Wang, Jinyan, Wang, Jun, Wang, P., Xue, Y., 2015a. Paeoniflorin attenuates Aβ1-42-induced inflammation and chemotaxis of microglia in vitro and inhibits NF-κB and VEGF/Flt-1 signaling pathways. Brain Res. 1618, 149–158. doi:10.1016/j.brainres.2015.05.035

Liu, H., Wang, Jinyan, Wang, Jun, Wang, P., Xue, Y., 2015b. Paeoniflorin attenuates Aβ1-42-induced inflammation and chemotaxis of microglia in vitro and inhibits NF-κB- and VEGF/Flt-1 signaling pathways. Brain Res. 1618, 149–158.

doi:10.1016/j.brainres.2015.05.035

Liu, M., Zhao, J., Chen, K., Bian, X., Wang, C., Shi, Y., Wang, J.M., 2012. G protein-coupled receptor FPR1 as a pharmacologic target in inflammation and human glioblastoma. Int. Immunopharmacol. 14, 283–288. doi:10.1016/j.intimp.2012.07.015

Liu, Q., Kawai, H., Berg, D.K., 2001. beta -Amyloid peptide blocks the response of alpha 7-containing nicotinic receptors on hippocampal neurons. Proc. Natl. Acad. Sci. U. S. A. 98, 4734–9. doi:10.1073/pnas.081553598

Liu, X., Zeng, K., Li, M., Wang, Q., Liu, R., Zhang, B., Wang, J.-Z., Shu, X., Wang, X., 2017. Expression of P301L-hTau in mouse MEC induces hippocampus-dependent memory deficit. Sci. Rep. 7, 3914. doi:10.1038/s41598-017-04305-4

Liu, Y., Kintner, D.B., Chanana, V., Algharabli, J., Chen, X., Gao, Y., Chen, J., Ferrazzano, P., Olson, J.K., Sun, D., 2010. Activation of Microglia Depends on Na+/H+ Exchange-Mediated H+ Homeostasis. J. Neurosci. 30, 15210–15220. doi:10.1523/JNEUROSCI.3950-10.2010

Lloyd, A.F., Davies, C.L., Holloway, R.K., Labrak, Y., Ireland, G., Carradori, D., Dillenburg, A., Borger, E., Soong, D., Richardson, J.C., Kuhlmann, T., Williams, A., Pollard, J.W., des Rieux, A., Priller, J., Miron, V.E., 2019. Central nervous system regeneration is driven by microglia necroptosis and repopulation. Nat. Neurosci. 22, 1046–1052. doi:10.1038/s41593-019-0418-z

Lobo-Silva, D., Carriche, G.M., Castro, A.G., Roque, S., Saraiva, M., 2016. Balancing the immune response in the brain: IL-10 and its regulation. J. Neuroinflammation 13, 297. doi:10.1186/s12974-016-0763-8

Locatelli, I., Sutti, S., Jindal, A., Vacchiano, M., Bozzola, C., Reutelingsperger, C., Kusters, D., Bena, S., Parola, M., Paternostro, C., Bugianesi, E., McArthur, S., Albano, E., Perretti, M., 2014. Endogenous annexin A1 is a novel protective determinant in nonalcoholic steatohepatitis in mice. Hepatology 60, 531–544. doi:10.1002/hep.27141

Loeffler, D.A., Camp, D.M., Bennett, D.A., 2008. Plaque complement activation and cognitive loss in Alzheimer's disease. J. Neuroinflammation 5, 9. doi:10.1186/1742-2094-5-9

Loiola, R.A., Wickstead, E.S., Solito, E., McArthur, S., 2019. Estrogen Promotes Pro-resolving Microglial Behavior and Phagocytic Cell Clearance Through the Actions of Annexin A1. Front. Endocrinol. (Lausanne). 10, 420. doi:10.3389/fendo.2019.00420

Lomakin, A., Teplow, D.B., Kirschner, D.A., Benedek, G.B., 1997. Kinetic theory of fibrillogenesis of amyloid beta-protein. Proc. Natl. Acad. Sci. U. S. A. 94, 7942–7.

López-Picón, F.R., Snellman, A., Eskola, O., Helin, S., Solin, O., Haaparanta-Solin, M., Rinne, J.O., 2018. Neuroinflammation Appears Early on PET Imaging and Then Plateaus in a Mouse Model of Alzheimer Disease. J. Nucl. Med. 59, 509–515. doi:10.2967/jnumed.117.197608

López, N., Tormo, C., De Blas, I., Llinares, I., Alom, J., 2013. Oxidative stress in Alzheimer's disease and mild cognitive impairment with high sensitivity and specificity. J. Alzheimer's Dis. 33, 823–829. doi:10.3233/JAD-2012-121528

Lu, Y.-C., Yeh, W.-C., Ohashi, P.S., 2008. LPS/TLR4 signal transduction pathway. Cytokine 42, 145–151. doi:10.1016/j.cyto.2008.01.006

Lucin, K.M., O'Brien, C.E., Bieri, G., Czirr, E., Mosher, K.I., Abbey, R.J., Mastroeni, D.F., Rogers, J., Spencer, B., Masliah, E., Wyss-Coray, T., 2013. Microglial Beclin 1 Regulates Retromer Trafficking and Phagocytosis and Is Impaired in Alzheimer's Disease. Neuron 79, 873–886. doi:10.1016/j.neuron.2013.06.046

Luo, Y., Bolon, B., Kahn, S., Bennett, B.D., Babu-Khan, S., Denis, P., Fan, W., Kha, H., Zhang, J., Gong, Y., Martin, L., Louis, J.C., Yan, Q., Richards, W.G., Citron, M., Vassar, R., 2001. Mice deficient in BACE1, the Alzheimer's beta-secretase, have normal phenotype and abolished beta-amyloid generation. Nat. Neurosci. 4, 231–2. doi:10.1038/85059

Lüth, H.J., Holzer, M., Gärtner, U., Staufenbiel, M., Arendt, T., 2001. Expression of endothelial and inducible NOS-isoforms is increased in Alzheimer's disease, in APP23 transgenic mice and after experimental brain lesion in rat: evidence for an induction by amyloid pathology. Brain Res. 913, 57–67. doi:10.1016/s0006-8993(01)02758-5

Ma, M.W., Wang, J., Zhang, Q., Wang, R., Dhandapani, K.M., Vadlamudi, R.K., Brann, D.W., 2017. NADPH oxidase in brain injury and neurodegenerative disorders. Mol. Neurodegener. 12, 7. doi:10.1186/s13024-017-0150-7

Ma, Q., Zhang, Z., Shim, J.-K., Venkatraman, T.N., Lascola, C.D., Quinones, Q.J., Mathew, J.P., Terrando, N., Podgoreanu, M. V, 2019. Annexin A1 Bioactive Peptide Promotes Resolution of Neuroinflammation in a Rat Model of Exsanguinating Cardiac Arrest Treated by Emergency Preservation and Resuscitation. Front. Neurosci. 13, 608. doi:10.3389/fnins.2019.00608

Mächler, P., Wyss, M.T., Elsayed, M., Stobart, J., Gutierrez, R., von Faber-Castell, A., Kaelin, V., Zuend, M., San Martín, A., Romero-Gómez, I., Baeza-Lehnert, F., Lengacher, S., Schneider, B.L., Aebischer, P., Magistretti, P.J., Barros, L.F., Weber, B., 2016. In Vivo Evidence for a Lactate Gradient from Astrocytes to Neurons. Cell Metab. 23, 94–102. doi:10.1016/j.cmet.2015.10.010

Maderna, P., Godson, C., 2009. Lipoxins: resolutionary road. Br. J. Pharmacol. 158, 947–59. doi:10.1111/j.1476-5381.2009.00386.x

Magistretti, P.J., Allaman, I., 2015. A Cellular Perspective on Brain Energy Metabolism and Functional Imaging. Neuron 86, 883–901. doi:10.1016/J.NEURON.2015.03.035

Majd, S., Majd, Z., Koblar, S., Power, J., 2018. Beta estradiol and norepinephrine treatment of differentiated SH-SY5Y cells enhances tau phosphorylation at (Ser396) and (Ser262) via AMPK but not mTOR signaling pathway. Mol. Cell. Neurosci. 88, 201–211. doi:10.1016/j.mcn.2018.02.004

Malik, M., Parikh, I., Vasquez, J.B., Smith, C., Tai, L., Bu, G., LaDu, M.J., Fardo, D.W., Rebeck, G.W., Estus, S., 2015. Genetics ignite focus on microglial inflammation in Alzheimer's disease. Mol. Neurodegener. 10, 52. doi:10.1186/s13024-015-0048-1

Malinski, T., 2007. Nitric oxide and nitroxidative stress in Alzheimer's disease. J. Alzheimer's Dis. doi:10.3233/JAD-2007-11208

Manczak, M., Reddy, P.H., 2013. Abnormal interaction of oligomeric amyloid-β with phosphorylated tau: implications to synaptic dysfunction and neuronal damage. J. Alzheimers. Dis. 36, 285–95. doi:10.3233/JAD-130275

Mander, P.K., Jekabsone, A., Brown, G.C., 2006. Microglia Proliferation Is Regulated by Hydrogen Peroxide from NADPH Oxidase. J. Immunol. 176, 1046–1052. doi:10.4049/jimmunol.176.2.1046

Mao, P., Manczak, M., Calkins, M.J., Truong, Q., Reddy, T.P., Reddy, A.P., Shirendeb, U., Lo, H.-H., Rabinovitch, P.S., Reddy, P.H., 2012. Mitochondria-targeted catalase reduces abnormal APP processing, amyloid production and BACE1 in a mouse model of Alzheimer's disease: implications for neuroprotection and lifespan extension. Hum. Mol. Genet. 21, 2973–2990. doi:10.1093/hmg/dds128

Maphis, N., Xu, G., Kokiko-Cochran, O.N., Jiang, S., Cardona, A., Ransohoff, R.M., Lamb, B.T., Bhaskar, K., 2015. Reactive microglia drive tau pathology and contribute to the spreading of pathological tau in the brain. Brain 138, 1738–1755. doi:10.1093/brain/awv081

Mariappan, N., Elks, C.M., Sriramula, S., Guggilam, A., Liu, Z., Borkhsenious, O., Francis, J., 2010. NF-κB-induced oxidative stress contributes to mitochondrial and cardiac dysfunction in type II diabetes. Cardiovasc. Res. 85, 473–483. doi:10.1093/cvr/cvp305

Marolda, R., Ciotti, M.T., Matrone, C., Possenti, R., Calissano, P., Cavallaro, S., Severini, C., 2012. Substance P activates ADAM9 mRNA expression and induces α-secretase-mediated amyloid precursor protein cleavage. Neuropharmacology 62, 1954–1963. doi:10.1016/j.neuropharm.2011.12.025

Martin, C.J., Peters, K.N., Behar, S.M., 2014. Macrophages clean up: efferocytosis and microbial control. Curr. Opin. Microbiol. 17, 17–23. doi:10.1016/j.mib.2013.10.007

Masters, C.L., Bateman, R., Blennow, K., Rowe, C.C., Sperling, R.A., Cummings, J.L., 2015. Alzheimer's disease. Nat. Rev. Dis. Prim. 1, 15056. doi:10.1038/nrdp.2015.56

Mathew, A., Lindsley, T.A., Sheridan, A., Bhoiwala, D.L., Hushmendy, S.F., Yager, E.J., Ruggiero, E.A., Crawford, D.R., 2012. Degraded Mitochondrial DNA is a Newly Identified Subtype of the Damage Associated Molecular Pattern (DAMP) Family and Possible Trigger of Neurodegeneration. J. Alzheimer's Dis. 30, 617–627. doi:10.3233/JAD-2012-120145

Matsuoka, Y., Picciano, M., Malester, B., LaFrancois, J., Zehr, C., Daeschner, J.M., Olschowka, J.A., Fonseca, M.I., O'Banion, M.K., Tenner, A.J., Lemere, C.A., Duff, K., 2001. Inflammatory responses to amyloidosis in a transgenic mouse model of Alzheimer's disease. Am. J. Pathol. 158, 1345–54. doi:10.1016/S0002-9440(10)64085-0

Mawuenyega, K.G., Sigurdson, W., Ovod, V., Munsell, L., Kasten, T., Morris, J.C., Yarasheski, K.E., Bateman, R.J., 2010. Decreased clearance of CNS β-amyloid in Alzheimer's disease. Science (80-.). 330, 1774. doi:10.1126/science.1197623

McArthur, S., Cristante, E., Paterno, M., Christian, H., Roncaroli, F., Gillies, G.E., Solito, E., 2010. Annexin A1: a central player in the anti-inflammatory and neuroprotective role of microglia. J. Immunol. 185, 6317–28. doi:10.4049/jimmunol.1001095

McArthur, S., Gobbetti, T., Juban, G., Desgeorges, T., Theret, M., Gondin, J., Toller-Kawahisa, J.E., Reutelingsperger, C.P., Perretti, M., Mounier, R., 2018. Annexin A1 drives macrophage skewing towards a resolving phenotype to accelerate the regeneration of muscle injury through AMPK activation. bioRxiv 375709. doi:10.1101/375709

McArthur, S., Gobbetti, T., Kusters, D.H.M., Reutelingsperger, C.P., Flower, R.J., Perretti, M., 2015. Definition of a Novel Pathway Centered on Lysophosphatidic Acid To Recruit Monocytes during the Resolution Phase of Tissue Inflammation. J. Immunol. 195, 1139–1151. doi:10.4049/jimmunol.1500733

McArthur, S., Yazid, S., Christian, H., Sirha, R., Flower, R., Buckingham, J., Solito, E., 2009. Annexin A1 regulates hormone exocytosis through a mechanism involving actin reorganization. FASEB J. 23, 4000–4010. doi:10.1096/fj.09-131391

McGeer, P.L., McGeer, E.G., 2013. The amyloid cascade-inflammatory hypothesis of Alzheimer disease: implications for therapy. Acta Neuropathol. 126, 479–497. doi:10.1007/s00401-013-1177-7

McPherson, C.A., Merrick, B.A., Harry, G.J., 2014. In vivo molecular markers for pro-inflammatory cytokine M1 stage and resident microglia in trimethyltin-induced hippocampal injury. Neurotox. Res. 25, 45–56. doi:10.1007/s12640-013-9422-3

Mecca, C., Giambanco, I., Donato, R., Arcuri, C., 2018. Microglia and aging: The role of the TREM2–DAP12 and CX3CL1-CX3CR1 Axes. Int. J. Mol. Sci. 19, 318. doi:10.3390/ijms19010318

Mehta, A., Prabhakar, M., Kumar, P., Deshmukh, R., Sharma, P.L., 2013. Excitotoxicity: Bridge to various triggers in neurodegenerative disorders. Eur. J. Pharmacol. 698, 6–18. doi:10.1016/j.ejphar.2012.10.032

Mele, L., Paino, F., Papaccio, F., Regad, T., Boocock, D., Stiuso, P., Lombardi, A., Liccardo, D., Aquino, G., Barbieri, A., Arra, C., Coveney, C., La Noce, M., Papaccio, G., Caraglia, M., Tirino, V., Desiderio, V., 2018. A new inhibitor of glucose-6-phosphate dehydrogenase blocks pentose phosphate pathway and suppresses malignant proliferation and metastasis in vivo article. Cell Death Dis. 9, 572. doi:10.1038/s41419-018-0635-5

Mendez, F.M., Paholpak, P., Lin, A., Zhang, J., Teng, E., 2015. Prevalence of Traumatic Brain Injury in Early Versus Late-Onset Alzheimer's Disease. J. Alzheimer's Dis. 47, 985–93.

Meng, X.-F., Yu, J.-T., Wang, H.-F., Tan, M.-S., Wang, C., Tan, C.-C., Tan, L., 2014. Midlife vascular risk factors and the risk of Alzheimer's disease: a systematic review and meta-analysis. J. Alzheimers. Dis. 42, 1295–310. doi:10.3233/JAD-140954

Mergenthaler, P., Lindauer, U., Dienel, G.A., Meisel, A., 2013. Sugar for the brain: the role of glucose in physiological and pathological brain function. Trends Neurosci. 36, 587–97. doi:10.1016/j.tins.2013.07.001

Merino, J.J., Bellver-Landete, V., Oset-Gasque, M.J., Cubelos, B., 2015. CXCR4/CXCR7 Molecular Involvement in Neuronal and Neural Progenitor Migration: Focus in CNS Repair. J. Cell. Physiol. 230, 27–42. doi:10.1002/jcp.24695

Meyer, P.-F., Tremblay-Mercier, J., Leoutsakos, J., Madjar, C., Lafaille-Maignan, M.-É., Savard, M., Rosa-Neto, P., Poirier, J., Etienne, P., Breitner, J., PREVENT-AD Research Group, 2019. INTREPAD: A randomized trial of naproxen to slow progress of presymptomatic Alzheimer disease. Neurology 92, e2070–e2080. doi:10.1212/WNL.0000000000007232

Miao, G.-S., Liu, Z.-H., Wei, S.-X., Luo, J.-G., Fu, Z.-J., Sun, T., 2015. Lipoxin A4 attenuates radicular pain possibly by inhibiting spinal ERK, JNK and NF-κB/p65 and cytokine signals, but not p38, in a rat model of non-compressive lumbar disc herniation. Neuroscience 300, 10–18. doi:10.1016/j.neuroscience.2015.04.060

Micheau, J., Marighetto, A., 2011. Acetylcholine and memory: A long, complex and chaotic but still living relationship. Behav. Brain Res. 221, 424–429. doi:10.1016/j.bbr.2010.11.052

Migeotte, I., Communi, D., Parmentier, M., 2006. Formyl peptide receptors: A promiscuous subfamily of G protein-coupled receptors controlling immune responses. Cytokine Growth Factor Rev. 17, 501–519. doi:10.1016/j.cytogfr.2006.09.009

Mills, E.L., Kelly, B., Logan, A., Costa, A.S.H., Varma, M., Bryant, C.E., Tourlomousis, P., Däbritz, J.H.M., Gottlieb, E., Latorre, I., Corr, S.C., McManus, G., Ryan, D., Jacobs, H.T., Szibor, M., Xavier, R.J., Braun, T., Frezza, C., Murphy, M.P., O'Neill, L.A., 2016. Succinate Dehydrogenase Supports Metabolic Repurposing of Mitochondria to Drive Inflammatory Macrophages. Cell 167, 457-470.e13. doi:10.1016/j.cell.2016.08.064

Mink, J.W., Blumenschine, R.J., Adams, D.B., 1981. Ratio of central nervous system to body metabolism in vertebrates: its constancy and functional basis. Am. J. Physiol. 241, R203-12. doi:10.1152/ajpregu.1981.241.3.R203

Mireille, B., Igor, A., Pierre J, M., 2011. Brain Energy Metabolism: Focus on Astrocyte-Neuron Metabolic Cooperation. Cell Metab. 14. doi:10.1016/J.CMET.2011.08.016

Misiak, B., Leszek, J., Kiejna, A., 2012. Metabolic syndrome, mild cognitive impairment and Alzheimer's disease-The emerging role of systemic low-grade inflammation and adiposity. Brain Res. Bull. doi:10.1016/j.brainresbull.2012.08.003

Misko, T.P., Schilling, R.J., Salvemini, D., Moore, W.M., Currie, M.G., 1993. A Fluorometric Assay for the Measurement of Nitrite in Biological Samples. Anal. Biochem. 214, 11–16. doi:10.1006/abio.1993.1449

Mittal, M., Siddiqui, M.R., Tran, K., Reddy, S.P., Malik, A.B., 2014. Reactive Oxygen Species in Inflammation and Tissue Injury. Antioxid. Redox Signal. 20, 1126–1167. doi:10.1089/ars.2012.5149

Mizwicki, M.T., Liu, G., Fiala, M., Magpantay, L., Sayre, J., Siani, A., Mahanian, M., Weitzman, R., Hayden, E.Y., Rosenthal, M.J., Nemere, I., Ringman, J., Teplow, D.B., 2013. 1α,25-Dihydroxyvitamin D3 and Resolvin D1 Retune the Balance between Amyloid-β Phagocytosis and Inflammation in Alzheimer's Disease Patients. J. Alzheimer's Dis. 34, 155–170. doi:10.3233/JAD-121735

Monson, N.L., Ireland, S.J., Ligocki, A.J., Chen, D., Rounds, W.H., Li, M., Huebinger, R.M., Munro Cullum, C., Greenberg, B.M., Stowe, A.M., Zhang, R., 2014. Elevated CNS Inflammation in Patients with Preclinical Alzheimer's Disease. J. Cereb. Blood Flow Metab. 34, 30–33. doi:10.1038/jcbfm.2013.183

Mookerjee, S.A., Gerencser, A.A., Nicholls, D.G., Brand, M.D., 2017. Quantifying intracellular rates of glycolytic and oxidative ATP production and consumption using extracellular flux measurements. J. Biol. Chem. 292, 7189–7207. doi:10.1074/jbc.M116.774471

Morales, I., Guzmán-Martínez, L., Cerda-Troncoso, C., Farías, G.A., Maccioni, R.B., 2014. Neuroinflammation in the pathogenesis of Alzheimer's disease. A rational framework for the search of novel therapeutic approaches. Front. Cell. Neurosci. 8, 112. doi:10.3389/fncel.2014.00112

Moran, C., Beare, R., Phan, T.G., Bruce, D.G., Callisaya, M.L., Srikanth, V., 2015. Type 2 diabetes mellitus and biomarkers of neurodegeneration. Neurology 85, 1123–1130. doi:10.1212/WNL.0000000000001982

Moreno-Gonzalez, I., Edwards III, G., Salvadores, N., Shahnawaz, M., Diaz-Espinoza, R., Soto, C., 2017. Molecular interaction between type 2 diabetes and Alzheimer's disease through cross-seeding of protein misfolding. Mol. Psychiatry 22, 1327–1334. doi:10.1038/mp.2016.230

Moroni, F., Ammirati, E., Magnoni, M., D'Ascenzo, F., Anselmino, M., Anzalone, N., Rocca, M.A., Falini, A., Filippi, M., Camici, P.G., 2016. Carotid atherosclerosis, silent ischemic brain damage and brain atrophy: A systematic review and meta-analysis. Int. J. Cardiol. 223, 681–687. doi:10.1016/j.ijcard.2016.08.234

Morozov, Y.M., Datta, D., Paspalas, C.D., Arnsten, A.F.T., 2017. Ultrastructural evidence for impaired mitochondrial fission in the aged rhesus monkey dorsolateral prefrontal cortex. Neurobiol. Aging 51, 9–18. doi:10.1016/j.neurobiolaging.2016.12.001

Morris, M., Maeda, S., Vossel, K., Mucke, L., 2011. The many faces of tau. Neuron 70, 410–26. doi:10.1016/j.neuron.2011.04.009

Mottola, G., Chatterjee, A., Wu, B., Chen, M., Conte, M.S., 2017. Aspirin-triggered resolvin D1 attenuates PDGF-induced vascular smooth muscle cell migration via the cyclic adenosine monophosphate/protein kinase A (cAMP/PKA) pathway. PLoS One 12, e0174936. doi:10.1371/journal.pone.0174936

Mozurkewich, E.L., Greenwood, M., Clinton, C., Berman, D., Romero, V., Djuric, Z., Qualls, C., Gronert, K., 2016. Pathway Markers for Pro-resolving Lipid Mediators in Maternal and Umbilical Cord Blood: A Secondary Analysis of the Mothers, Omega-3, and Mental Health Study. Front. Pharmacol. 07, 274. doi:10.3389/fphar.2016.00274

Mudò, G., Frinchi, M., Nuzzo, D., Scaduto, P., Plescia, F., Massenti, M.F., Di Carlo, M., Cannizzaro, C., Cassata, G., Cicero, L., Ruscica, M., Belluardo, N., Grimaldi, L.M., 2019. Anti-inflammatory and cognitive effects of interferon-β1a (IFNβ1a) in a rat model of Alzheimer's disease. J. Neuroinflammation 16, 44. doi:10.1186/s12974-019-1417-4

Muirhead, K.E.A., Borger, E., Aitken, L., Conway, S.J., Gunn-Moore, F.J., 2010. The consequences of mitochondrial amyloid β-peptide in Alzheimer's disease. Biochem. J. 426, 255–270. doi:10.1042/BJ20091941

Mullarky, E., Cantley, L.C., 2015. Diverting Glycolysis to Combat Oxidative Stress, in: Innovative Medicine. Springer Japan, Tokyo, pp. 3–23. doi:10.1007/978-4-431-55651-0_1

Müller-Schiffmann, A., Herring, A., Abdel-Hafiz, L., Chepkova, A.N., Schäble, S., Wedel, D., Horn, A.H.C., Sticht, H., de Souza Silva, M.A., Gottmann, K., Sergeeva, O.A., Huston, J.P., Keyvani, K., Korth, C., 2016. Amyloid-β dimers in the absence of plaque pathology impair learning and synaptic plasticity. Brain 139, 509–525. doi:10.1093/brain/awv355

Müller, N., Weidinger, E., Leitner, B., Schwarz, M.J., 2015. The role of inflammation in schizophrenia. Front. Neurosci. 9, 372. doi:10.3389/fnins.2015.00372

Müller, U.C., Deller, T., Korte, M., 2017. Not just amyloid: physiological functions of the amyloid precursor protein family. Nat. Rev. Neurosci. 18, 281–298. doi:10.1038/nrn.2017.29

Murphy, M.P., LeVine, H., III, 2010. Alzheimer's disease and the amyloid-beta peptide. J. Alzheimers. Dis. 19, 311–23. doi:10.3233/JAD-2010-1221

Murphy, S.L., Xu, J., Kochanek, K.D., 2013. Deaths: final data for 2010. Natl. Vital Stat. Rep. 61, 1–117.

Murray, P.J., Allen, J.E., Biswas, S.K., Fisher, E.A., Gilroy, D.W., Goerdt, S., Gordon, S., Hamilton, J.A., Ivashkiv, L.B., Lawrence, T., Locati, M., Mantovani, A., Martinez, F.O., Mege, J.-L., Mosser, D.M., Natoli, G., Saeij, J.P., Schultze, J.L., Shirey, K.A., Sica, A., Suttles, J., Udalova, I., van Ginderachter, J.A., Vogel, S.N., Wynn, T.A., 2014. Macrophage Activation and Polarization: Nomenclature and Experimental Guidelines. Immunity 41, 14–20. doi:10.1016/j.immuni.2014.06.008

Musiek, E.S., Holtzman, D.M., 2015. Three dimensions of the amyloid hypothesis: time, space and "wingmen". Nat. Neurosci. 18, 800–6. doi:10.1038/nn.4018

Nadkarni, S., McArthur, S., 2013. Oestrogen and immunomodulation: new mechanisms that impact on peripheral and central immunity. Curr. Opin. Pharmacol. 13, 576–581. doi:10.1016/j.coph.2013.05.007

Naga, K.K., Sullivan, P.G., Geddes, J.W., 2007. High Cyclophilin D Content of Synaptic Mitochondria Results in Increased Vulnerability to Permeability Transition. J. Neurosci. 27, 7469–7475. doi:10.1523/JNEUROSCI.0646-07.2007

Naj, A.C., Jun, G., Beecham, G.W., Wang, L.-S., Vardarajan, B.N., Buros, J., Gallins, P.J., Buxbaum, J.D., Jarvik, G.P., Crane, P.K., Larson, E.B., Bird, T.D., Boeve, B.F., Graff-Radford, N.R., De Jager, P.L., Evans, D., Schneider, J.A., Carrasquillo, M.M., Ertekin-Taner, N., Younkin, S.G., Cruchaga, C., Kauwe, J.S.K., Nowotny, P., Kramer, P., Hardy, J., Huentelman, M.J., Myers, A.J., Barmada, M.M., Demirci, F.Y., Baldwin, C.T., Green, R.C., Rogaeva, E., St George-Hyslop, P., Arnold, S.E., Barber, R., Beach, T., Bigio, E.H., Bowen, J.D., Boxer, A., Burke, J.R., Cairns, N.J., Carlson, C.S., Carney, R.M., Carroll, S.L., Chui, H.C., Clark, D.G., Corneveaux, J., Cotman, C.W., Cummings, J.L., DeCarli, C., DeKosky, S.T., Diaz-Arrastia, R., Dick, M., Dickson, D.W., Ellis, W.G., Faber, K.M., Fallon, K.B., Farlow, M.R., Ferris, S., Frosch, M.P., Galasko, D.R., Ganguli, M., Gearing, M., Geschwind, D.H., Ghetti, B., Gilbert, J.R., Gilman, S., Giordani, B., Glass, J.D., Growdon, J.H., Hamilton, R.L., Harrell, L.E., Head, E., Honig, L.S., Hulette, C.M., Hyman, B.T., Jicha, G.A., Jin, L.-W., Johnson, N., Karlawish, J., Karydas, A., Kaye, J.A., Kim, R., Koo, E.H., Kowall, N.W., Lah, J.J., Levey, A.I., Lieberman, A.P., Lopez, O.L., Mack, W.J., Marson, D.C., Martiniuk, F., Mash, D.C., Masliah, E., McCormick, W.C., McCurry, S.M., McDavid, A.N., McKee, A.C., Mesulam, M., Miller, B.L., Miller, C.A., Miller, J.W., Parisi, J.E., Perl, D.P., Peskind, E., Petersen, R.C., Poon, W.W., Quinn, J.F., Rajbhandary, R.A., Raskind, M., Reisberg, B., Ringman, J.M., Roberson, E.D., Rosenberg, R.N., Sano, M., Schneider, L.S., Seeley, W., Shelanski, M.L., Slifer, M.A., Smith, C.D., Sonnen, J.A., Spina, S., Stern, R.A., Tanzi, R.E., Trojanowski, J.Q., Troncoso, J.C., Van Deerlin, V.M., Vinters, H. V, Vonsattel, J.P., Weintraub, S., Welsh-Bohmer, K.A., Williamson, J., Woltjer, R.L., Cantwell, L.B., Dombroski, B.A., Beekly, D., Lunetta, K.L., Martin, E.R., Kamboh, M.I., Saykin, A.J., Reiman, E.M., Bennett, D.A., Morris, J.C., Montine, T.J., Goate, A.M., Blacker, D., Tsuang, D.W., Hakonarson, H., Kukull, W.A., Foroud, T.M., Haines, J.L., Mayeux, R., Pericak-Vance, M.A., Farrer, L.A., Schellenberg, G.D., 2011. Common variants at MS4A4/MS4A6E, CD2AP, CD33 and EPHA1 are associated with late-onset Alzheimer's disease. Nat. Genet. 43, 436–41. doi:10.1038/ng.801

Najjar, S., Pearlman, D.M., 2015. Neuroinflammation and white matter pathology in schizophrenia: systematic review. Schizophr. Res. 161, 102–112. doi:10.1016/j.schres.2014.04.041

Nathan, C., Calingasan, N., Nezezon, J., Ding, A., Lucia, M.S., La Perle, K., Fuortes, M., Lin, M., Ehrt, S., Kwon, N.S., Chen, J., Vodovotz, Y., Kipiani, K., Beal, M.F., 2005. Protection from Alzheimer's-like disease in the mouse by genetic ablation of inducible nitric oxide synthase. J. Exp. Med. 202, 1163–1169. doi:10.1084/jem.20051529

Nathan, C., Cunningham-Bussel, A., 2013. Beyond oxidative stress: an immunologist's

guide to reactive oxygen species. Nat. Rev. Immunol. 13, 349–61. doi:10.1038/nri3423

Nation, D.A., Sweeney, M.D., Montagne, A., Sagare, A.P., D'Orazio, L.M., Pachicano, M., Sepehrband, F., Nelson, A.R., Buennagel, D.P., Harrington, M.G., Benzinger, T.L.S., Fagan, A.M., Ringman, J.M., Schneider, L.S., Morris, J.C., Chui, H.C., Law, M., Toga, A.W., Zlokovic, B. V., 2019. Blood–brain barrier breakdown is an early biomarker of human cognitive dysfunction. Nat. Med. 25, 270–276. doi:10.1038/s41591-018-0297-y

Nciri, R., Desmoulin, F., Allagui, M.S., Murat, J.-C., Feki, A. El, Vincent, C., Croute, F., 2013. Neuroprotective effects of chronic exposure of SH-SY5Y to low lithium concentration involve glycolysis stimulation, extracellular pyruvate accumulation and resistance to oxidative stress. Int. J. Neuropsychopharmacol. 16, 365–376. doi:10.1017/S1461145712000132

Ndengele, M.M., Muscoli, C., Wang, Z.Q., Doyle, T.M., Matuschak, G.M., Salvemini, D., 2005. Superoxide potentiates NF-kappaB activation and modulates endotoxin-induced cytokine production in alveolar macrophages. Shock 23, 186–93.

Neher, J.J., Neniskyte, U., Zhao, J.-W., Bal-Price, A., Tolkovsky, A.M., Brown, G.C., 2011. Inhibition of microglial phagocytosis is sufficient to prevent inflammatory neuronal death. J. Immunol. 186, 4973–83. doi:10.4049/jimmunol.1003600

Newton, K., Dixit, V.M., 2012. Signaling in innate immunity and inflammation. Cold Spring Harb. Perspect. Biol. 4. doi:10.1101/cshperspect.a006049

Ni, C.-H., Yu, C.-S., Lu, H.-F., Yang, J.-S., Huang, H.-Y., Chen, P.-Y., Wu, S.-H., Ip, S.-W., Chiang, S.-Y., Lin, J.-G., Chung, J.-G., 2014. Chrysophanol-induced cell death (necrosis) in human lung cancer A549 cells is mediated through increasing reactive oxygen species and decreasing the level of mitochondrial membrane potential. Environ. Toxicol. 29, 740–749. doi:10.1002/tox.21801

Ni, R., Marutle, A., Nordberg, A., 2013. Modulation of alpha7 nicotinic acetylcholine receptor and fibrillar amyloid-beta interactions in Alzheimer's disease brain. J. Alzheimer's Dis. 33, 841–851. doi:10.3233/JAD-2012-121447

Niciu, M., Kelmendi, B., Sanacora, G., 2012. Overview of Glutermatergic Neurotransmission in Nervous System. Pharmacol Biochem Behav 100, 656–664. doi:10.1016/j.pbb.2011.08.008.Overview

Nielsen, O.H., Ainsworth, M.A., 2013. Tumor Necrosis Factor Inhibitors for Inflammatory Bowel Disease. N. Engl. J. Med. 369, 754–762. doi:10.1056/NEJMct1209614

Nimmerjahn, A., Kirchhoff, F., Helmchen, F., 2005. Resting microglial cells are highly dynamic surveillants of brain parenchyma in vivo. Science (80-.). 308, 1314–1318. doi:10.1126/science.1110647

Nunomura, A., Perry, G., Aliev, G., Hirai, K., Takeda, A., Balraj, E.K., Jones, P.K., Ghanbari, H., Wataya, T., Shimohama, S., Chiba, S., Atwood, C.S., Petersen, R.B., Smith, M.A., 2001. Oxidative damage is the earliest event in Alzheimer disease. J. Neuropathol. Exp. Neurol. 60, 759–767. doi:10.1093/jnen/60.8.759

O'Neill, L.A.J., Hardie, D.G., 2013. Metabolism of inflammation limited by AMPK and pseudo-starvation. Nature 493, 346–355. doi:10.1038/nature11862

O'Neill, L.A.J., Kishton, R.J., Rathmell, J., 2016. A guide to immunometabolism for immunologists. Nat. Rev. Immunol. 16, 553–65. doi:10.1038/nri.2016.70

O'Neill, L.A.J., Pearce, E.J., 2016. Immunometabolism governs dendritic cell and macrophage function. J. Exp. Med. 213, 15–23. doi:10.1084/jem.20151570

Oe, T., Sasayama, T., Nagashima, T., Muramoto, M., Yamazaki, T., Morikawa, N., Okitsu, O., Nishimura, S., Aoki, T., Katayama, Y., Kita, Y., 2005. Differences in gene expression profile among SH-SY5Y neuroblastoma subclones with different neurite outgrowth responses to nerve growth factor. J. Neurochem. 94, 1264–1276. doi:10.1111/j.1471-4159.2005.03273.x

Ojala, J.O., Sutinen, E.M., 2017. The Role of Interleukin-18, Oxidative Stress and

Metabolic Syndrome in Alzheimer's Disease. J. Clin. Med. 6, 55. doi:10.3390/jcm6050055

Olah, M., Patrick, E., Villani, A.C., Xu, J., White, C.C., Ryan, K.J., Piehowski, P., Kapasi, A., Nejad, P., Cimpean, M., Connor, S., Yung, C.J., Frangieh, M., McHenry, A., Elyaman, W., Petyuk, V., Schneider, J.A., Bennett, D.A., De Jager, P.L., Bradshaw, E.M., 2018. A transcriptomic atlas of aged human microglia. Nat. Commun. 9, 539. doi:10.1038/s41467-018-02926-5

Oliveira, J.M., Henriques, A.G., Martins, F., Rebelo, S., da Cruz e Silva, O.A.B., 2015. Amyloid-β Modulates Both AβPP and Tau Phosphorylation. J. Alzheimers. Dis. 45, 495–507. doi:10.3233/JAD-142664

Olney, J.W., Sharpe, L.G., 1969. Brain lesions in an infant rhesus monkey treated with monsodium glutamate. Science 166, 386–8.

Opazo, C., Huang, X., Cherny, R.A., Moir, R.D., Roher, A.E., White, A.R., Cappai, R., Masters, C.L., Tanzi, R.E., Inestrosa, N.C., Bush, A.I., 2002. Metalloenzyme-like activity of Alzheimer's disease beta-amyloid: Cu-dependent catalytic conversion of dopamine, cholesterol, and biological reducing agents to neurotoxic H2O2. J. Biol. Chem. 277, 40302–40308. doi:10.1074/jbc.M206428200

Orešič, M., Hyötyläinen, T., Herukka, S.-K., Sysi-Aho, M., Mattila, I., Seppänan-Laakso, T., Julkunen, V., Gopalacharyulu, P. V, Hallikainen, M., Koikkalainen, J., Kivipelto, M., Helisalmi, S., Lötjönen, J., Soininen, H., 2011. Metabolome in progression to Alzheimer's disease. Transl. Psychiatry 1, e57–e57. doi:10.1038/tp.2011.55

Orihuela, R., McPherson, C.A., Harry, G.J., 2016. Microglial M1/M2 polarization and metabolic states. Br. J. Pharmacol. 173, 649–65. doi:10.1111/bph.13139

Orre, M., Kamphuis, W., Osborn, L.M., Jansen, A.H.P., Kooijman, L., Bossers, K., Hol, E.M., 2014. Isolation of glia from Alzheimer's mice reveals inflammation and dysfunction. Neurobiol. Aging 35, 2746–2760. doi:10.1016/j.neurobiolaging.2014.06.004

Orsini, F., De Blasio, D., Zangari, R., Zanier, E.R., De Simoni, M.-G., 2014. Versatility of the complement system in neuroinflammation, neurodegeneration and brain homeostasis. Front. Cell. Neurosci. 8, 380. doi:10.3389/fncel.2014.00380

Ossenkoppele, R., Schonhaut, D.R., Schöll, M., Lockhart, S.N., Ayakta, N., Baker, S.L., O'Neil, J.P., Janabi, M., Lazaris, A., Cantwell, A., Vogel, J., Santos, M., Miller, Z.A., Bettcher, B.M., Vossel, K.A., Kramer, J.H., Gorno-Tempini, M.L., Miller, B.L., Jagust, W.J., Rabinovici, G.D., 2016. Tau PET patterns mirror clinical and neuroanatomical variability in Alzheimer's disease. Brain 139, 1551–1567. doi:10.1093/brain/aww027

Ovchinnikov, D.A., 2008. Macrophages in the embryo and beyond: Much more than just giant phagocytes. genesis 46, 447–462. doi:10.1002/dvg.20417

Oz, M., Lorke, D.E., Yang, K.-H.S., Petroianu, G., 2013. On the interaction of β-amyloid peptides and α7-nicotinic acetylcholine receptors in Alzheimer's disease. Curr. Alzheimer Res. 10, 618–30.

Paci, P., Gabriele, S., Ris, L., 2017. A new method allowing long-term potentiation recordings in hippocampal organotypic slices. Brain Behav. 7, e00692. doi:10.1002/brb3.692

Paiva, C.N., Bozza, M.T., 2014. Are reactive oxygen species always detrimental to pathogens? Antioxid. Redox Signal. 20, 1000–37. doi:10.1089/ars.2013.5447

Pallen, M.J., 2011. Time to recognise that mitochondria are bacteria? Trends Microbiol. 19, 58–64. doi:10.1016/j.tim.2010.11.001

Pallo, S.P., DiMaio, J., Cook, A., Nilsson, B., Johnson, G.V.W., 2016. Mechanisms of tau and Aβ-induced excitotoxicity. Brain Res. 1634, 119–131. doi:10.1016/j.brainres.2015.12.048

Palsson-McDermott, E.M., Curtis, A.M., Goel, G., Lauterbach, M.A.R., Sheedy, F.J., Gleeson, L.E., van den Bosch, M.W.M., Quinn, S.R., Domingo-Fernandez, R., Johnston, D.G.W., Jiang, J., Israelsen, W.J., Keane, J., Thomas, C., Clish, C.,

Vander Heiden, M., Xavier, R.J., O'Neill, L.A.J., Xavier, R.J., O'Neill, L.A.J., 2015. Pyruvate Kinase M2 Regulates Hif-1α Activity and IL-1β Induction and Is a Critical Determinant of the Warburg Effect in LPS-Activated Macrophages. Cell Metab. 21, 65–80. doi:10.1016/j.cmet.2014.12.005

Palsson-McDermott, E.M., O'Neill, L.A.J., 2013. The Warburg effect then and now: From cancer to inflammatory diseases. BioEssays 35, 965–973. doi:10.1002/bies.201300084

Palutke, M., KuKuruga, D., Wolfe, D., Roher, A., 1987. Flow cytometric purification of Alzheimer's disease amyloid plaque core protein using thioflavin T. Cytometry 8, 494–9. doi:10.1002/cyto.990080510

Pan, X.D., Zhu, Y.G., Lin, N., Zhang, J., Ye, Q.Y., Huang, H.P., Chen, X.C., 2011. Microglial phagocytosis induced by fibrillar β-amyloid is attenuated by oligomeric β-amyloid: Implications for Alzheimer's disease. Mol. Neurodegener. 6, 45. doi:10.1186/1750-1326-6-45

Panaro, M.A., Acquafredda, A., Sisto, M., Lisi, S., Maffione, A.B., Mitolo, V., 2006. Biological Role of the N-Formyl Peptide Receptors. Immunopharmacol. Immunotoxicol. 28, 103–127. doi:10.1080/08923970600625975

Panayi, G.S., Corrigall, V.M., Henderson, B., 2004. Stress cytokines: pivotal proteins in immune regulatory networks. Curr. Opin. Immunol. 16, 531–534. doi:10.1016/j.coi.2004.05.017

Panza, F., Lozupone, M., Logroscino, G., Imbimbo, B.P., 2019. A critical appraisal of amyloid-β-targeting therapies for Alzheimer disease. Nat. Rev. Neurol. 15, 73–88. doi:10.1038/s41582-018-0116-6

Panza, F., Solfrizzi, V., Seripa, D., Imbimbo, B.P., Lozupone, M., Santamato, A., Tortelli, R., Galizia, I., Prete, C., Daniele, A., Pilotto, A., Greco, A., Logroscino, G., 2016. Tau-based therapeutics for Alzheimer's disease: active and passive immunotherapy. Immunotherapy 8, 1119–1134. doi:10.2217/imt-2016-0019

Paolicelli, R.C., Bolasco, G., Pagani, F., Maggi, L., Scianni, M., Panzanelli, P., Giustetto, M., Ferreira, T.A., Guiducci, E., Dumas, L., Ragozzino, D., Gross, C.T., 2011. Synaptic pruning by microglia is necessary for normal brain development. Science (80-.). 333, 1456–1458. doi:10.1126/science.1202529

Paolicelli, R.C., Jawaid, A., Henstridge, C.M., Valeri, A., Merlini, M., Robinson, J.L., Lee, E.B., Rose, J., Appel, S., Lee, V.M.-Y., Trojanowski, J.Q., Spires-Jones, T., Schulz, P.E., Rajendran, L., 2017. TDP-43 Depletion in Microglia Promotes Amyloid Clearance but Also Induces Synapse Loss. Neuron 95, 297-308.e6. doi:10.1016/j.neuron.2017.05.037

Parajuli, B., Sonobe, Y., Kawanokuchi, J., Doi, Y., Noda, M., Takeuchi, H., Mizuno, T., Suzumura, A., 2012. GM-CSF increases LPS-induced production of proinflammatory mediators via upregulation of TLR4 and CD14 in murine microglia. J. Neuroinflammation 9, 268. doi:10.1186/1742-2094-9-268

Parbo, P., Ismail, R., Hansen, K. V., Amidi, A., Mårup, F.H., Gottrup, H., Brændgaard, H., Eriksson, B.O., Eskildsen, S.F., Lund, T.E., Tietze, A., Edison, P., Pavese, N., Stokholm, M.G., Borghammer, P., Hinz, R., Aanerud, J., Brooks, D.J., 2017. Brain inflammation accompanies amyloid in the majority of mild cognitive impairment cases due to Alzheimer's disease. Brain 140, 2002–2011. doi:10.1093/brain/awx120

Parente, L., Solito, E., 2004. Annexin 1: more than an anti-phospholipase protein. Inflamm. Res. 53, 125–32. doi:10.1007/s00011-003-1235-z

Park, J., Min, J.-S., Kim, B., Chae, U.-B., Yun, J.W., Choi, M.-S., Kong, I.-K., Chang, K.-T., Lee, D.-S., 2015. Mitochondrial ROS govern the LPS-induced pro-inflammatory response in microglia cells by regulating MAPK and NF-κB pathways. Neurosci. Lett. 584, 191–196. doi:10.1016/j.neulet.2014.10.016

Park, J., Wetzel, I., Marriott, I., Dréau, D., D'Avanzo, C., Kim, D.Y., Tanzi, R.E., Cho, H., 2018. A 3D human triculture system modeling neurodegeneration and neuroinflammation in Alzheimer's disease. Nat. Neurosci. 21, 941–951.

doi:10.1038/s41593-018-0175-4

Park, T., Chen, H., Kevala, K., Lee, J.-W., Kim, H.-Y., 2016. N-Docosahexaenoylethanolamine ameliorates LPS-induced neuroinflammation via cAMP/PKA-dependent signaling. J. Neuroinflammation 13, 284. doi:10.1186/s12974-016-0751-z

Parsons, C.G., Danysz, W., Dekundy, A., Pulte, I., 2013. Memantine and cholinesterase inhibitors: Complementary mechanisms in the treatment of Alzheimer's disease. Neurotox. Res. 24, 358–369. doi:10.1007/s12640-013-9398-z

Partida-Sánchez, S., Cockayne, D.A., Monard, S., Jacobson, E.L., Oppenheimer, N., Garvy, B., Kusser, K., Goodrich, S., Howard, M., Harmsen, A., Randall, T.D., Lund, F.E., 2001. Cyclic ADP-ribose production by CD38 regulates intracellular calcium release, extracellular calcium influx and chemotaxis in neutrophils and is required for bacterial clearance in vivo. Nat. Med. 7, 1209–1216. doi:10.1038/nm1101-1209

Pascoal, T.A., Mathotaarachchi, S., Kang, M.S., Mohaddes, S., Shin, M., Park, A.Y., Parent, M.J., Benedet, A.L., Chamoun, M., Therriault, J., Hwang, H., Cuello, A.C., Misic, B., Soucy, J.P., Aston, J.A.D., Gauthier, S., Rosa-Neto, P., 2019. Aβ-induced vulnerability propagates via the brain's default mode network. Nat. Commun. 10, 2353. doi:10.1038/s41467-019-10217-w

Patel, M.M., Patel, B.M., 2017. Crossing the Blood-Brain Barrier: Recent Advances in Drug Delivery to the Brain. CNS Drugs 31, 109–133. doi:10.1007/s40263-016-0405-9

Pearson, H.A., Peers, C., 2006. Physiological roles for amyloid beta peptides. J. Physiol. 575, 5–10. doi:10.1113/jphysiol.2006.111203

Perretti, M., Cooper, D., Dalli, J., Norling, L. V., 2017a. Immune resolution mechanisms in inflammatory arthritis. Nat. Rev. Rheumatol. 13, 87–99. doi:10.1038/nrrheum.2016.193

Perretti, M., D'Acquisto, F., 2009. Annexin A1 and glucocorticoids as effectors of the resolution of inflammation. Nat. Rev. Immunol. 9, 62–70. doi:10.1038/nri2470

Perretti, M., Di Filippo, C., D'Amico, M., Dalli, J., 2017b. Characterizing the anti-inflammatory and tissue protective actions of a novel Annexin A1 peptide. PLoS One 12, e0175786. doi:10.1371/journal.pone.0175786

Perry, E.K., Tomlinson, B.E., Blessed, G., Bergmann, K., Gibson, P.H., Perry, R.H., 1978. Correlation of cholinergic abnormalities with senile plaques and mental test scores in senile dementia. Br. Med. J. 2, 1457–9.

Perry, V.H., Holmes, C., 2014. Microglial priming in neurodegenerative disease. Nat. Rev. Neurol. 10, 217–224. doi:10.1038/nrneurol.2014.38

Perry, V.H., Teeling, J., 2013. Microglia and macrophages of the central nervous system: the contribution of microglia priming and systemic inflammation to chronic neurodegeneration. Semin. Immunopathol. 35, 601–12. doi:10.1007/s00281-013-0382-8

Petri, M.H., Laguna-Fernandez, A., Arnardottir, H., Wheelock, C.E., Perretti, M., Hansson, G.K., Bäck, M., 2017. Aspirin-triggered lipoxin A4 inhibits atherosclerosis progression in apolipoprotein E $^{-/-}$ mice. Br. J. Pharmacol. doi:10.1111/bph.13707

Pike, C.J., Carroll, J.C., Rosario, E.R., Barron, A.M., 2009. Protective actions of sex steroid hormones in Alzheimer's disease. Front. Neuroendocrinol. 30, 239–258. doi:10.1016/j.yfrne.2009.04.015

Pinho, C.M., Teixeira, P.F., Glaser, E., 2014. Mitochondrial import and degradation of amyloid-β peptide. Biochim. Biophys. Acta - Bioenerg. 1837, 1069–1074. doi:10.1016/j.bbabio.2014.02.007

Pivovarova, O., Höhn, A., Grune, T., Pfeiffer, A.F.H., Rudovich, N., 2016. Insulin-degrading enzyme: new therapeutic target for diabetes and Alzheimer's disease? Ann. Med. 48, 614–624. doi:10.1080/07853890.2016.1197416

Plant, L.D., Boyle, J.P., Smith, I.F., Peers, C., Pearson, H.A., 2003. The production of amyloid beta peptide is a critical requirement for the viability of central neurons. J.

Neurosci. 23, 5531–5.

Pliássova, A., Lopes, J.P., Lemos, C., Oliveira, C.R., Cunha, R.A., Agostinho, P., 2015. The Association of Amyloid-β Protein Precursor With α- and β-Secretases in Mouse Cerebral Cortex Synapses Is Altered in Early Alzheimer's Disease. Mol. Neurobiol. doi:10.1007/s12035-015-9491-9

Pollard, A.K., Craig, E.L., Chakrabarti, L., 2016. Mitochondrial Complex 1 Activity Measured by Spectrophotometry Is Reduced across All Brain Regions in Ageing and More Specifically in Neurodegeneration. PLoS One 11, e0157405. doi:10.1371/journal.pone.0157405

Pontecorvo, M.J., Devous, M.D., Kennedy, I., Navitsky, M., Lu, M., Galante, N., Salloway, S., Doraiswamy, P.M., Southekal, S., Arora, A.K., McGeehan, A., Lim, N.C., Xiong, H., Truocchio, S.P., Joshi, A.D., Shcherbinin, S., Teske, B., Fleisher, A.S., Mintun, M.A., 2019. A multicentre longitudinal study of flortaucipir (18F) in normal ageing, mild cognitive impairment and Alzheimer's disease dementia. Brain 142, 1723–1735. doi:10.1093/brain/awz090

Pooler, A.M., Polydoro, M., Wegmann, S.K., Pitstick, R., Kay, K.R., Sanchez, L., Carlson, G.A., Gomez-Isla, T., Albers, M.W., Spires-Jones, T.L., Hyman, B.T., 2013. Tau-amyloid interactions in the rTgTauEC model of early Alzheimer's disease suggest amyloid-induced disruption of axonal projections and exacerbated axonal pathology. J. Comp. Neurol. 521, 4236–4248. doi:10.1002/cne.23411

Popp, J., Oikonomidi, A., Tautvydaitė, D., Dayon, L., Bacher, M., Migliavacca, E., Henry, H., Kirkland, R., Severin, I., Wojcik, J., Bowman, G.L., 2017. Markers of neuroinflammation associated with Alzheimer's disease pathology in older adults. Brain. Behav. Immun. 62, 203–211. doi:10.1016/j.bbi.2017.01.020

Porrini, V., Lanzillotta, A., Branca, C., Benarese, M., Parrella, E., Lorenzini, L., Calzà, L., Flaibani, R., Spano, P.F., Imbimbo, B.P., Pizzi, M., 2015. CHF5074 (CSP-1103) induces microglia alternative activation in plaque-free Tg2576 mice and primary glial cultures exposed to beta-amyloid. Neuroscience 302, 112–120. doi:10.1016/j.neuroscience.2014.10.029

Postina, R., 2012. Activation of α-secretase cleavage. J. Neurochem. 120, 46–54. doi:10.1111/j.1471-4159.2011.07459.x

Postina, R., 2008. A Closer Look at alpha-Secretase. Curr. Alzheimer Res. 179–186. doi:10.2174/156720508783954668

Prevete, N., Liotti, F., Marone, G., Melillo, R.M., de Paulis, A., 2015. Formyl peptide receptors at the interface of inflammation, angiogenesis and tumor growth. Pharmacol. Res. 102, 184–191. doi:10.1016/j.phrs.2015.09.017

Prince, M., Bryce, R., Albanese, E., Wimo, A., Ribeiro, W., Ferri, C.P., 2013. The global prevalence of dementia: a systematic review and metaanalysis. Alzheimers Dement 9, 63-75 e2. doi:10.1016/j.jalz.2012.11.007

Prince, M., Knapp, M., Guerchet, M., McCrone, P., Prina, M., Comas-Herrera, A., Wittenberg, R., Adelaja, B., Hu, B., King, D., Rehill, A., Salimkumar, D., 2014. Dementia UK: Update. Alzheimer's Society, London. doi:10.1007/s13398-014-0173-7.2

Prince, M., Wimo, A., Guerchet, M., Gemma-Claire, A., Wu, Y.-T., Prina, M., 2015. World Alzheimer Report 2015: The Global Impact of Dementia - An analysis of prevalence, incidence, cost and trends. Alzheimer's Dis. Int. 84. doi:10.1111/j.0963-7214.2004.00293.x

Purvis, G.S.D., Collino, M., Loiola, R.A., Baragetti, A., Chiazza, F., Brovelli, M., Sheikh, M.H., Collotta, D., Cento, A., Mastrocola, R., Aragno, M., Cutrin, J.C., Reutelingsperger, C., Grigore, L., Catapano, A.L., Yaqoob, M.M., Norata, G.D., Solito, E., Thiemermann, C., 2019. Identification of Annexina1 as an endogenous regulator of RhoA, and its role in the pathophysiology and experimental therapy of type-2 diabetes. Front. Immunol. 10, 571. doi:10.3389/fimmu.2019.00571

Puzzo, D., Privitera, L., Leznik, E., Fa, M., Staniszewski, A., Palmeri, A., Arancio, O.,

2008. Picomolar amyloid-b positively modulates synaptic plasticity and memory in hippocampus. J. Neurosci. 28, 14537–14545. doi:10.1523/jneurosci.2692-08.2008

Qin, C.X., May, L.T., Li, R., Cao, N., Rosli, S., Deo, M., Alexander, A.E., Horlock, D., Bourke, J.E., Yang, Y.H., Stewart, A.G., Kaye, D.M., Du, X.-J., Sexton, P.M., Christopoulos, A., Gao, X.-M., Ritchie, R.H., 2017. Small-molecule-biased formyl peptide receptor agonist compound 17b protects against myocardial ischaemia-reperfusion injury in mice. Nat. Commun. 8, 14232. doi:10.1038/ncomms14232

Qin, L., Crews, F.T., 2012. NADPH oxidase and reactive oxygen species contribute to alcohol-induced microglial activation and neurodegeneration. J. Neuroinflammation 9, 491. doi:10.1186/1742-2094-9-5

Qin, L., Liu, Y., Cooper, C., Liu, B., Wilson, B., Hong, J.S., 2002. Microglia enhance β-amyloid peptide-induced toxicity in cortical and mesencephalic neurons by producing reactive oxygen species. J. Neurochem. 83, 973–983. doi:10.1046/j.1471-4159.2002.01210.x

Quiroz, Y.T., Sperling, R.A., Norton, D.J., Baena, A., Arboleda-Velasquez, J.F., Cosio, D., Schultz, A., Lapoint, M., Guzman-Velez, E., Miller, J.B., Kim, L.A., Chen, K., Tariot, P.N., Lopera, F., Reiman, E.M., Johnson, K.A., 2018. Association between amyloid and tau accumulation in young adults with autosomal dominant Alzheimer disease. JAMA Neurol. 75, 548–556. doi:10.1001/jamaneurol.2017.4907

Radi, R., 2018. Oxygen radicals, nitric oxide, and peroxynitrite: Redox pathways in molecular medicine. Proc. Natl. Acad. Sci. 115, 5839–5848. doi:10.1073/pnas.1804932115

Ragsdale, R.L., Grasso, R.J., 1989. An improved spectrofluorometric assay for quantitating yeast phagocytosis in cultures of murine peritoneal macrophages. J. Immunol. Methods 123, 259–67.

Raikwar, S.P., Thangavel, R., Dubova, I., Selvakumar, G.P., Ahmed, M.E., Kempuraj, D., Zaheer, S.A., Iyer, S.S., Zaheer, A., 2019. Targeted Gene Editing of Glia Maturation Factor in Microglia: a Novel Alzheimer's Disease Therapeutic Target. Mol. Neurobiol. 56, 378–393. doi:10.1007/s12035-018-1068-y

Rajaiah, R., Perkins, D.J., Ireland, D.D.C., Vogel, S.N., 2015. CD14 dependence of TLR4 endocytosis and TRIF signaling displays ligand specificity and is dissociable in endotoxin tolerance. Proc. Natl. Acad. Sci. U. S. A. 112, 8391–6. doi:10.1073/pnas.1424980112

Rajaram, M.V.S., Arnett, E., Azad, A.K., Guirado, E., Ni, B., Gerberick, A.D., He, L.Z., Keler, T., Thomas, L.J., Lafuse, W.P., Schlesinger, L.S., 2017. M. tuberculosis-Initiated Human Mannose Receptor Signaling Regulates Macrophage Recognition and Vesicle Trafficking by FcRγ-Chain, Grb2, and SHP-1. Cell Rep. 21, 126–140. doi:10.1016/j.celrep.2017.09.034

Ransohoff, R.M., El Khoury, J., 2015. Microglia in Health and Disease. Cold Spring Harb. Perspect. 8, a020560. doi:10.1016/j.mito.2018.06.006

Ransohoff, R.M., Schafer, D., Vincent, A., Blachère, N.E., Bar-Or, A., 2015. Neuroinflammation: Ways in Which the Immune System Affects the Brain. Neurotherapeutics 12, 896–909. doi:10.1007/s13311-015-0385-3

Raux, G., 2005. Molecular diagnosis of autosomal dominant early onset Alzheimer's disease: an update. J. Med. Genet. 42, 793–795. doi:10.1136/jmg.2005.033456

Rawson, F.J., Hicks, J., Dodd, N., Abate, W., Garrett, D.J., Yip, N., Fejer, G., Downard, A.J., R Baronian, K.H., Jackson, S.K., Mendes, P.M., 2015. Fast, Ultrasensitive Detection of Reactive Oxygen Species Using a Carbon Nanotube Based-Electrocatalytic Intracellular Sensor. doi:10.1021/acsami.5b06493

Reiman, E.M., Chen, K., Liu, X., Bandy, D., Yu, M., Lee, W., Ayutyanont, N., Keppler, J., Reeder, S.A., Langbaum, J.B.S., Alexander, G.E., Klunk, W.E., Mathis, C.A., Price, J.C., Aizenstein, H.J., DeKosky, S.T., Caselli, R.J., 2009. Fibrillar amyloid- burden in cognitively normal people at 3 levels of genetic risk for Alzheimer's disease. Proc. Natl. Acad. Sci. U. S. A. 106, 6820–6825. doi:10.1073/pnas.0900345106

Reines, S.A., Block, G.A., Morris, J.C., Liu, G., Nessly, M.L., Lines, C.R., Norman, B.A., Baranak, C.C., Rofecoxib Protocol 091 Study Group, 2004. Rofecoxib: no effect on Alzheimer's disease in a 1-year, randomized, blinded, controlled study. Neurology 62, 66–71.

Réu, P., Khosravi, A., Bernard, S., Mold, J.E., Salehpour, M., Alkass, K., Perl, S., Tisdale, J., Possnert, G., Druid, H., Frisén, J., 2017. The Lifespan and Turnover of Microglia in the Human Brain. Cell Rep. 20, 779–784. doi:10.1016/j.celrep.2017.07.004

Ries, M., Loiola, R., Shah, U.N., Gentleman, S.M., Solito, E., Sastre, M., 2016. The anti-inflammatory Annexin A1 induces the clearance and degradation of the amyloid-β peptide. J. Neuroinflammation 13, 234. doi:10.1186/s12974-016-0692-6

Ries, M., Sastre, M., 2016. Mechanisms of Aβ clearance and degradation by glial cells. Front. Aging Neurosci. doi:10.3389/fnagi.2016.00160

Ripoli, C., Cocco, S., Li Puma, D.D., Piacentini, R., Mastrodonato, A., Scala, F., Puzzo, D., D'Ascenzo, M., Grassi, C., 2014. Intracellular Accumulation of Amyloid-β (Aβ) Protein Plays a Major Role in Aβ-Induced Alterations of Glutamatergic Synaptic Transmission and Plasticity. J. Neurosci. 34, 12893–12903. doi:10.1523/jneurosci.1201-14.2014

Ritzel, R.M., Patel, A.R., Pan, S., Crapser, J., Hammond, M., Jellison, E., McCullough, L.D., 2015. Age- and location-related changes in microglial function. Neurobiol. Aging 36, 2153–63. doi:10.1016/j.neurobiolaging.2015.02.016

Rivera, A., Siracusa, M.C., Yap, G.S., Gause, W.C., 2016. Innate cell communication kick-starts pathogen-specific immunity. Nat. Immunol. 17, 356–363. doi:10.1038/ni.3375

Rodríguez-Prados, J.-C., Través, P.G., Cuenca, J., Rico, D., Aragonés, J., Martín-Sanz, P., Cascante, M., Boscá, L., 2010. Substrate fate in activated macrophages: a comparison between innate, classic, and alternative activation. J. Immunol. 185, 605–14. doi:10.4049/jimmunol.0901698

Rogaev, E.I., Sherrington, R., Rogaeva, E. a, Levesque, G., Ikeda, M., Liang, Y., Chi, H., Lin, C., Holman, K., Tsuda, T., 1995. Familial Alzheimer's disease in kindreds with missense mutations in a gene on chromosome 1 related to the Alzheimer's disease type 3 gene. Nature 376, 775–778. doi:10.1038/376775a0

Rogers, J.T., Morganti, J.M., Bachstetter, A.D., Hudson, C.E., Peters, M.M., Grimmig, B.A., Weeber, E.J., Bickford, P.C., Gemma, C., 2011. CX3CR1 deficiency leads to impairment of hippocampal cognitive function and synaptic plasticity. J. Neurosci. 31, 16241–50. doi:10.1523/JNEUROSCI.3667-11.2011

Romero-Calvo, I., Ocón, B., Martínez-Moya, P., Suárez, M.D., Zarzuelo, A., Martínez-Augustin, O., de Medina, F.S., 2010. Reversible Ponceau staining as a loading control alternative to actin in Western blots. Anal. Biochem. 401, 318–320. doi:10.1016/j.ab.2010.02.036

Rosales-Corral, S., Acuna-Castroviejo, D., Tan, D.X., López-Armas, G., Cruz-Ramos, J., Munoz, R., Melnikov, V.G., Manchester, L.C., Reiter, R.J., 2012. Accumulation of Exogenous Amyloid-Beta Peptide in Hippocampal Mitochondria Causes Their Dysfunction: A Protective Role for Melatonin. Oxid. Med. Cell. Longev. 2012, 1–15. doi:10.1155/2012/843649

Rovelet-Lecrux, A., Legallic, S., Wallon, D., Flaman, J.-M., Martinaud, O., Bombois, S., Rollin-Sillaire, A., Michon, A., Le Ber, I., Pariente, J., Puel, M., Paquet, C., Croisile, B., Thomas-Antérion, C., Vercelletto, M., Lévy, R., Frébourg, T., Hannequin, D., Campion, D., 2012. A genome-wide study reveals rare CNVs exclusive to extreme phenotypes of Alzheimer disease. Eur. J. Hum. Genet. 20, 613–7. doi:10.1038/ejhg.2011.225

Rubartelli, A., Lotze, M.T., 2007. Inside, outside, upside down: damage-associated molecular-pattern molecules (DAMPs) and redox. Trends Immunol. 28, 429–436. doi:10.1016/j.it.2007.08.004

Ruska, E., 1986. The emergence of the electron microscope: Connection between Realization and First Patent Application, Documents of an Invention. J. Ultrastruct.

Mol. Struct. Res. 95, 3–28. doi:10.1016/0889-1605(86)90025-X

Russo, I., Bubacco, L., Greggio, E., 2014. LRRK2 and neuroinflammation: partners in crime in Parkinson's disease? J. Neuroinflammation 11, 52. doi:10.1186/1742-2094-11-52

Sabaté, R., Estelrich, J., 2005. Evidence of the existence of micelles in the fibrillogenesis of beta-amyloid peptide. J. Phys. Chem. B 109, 11027–32. doi:10.1021/jp050716m

Sáez-Orellana, F., Godoy, P.A., Bastidas, C.Y., Silva-Grecchi, T., Guzmán, L., Aguayo, L.G., Fuentealba, J., 2016. ATP leakage induces P2XR activation and contributes to acute synaptic excitotoxicity induced by soluble oligomers of β-amyloid peptide in hippocampal neurons. Neuropharmacology 100, 116–123. doi:10.1016/j.neuropharm.2015.04.005

Saido, T., Leissring, M.A., 2012. Proteolytic degradation of amyloid β-protein. Cold Spring Harb. Perspect. Med. 2, a006379. doi:10.1101/cshperspect.a006379

Sala Frigerio, C., Wolfs, L., Fattorelli, N., Thrupp, N., Voytyuk, I., Schmidt, I., Mancuso, R., Chen, W.-T., Woodbury, M.E., Srivastava, G., Möller, T., Hudry, E., Das, S., Saido, T., Karran, E., Hyman, B., Perry, V.H., Fiers, M., De Strooper, B., 2019. The Major Risk Factors for Alzheimer's Disease: Age, Sex, and Genes Modulate the Microglia Response to Aβ Plaques. Cell Rep. 27, 1293-1306.e6. doi:10.1016/j.celrep.2019.03.099

Salloway, S., Sperling, R., Fox, N.C., Blennow, K., Klunk, W., Raskind, M., Sabbagh, M., Honig, L.S., Porsteinsson, A.P., Ferris, S., Reichert, M., Ketter, N., Nejadnik, B., Guenzler, V., Miloslavsky, M., Wang, D., Lu, Y., Lull, J., Tudor, I.C., Liu, E., Grundman, M., Yuen, E., Black, R., Brashear, H.R., Bapineuzumab 301 and 302 Clinical Trial Investigators, 2014. Two Phase 3 Trials of Bapineuzumab in Mild-to-Moderate Alzheimer's Disease. N. Engl. J. Med. 370, 322–333. doi:10.1056/NEJMoa1304839

Salminen, A., Ojala, J., Kauppinen, A., Kaarniranta, K., Suuronen, T., 2009. Inflammation in Alzheimer's disease: Amyloid-β oligomers trigger innate immunity defence via pattern recognition receptors. Prog. Neurobiol. 87, 181–194. doi:10.1016/j.pneurobio.2009.01.001

Salter, M.W., Beggs, S., 2014. Sublime microglia: expanding roles for the guardians of the CNS. Cell 158, 15–24. doi:10.1016/j.cell.2014.06.008

Salter, M.W., Stevens, B., 2017. Microglia emerge as central players in brain disease. Nat. Med. 23, 1018–1027. doi:10.1038/nm.4397

Salvi, V., Sozio, F., Sozzani, S., Del Prete, A., 2017. Role of Atypical Chemokine Receptors in Microglial Activation and Polarization. Front. Aging Neurosci. 9, 148. doi:10.3389/fnagi.2017.00148

Sanders, N.T., Dutson, D.J., Durrant, J.W., Lewis, J.B., Wilcox, S.H., Winden, D.R., Arroyo, J.A., Bikman, B.T., Reynolds, P.R., 2017. Cigarette smoke extract (CSE) induces RAGE-mediated inflammation in the Ca9-22 gingival carcinoma epithelial cell line. Arch. Oral Biol. 80, 95–100. doi:10.1016/j.archoralbio.2017.03.021

SanMartín, C.D., Veloso, P., Adasme, T., Lobos, P., Bruna, B., Galaz, J., García, A., Hartel, S., Hidalgo, C., Paula-Lima, A.C., 2017. RyR2-Mediated Ca2+ Release and Mitochondrial ROS Generation Partake in the Synaptic Dysfunction Caused by Amyloid β Peptide Oligomers. Front. Mol. Neurosci. 10, 115. doi:10.3389/fnmol.2017.00115

Sansbury, B.E., Spite, M., 2016. Resolution of Acute Inflammation and the Role of Resolvins in Immunity, Thrombosis, and Vascular Biology. Circ. Res. 119, 113–30. doi:10.1161/CIRCRESAHA.116.307308

Santoni, G., Cardinali, C., Morelli, M., Santoni, M., Nabissi, M., Amantini, C., 2015. Danger- and pathogen-associated molecular patterns recognition by pattern-recognition receptors and ion channels of the transient receptor potential family triggers the inflammasome activation in immune cells and sensory neurons. J. Neuroinflammation 12, 21. doi:10.1186/s12974-015-0239-2

Saraiva, M., O'Garra, A., 2010. The regulation of IL-10 production by immune cells. Nat. Rev. Immunol. 10, 170–181. doi:10.1038/nri2711

Sasaki, A., Yamaguchi, H., Horikoshi, Y., Tanaka, G., Nakazato, Y., 2004. Expression of glucose transporter 5 by microglia in human gliomas. Neuropathol. Appl. Neurobiol. 30, 447–455. doi:10.1111/j.1365-2990.2004.00556.x

Sastre, M., Walter, J., Gentleman, S.M., 2008. Interactions between APP secretases and inflammatory mediators. J. Neuroinflammation 5, 25. doi:10.1186/1742-2094-5-25

Sato, N., Morishita, R., 2014. Brain alterations and clinical symptoms of dementia in diabetes: aβ/tau-dependent and independent mechanisms. Front. Endocrinol. (Lausanne). 5, 143. doi:10.3389/fendo.2014.00143

Savage, J.C., Jay, T., Goduni, E., Quigley, C., Mariani, M.M., Malm, T., Ransohoff, R.M., Lamb, B.T., Landreth, G.E., 2015. Nuclear Receptors License Phagocytosis by Trem2+ Myeloid Cells in Mouse Models of Alzheimer's Disease. J. Neurosci. 35, 6532–6543. doi:10.1523/JNEUROSCI.4586-14.2015

Schafer, D.P., Lehrman, E.K., Kautzman, A.G., Koyama, R., Mardinly, A.R., Yamasaki, R., Ransohoff, R.M., Greenberg, M.E., Barres, B.A., Stevens, B., 2012. Microglia Sculpt Postnatal Neural Circuits in an Activity and Complement-Dependent Manner. Neuron 74, 691–705. doi:10.1016/j.neuron.2012.03.026

Schepetkin, I.A., Khlebnikov, A.I., Giovannoni, M.P., Kirpotina, L.N., Cilibrizzi, A., Quinn, M.T., 2014. Development of small molecule non-peptide formyl peptide receptor (FPR) ligands and molecular modeling of their recognition. Curr. Med. Chem. 21, 1478–504.

Schmiedel, B.J., Singh, D., Madrigal, A., Valdovino-Gonzalez, A.G., White, B.M., Zapardiel-Gonzalo, J., Ha, B., Altay, G., Greenbaum, J.A., McVicker, G., Seumois, G., Rao, A., Kronenberg, M., Peters, B., Vijayanand, P., 2018. Impact of Genetic Polymorphisms on Human Immune Cell Gene Expression. Cell 175, 1701-1715.e16. doi:10.1016/j.cell.2018.10.022

Schurr, A., Payne, R.S., Miller, J.J., Rigor, B.M., 1997. Glia are the main source of lactate utilized by neurons for recovery of function posthypoxia. Brain Res. 774, 221–4. doi:10.1016/s0006-8993(97)81708-8

Scialò, F., Fernández-Ayala, D.J., Sanz, A., 2017. Role of Mitochondrial Reverse Electron Transport in ROS Signaling: Potential Roles in Health and Disease. Front. Physiol. 8, 428. doi:10.3389/fphys.2017.00428

Sehlin, D., Fang, X.T., Cato, L., Antoni, G., Lannfelt, L., Syvänen, S., 2016. Antibody-based PET imaging of amyloid beta in mouse models of Alzheimer's disease. Nat. Commun. 7, 10759. doi:10.1038/ncomms10759

Sepulveda, F.J., Parodi, J., Peoples, R.W., Opazo, C., Aguayo, L.G., 2010. Synaptotoxicity of Alzheimer Beta Amyloid Can Be Explained by Its Membrane Perforating Property. PLoS One 5, e11820. doi:10.1371/journal.pone.0011820

Serhan, C.N., Chiang, N., Dalli, J., 2015. The resolution code of acute inflammation: Novel pro-resolving lipid mediators in resolution. Semin. Immunol. 27, 200–215. doi:10.1016/j.smim.2015.03.004

Serrano-Pozo, A., Frosch, M.P., Masliah, E., Hyman, B.T., 2011. Neuropathological Alterations in Alzheimer Disease. Cold Spring Harb. Perspect. Med. 1, a006189. doi:10.1101/cshperspect.a006189

Serrano-Pozo, A., Gómez-Isla, T., Growdon, J.H., Frosch, M.P., Hyman, B.T., 2013. A Phenotypic Change But Not Proliferation Underlies Glial Responses in Alzheimer Disease. Am. J. Pathol. 182, 2332–2344. doi:10.1016/j.ajpath.2013.02.031

Serres, S., Bezancon, E., Franconi, J.-M., Merle, M., 2005. Ex vivo NMR study of lactate metabolism in rat brain under various depressed states. J. Neurosci. Res. 79, 19–25. doi:10.1002/jnr.20277

Seshadri, S., Beiser, A., Kelly-Hayes, M., Kase, C.S., Au, R., Kannel, W.B., Wolf, P.A., 2006. The Lifetime Risk of Stroke: Estimates From the Framingham Study. Stroke

37, 345–350. doi:10.1161/01.STR.0000199613.38911.b2

Shankar, G.M., Li, S., Mehta, T.H., Garcia-Munoz, A., Shepardson, N.E., Smith, I., Brett, F.M., Farrell, M.A., Rowan, M.J., Lemere, C.A., Regan, C.M., Walsh, D.M., Sabatini, B.L., Selkoe, D.J., 2008. Amyloid-β protein dimers isolated directly from Alzheimer's brains impair synaptic plasticity and memory. Nat. Med. 14, 837–842. doi:10.1038/nm1782

Shannon, B.J., Vaishnavi, S.N., Vlassenko, A.G., Shimony, J.S., Rutlin, J., Raichle, M.E., 2016. Brain aerobic glycolysis and motor adaptation learning. Proc. Natl. Acad. Sci. 113, E3782–E3791. doi:10.1073/pnas.1604977113

Sharba, S., Venkatakrishnan, V., Padra, M., Winther, M., Gabl, M., Sundqvist, M., Wang, J., Forsman, H., Linden, S.K., 2019. Formyl peptide receptor 2 orchestrates mucosal protection against Citrobacter rodentium infection. Virulence 10, 610–624. doi:10.1080/21505594.2019.1635417

Shen, Y., Joachimiak, A., Rich Rosner, M., Tang, W.-J., 2006. Structures of human insulin-degrading enzyme reveal a new substrate recognition mechanism. Nature 443, 870–874. doi:10.1038/nature05143

Sheng, J., Ruedl, C., Karjalainen, K., 2015. Most Tissue-Resident Macrophages Except Microglia Are Derived from Fetal Hematopoietic Stem Cells. Immunity 43, 382–93. doi:10.1016/j.immuni.2015.07.016

Shepherd, C., McCann, H., Halliday, G.M., 2009. Variations in the neuropathology of familial Alzheimer's disease. Acta Neuropathol. 118, 37–52. doi:10.1007/s00401-009-0521-4

Sherrington, R., Rogaev, E.I., Liang, Y., Rogaeva, E.A., Levesque, G., Ikeda, M., Chi, H., Lin, C., Li, G., Holman, K., Tsuda, T., Mar, L., Foncin, J.F., Bruni, A.C., Montesi, M.P., Sorbi, S., Rainero, I., Pinessi, L., Nee, L., Chumakov, I., Pollen, D., Brookes, A., Sanseau, P., Polinsky, R.J., Wasco, W., Da Silva, H.A., Haines, J.L., Perkicak-Vance, M.A., Tanzi, R.E., Roses, A.D., Fraser, P.E., Rommens, J.M., St George-Hyslop, P.H., 1995. Cloning of a gene bearing missense mutations in early-onset familial Alzheimer's disease. Nature 375, 754–760. doi:10.1038/375754a0

Shi, J.-Q., Shen, W., Chen, J., Wang, B.-R., Zhong, L.-L., Zhu, Y.-W., Zhu, H.-Q., Zhang, Q.-Q., Zhang, Y.-D., Xu, J., 2011. Anti-TNF-α reduces amyloid plaques and tau phosphorylation and induces CD11c-positive dendritic-like cell in the APP/PS1 transgenic mouse brains. Brain Res. 1368, 239–47. doi:10.1016/j.brainres.2010.10.053

Shi, Y., Holtzman, D.M., 2018. Interplay between innate immunity and Alzheimer disease: APOE and TREM2 in the spotlight. Nat. Rev. Immunol. 18, 759–772. doi:10.1038/s41577-018-0051-1

Shi, Y., Yamada, K., Liddelow, S.A., Smith, S.T., Zhao, L., Luo, W., Tsai, R.M., Spina, S., Grinberg, L.T., Rojas, J.C., Gallardo, G., Wang, K., Roh, J., Robinson, G., Finn, M.B., Jiang, H., Sullivan, P.M., Baufeld, C., Wood, M.W., Sutphen, C., McCue, L., Xiong, C., Del-Aguila, J.L., Morris, J.C., Cruchaga, C., Fagan, A.M., Miller, B.L., Boxer, A.L., Seeley, W.W., Butovsky, O., Barres, B.A., Paul, S.M., Holtzman, D.M., Holtzman, D.M., 2017. ApoE4 markedly exacerbates tau-mediated neurodegeneration in a mouse model of tauopathy. Nature 549, 523–527. doi:10.1038/nature24016

Shih, R.-H., Wang, C.-Y., Yang, C.-M., 2015. NF-kappaB Signaling Pathways in Neurological Inflammation: A Mini Review. Front. Mol. Neurosci. 8, 1–8. doi:10.3389/fnmol.2015.00077

Shipley, M.M., Mangold, C.A., Szpara, M.L., 2016. Differentiation of the SH-SY5Y Human Neuroblastoma Cell Line. J. Vis. Exp. 53193. doi:10.3791/53193

Shoeb, M., Ansari, N.H., Srivastava, S.K., Ramana, K. V, 2014. 4-Hydroxynonenal in the pathogenesis and progression of human diseases. Curr. Med. Chem. 21, 230–7.

Shulman, R.G., Blamire, A.M., Rothman, D.L., McCarthy, G., 1993. Nuclear magnetic resonance imaging and spectroscopy of human brain function. Proc. Natl. Acad. Sci.

90, 3127–3133. doi:10.1073/pnas.90.8.3127

Sica, A., Mantovani, A., 2012. Macrophage plasticity and polarization: in vivo veritas. J. Clin. Invest. 122, 787–795. doi:10.1172/JCI59643

Siddiqui, T.A., Lively, S., Schlichter, L.C., 2016. Complex molecular and functional outcomes of single versus sequential cytokine stimulation of rat microglia. J. Neuroinflammation 13, 66. doi:10.1186/s12974-016-0531-9

Sierra, A., de Castro, F., del Río-Hortega, J., Rafael Iglesias-Rozas, J., Garrosa, M., Kettenmann, H., 2016. The “Big-Bang” for modern glial biology: Translation and comments on Pío del Río-Hortega 1919 series of papers on microglia. Glia 64, 1801–1840. doi:10.1002/glia.23046

Silhavy, T.J., Kahne, D., Walker, S., 2010. The Bacterial Cell Envelope. Cold Spring Harb. Perspect. Biol. 2, a000414–a000414. doi:10.1101/cshperspect.a000414

Silverman, S.M., Kim, B.J., Howell, G.R., Miller, J., John, S.W.M., Wordinger, R.J., Clark, A.F., 2016. C1q propagates microglial activation and neurodegeneration in the visual axis following retinal ischemia/reperfusion injury. Mol. Neurodegener. 11, 24. doi:10.1186/s13024-016-0089-0

Šimić, G., Babić Leko, M., Wray, S., Harrington, C., Delalle, I., Jovanov-Milošević, N., Bažadona, D., Buée, L., de Silva, R., Giovanni, G. Di, Wischik, C., Hof, P.R., 2016. Tau protein hyperphosphorylation and aggregation in alzheimer’s disease and other tauopathies, and possible neuroprotective strategies. Biomolecules 6, 2–28. doi:10.3390/biom6010006

Sims, R., van der Lee, S.J., Naj, A.C., Bellenguez, C., Badarinarayan, N., Jakobsdottir, J., Kunkle, B.W., Boland, A., Raybould, R., Bis, J.C., Martin, E.R., Grenier-Boley, B., Heilmann-Heimbach, S., Chouraki, V., Kuzma, A.B., Sleegers, K., Vronskaya, M., Ruiz, A., Graham, R.R., Olaso, R., Hoffmann, P., Grove, M.L., Vardarajan, B.N., Hiltunen, M., Nöthen, M.M., White, C.C., Hamilton-Nelson, K.L., Epelbaum, J., Maier, W., Choi, S.-H., Beecham, G.W., Dulary, C., Herms, S., Smith, A. V, Funk, C.C., Derbois, C., Forstner, A.J., Ahmad, S., Li, H., Bacq, D., Harold, D., Satizabal, C.L., Valladares, O., Squassina, A., Thomas, R., Brody, J.A., Qu, L., Sánchez-Juan, P., Morgan, T., Wolters, F.J., Zhao, Y., Garcia, F.S., Denning, N., Fornage, M., Malamon, J., Naranjo, M.C.D., Majounie, E., Mosley, T.H., Dombroski, B., Wallon, D., Lupton, M.K., Dupuis, J., Whitehead, P., Fratiglioni, L., Medway, C., Jian, X., Mukherjee, S., Keller, L., Brown, K., Lin, H., Cantwell, L.B., Panza, F., McGuinness, B., Moreno-Grau, S., Burgess, J.D., Solfrizzi, V., Proitsi, P., Adams, H.H., Allen, M., Seripa, D., Pastor, P., Cupples, L.A., Price, N.D., Hannequin, D., Frank-García, A., Levy, D., Chakrabarty, P., Caffarra, P., Giegling, I., Beiser, A.S., Giedraitis, V., Hampel, H., Garcia, M.E., Wang, X., Lannfelt, L., Mecocci, P., Eiriksdottir, G., Crane, P.K., Pasquier, F., Boccardi, V., Henández, I., Barber, R.C., Scherer, M., Tarraga, L., Adams, P.M., Leber, M., Chen, Y., Albert, M.S., Riedel-Heller, S., Emilsson, V., Beekly, D., Braae, A., Schmidt, R., Blacker, D., Masullo, C., Schmidt, H., Doody, R.S., Spalletta, G., Jr, W.T.L., Fairchild, T.J., Bossù, P., Lopez, O.L., Frosch, M.P., Sacchinelli, E., Ghetti, B., Yang, Q., Huebinger, R.M., Jessen, F., Li, S., Kamboh, M.I., Morris, J., Sotolongo-Grau, O., Katz, M.J., Corcoran, C., Dunstan, M., Braddel, A., Thomas, C., Meggy, A., Marshall, R., Gerrish, A., Chapman, J., Aguilar, M., Taylor, S., Hill, M., Fairén, M.D., Hodges, A., Vellas, B., Soininen, H., Kloszewska, I., Daniilidou, M., Uphill, J., Patel, Y., Hughes, J.T., Lord, J., Turton, J., Hartmann, A.M., Cecchetti, R., Fenoglio, C., Serpente, M., Arcaro, M., Caltagirone, C., Orfei, M.D., Ciaramella, A., Pichler, S., Mayhaus, M., Gu, W., Lleó, A., Fortea, J., Blesa, R., Barber, I.S., Brookes, K., Cupidi, C., Maletta, R.G., Carrell, D., Sorbi, S., Moebus, S., Urbano, M., Pilotto, A., Kornhuber, J., Bosco, P., Todd, S., Craig, D., Johnston, J., Gill, M., Lawlor, B., Lynch, A., Fox, N.C., Hardy, J., Albin, R.L., Apostolova, L.G., Arnold, S.E., Asthana, S., Atwood, C.S., Baldwin, C.T., Barnes, L.L., Barral, S., Beach, T.G., Becker, J.T., Bigio, E.H., Bird, T.D., Boeve, B.F., Bowen, J.D., Boxer, A., Burke, J.R., Burns, J.M., Buxbaum, J.D., Cairns, N.J., Cao, C., Carlson, C.S., Carlsson, C.M., Carney, R.M., Carrasquillo, M.M., Carroll, S.L., Diaz, C.C., Chui, H.C., Clark, D.G., Cribbs, D.H., Crocco, E.A., DeCarli, C., Dick, M., Duara, R., Evans, D.A., Faber, K.M., Fallon, K.B., Fardo, D.W., Farlow, M.R., Ferris, S., Foroud, T.M.,

Galasko, D.R., Gearing, M., Geschwind, D.H., Gilbert, J.R., Graff-Radford, N.R., Green, R.C., Growdon, J.H., Hamilton, R.L., Harrell, L.E., Honig, L.S., Huentelman, M.J., Hulette, C.M., Hyman, B.T., Jarvik, G.P., Abner, E., Jin, L.-W., Jun, G., Karydas, A., Kaye, J.A., Kim, R., Kowall, N.W., Kramer, J.H., LaFerla, F.M., Lah, J.J., Leverenz, J.B., Levey, A.I., Li, G., Lieberman, A.P., Lunetta, K.L., Lyketsos, C.G., Marson, D.C., Martiniuk, F., Mash, D.C., Masliah, E., McCormick, W.C., McCurry, S.M., McDavid, A.N., McKee, A.C., Mesulam, M., Miller, B.L., Miller, C.A., Miller, J.W., Morris, J.C., Murrell, J.R., Myers, A.J., O'Bryant, S., Olichney, J.M., Pankratz, V.S., Parisi, J.E., Paulson, H.L., Perry, W., Peskind, E., Pierce, A., Poon, W.W., Potter, H., Quinn, J.F., Raj, A., Raskind, M., Reisberg, B., Reitz, C., Ringman, J.M., Roberson, E.D., Rogaeva, E., Rosen, H.J., Rosenberg, R.N., Sager, M.A., Saykin, A.J., Schneider, J.A., Schneider, L.S., Seeley, W.W., Smith, A.G., Sonnen, J.A., Spina, S., Stern, R.A., Swerdlow, R.H., Tanzi, R.E., Thornton-Wells, T.A., Trojanowski, J.Q., Troncoso, J.C., Van Deerlin, V.M., Van Eldik, L.J., Vinters, H. V, Vonsattel, J.P., Weintraub, S., Welsh-Bohmer, K.A., Wilhelmsen, K.C., Williamson, J., Wingo, T.S., Woltjer, R.L., Wright, C.B., Yu, C.-E., Yu, L., Garzia, F., Golamaully, F., Septier, G., Engelborghs, S., Vandenberghe, R., De Deyn, P.P., Fernadez, C.M., Benito, Y.A., Thonberg, H., Forsell, C., Lilius, L., Kinhult-Stählbom, A., Kilander, L., Brundin, R., Concari, L., Helisalmi, S., Koivisto, A.M., Haapasalo, A., Dermecourt, V., Fievet, N., Hanon, O., Dufouil, C., Brice, A., Ritchie, K., Dubois, B., Himali, J.J., Keene, C.D., Tschanz, J., Fitzpatrick, A.L., Kukull, W.A., Norton, M., Aspelund, T., Larson, E.B., Munger, R., Rotter, J.I., Lipton, R.B., Bullido, M.J., Hofman, A., Montine, T.J., Coto, E., Boerwinkle, E., Petersen, R.C., Alvarez, V., Rivadeneira, F., Reiman, E.M., Gallo, M., O'Donnell, C.J., Reisch, J.S., Bruni, A.C., Royall, D.R., Dichgans, M., Sano, M., Galimberti, D., St George-Hyslop, P., Scarpini, E., Tsuang, D.W., Mancuso, M., Bonuccelli, U., Winslow, A.R., Daniele, A., Wu, C.-K., Peters, O., Nacmias, B., Riemenschneider, M., Heun, R., Brayne, C., Rubinsztein, D.C., Bras, J., Guerreiro, R., Al-Chalabi, A., Shaw, C.E., Collinge, J., Mann, D., Tsolaki, M., Clarimón, J., Sussams, R., Lovestone, S., O'Donovan, M.C., Owen, M.J., Behrens, T.W., Mead, S., Goate, A.M., Uitterlinden, A.G., Holmes, C., Cruchaga, C., Ingelsson, M., Bennett, D.A., Powell, J., Golde, T.E., Graff, C., De Jager, P.L., Morgan, K., Ertekin-Taner, N., Combarros, O., Psaty, B.M., Passmore, P., Younkin, S.G., Berr, C., Gudnason, V., Rujescu, D., Dickson, D.W., Dartigues, J.-F., DeStefano, A.L., Ortega-Cubero, S., Hakonarson, H., Campion, D., Boada, M., Kauwe, J.K., Farrer, L.A., Van Broeckhoven, C., Ikram, M.A., Jones, L., Haines, J.L., Tzourio, C., Launer, L.J., Escott-Price, V., Mayeux, R., Deleuze, J.-F., Amin, N., Holmans, P.A., Pericak-Vance, M.A., Amouyel, P., van Duijn, C.M., Ramirez, A., Wang, L.-S., Lambert, J.-C., Seshadri, S., Williams, J., Schellenberg, G.D., Williams, J., Schellenberg, G.D., 2017. Rare coding variants in PLCG2, ABI3, and TREM2 implicate microglial-mediated innate immunity in Alzheimer's disease. Nat. Genet. 49, 1373–1384. doi:10.1038/ng.3916

Singel, K.L., Segal, B.H., 2016. NOX2-dependent regulation of inflammation. Clin. Sci. 130, 479–490. doi:10.1042/CS20150660

Singh, B., Parsaik, A.K., Mielke, M.M., Erwin, P.J., Knopman, D.S., Petersen, R.C., Roberts, R.O., 2014. Association of Mediterranean Diet with Mild Cognitive Impairment and Alzheimer's Disease: A Systematic Review and Meta-Analysis. J. Alzheimer's Dis. 39, 271–282. doi:10.3233/JAD-130830

Singhrao, S.K., Harding, A., Poole, S., Kesavalu, L., Crean, S., 2015. Porphyromonas gingivalis Periodontal Infection and Its Putative Links with Alzheimer's Disease. Mediators Inflamm. 2015, 137357. doi:10.1155/2015/137357

Skarke, C., Alamuddin, N., Lawson, J.A., Li, X., Ferguson, J.F., Reilly, M.P., FitzGerald, G.A., 2015. Bioactive products formed in humans from fish oils. J. Lipid Res. 56, 1808–20. doi:10.1194/jlr.M060392

Solito, E., Sastre, M., 2012. Microglia function in Alzheimer's disease. Front. Pharmacol. 3, 14. doi:10.3389/fphar.2012.00014

Song, M., Xiong, J., Wang, Y., Tang, J., Zhang, B., Bai, Y., 2012. VIP Enhances Phagocytosis of Fibrillar Beta-Amyloid by Microglia and Attenuates Amyloid

Deposition in the Brain of APP/PS1 Mice. PLoS One 7, e29790. doi:10.1371/journal.pone.0029790

Sorce, S., Stocker, R., Seredenina, T., Holmdahl, R., Aguzzi, A., Chio, A., Depaulis, A., Heitz, F., Olofsson, P., Olsson, T., Duveau, V., Sanoudou, D., Skosgater, S., Vlahou, A., Wasquel, D., Krause, K.-H., Jaquet, V., 2017. NADPH oxidases as drug targets and biomarkers in neurodegenerative diseases: What is the evidence? Free Radic. Biol. Med. 112, 387–396. doi:10.1016/j.freeradbiomed.2017.08.006

Sotelo-Hitschfeld, T., Niemeyer, M.I., Machler, P., Ruminot, I., Lerchundi, R., Wyss, M.T., Stobart, J., Fernandez-Moncada, I., Valdebenito, R., Garrido-Gerter, P., Contreras-Baeza, Y., Schneider, B.L., Aebischer, P., Lengacher, S., San Martin, A., Le Douce, J., Bonvento, G., Magistretti, P.J., Sepulveda, F. V., Weber, B., Barros, L.F., 2015. Channel-Mediated Lactate Release by K+-Stimulated Astrocytes. J. Neurosci. 35, 4168–4178. doi:10.1523/JNEUROSCI.5036-14.2015

Souza, D.G., Fagundes, C.T., Amaral, F.A., Cisalpino, D., Sousa, L.P., Vieira, A.T., Pinho, V., Nicoli, J.R., Vieira, L.Q., Fierro, I.M., Teixeira, M.M., 2007. The Required Role of Endogenously Produced Lipoxin A4 and Annexin-1 for the Production of IL-10 and Inflammatory Hyporesponsiveness in Mice. J. Immunol. 179, 8533–8543. doi:10.4049/jimmunol.179.12.8533

Spangenberg, E.E., Lee, R.J., Najafi, A.R., Rice, R.A., Elmore, M.R.P., Blurton-Jones, M., West, B.L., Green, K.N., 2016. Eliminating microglia in Alzheimer's mice prevents neuronal loss without modulating amyloid-β pathology. Brain 139, 1265–1281. doi:10.1093/brain/aww016

Spires-Jones, T.L., Hyman, B.T., 2014. The Intersection of Amyloid Beta and Tau at Synapses in Alzheimer's Disease. Neuron 82, 756–771. doi:10.1016/j.neuron.2014.05.004

Spooner, R., Yilmaz, O., 2011. The role of reactive-oxygen-species in microbial persistence and inflammation. Int. J. Mol. Sci. 12, 334–52. doi:10.3390/ijms12010334

Srinivasan, K., Friedman, B.A., Larson, J.L., Lauffer, B.E., Goldstein, L.D., Appling, L.L., Borneo, J., Poon, C., Ho, T., Cai, F., Steiner, P., Van Der Brug, M.P., Modrusan, Z., Kaminker, J.S., Hansen, D. V, 2016. Untangling the brain's neuroinflammatory and neurodegenerative transcriptional responses. Nat. Commun. 7, 11295. doi:10.1038/ncomms11295

Stahon, K.E., Bastian, C., Griffith, S., Kidd, G.J., Brunet, S., Baltan, S., 2016. Age-Related Changes in Axonal and Mitochondrial Ultrastructure and Function in White Matter. J. Neurosci. 36, 9990–10001. doi:10.1523/JNEUROSCI.1316-16.2016

Steen, E., Terry, B.M., Rivera, E.J., Cannon, J.L., Neely, T.R., Tavares, R., Xu, X.J., Wands, J.R., de la Monte, S.M., 2005. Impaired insulin and insulin-like growth factor expression and signaling mechanisms in Alzheimer's disease--is this type 3 diabetes? J. Alzheimers. Dis. 7, 63–80.

Stelzmann, R.A., Norman Schnitzlein, H., Reed Murtagh, F., 1995. An english translation of alzheimer's 1907 paper, "über eine eigenartige erkankung der hirnrinde." Clin. Anat. 8, 429–431. doi:10.1002/ca.980080612

Stempel, H., Jung, M., Pérez-Gómez, A., Leinders-Zufall, T., Zufall, F., Bufe, B., 2016. Strain-specific Loss of Formyl Peptide Receptor 3 in the Murine Vomeronasal and Immune Systems. J. Biol. Chem. 291, 9762–75. doi:10.1074/jbc.M116.714493

Stepniewski, T.M., Filipek, S., 2015. Non-peptide ligand binding to the formyl peptide receptor FPR2—A comparison to peptide ligand binding modes. Bioorg. Med. Chem. 23, 4072–4081. doi:10.1016/j.bmc.2015.03.062

Stienstra, R., Netea-Maier, R.T., Riksen, N.P., Joosten, L.A.B., Netea, M.G., 2017. Specific and Complex Reprogramming of Cellular Metabolism in Myeloid Cells during Innate Immune Responses. Cell Metab. 26, 142–156. doi:10.1016/j.cmet.2017.06.001

Stine, B., Jungbauer, L., Chunjiang, Y., LaDu, M., 2011. Preparing Synthetic Aβ in Different Aggregation States. Methods Mol. Biol. 670, 13–32. doi:10.1007/978-1-

60761-744-0

Sturchler-Pierrat, C., Abramowski, D., Duke, M., Wiederhold, K.H., Mistl, C., Rothacher, S., Ledermann, B., Bürki, K., Frey, P., Paganetti, P.A., Waridel, C., Calhoun, M.E., Jucker, M., Probst, A., Staufenbiel, M., Sommer, B., 1997. Two amyloid precursor protein transgenic mouse models with Alzheimer disease-like pathology. Proc. Natl. Acad. Sci. U. S. A. 94, 13287–92.

Sun, Q., Jia, N., Wang, W., Jin, H., Xu, J., Hu, H., 2014. Protective Effects of Astragaloside IV against Amyloid Beta1-42 Neurotoxicity by Inhibiting the Mitochondrial Permeability Transition Pore Opening. PLoS One 9, e98866. doi:10.1371/journal.pone.0098866

Suzuki, A., Stern, S.A., Bozdagi, O., Huntley, G.W., Walker, R.H., Magistretti, P.J., Alberini, C.M., 2011. Astrocyte-neuron lactate transport is required for long-term memory formation. Cell 144, 810–23. doi:10.1016/j.cell.2011.02.018

Swaminathan, A., Jicha, G.A., 2014. Nutrition and prevention of Alzheimer's dementia. Front. Aging Neurosci. 6, 1–13. doi:10.3389/fnagi.2014.00282

Sydow, A., Van der Jeugd, A., Zheng, F., Ahmed, T., Balschun, D., Petrova, O., Drexler, D., Zhou, L., Rune, G., Mandelkow, E., D'Hooge, R., Alzheimer, C., Mandelkow, E.-M., 2011. Tau-Induced Defects in Synaptic Plasticity, Learning, and Memory Are Reversible in Transgenic Mice after Switching Off the Toxic Tau Mutant. J. Neurosci. 31, 2511–2525. doi:10.1523/JNEUROSCI.5245-10.2011

Taetzsch, T., Levesque, S., McGraw, C., Brookins, S., Luqa, R., Bonini, M.G., Mason, R.P., Oh, U., Block, M.L., 2015. Redox regulation of NF-κB p50 and M1 polarization in microglia. Glia 63, 423–40. doi:10.1002/glia.22762

Taipa, R., Ferreira, V., Brochado, P., Robinson, A., Reis, I., Marques, F., Mann, D.M., Melo-Pires, M., Sousa, N., 2018. Inflammatory pathology markers (activated microglia and reactive astrocytes) in early and late onset Alzheimer disease: a *post mortem* study. Neuropathol. Appl. Neurobiol. 44, 298–313. doi:10.1111/nan.12445

Takuma, K., Yao, J., Huang, J., Xu, H., Chen, X., Luddy, J., Trillat, A.-C., Stern, D.M., Arancio, O., Yan, S.S., 2005. ABAD enhances Abeta-induced cell stress via mitochondrial dysfunction. FASEB J. 19, 597–8. doi:10.1096/fj.04-2582fje

Talbot, K., Wang, H.-Y., Kazi, H., Han, L.-Y., Bakshi, K.P., Stucky, A., Fuino, R.L., Kawaguchi, K.R., Samoyedny, A.J., Wilson, R.S., Arvanitakis, Z., Schneider, J.A., Wolf, B.A., Bennett, D.A., Trojanowski, J.Q., Arnold, S.E., 2012. Demonstrated brain insulin resistance in Alzheimer's disease patients is associated with IGF-1 resistance, IRS-1 dysregulation, and cognitive decline. J. Clin. Invest. 122, 1316–38. doi:10.1172/JCI59903

Tan, J.L., Tan, Y.Z., Muljadi, R., Chan, S.T., Lau, S.N., Mockler, J.C., Wallace, E.M., Lim, R., 2017. Amnion Epithelial Cells Promote Lung Repair via Lipoxin A $_4$. Stem Cells Transl. Med. 6, 1085–1095. doi:10.5966/sctm.2016-0077

Tan, Z., Xie, N., Banerjee, S., Cui, H., Fu, M., Thannickal, V.J., Liu, G., 2015. The monocarboxylate transporter 4 is required for glycolytic reprogramming and inflammatory response in macrophages. J. Biol. Chem. 290, 46–55. doi:10.1074/jbc.M114.603589

Tang, B.L., 2009. Neuronal protein trafficking associated with Alzheimer disease: From APP and BACE1 to glutamate receptors. Cell Adhes. Migr. 3, 118–128. doi:10.4161/cam.3.1.7254

Tang, D., Kang, R., Coyne, C.B., Zeh, H.J., Lotze, M.T., 2012. PAMPs and DAMPs: signal 0s that spur autophagy and immunity. Immunol. Rev. 249, 158–75. doi:10.1111/j.1600-065X.2012.01146.x

Tang, Y., Le, W., 2016. Differential Roles of M1 and M2 Microglia in Neurodegenerative Diseases. Mol. Neurobiol. 53, 1181–1194. doi:10.1007/s12035-014-9070-5

Tanokashira, D., Mamada, N., Yamamoto, F., Taniguchi, K., Tamaoka, A., Lakshmana, M.K., Araki, W., 2017. The neurotoxicity of amyloid β-protein oligomers is reversible

in a primary neuron model. Mol. Brain 10, 4. doi:10.1186/s13041-016-0284-5

Tanzi, R.E., 2012. The Genetics of Alzheimer disease. Cold Spring Harb. Perspect. Med. 2, a006296. doi:10.1101/cshperspect.a006296

Texidó, L., Martín-Satué, M., Alberdi, E., Solsona, C., Matute, C., 2011. Amyloid beta peptide oligomers directly activate NMDA receptors. Cell Calcium 49, 184–190. doi:10.1016/j.ceca.2011.02.001

Thériault, P., Rivest, S., 2016. Microglia: Senescence Impairs Clearance of Myelin Debris. Curr. Biol. doi:10.1016/j.cub.2016.06.066

Thomsen, M.S., Andreasen, J.T., Arvaniti, M., Kohlmeier, K.A., 2016. Nicotinic acetylcholine receptors in the pathophysiology of Alzheimer's disease: The role of protein-protein interactions in current and future treatment. Curr. Pharm. Des.

Tiffany, H.L., Lavigne, M.C., Cui, Y.H., Wang, J.M., Leto, T.L., Gao, J.L., Murphy, P.M., 2001. Amyloid-beta induces chemotaxis and oxidant stress by acting at formylpeptide receptor 2, a G protein-coupled receptor expressed in phagocytes and brain. J. Biol. Chem. 276, 23645–52. doi:10.1074/jbc.M101031200

Timmerman, R., Burm, S.M., Bajramovic, J.J., 2018. An Overview of in vitro Methods to Study Microglia. Front. Cell. Neurosci. 12, 242. doi:10.3389/fncel.2018.00242

Ting, J., Williams, K., 2005. The CATERPILLER family: An ancient family of immune/apoptotic proteins. Clin. Immunol. 115, 33–37. doi:10.1016/j.clim.2005.02.007

Tóbon-Velasco, J.C., Cuevas, E., Torres-Ramos, M.A., 2014. Receptor for AGEs (RAGE) as mediator of NF-kB pathway activation in neuroinflammation and oxidative stress. CNS Neurol. Disord. Drug Targets 13, 1615–26.

Togo, T., Akiyama, H., Kondo, H., Ikeda, K., Kato, M., Iseki, E., Kosaka, K., 2000. Expression of CD40 in the brain of Alzheimer's disease and other neurological diseases. Brain Res. 885, 117–21.

Tomiyama, T., Matsuyama, S., Iso, H., Umeda, T., Takuma, H., Ohnishi, K., Ishibashi, K., Teraoka, R., Sakama, N., Yamashita, T., Nishitsuji, K., Ito, K., Shimada, H., Lambert, M.P., Klein, W.L., Mori, H., 2010. A Mouse Model of Amyloid Beta Oligomers: Their Contribution to Synaptic Alteration, Abnormal Tau Phosphorylation, Glial Activation, and Neuronal Loss In Vivo. J. Neurosci. 30, 4845–4856. doi:10.1523/JNEUROSCI.5825-09.2010

Trentin, P.G., Ferreira, T.P.T., Arantes, A.C.S., Ciambarella, B.T., Cordeiro, R.S.B., Flower, R.J., Perretti, M., Martins, M.A., Silva, P.M.R., 2015. Annexin A1 mimetic peptide controls the inflammatory and fibrotic effects of silica particles in mice. Br. J. Pharmacol. 172, 3058–71. doi:10.1111/bph.13109

Treusch, S., Cyr, D.M., Lindquist, S., 2009. Amyloid deposits: protection against toxic protein species? Cell Cycle 8, 1668–74. doi:10.4161/cc.8.11.8503

Ulrich, J.D., Ulland, T.K., Colonna, M., Holtzman, D.M., 2017. Elucidating the Role of TREM2 in Alzheimer's Disease. Neuron 94, 237–248. doi:10.1016/j.neuron.2017.02.042

Underhill, D.M., Goodridge, H.S., 2012. Information processing during phagocytosis. Nat. Rev. Immunol. 12, 492–502. doi:10.1038/nri3244

Underhill, D.M., Gordon, S., Imhof, B.A., Núñez, G., Bousso, P., 2016. Élie Metchnikoff (1845–1916): celebrating 100 years of cellular immunology and beyond. Nat. Rev. Immunol. 16, 651–656. doi:10.1038/nri.2016.89

United Nations, 2015. World Population Prospects: The 2015 Revision, Key Findings and Advance Tables, World Population Prospects.

Urrutia, P.J., Hirsch, E.C., González-Billault, C., Núñez, M.T., 2017. Hepcidin attenuates amyloid beta-induced inflammatory and pro-oxidant responses in astrocytes and microglia. J. Neurochem. 142, 140–152. doi:10.1111/jnc.14005

Valko, M., Leibfritz, D., Moncol, J., Cronin, M.T.D., Mazur, M., Telser, J., 2007. Free

radicals and antioxidants in normal physiological functions and human disease. Int. J. Biochem. Cell Biol. 39, 44–84. doi:10.1016/j.biocel.2006.07.001

Van Helmond, Z., Miners, J.S., Kehoe, P.G., Love, S., 2010. Higher Soluble Amyloid β Concentration in Frontal Cortex of Young Adults than in Normal Elderly or Alzheimer's Disease. Brain Pathol. 20, 787–793. doi:10.1111/j.1750-3639.2010.00374.x

Vander Heiden, M.G., Cantley, L.C., Thompson, C.B., 2009. Understanding the Warburg Effect: The Metabolic Requirements of Cell Proliferation. Science 324, 1029–1033. doi:10.1126/science.1160809

Vandresen-Filho, S., Martins, W.C., Bertoldo, D.B., Mancini, G., Herculano, B.A., de Bem, A.F., Tasca, C.I., 2013. Atorvastatin prevents cell damage via modulation of oxidative stress, glutamate uptake and glutamine synthetase activity in hippocampal slices subjected to oxygen/glucose deprivation. Neurochem. Int. 62, 948–55. doi:10.1016/j.neuint.2013.03.002

Vara, D., Watt, J.M., Fortunato, T.M., Mellor, H., Burgess, M., Wicks, K., Mace, K., Reeksting, S., Lubben, A., Wheeler-Jones, C.P.D., Pula, G., 2018. Direct Activation of NADPH Oxidase 2 by 2-Deoxyribose-1-Phosphate Triggers Nuclear Factor Kappa B-Dependent Angiogenesis. Antioxid. Redox Signal. 28, 110–130. doi:10.1089/ars.2016.6869

Vassar, R., Bennett, B.D., Babu-Khan, S., Kahn, S., Mendiaz, E.A., Denis, P., Teplow, D.B., Ross, S., Amarante, P., Loeloff, R., Luo, Y., Fisher, S., Fuller, J., Edenson, S., Lile, J., Jarosinski, M.A., Biere, A.L., Curran, E., Burgess, T., Louis, J.C., Collins, F., Treanor, J., Rogers, G., Citron, M., 1999. Beta-secretase cleavage of Alzheimer's amyloid precursor protein by the transmembrane aspartic protease BACE. Science 286, 735–41.

Vazquez, A., Liu, J., Zhou, Y., Oltvai, Z.N., 2010. Catabolic efficiency of aerobic glycolysis: The Warburg effect revisited. BMC Syst. Biol. 4, 58. doi:10.1186/1752-0509-4-58

Vekrellis, K., Ye, Z., Qiu, W.Q., Walsh, D., Hartley, D., Chesneau, V., Rosner, M.R., Selkoe, D.J., 2000. Neurons regulate extracellular levels of amyloid beta-protein via proteolysis by insulin-degrading enzyme. J. Neurosci. 20, 1657–65.

Venegas, C., Heneka, M.T., 2017. Danger-associated molecular patterns in Alzheimer's disease. J. Leukoc. Biol. 101, 87–98. doi:10.1189/jlb.3MR0416-204R

Verdile, G., Keane, K.N., Cruzat, V.F., Medic, S., Sabale, M., Rowles, J., Wijesekara, N., Martins, R.N., Fraser, P.E., Newsholme, P., 2015. Inflammation and Oxidative Stress: The Molecular Connectivity between Insulin Resistance, Obesity, and Alzheimer's Disease. Mediators Inflamm. 2015. doi:10.1155/2015/105828

Vessoni, A.T., Quinet, A., Andrade-Lima, L.C. de, Martins, D.J., Garcia, C.C.M., Rocha, C.R.R., Vieira, D.B., Menck, C.F.M., 2016. Chloroquine-induced glioma cells death is associated with mitochondrial membrane potential loss, but not oxidative stress. Free Radic. Biol. Med. 90, 91–100. doi:10.1016/j.freeradbiomed.2015.11.008

Vezzani, A., French, J., Bartfai, T., Baram, T.Z., 2011. The role of inflammation in epilepsy. Nat. Rev. Neurol. 7, 31–40. doi:10.1038/nrneurol.2010.178

Vilhardt, F., Haslund-Vinding, J., Jaquet, V., McBean, G., 2017. Microglia antioxidant systems and redox signalling. Br. J. Pharmacol. 174, 1719–1732. doi:10.1111/bph.13426

Villegas-Llerena, C., Phillips, A., Reitboeck, P.G., Hardy, J., Pocock, J.M., 2016. Microglial genes regulating neuroinflammation in the progression of Alzheimer's disease. Curr. Opin. Neurobiol. 36, 74–81. doi:10.1016/j.conb.2015.10.004

Vingtdeux, V., Marambaud, P., 2012. Identification and biology of α-secretase. J. Neurochem. 120, 34–45. doi:10.1111/j.1471-4159.2011.07477.x

Vistoli, G., De Maddis, D., Cipak, A., Zarkovic, N., Carini, M., Aldini, G., 2013. Advanced glycoxidation and lipoxidation end products (AGEs and ALEs): an overview of their

mechanisms of formation. Free Radic. Res. 47 Suppl 1, 3–27. doi:10.3109/10715762.2013.815348

Vital, S.A., Becker, F., Holloway, P.M., Russell, J., Perretti, M., Granger, D.N., Gavins, F.N.E., 2016. Fpr2/ALX Regulates Neutrophil-Platelet Aggregation and Attenuates Cerebral Inflammation: Impact for Therapy in Cardiovascular Disease. Circulation 133, 2169–2179. doi:10.1161/CIRCULATIONAHA.115.020633

Vlassenko, A.G., Gordon, B.A., Goyal, M.S., Su, Y., Blazey, T.M., Durbin, T.J., Couture, L.E., Christensen, J.J., Jafri, H., Morris, J.C., Raichle, M.E., Benzinger, T.L.-S., 2018. Aerobic glycolysis and tau deposition in preclinical Alzheimer's disease. Neurobiol. Aging 67, 95–98. doi:10.1016/j.neurobiolaging.2018.03.014

von Bartheld, C.S., Bahney, J., Herculano-Houzel, S., 2016. The search for true numbers of neurons and glial cells in the human brain: A review of 150 years of cell counting. J. Comp. Neurol. 524, 3865–3895. doi:10.1002/cne.24040

Wadhwa, M., Prabhakar, A., Ray, K., Roy, K., Kumari, P., Jha, P.K., Kishore, K., Kumar, S., Panjwani, U., 2017. Inhibiting the microglia activation improves the spatial memory and adult neurogenesis in rat hippocampus during 48h of sleep deprivation. J. Neuroinflammation 14, 222. doi:10.1186/s12974-017-0998-z

Walker, D.G., Lue, L.-F., 2015. Immune phenotypes of microglia in human neurodegenerative disease: challenges to detecting microglial polarization in human brains. Alzheimers. Res. Ther. 7, 56. doi:10.1186/s13195-015-0139-9

Walker, J.M., Kruger, N.J., 2003. The Bradford Method for Protein Quantitation, in: Basic Protein and Peptide Protocols. Humana Press, New Jersey, pp. 9–16. doi:10.1385/0-89603-268-x:9

Walker, K.A., Gottesman, R.F., Wu, A., Knopman, D.S., Gross, A.L., Mosley, T.H., Selvin, E., Windham, B.G., 2019. Systemic inflammation during midlife and cognitive change over 20 years: The ARIC Study. Neurology 92, e1256–e1267. doi:10.1212/WNL.0000000000007094

Walsh, D.M., Klyubin, I., Fadeeva, J. V, Cullen, W.K., Anwyl, R., Wolfe, M.S., Rowan, M.J., Selkoe, D.J., 2002. Naturally secreted oligomers of amyloid beta protein potently inhibit hippocampal long-term potentiation in vivo. Nature 416, 535–539. doi:10.1038/416535a

Wan, C.P., Park, C.S., Lau, B.H., 1993. A rapid and simple microfluorometric phagocytosis assay. J. Immunol. Methods 162, 1–7.

Wang, B.-R., Shi, J.-Q., Ge, N.-N., Ou, Z., Tian, Y.-Y., Jiang, T., Zhou, J.-S., Xu, J., Zhang, Y.-D., 2018. PM2.5 exposure aggravates oligomeric amyloid beta-induced neuronal injury and promotes NLRP3 inflammasome activation in an in vitro model of Alzheimer's disease. J. Neuroinflammation 15, 132. doi:10.1186/s12974-018-1178-5

Wang, H.-M., Zhang, T., Huang, J.-K., Sun, X.-J., 2013. 3-N-butylphthalide (NBP) attenuates the amyloid-β-induced inflammatory responses in cultured astrocytes via the nuclear factor-κB signaling pathway. Cell. Physiol. Biochem. 32, 235–42. doi:10.1159/000350139

Wang, H., Blackall, M., Sominsky, L., Spencer, S.J., Vlahos, R., Churchill, M., Bozinovski, S., 2018. Increased hypothalamic microglial activation after viral-induced pneumococcal lung infection is associated with excess serum amyloid A production. J. Neuroinflammation 15, 200. doi:10.1186/s12974-018-1234-1

Wang, J., Lu, R., Yang, J., Li, H., He, Z., Jing, N., Wang, X., Wang, Y., 2015. TRPC6 specifically interacts with APP to inhibit its cleavage by γ-secretase and reduce Aβ production. Nat. Commun. 6, 8876. doi:10.1038/ncomms9876

Wang, L., Pavlou, S., Du, X., Bhuckory, M., Xu, H., Chen, M., 2019. Glucose transporter 1 critically controls microglial activation through facilitating glycolysis. Mol. Neurodegener. 14, 2. doi:10.1186/s13024-019-0305-9

Wang, R., Reddy, P.H., 2017. Role of Glutamate and NMDA Receptors in Alzheimer's Disease. J. Alzheimers. Dis. 57, 1041–1048. doi:10.3233/JAD-160763

Wang, W., Li, T., Wang, X., Yuan, W., Cheng, Y., Zhang, H., Xu, E., Zhang, Y., Shi, S., Ma, D., Han, W., 2015. FAM19A4 is a novel cytokine ligand of formyl peptide receptor 1 (FPR1) and is able to promote the migration and phagocytosis of macrophages. Cell. Mol. Immunol. 12, 615–624. doi:10.1038/cmi.2014.61

Wang, X., Zhu, M., Hjorth, E., Cortés-Toro, V., Eyjolfsdottir, H., Graff, C., Nennesmo, I., Palmblad, J., Eriksdotter, M., Sambamurti, K., Fitzgerald, J.M., Serhan, C.N., Granholm, A.-C., Schultzberg, M., 2015. Resolution of inflammation is altered in Alzheimer's disease. Alzheimer's Dement. 11, 40-50.e2. doi:10.1016/j.jalz.2013.12.024

Wang, Y.-P., Zhou, L.-S., Zhao, Y.-Z., Wang, S.-W., Chen, L.-L., Liu, L.-X., Ling, Z.-Q., Hu, F.-J., Sun, Y.-P., Zhang, J.-Y., Yang, C., Yang, Y., Xiong, Y., Guan, K.-L., Ye, D., 2014. Regulation of G6PD acetylation by KAT9/SIRT2 modulates NADPH homeostasis and cell survival during oxidative stress. EMBO J. doi:10.1002/embj.201387224

Wang, Y., Branicky, R., Noë, A., Hekimi, S., 2018. Superoxide dismutases: Dual roles in controlling ROS damage and regulating ROS signaling. J. Cell Biol. 217, 1915–1928. doi:10.1083/jcb.201708007

Wang, Y., Cella, M., Mallinson, K., Ulrich, J.D., Young, K.L., Robinette, M.L., Gilfillan, S., Krishnan, G.M., Sudhakar, S., Zinselmeyer, B.H., Holtzman, D.M., Cirrito, J.R., Colonna, M., 2015. TREM2 lipid sensing sustains the microglial response in an Alzheimer's disease model. Cell 160, 1061–71. doi:10.1016/j.cell.2015.01.049

Wang, Z., Li, S., Cao, Y., Tian, X., Zeng, R., Liao, D.F., Cao, D., 2016. Oxidative stress and carbonyl lesions in ulcerative colitis and associated colorectal cancer. Oxid. Med. Cell. Longev. 2016, 9875298. doi:10.1155/2016/9875298

Wang, Z., Wei, X., Liu, K., Zhang, X., Yang, F., Zhang, H., He, Y., Zhu, T., Li, F., Shi, W., Zhang, Y., Xu, H., Liu, J., Yi, F., 2013. NOX2 deficiency ameliorates cerebral injury through reduction of complexin II-mediated glutamate excitotoxicity in experimental stroke. Free Radic. Biol. Med. 65, 942–51. doi:10.1016/j.freeradbiomed.2013.08.166

Ward, S.M., Himmelstein, D.S., Lancia, J.K., Binder, L.I., 2012. Tau oligomers and tau toxicity in neurodegenerative disease. Biochem. Soc. Trans. 40, 667–71. doi:10.1042/BST20120134

Wendeln, A.-C., Degenhardt, K., Kaurani, L., Gertig, M., Ulas, T., Jain, G., Wagner, J., Häsler, L.M., Wild, K., Skodras, A., Blank, T., Staszewski, O., Datta, M., Centeno, T.P., Capece, V., Islam, M.R., Kerimoglu, C., Staufenbiel, M., Schultze, J.L., Beyer, M., Prinz, M., Jucker, M., Fischer, A., Neher, J.J., 2018. Innate immune memory in the brain shapes neurological disease hallmarks. Nature 556, 332–338. doi:10.1038/s41586-018-0023-4

Wendt, S., Maricos, M., Vana, N., Meyer, N., Guneykaya, D., Semtner, M., Kettenmann, H., 2017. Changes in phagocytosis and potassium channel activity in microglia of 5xFAD mice indicate alterations in purinergic signaling in a mouse model of Alzheimer's disease. Neurobiol. Aging 58, 41–53. doi:10.1016/j.neurobiolaging.2017.05.027

Wenzel-Seifert, K., Seifert, R., 1993. Cyclosporin H is a potent and selective formyl peptide receptor antagonist. Comparison with N-t-butoxycarbonyl-L-phenylalanyl-L-leucyl-L-phenylalanyl-L- leucyl-L-phenylalanine and cyclosporins A, B, C, D, and E. J. Immunol. 150, 4591–9.

West, A.P., Brodsky, I.E., Rahner, C., Woo, D.K., Erdjument-Bromage, H., Tempst, P., Walsh, M.C., Choi, Y., Shadel, G.S., Ghosh, S., 2011. TLR signalling augments macrophage bactericidal activity through mitochondrial ROS. Nature 472, 476–480. doi:10.1038/nature09973

Wilcock, D.M., Griffin, W.S.T., 2013. Down's syndrome, neuroinflammation, and Alzheimer neuropathogenesis. J. Neuroinflammation 10, 864. doi:10.1186/1742-2094-10-84

Wilkinson, B.L., Cramer, P.E., Varvel, N.H., Reed-Geaghan, E., Jiang, Q., Szabo, A.,

Herrup, K., Lamb, B.T., Landreth, G.E., 2012. Ibuprofen attenuates oxidative damage through NOX2 inhibition in Alzheimer's disease. Neurobiol. Aging 33, 197.e21-197.e32. doi:10.1016/j.neurobiolaging.2010.06.014

Winterbourn, C.C., Kettle, A.J., 2013. Redox Reactions and Microbial Killing in the Neutrophil Phagosome. Antioxid. Redox Signal. 18, 642–660. doi:10.1089/ars.2012.4827

Wisniewski, T., Goñi, F., 2015. Immunotherapeutic Approaches for Alzheimer's Disease. Neuron 85, 1162–1176. doi:10.1016/j.neuron.2014.12.064

Wolf, S.A., Boddeke, H.W.G.M., Kettenmann, H., 2017. Microglia in Physiology and Disease. Annu. Rev. Physiol. 79, 619–643. doi:10.1146/annurev-physiol-022516-034406

Woodling, N.S., Colas, D., Wang, Q., Minhas, P., Panchal, M., Liang, X., Mhatre, S.D., Brown, H., Ko, N., Zagol-Ikapitte, I., van der Hart, M., Khroyan, T. V., Chuluun, B., Priyam, P.G., Milne, G.L., Rassoulpour, A., Boutaud, O., Manning-Boğ, A.B., Heller, H.C., Andreasson, K.I., 2016. Cyclooxygenase inhibition targets neurons to prevent early behavioural decline in Alzheimer's disease model mice. Brain 139, 2063–2081. doi:10.1093/brain/aww117

Woodward, E.A., Prêle, C.M., Nicholson, S.E., Kolesnik, T.B., Hart, P.H., 2010. The anti-inflammatory effects of interleukin-4 are not mediated by suppressor of cytokine signalling-1 (SOCS1). Immunology 131, 118–27. doi:10.1111/j.1365-2567.2010.03281.x

Wu, D., Yotnda, P., 2011. Production and detection of reactive oxygen species (ROS) in cancers. J. Vis. Exp. doi:10.3791/3357

Wu, L.-J., Wu, G., Sharif, M.R.A., Baker, A., Jia, Y., Fahey, F.H., Luo, H.R., Feener, E.P., Clapham, D.E., 2012. The voltage-gated proton channel Hv1 enhances brain damage from ischemic stroke. Nat. Neurosci. 15, 565.

Wu, S.C., Cao, Z.S., Chang, K.M., Juang, J.L., 2017. Intestinal microbial dysbiosis aggravates the progression of Alzheimer's disease in Drosophila. Nat. Commun. 8, 24. doi:10.1038/s41467-017-00040-6

Wu, Y.-T., Beiser, A.S., Breteler, M.M.B., Fratiglioni, L., Helmer, C., Hendrie, H.C., Honda, H., Ikram, M.A., Langa, K.M., Lobo, A., Matthews, F.E., Ohara, T., Pérès, K., Qiu, C., Seshadri, S., Sjölund, B.-M., Skoog, I., Brayne, C., 2017. The changing prevalence and incidence of dementia over time - current evidence. Nat. Rev. Neurol. 13, 327–339. doi:10.1038/nrneurol.2017.63

Wu, Y.T., Fratiglioni, L., Matthews, F.E., Lobo, A., Breteler, M.M., Skoog, I., Brayne, C., 2015. Dementia in western Europe: epidemiological evidence and implications for policy making. Lancet Neurol. 4422, 1–9. doi:10.1016/S1474-4422(15)00092-7

Wyss, M.T., Jolivet, R., Buck, A., Magistretti, P.J., Weber, B., 2011. In Vivo Evidence for Lactate as a Neuronal Energy Source. J. Neurosci. 31, 7477–7485. doi:10.1523/JNEUROSCI.0415-11.2011

Wyssenbach, A., Quintela, T., Llavero, F., Zugaza, J.L., Matute, C., Alberdi, E., 2016. Amyloid β-induced astrogliosis is mediated by β1-integrin via NADPH oxidase 2 in Alzheimer's disease. Aging Cell 15, 1140–1152. doi:10.1111/acel.12521

Xiang, B., Xiao, C., Shen, T., Li, X., 2018. Anti-inflammatory effects of anisalcohol on lipopolysaccharide-stimulated BV2 microglia via selective modulation of microglia polarization and down-regulation of NF-κB p65 and JNK activation. Mol. Immunol. 95, 39–46. doi:10.1016/j.molimm.2018.01.011

Xing, S., Shen, D., Chen, C., Wang, J., Liu, T., Yu, Z., 2013. Regulation of neuronal toxicity of β-amyloid oligomers by surface ATP synthase. Mol. Med. Rep. 8, 1689–1694. doi:10.3892/mmr.2013.1722

Yamin, G., Teplow, D.B., 2017. Pittsburgh Compound-B (PiB) binds amyloid β-protein protofibrils. J. Neurochem. 140, 210–215. doi:10.1111/jnc.13887

Yan, S. Du, Stern, D.M., 2005. Mitochondrial dysfunction and Alzheimer's disease: Role of

amyloid-beta peptide alcohol dehydrogenase (ABAD). Int. J. Exp. Pathol. 86, 161–171. doi:10.1111/j.0959-9673.2005.00427.x

Yan, N., 2017. A Glimpse of Membrane Transport through Structures-Advances in the Structural Biology of the GLUT Glucose Transporters. J. Mol. Biol. 429, 2710–2725. doi:10.1016/j.jmb.2017.07.009

Yan, S.D., Chen, X., Fu, J., Chen, M., Zhu, H., Roher, A., Slattery, T., Zhao, L., Nagashima, M., Morser, J., Migheli, A., Nawroth, P., Stern, D., Schmidt, A.M., 1996. RAGE and amyloid-beta peptide neurotoxicity in Alzheimer's disease. Nature 382, 685–91. doi:10.1038/382685a0

Yang, F., Tang, E., Guan, K., Wang, C.-Y., 2003. IKK Plays an Essential Role in the Phosphorylation of RelA/p65 on Serine 536 Induced by Lipopolysaccharide. J. Immunol. 170, 5630–5635. doi:10.4049/jimmunol.170.11.5630

Yang, J., Jiang, Z., Fitzgerald, D.C., Ma, C., Yu, S., Li, H., Zhao, Z., Li, Y., Ciric, B., Curtis, M., Rostami, A., Zhang, G.-X., 2009. Adult neural stem cells expressing IL-10 confer potent immunomodulation and remyelination in experimental autoimmune encephalitis. J. Clin. Invest. 119, 3678–3691. doi:10.1172/JCI37914

Yang, J., Ruchti, E., Petit, J.-M., Jourdain, P., Grenningloh, G., Allaman, I., Magistretti, P.J., 2014. Lactate promotes plasticity gene expression by potentiating NMDA signaling in neurons. Proc. Natl. Acad. Sci. U. S. A. 111, 12228–33. doi:10.1073/pnas.1322912111

Yang, L.-B., Lindholm, K., Yan, R., Citron, M., Xia, W., Yang, X.-L., Beach, T., Sue, L., Wong, P., Price, D., Li, R., Shen, Y., 2003. Elevated beta-secretase expression and enzymatic activity detected in sporadic Alzheimer disease. Nat. Med. 9, 3–4. doi:10.1038/nm0103-3

Yang, T., Li, S., Xu, H., Walsh, D.M., Selkoe, D.J., 2017. Large Soluble Oligomers of Amyloid β-Protein from Alzheimer Brain Are Far Less Neuroactive Than the Smaller Oligomers to Which They Dissociate. J. Neurosci. 37, 152–163. doi:10.1523/JNEUROSCI.1698-16.2016

Yao, J., Du, H., Yan, S., Fang, F., Wang, C., Lue, L.-F., Guo, L., Chen, D., Stern, D.M., Gunn Moore, F.J., Xi Chen, J., Arancio, O., Yan, S.S., 2011. Inhibition of amyloid-beta (Abeta) peptide-binding alcohol dehydrogenase-Abeta interaction reduces Abeta accumulation and improves mitochondrial function in a mouse model of Alzheimer's disease. J. Neurosci. 31, 2313–20. doi:10.1523/JNEUROSCI.4717-10.2011

Yao, Y., Li, J., Niu, Y., Yu, J., Yan, L., Miao, Z., Zhao, X., Li, Y., Yao, W., Zheng, P., Li, W., 2015. Resveratrol inhibits oligomeric Aβ-induced microglial activation via NADPH oxidase. Mol. Med. Rep. 12, 6133–9. doi:10.3892/mmr.2015.4199

Yaron, J.R., Gangaraju, S., Rao, M.Y., Kong, X., Zhang, L., Su, F., Tian, Y., Glenn, H.L., Meldrum, D.R., 2015. K+ regulates Ca2+ to drive inflammasome signaling: Dynamic visualization of ion flux in live cells. Cell Death Dis. 6, e1954–e1954. doi:10.1038/cddis.2015.277

Yasojima, K., Schwab, C., McGeer, E.G., McGeer, P.L., 1999. Up-Regulated Production and Activation of the Complement System in Alzheimer's Disease Brain. Am. J. Pathol. 154, 927–936. doi:10.1016/S0002-9440(10)65340-0

Yasuno, F., Kosaka, J., Ota, M., Higuchi, M., Ito, H., Fujimura, Y., Nozaki, S., Takahashi, S., Mizukami, K., Asada, T., Suhara, T., 2012. Increased binding of peripheral benzodiazepine receptor in mild cognitive impairment-dementia converters measured by positron emission tomography with [^{11}C]DAA1106. Psychiatry Res. 203, 67–74. doi:10.1016/j.pscychresns.2011.08.013

Yauger, Y.J., Bermudez, S., Moritz, K.E., Glaser, E., Stoica, B., Byrnes, K.R., 2019. Iron accentuated reactive oxygen species release by NADPH oxidase in activated microglia contributes to oxidative stress in vitro. J. Neuroinflammation 16, 41. doi:10.1186/s12974-019-1430-7

Ye, C.Y., Lei, Y., Tang, X.C., Zhang, H.Y., 2015. Donepezil attenuates Aβ-associated

mitochondrial dysfunction and reduces mitochondrial Aβ accumulation in vivo and in vitro. Neuropharmacology 95, 29–36. doi:10.1016/j.neuropharm.2015.02.020

Ye, R.D., Boulay, F., Wang, J.M., Dahlgren, C., Gerard, C., Parmentier, M., Serhan, C.N., Murphy, P.M., 2009. International Union of Basic and Clinical Pharmacology. LXXIII. Nomenclature for the Formyl Peptide Receptor (FPR) Family. Pharmacol. Rev. 61, 119–161. doi:10.1124/pr.109.001578

Yi, G., Sze, S.-H., Thon, M.R., 2007. Identifying clusters of functionally related genes in genomes. Bioinformatics 23, 1053–1060. doi:10.1093/bioinformatics/btl673

Yin, Z., Raj, D., Saiepour, N., Van Dam, D., Brouwer, N., Holtman, I.R., Eggen, B.J.L., Möller, T., Tamm, J.A., Abdourahman, A., Hol, E.M., Kamphuis, W., Bayer, T.A., De Deyn, P.P., Boddeke, E., 2017. Immune hyperreactivity of Aβ plaque-associated microglia in Alzheimer's disease. Neurobiol. Aging. doi:10.1016/j.neurobiolaging.2017.03.021

Yokoyama, J.S., Wang, Y., Schork, A.J., Thompson, W.K., Karch, C.M., Cruchaga, C., McEvoy, L.K., Witoelar, A., Chen, C.H., Holland, D., Brewer, J.B., Franke, A., Dillon, W.P., Wilson, D.M., Mukherjee, P., Hess, C.P., Miller, Z., Bonham, L.W., Shen, J., Rabinovici, G.D., Rosen, H.J., Miller, B.L., Hyman, B.T., Schellenberg, G.D., Karlsen, T.H., Andreassen, O.A., Dale, A.M., Desikan, R.S., 2016. Association between genetic traits for immune-mediated diseases and Alzheimer disease. JAMA Neurol. 73, 691–697. doi:10.1001/jamaneurol.2016.0150

Yoon, S.O., Park, D.J., Ryu, J.C., Ozer, H.G., Tep, C., Shin, Y.J., Lim, T.H., Pastorino, L., Kunwar, A.J., Walton, J.C., Nagahara, A.H., Lu, K.P., Nelson, R.J., Tuszynski, M.H., Huang, K., 2012. JNK3 perpetuates metabolic stress induced by Aβ peptides. Neuron 75, 824–37. doi:10.1016/j.neuron.2012.06.024

Yoshiyama, Y., Higuchi, M., Zhang, B., Huang, S.-M., Iwata, N., Saido, T.C., Maeda, J., Suhara, T., Trojanowski, J.Q., Lee, V.M.-Y., 2007. Synapse Loss and Microglial Activation Precede Tangles in a P301S Tauopathy Mouse Model. Neuron 53, 337–351. doi:10.1016/j.neuron.2007.01.010

Youssef, M., Ibrahim, A., Akashi, K., Hossain, M.S., 2019. PUFA-Plasmalogens Attenuate the LPS-Induced Nitric Oxide Production by Inhibiting the NF-kB, p38 MAPK and JNK Pathways in Microglial Cells. Neuroscience 397, 18–30. doi:10.1016/j.neuroscience.2018.11.030

Yu, Y., Ye, R.D., 2014. Microglial Aβ Receptors in Alzheimer's Disease. Cell. Mol. Neurobiol. 35, 71–83. doi:10.1007/s10571-014-0101-6

Yun, S.P., Kam, T.-I., Panicker, N., Kim, SangMin, Oh, Y., Park, J.-S., Kwon, S.-H., Park, Y.J., Karuppagounder, S.S., Park, H., Kim, Sangjune, Oh, N., Kim, N.A., Lee, Saebom, Brahmachari, S., Mao, X., Lee, J.H., Kumar, M., An, D., Kang, S.-U., Lee, Y., Lee, K.C., Na, D.H., Kim, D., Lee, S.H., Roschke, V. V., Liddelow, S.A., Mari, Z., Barres, B.A., Dawson, V.L., Lee, Seulki, Dawson, T.M., Ko, H.S., 2018. Block of A1 astrocyte conversion by microglia is neuroprotective in models of Parkinson's disease. Nat. Med. 24, 931. doi:10.1038/S41591-018-0051-5

Zanjani, H., Finch, C.E., Kemper, C., Atkinson, J., McKeel, D., Morris, J.C., Price, J.L., 2005. Complement activation in very early Alzheimer disease. Alzheimer Dis. Assoc. Disord. 19, 55–66.

Zenaro, E., Pietronigro, E., Della Bianca, V., Piacentino, G., Marongiu, L., Budui, S., Turano, E., Rossi, B., Angiari, S., Dusi, S., Montresor, A., Carlucci, T., Nanì, S., Tosadori, G., Calciano, L., Catalucci, D., Berton, G., Bonetti, B., Constantin, G., 2015. Neutrophils promote Alzheimer's disease-like pathology and cognitive decline via LFA-1 integrin. Nat. Med. 21, 880–6. doi:10.1038/nm.3913

Zhang-Haagen, B., Biehl, R., Nagel-Steger, L., Radulescu, A., Richter, D., Willbold, D., 2016. Monomeric Amyloid Beta Peptide in Hexafluoroisopropanol Detected by Small Angle Neutron Scattering. PLoS One 11, e0150267. doi:10.1371/journal.pone.0150267

Zhang, B., Gaiteri, C., Bodea, L.-G., Wang, Z., McElwee, J., Podtelezhnikov, A.A., Zhang,

C., Xie, T., Tran, L., Dobrin, R., Fluder, E., Clurman, B., Melquist, S., Narayanan, M., Suver, C., Shah, H., Mahajan, M., Gillis, T., Mysore, J., MacDonald, M.E., Lamb, J.R., Bennett, D.A., Molony, C., Stone, D.J., Gudnason, V., Myers, A.J., Schadt, E.E., Neumann, H., Zhu, J., Emilsson, V., 2013. Integrated Systems Approach Identifies Genetic Nodes and Networks in Late-Onset Alzheimer's Disease. Cell 153, 707–720. doi:10.1016/j.cell.2013.03.030

Zhang, C., Wang, Y., Wang, D., Zhang, J., Zhang, F., 2018. NSAID exposure and risk of Alzheimer's disease: An updated meta-analysis from cohort studies. Front. Aging Neurosci. 10, 83. doi:10.3389/fnagi.2018.00083

Zhang, H., Ma, Q., Zhang, Y., Xu, H., 2012. Proteolytic processing of Alzheimer's β-amyloid precursor protein. J. Neurochem. 120 Suppl, 9–21. doi:10.1111/j.1471-4159.2011.07519.x

Zhang, J., 2015. Mapping neuroinflammation in frontotemporal dementia with molecular PET imaging. J. Neuroinflammation 12, 108. doi:10.1186/s12974-015-0236-5

Zhang, L., Wang, G., Chen, X., Xue, X., Guo, Q., Liu, M., Zhao, J., 2017. Formyl peptide receptors promotes neural differentiation in mouse neural stem cells by ROS generation and regulation of PI3K-AKT signaling. Sci. Rep. 7, 206. doi:10.1038/s41598-017-00314-5

Zhang, L., Zhou, Z., Zhai, W., Pang, J., Mo, Y., Yang, G., Qu, Z., Hu, Y., 2019. Safflower yellow attenuates learning and memory deficits in amyloid β-induced Alzheimer's disease rats by inhibiting neuroglia cell activation and inflammatory signaling pathways. Metab. Brain Dis. 34, 927–939. doi:10.1007/s11011-019-00398-0

Zhang, P., Kishimoto, Y., Grammatikakis, I., Gottimukkala, K., Cutler, R.G., Zhang, S., Abdelmohsen, K., Bohr, V.A., Misra Sen, J., Gorospe, M., Mattson, M.P., 2019. Senolytic therapy alleviates Aβ-associated oligodendrocyte progenitor cell senescence and cognitive deficits in an Alzheimer's disease model. Nat. Neurosci. 22, 719–728. doi:10.1038/s41593-019-0372-9

Zhang, Q., Lenardo, M.J., Baltimore, D., 2017. 30 Years of NF-κB: A Blossoming of Relevance to Human Pathobiology. Cell 168, 37–57. doi:10.1016/j.cell.2016.12.012

Zhang, R., Miller, R.G., Madison, C., Jin, X., Honrada, R., Harris, W., Katz, J., Forshew, D.A., McGrath, M.S., 2013. Systemic immune system alterations in early stages of Alzheimer's disease. J. Neuroimmunol. 256, 38–42. doi:10.1016/j.jneuroim.2013.01.002

Zhang, R., Zhang, N., Zhang, H., Liu, C., Dong, X., Wang, X., Zhu, Y., Xu, C., Liu, L., Yang, S., Huang, S., Chen, L., 2017. Celastrol prevents cadmium-induced neuronal cell death by blocking reactive oxygen species-mediated mammalian target of rapamycin pathway. Br. J. Pharmacol. 174, 82–100. doi:10.1111/bph.13655

Zhang, X., Li, Y., Xu, H., Zhang, Y.-W., 2014. The γ-secretase complex: from structure to function. Front. Cell. Neurosci. 8, 427. doi:10.3389/fncel.2014.00427

Zhang, Y., Sloan, S.A., Clarke, L.E., Caneda, C., Plaza, C.A., Blumenthal, P.D., Vogel, H., Steinberg, G.K., Edwards, M.S.B., Li, G., Duncan, J.A., Cheshier, S.H., Shuer, L.M., Chang, E.F., Grant, G.A., Gephart, M.G.H., Barres, B.A., 2016. Purification and Characterization of Progenitor and Mature Human Astrocytes Reveals Transcriptional and Functional Differences with Mouse. Neuron 89, 37–53. doi:10.1016/j.neuron.2015.11.013

Zhang, Y., Thompson, R., Zhang, H., Xu, H., 2011. APP processing in Alzheimer's disease. Mol. Brain 4, 3. doi:10.1186/1756-6606-4-3

Zhang, Z., Takeda-Uchimura, Y., Foyez, T., Ohtake-Niimi, S., Narentuya, Akatsu, H., Nishitsuji, K., Michikawa, M., Wyss-Coray, T., Kadomatsu, K., Uchimura, K., 2017. Deficiency of a sulfotransferase for sialic acid-modified glycans mitigates Alzheimer's pathology. Proc. Natl. Acad. Sci. U. S. A. 114, E2947–E2954. doi:10.1073/pnas.1615036114

Zhang, Z., Zhang, Z.-Y., Wu, Y., Schluesener, H.J., 2012. Lesional Accumulation of CD163+ Macrophages/microglia in Rat Traumatic Brain Injury. Brain Res. 1461,

102–110. doi:10.1016/j.brainres.2012.04.038

Zhao, Y., Zeng, Y., Wu, A., Yu, C., Tang, Y., Wang, X., Xiong, R., Chen, H., Wu, J., Qin, D., 2018. Lychee Seed Fraction Inhibits Aβ(1-42)-Induced Neuroinflammation in BV-2 Cells via NF-κB Signaling Pathway. Front. Pharmacol. 9, 380. doi:10.3389/fphar.2018.00380

Zhou, C., Zhang, S., Nanamori, M., Zhang, Y., Liu, Q., Li, N., Sun, M., Tian, J., Ye, P.P., Cheng, N., Ye, R.D., Wang, M.-W., 2007. Pharmacological characterization of a novel nonpeptide antagonist for formyl peptide receptor-like 1. Mol. Pharmacol. 72, 976–83. doi:10.1124/mol.107.037564

Zhou, J., Fonseca, M.I., Pisalyaput, K., Tenner, A.J., 2008. Complement C3 and C4 expression in C1q sufficient and deficient mouse models of Alzheimer's disease. J. Neurochem. 106, 2080–2092. doi:10.1111/j.1471-4159.2008.05558.x

Zhou, L., Brouwers, N., Benilova, I., Vandersteen, A., Mercken, M., Van Laere, K., Van Damme, P., Demedts, D., Van Leuven, F., Sleegers, K., Broersen, K., Van Broeckhoven, C., Vandenberghe, R., De Strooper, B., 2011. Amyloid precursor protein mutation E682K at the alternative β-secretase cleavage β'-site increases Aβ generation. EMBO Mol. Med. 3, 291–302. doi:10.1002/emmm.201100138

Zhou, X., Yuan, L., Zhao, X., Hou, C., Ma, W., Yu, H., Xiao, R., 2014. Genistein antagonizes inflammatory damage induced by β-amyloid peptide in microglia through TLR4 and NF-κB. Nutrition 30, 90–95. doi:10.1016/j.nut.2013.06.006

Zhou, Z., Peng, X., Insolera, R., Fink, D.J., Mata, M., 2009. IL-10 promotes neuronal survival following spinal cord injury. Exp. Neurol. 220, 183–90. doi:10.1016/j.expneurol.2009.08.018

Zhu, M., Wang, X., Hjorth, E., Colas, R.A., Schroeder, L., Granholm, A.-C., Serhan, C.N., Schultzberg, M., 2016. Pro-Resolving Lipid Mediators Improve Neuronal Survival and Increase Aβ42 Phagocytosis. Mol. Neurobiol. 53, 2733–49. doi:10.1007/s12035-015-9544-0

Zhu, Y.P., Brown, J.R., Sag, D., Zhang, L., Suttles, J., 2015. Adenosine 5′-Monophosphate–Activated Protein Kinase Regulates IL-10–Mediated Anti-Inflammatory Signaling Pathways in Macrophages. J. Immunol. 194, 584–594. doi:10.4049/jimmunol.1401024

Zilkha-Falb, R., Kaushansky, N., Kawakami, N., Ben-Nun, A., 2016. Post-CNS-inflammation expression of CXCL12 promotes the endogenous myelin/neuronal repair capacity following spontaneous recovery from multiple sclerosis-like disease. J. Neuroinflammation 13, 7. doi:10.1186/s12974-015-0468-4

Zotova, E., Bharambe, V., Cheaveau, M., Morgan, W., Holmes, C., Harris, S., Neal, J.W., Love, S., Nicoll, J.A.R., Boche, D., 2013. Inflammatory components in human Alzheimer's disease and after active amyloid-β42 immunization. Brain 136, 2677–2696. doi:10.1093/brain/awt210

Zusso, M., Mercanti, G., Belluti, F., Di Martino, R.M.C., Pagetta, A., Marinelli, C., Brun, P., Ragazzi, E., Lo, R., Stifani, S., Giusti, P., Moro, S., 2017. Phenolic 1,3-diketones attenuate lipopolysaccharide-induced inflammatory response by an alternative magnesium-mediated mechanism. Br. J. Pharmacol. 174, 1090–1103. doi:10.1111/bph.13746